Mechanics and Materials Center
TEXAS A&M UNIVERSITY
College Station, Texas

RESEARCH ON DAMAGE MODELS
FOR CONTINUOUS FIBER COMPOSITES

Final Technical Report

by

D.H. Allen

Aerospace Engineering Department
Texas A&M University

submitted to the

Air Force Office of Scientific Research
Office of Aerospace Research
United States Air Force

AD-A200 771

DTIC
ELECTE
OCT 1 2 1988

D

AD-A200 771

REPORT DOCUMENTATION PAGE

Form Approved
OMB No. 0704-0188

1a. REPORT SECURITY CLASSIFICATION	1b. RESTRICTIVE MARKINGS
unclassified	

2a. SECURITY CLASSIFICATION AUTHORITY	3. DISTRIBUTION/AVAILABILITY OF REPORT
2b. DECLASSIFICATION/DOWNGRADING SCHEDULE	unlimited

4. PERFORMING ORGANIZATION REPORT NUMBER(S)	5. MONITORING ORGANIZATION REPORT NUMBER(S)
MM 5023-88-8	AFOSR-TR- 88-1144

6a. NAME OF PERFORMING ORGANIZATION	6b. OFFICE SYMBOL (If applicable)	7a. NAME OF MONITORING ORGANIZATION
Aeropsace Engineering Dept.		Air Force Office of Scientific Research

6c. ADDRESS (City, State, and ZIP Code)	7b. ADDRESS (City, State, and ZIP Code)
Texas A&M University College Station, TX 77843	Bolling AFB Washington, DC 20332 - 6448

8a. NAME OF FUNDING/SPONSORING ORGANIZATION	8b. OFFICE SYMBOL (If applicable)	9. PROCUREMENT INSTRUMENT IDENTIFICATION NUMBER
Air Force Office of Scientific	NA	AFOSR-84-0067

8c. ADDRESS (City, State, and ZIP Code)	10. SOURCE OF FUNDING NUMBERS			
	PROGRAM ELEMENT NO.	PROJECT NO.	TASK NO.	WORK UNIT ACCESSION NO.
Bolling AFB Washington, DC 20332 6448	61102F	2302	B2	

11. TITLE (Include Security Classification)

Research on Damage Models for Continuous Fiber Composites - Final Technical Report

12. PERSONAL AUTHOR(S)
D.H. Allen

13a. TYPE OF REPORT	13b. TIME COVERED	14. DATE OF REPORT (Year, Month, Day)	15. PAGE COUNT
Final	FROM April 84 TO May 88	July 1988	

16. SUPPLEMENTARY NOTATION

17. COSATI CODES			18. SUBJECT TERMS (Continue on reverse if necessary and identify by block number)
FIELD	GROUP	SUB-GROUP	composites, continuum mechanics, damage, internal state variables, experimental mechanics, laminated composites (JES)

19. ABSTRACT (Continue on reverse if necessary and identify by block number)

This report summarizes research completed during a four year period under AFOSR grant no. AFOSR-84-0067 and originally detailed under Texas A&M Research Foundation proposal no. RF-84-34 and dated October 1983. The objective of this research has been to develop an accurate damage model for predicting strength and stiffness of continuous fiber laminated composite media subjected to fatigue or monotonic loading and to verify this model with experimental results obtained from composite specimens of selected geometry and makeup. Further details of this research can be found in the three previous annual reports available either from AFOSR or the author.

20. DISTRIBUTION/AVAILABILITY OF ABSTRACT	21. ABSTRACT SECURITY CLASSIFICATION
☒ UNCLASSIFIED/UNLIMITED ☐ SAME AS RPT. ☐ DTIC USERS	unclassified

22a. NAME OF RESPONSIBLE INDIVIDUAL	22b. TELEPHONE (Include Area Code)	22c. OFFICE SYMBOL
Lt. Col. G. Haritos	(202) 767-0463	AFOSR/NA

DD Form 1473, JUN 86   Previous editions are obsolete.

RESEARCH ON DAMAGE MODELS
FOR CONTINUOUS FIBER COMPOSITES

Final Technical Report

by

D.H. Allen

Aerospace Engineering Department
Texas A&M University

submitted to the

Air Force Office of Scientific Research
Office of Aerospace Research
United States Air Force

Accession For	
NTIS CRA&I	☑
DTIC TAB	☐
Unannounced	☐
Justification	

A-1
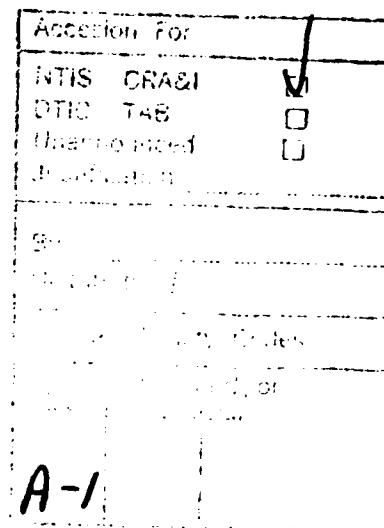
TABLE OF CONTENTS

1.0 INTRODUCTION

1.1 Summary

Continuous fiber composite laminates are known to undergo a substantial amount of complex load-induced damage which can adversely affect component performance. The nature of laminated composites is such that the material heterogeneity acts not only as a crack initiator, but also as a crack arrestor. Therefore, it is desirable to develop a model which accounts only for the average effects of small scale microcracks on the macroscale problem of interest. This approach, called continuum damage mechanics, has been successfully applied to isotropic media such as metals and concrete [2,3]. However, the application to laminated orthotropic composites has not been successfully demonstrated at this time. The principal difficulty in laminated composites, unlike metals and concrete, is that the layered orthotropy of the medium produces multiple damage modes, each possessed of some degree of anisotropy. Therefore, whereas it is often sufficient to deal with a single isotropic (scalar valued) damage tensor in initially isotropic and homogeneous media, this simplicity cannot be utilized in laminated composites. Furthermore, each of the damage mechanisms is interrelated and extremely difficult to distinguish experimentally. Finally, the damage may not be considered to be statistically homogeneous through the laminate thickness. Nevertheless, the application of continuum damage mechanics to laminated composites appears to be a fruitful quest because the alternative would be to attempt to solve a highly anisotropic multiply connected boundary value problem.

The ultimate objective of any continuum mechanics model is to design structural components so as to avoid failure. In the sense that laminated composites fail due to a complex sequence of damage events, it is essential to capture the important features of the damage process in order to accurately predict failure. Obviously this will be a complex task in laminated composites, but, as Einstein once put it, a good theory should be as simple as possible but no simpler than that.

The essential features of a continuum damage model for laminated composites are as follows: 1) identification and rigorous definition of the internal state variables characterizing each of the damage modes; 2)

1

development of stress-strain-damage constitutive equations; and 3) construction of damage evolution laws which accurately predict the genesis of each of the damage internal state variables as a function of load history. The primary difficulty lies in accomplishing this task in such a way that the model is independent of stacking sequence.

This report summarizes research completed during a four year period under AFOSR grant no. AFOSR-84-0067 and originally detailed under Texas A&M Research Foundation proposal no. RF-84-34 and dated October 1983. The objective of this research has been to develop an accurate damage model for predicting strength and stiffness of continuous fiber laminated composite media subjected to fatigue or monotonic loading and to verify this model with experimental results obtained from composite specimens of selected geometry and makeup. Further details of this research can be found in the three previous annual reports available either from AFOSR or the author.

1.2 Statement of Work

The following is a brief summary of work performed under the grant:

1) develop constitutive equations relating stresses to strains and damage internal state variables (ISV's) which may be used in a stress gradient field;

2) develop ISV growth laws as a function of load history for matrix cracking, interlaminar fracture, etc.;

3) develop finite element algorithms capable of evaluating ply properties in damaged components; and

4) perform experiments on components with selected stacking sequences in order to verify the model.

2

2.0 RESEARCH OVERVIEW

2.1 Summary of Completed Research

A substantial body of research has been completed under this grant, as evidenced by the publication list (see Section 3) and the thesis abstracts (see Section 4). The following is a summary of the major accomplishments to date.

1) In order to gain some insight about the general makeup of damage in laminated continuous fiber composites, two primarily experimental studies were undertaken (Section 2.2).

2) On the basis of the experimental studies, a general framework was developed using continuum damage mechanics to characterize the response of laminates with matrix cracks, and this model was compared to experimental evidence (Section 2.3).

3) The second order tensorial nature of the damage parameter was successfully demonstrated for the case of curved matrix cracks (Section 2.4).

4) Using the model developed above, a procedure was constructed with the aid of fracture mechanics to characterize the damage state for any laminate (Section 2.5).

5) The model was then extended to account for both matrix cracks and delaminations, and was successfully compared to experimental results (Section 2.6).

6) A micromechanics solution was obtained for laminates with matrix cracks and this result was utilized to demonstrate that the model is exact for the case of evenly distributed matrix cracks of constant size (Section 2.7).

7) The procedure was demonstrated for calculating ply level stresses and the effects of damage on these stresses (Section 2.8).

8) Development of damage evolution laws was initiated (Section 2.9).

9) A finite element program was developed for calculating the response of plates with spatially varying damage (Section 2.10).

The research grant has thus far resulted in a total of twelve publications in the open literature (see Section 3), ten conference presentations and two invited lectures (see Section 6). In addition, the program has produced two Ph.D.'s and four masters of science (see Section 4). All of these students have gone on to high visibility research positions (see Section 5).

The details of the research completed to date are contained in the research publications listed in Section 3, several of which are included in the appendix to this report. In the following sections the major achievements will be reviewed. However, in order to make this document more easily readable, these accomplishments will be discussed in summary rather than in detail.

2.2 Experimental Studies of Damage

The research program was initiated with a literature survey [1] which was undertaken to ascertain whether sufficient experimental data were available in the literature to obviate the necessity for performing in-house testing. It was found that no currently available research contained sufficiently detailed explanations of damage to characterize the model envisioned in this research effort. Therefore, it was decided to initiate our own experimental program under the auspices of the grant. Two M.S. theses resulted from this phase of the research [2,3].

The first study detailed the initiation and growth of matrix cracks in graphite-epoxy AS4-3502 cross-ply laminates. Primary attention was placed on identifying the mechanisms of initiation and growth of matrix cracks. Emphasis was also placed on observing the effect of these cracks on various components of stiffness loss.

A qualitative analysis was made to determine the significance of the damage events observed. These included crack density, stiffness reduction, crack shapes, development of crack surface area, and residual strain.

4

An array of seven cross-ply laminates was selected for study in order to examine the effect of the number of successive 90° plies on matrix crack damage. In addition, under appropriate loadings a highly developed state of matrix cracking can be obtained in the laminates without introducing other modes of damage, such as edge delamination.

In order to document the progression of matrix cracking one must nondestructively evaluate the damage in each laminate. This was accomplished by using edge replication and x-ray radiography. A typical edge replica showing damage in a cross-ply $[0/90_3]_s$ laminate is shown in Fig. 1. In this figure one can see three distinctly different types of matrix cracks: straight cracks, partial angled cracks and curved cracks. An x-ray radiograph of this same damage state is shown in Fig. 2. A straight crack appears as a sharp narrow band while a curved crack appears as a wider, fuzzy band. A typical progression of damage development is shown in Fig. 3. Other damage modes, including interlaminar delaminations and axial splitting, are visible in these radiographs. Interlaminar delaminations were observed to develop at the intersection of straight and curved cracks with the 0° interface as well as at the intersection of axial splits and transverse matrix cracks.

The experimental results showed a correlation between the number of curved cracks and the relative thickness of the 0° and 90° layers as well as the number of consecutive 90° plies. The bar chart in Fig. 4 shows the relationship between straight cracks and curved cracks for an increasing number of 90° plies in a $[0/90_n]_s$ laminate. It is interesting to note that for n greater than 2 there are more curved cracks than straight cracks.

The axial stiffness loss due to matrix cracking in five laminates was monitored during step-wise monotonic loadings. The stiffness was measured only on the unloading portion of the axial stress-strain curves. Thus, stiffness was used to indicate the degree of damage development during any monotonic loading step. The stiffness results are shown in Fig. 5. All curves represent an average of two or more replicate specimen results. The stiffness values are normalized to the undamaged stiffness and compared to the total crack density, which is the total number of straight cracks and curved cracks per unit length of specimen.

5

Z

STRAIGHT CRACK

X

LOADING DIRECTION

PARTIAL ANGLED
CRACK

CURVED CRACK

(A)
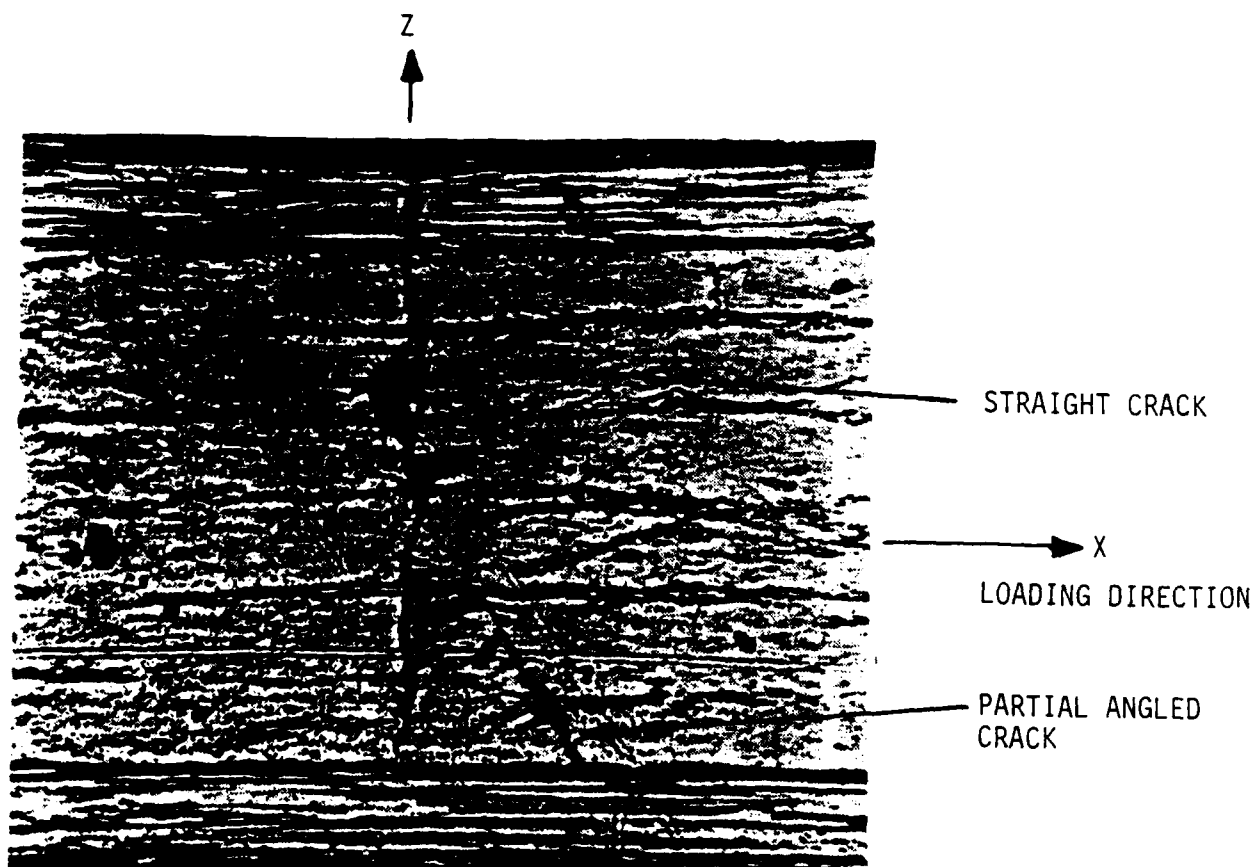
(B)
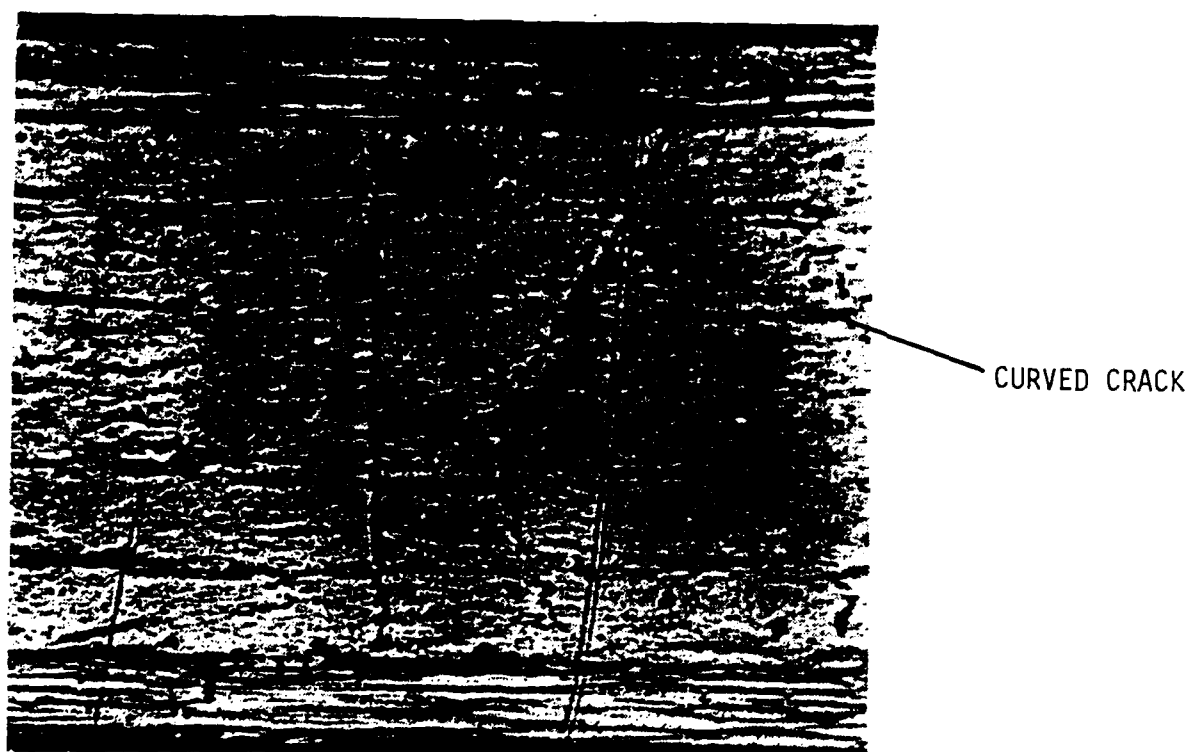
FIG. 1.   EDGE REPLICAS OF MATRIX CRACKS
        (A) PARTIAL ANGLE CRACKS
        (B) CURVED CRACKS

X

LOADING DIRECTION

angle crack
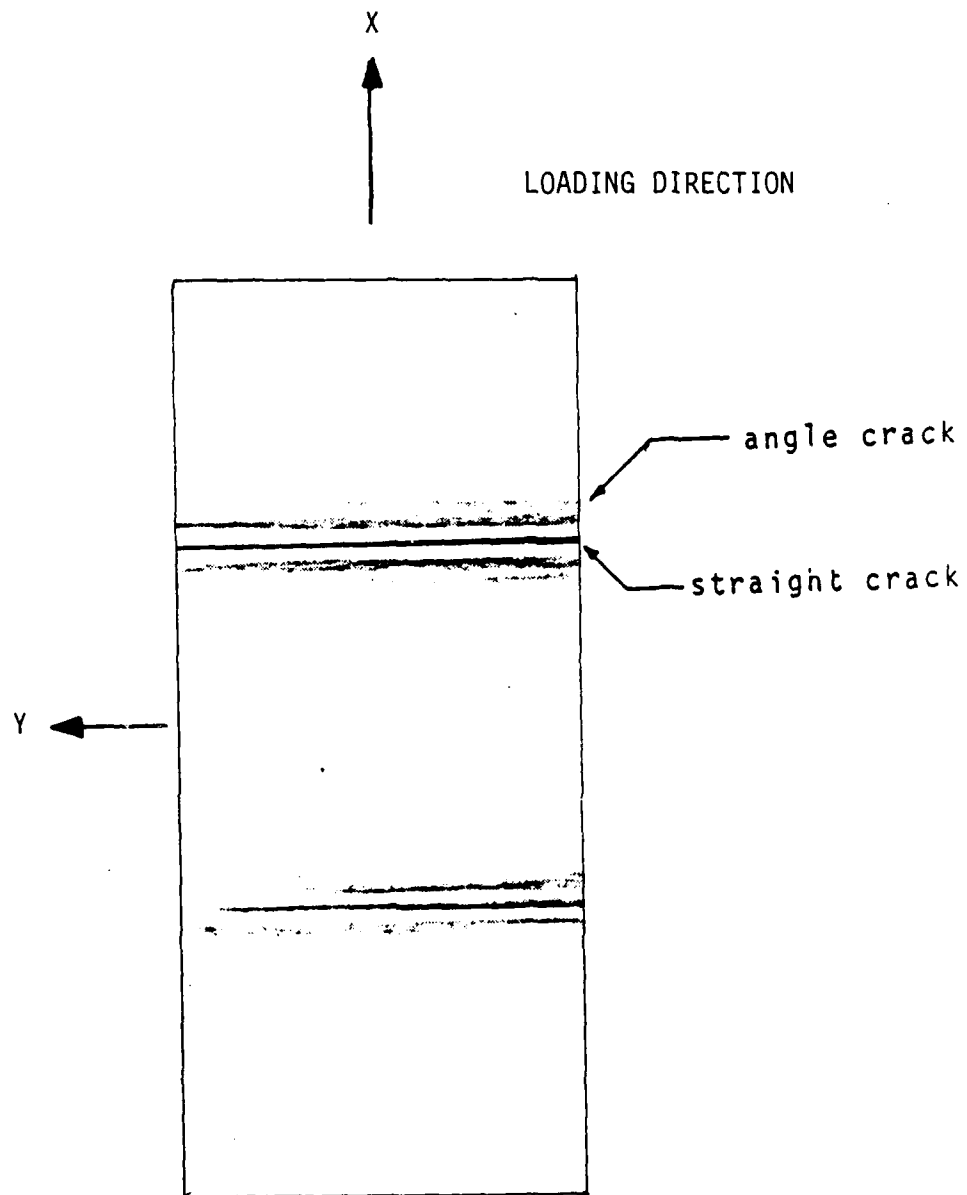
straight crack

Y

FIG. 2. DETAIL OF X-RAY RADIOGRAPH SHOWING DIFFERENCE
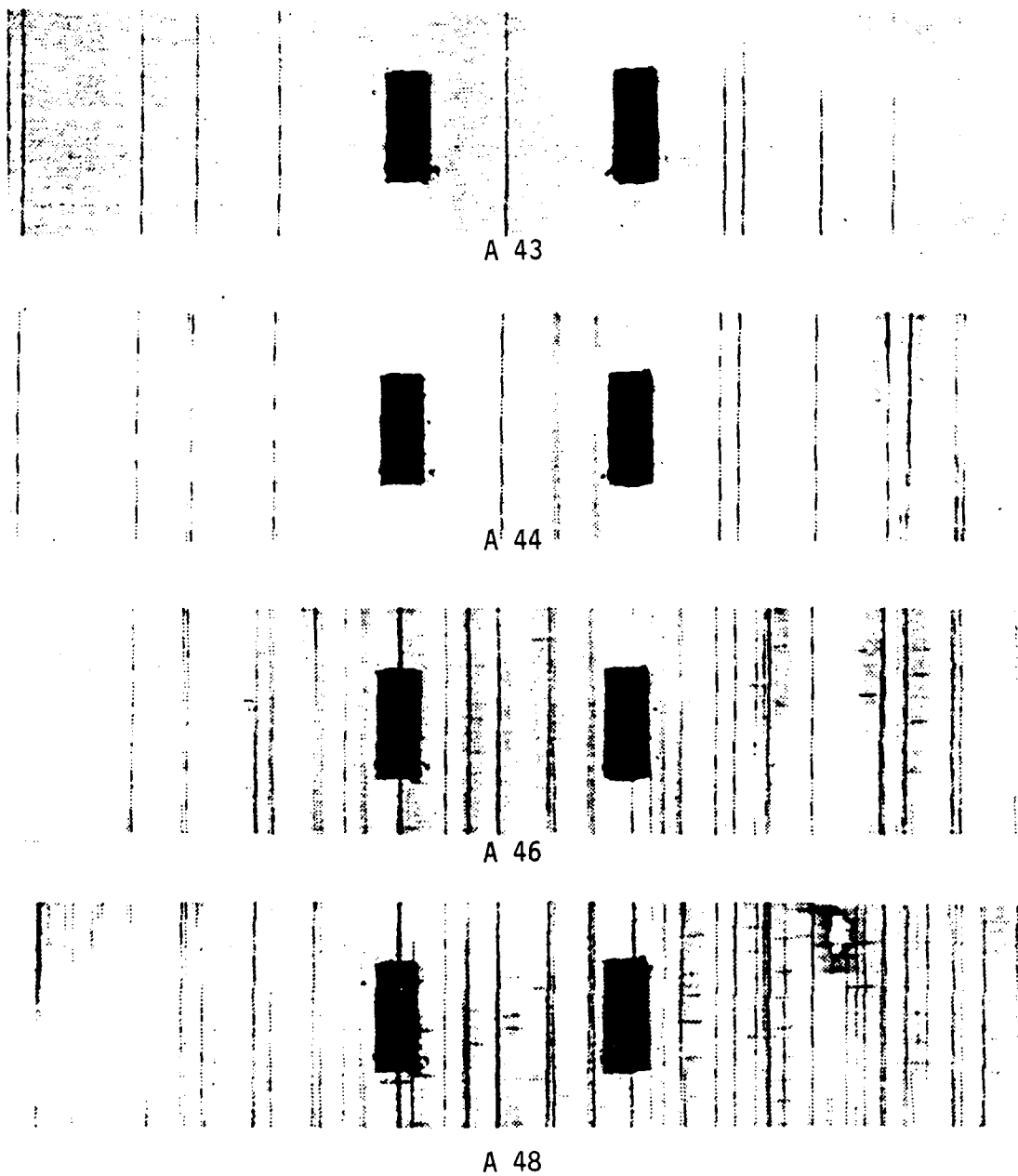BETWEEN STRAIGHT AND ANGLE CRACKS

A 43

A 44

A 46

A 48

FIG. 3. X-RAY RADIOGRAPHS SHOWING THE PROGRESSION
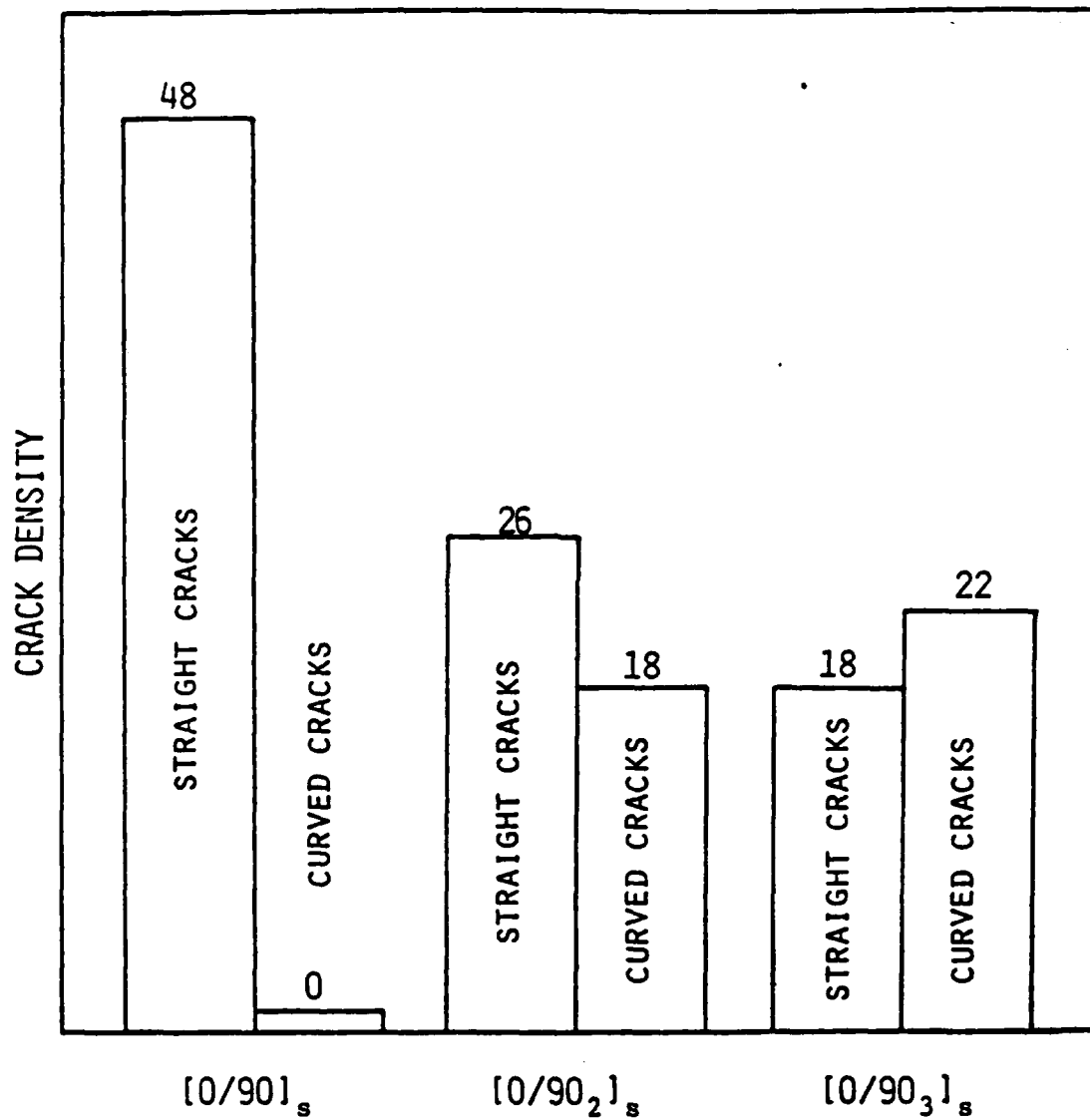OF DAMAGE IN A $[0/90_4]_s$ LAMINATE

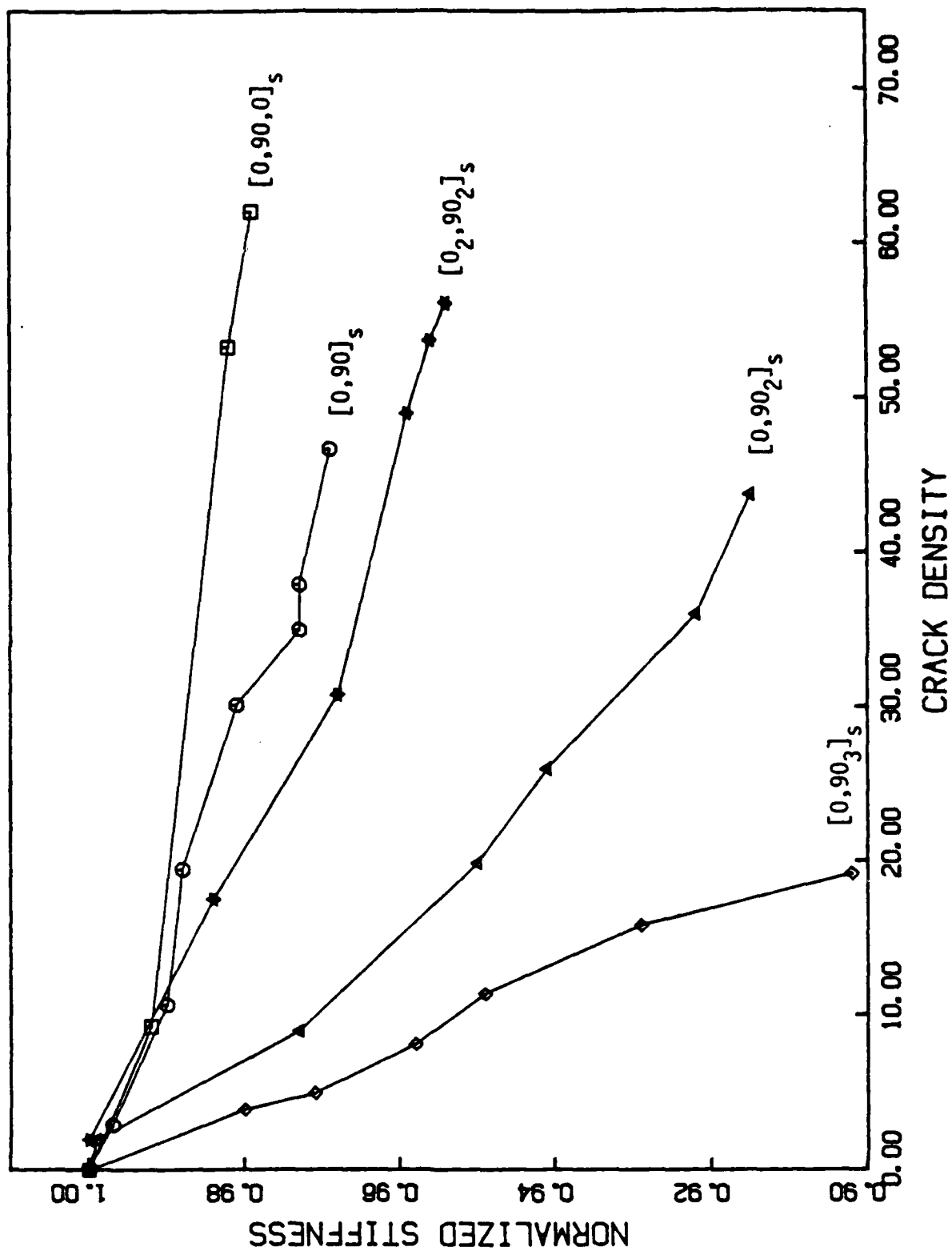Fig. 4. Increase in Curved Cracks as Number of Consecutive 90° Plies Increases.

Fig. 5. Axial Stiffness Loss in Cross-Ply Laminates for Matrix Cracking Only.

10

For $[0/90_n]_s$ laminates, where $n=\frac{1}{2}$, 1, 2, and 3, stiffness loss increases with increasing n. This is explained by the fact that for increasing n more load is carried by the 90° plies. Hence, for the same crack density (damage), the laminate with more 90° plies will lose more stiffness. This same trend can be explained by ply discount, though the ply discount method usually overestimates the total stiffness loss. It is noted that the last data points for the $[0/90/0]_s$ and $[0/90]_s$ were taken after application of 95 percent of the ultimate load, whereas the last data points for the remaining laminates correspond to the test termination loads when other damage modes began to occur.

For laminates with identical 0°/90° ratios such as the $[0/90]_s$ and $[0_2/90_2]_s$, the laminate with the higher consecutive number of 90° plies shows greater stiffness loss. This is due to the fact that the laminate with the higher consecutive number of 90°'s has more crack surface area for a given crack density resulting in a larger crack opening displacement. This implies that the constitutive model should reflect crack opening displacements in addition to surface area of cracks.

In order to understand what mechanisms control the geometry (location and orientation) of the curved cracks, a finite element model was developed to analyze the stress and strain fields in the vicinity of a straight crack [4]. Constant strain triangular elements (CST) were used to model an axial section through the thickness of a laminate. Internal boundary generation was also included. The ply level material constitution was assumed to be transversely isotropic elastic. The $[0/90_2]_s$ laminate was selected for detailed study.

The basic finite element mesh used to model the $[0/90_2]_s$ laminate with a straight matrix crack is shown in Fig. 6. The squares shown in the figure actually correspond to two "CST" elements. The broad dark line shown between the 0/90 interface represents the resin rich region where there are actually four rows of "CST" elements. The broad dark line shown between the 0/90 interface represents the resin rich region where there are actually four rows of "CST" elements. More elements were used in the interior 90° layer to increase the accuracy of the solution.

A typical crack family for a $[0/90_2]_s$ specimen is shown in Fig. 7. From edge replicas, the mean distance between a straight crack and its nearest
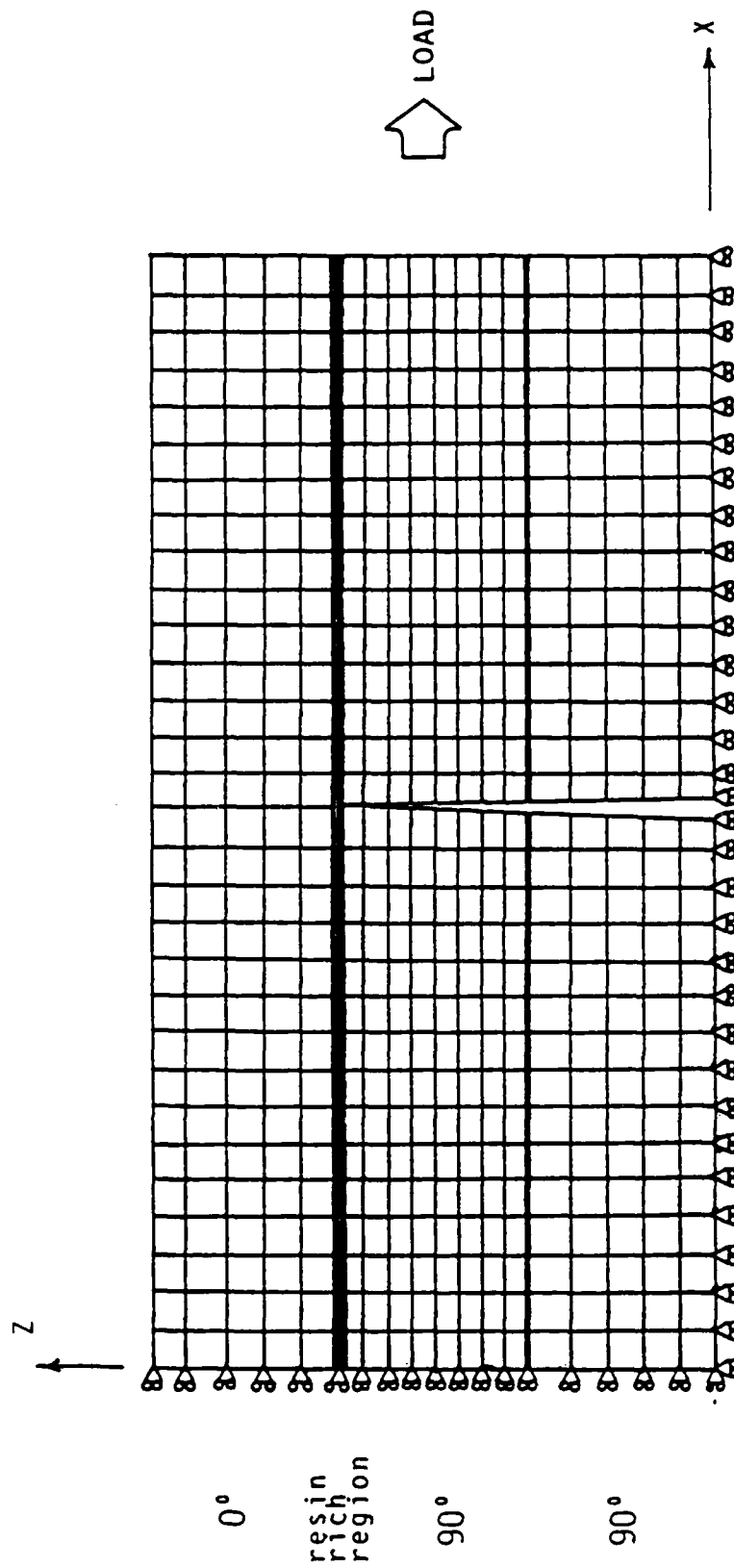
11

FIG. 6. FINITE ELEMENT MODEL OF A $[0/90_2]_s$

LAMINATE WITH A RESIN RICH REGION

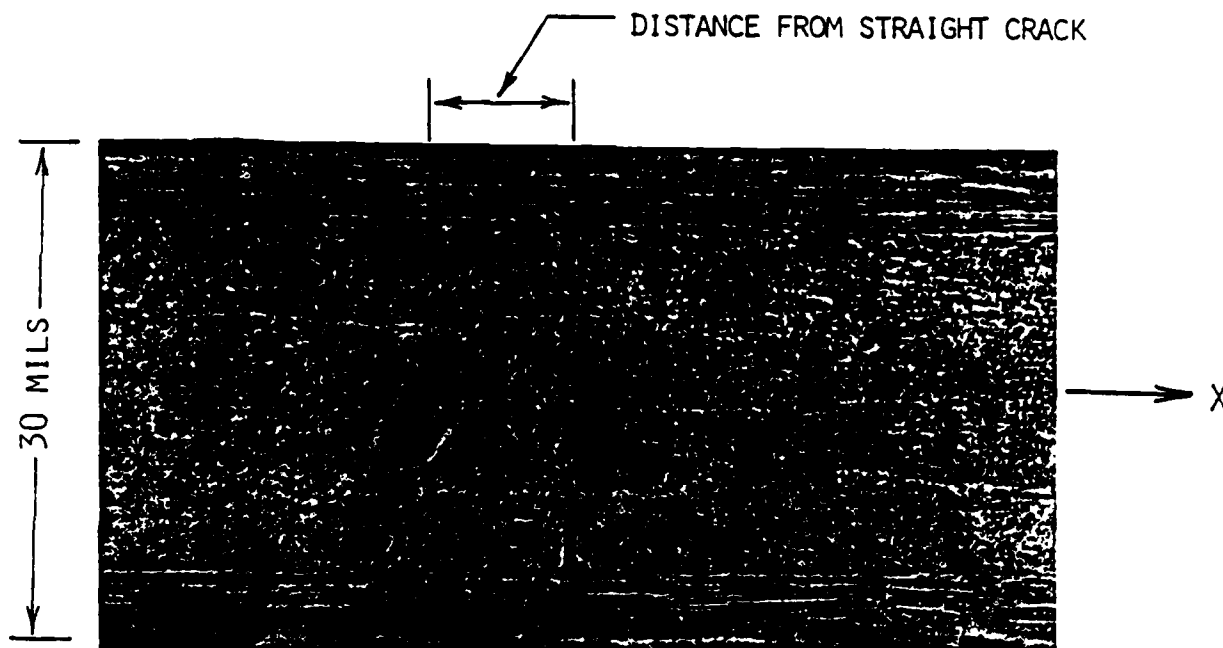DISTANCE FROM STRAIGHT CRACK

30 MILS

X

FIG. 7. TYPICAL CRACK FAMILY IN A $[0/90_2]_s$ LAMINATE

associated curved crack as measured at the 0/90 ply interface was found to be 9.8 mils (0.2489 mm), with a standard deviation of 2.08 mils (0.05283 mm). These statistical parameters were determined from 25 crack spacing measurements. The minimum spacing observed was 7.0 mils (0.1778 mm). The mean angle between the curved cracks and the normal to the interface was found to be 30°.

The distribution of maximum principal stress near the 0/90 interface determined by the finite element model is presented in Fig. 8. The principal stress has been plotted along each of the first three rows of elements, below the resin rich region. For comparison, Fig. 8 also shows the mean and minimum crack spacings that were determined experimentally.

The qualitative agreement between the experimental and finite element results supports the contention that curved cracks are caused by a rotation of the principal stresses which is induced by a shear lag effect resulting from the vertical matrix cracks. This phenomenon will be discussed further in Section 2.4.

The second experimental effort concentrated on the mechanics of delaminations. The initiation and growth of internal delaminations in laminated fiber-reinforced composites made of AS4/3502 graphite/epoxy was studied. Cross-ply laminates of the general type $[0_n/90_m]_s$ were subjected to a tension-tension cyclic load at 2.0 Hz and R=0.1 to develop internal delaminations. Isolation of internal delaminations from other major matrix fracture phenomena was the main reason for selecting cross-ply laminates for this study.

The X-ray radiography nondestructive method was used to record the internal delaminations at specified load cycles. In addition, Scanning Electron Microscopy was used to examine the damage state in the interior of the laminates. Also, the laminate mechanical properties E_{xx} and v_{xy} were measured at the cycles where the damage was recorded.

Following the characteristic damage state (CDS), all laminates first developed axial splits and then internal delaminations. Matrix fracture in the 0° layers initiated along transverse matrix cracks. Internal delaminations initiated at interfacial points where axial splits intersected transverse cracks. Two distinct patterns of axial splits and delaminations were observed. The $[0_2/90_2]_s$ laminate developed axial splits which completely
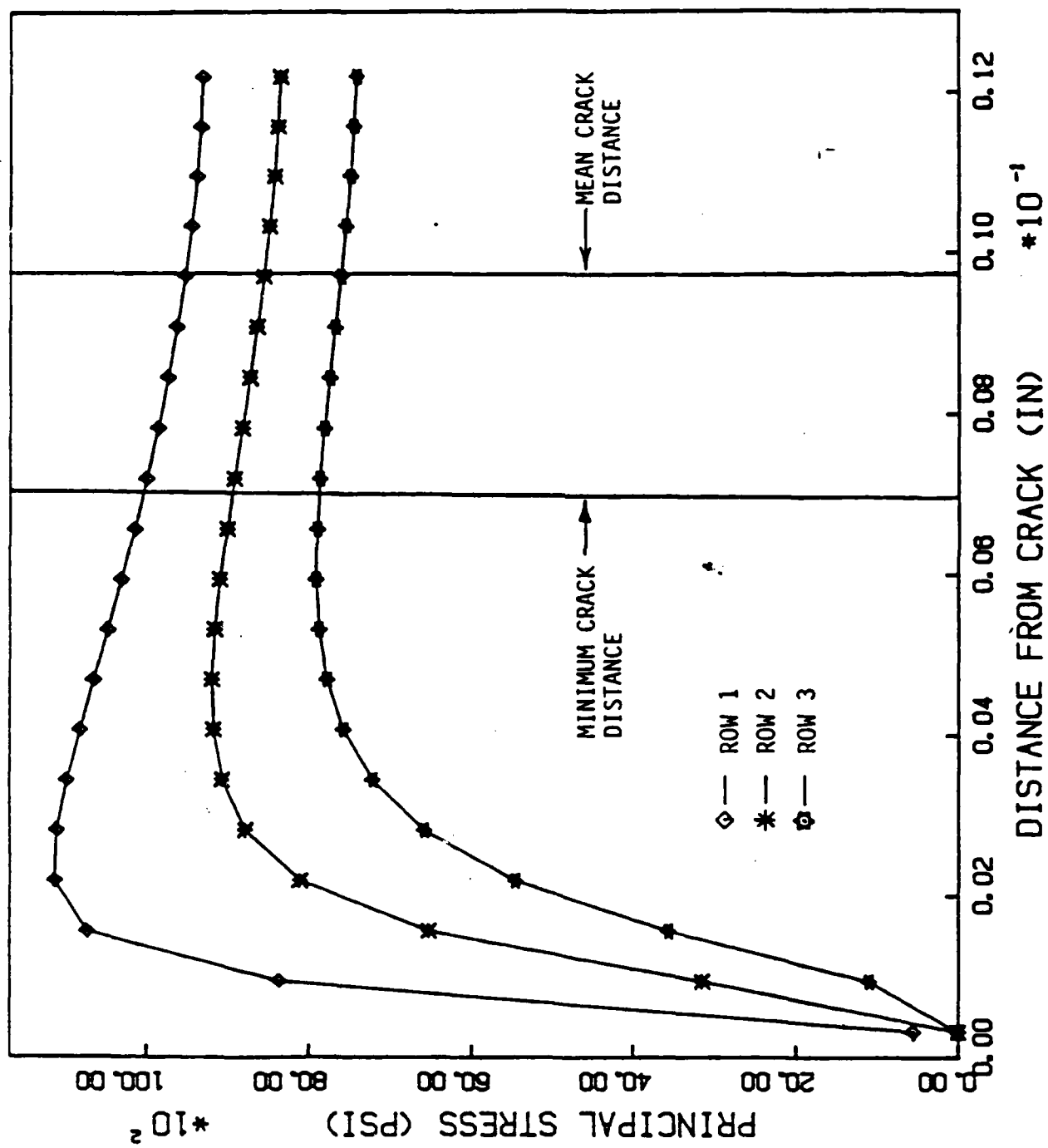
14

FIG. 8 Variation of Principal Stress Near the $0°/90°$ Interface.

extended to the specimen ends as shown in Fig. 9. Internal delaminations initiated at internal corner points and grew along axial splits to form axially continuous delaminations.

The $[0/90_2]_s$, $[0/90_3]_s$, and $[0/90]_s$ laminates first developed short axial splits and then internal delaminations which initiated at internal corner points. The delaminations preferred to initiate early in the fatigue life along closely packed transverse crack fronts intersected by a relatively large number of short axial splits as shown in Figure 10. These delaminations coalesced to form a continuous transverse delamination.

All laminates experienced a decrease in the axial modulus, E_{xx}, and in Poisson's ratio, ν_{xy}. The axial modulus exhibited a relatively small decrease, whereas the Poisson's ratio changed by a factor of 2 to 4 depending on the stacking sequence.

A stress analysis was employed to interpret the initiation and patterns of matrix cracking and delamination growth [4]. The results of the stress analysis were consistent with the observed experimental results. The analytical results suggest that axial splits initiate at transverse matrix cracks and delaminations initiate at the intersection of transverse and axial matrix cracks. The rate of growth of axial delaminations depends on the maximum stress, density of axial splits, and on the relative position of the axial splits along which the axial delaminations grow.

The observations made during the experimental program suggested several important factors which would have to be included in the model in order for it to be useful as a general theoretical tool. First, the model should include both matrix cracks and delamination damage parameters as independent state variables. Second, because different stacking sequences with identical numbers of plies could experience vastly different damage, the model must be independent of stacking sequence; that is, given the same input, the model should be capable of predicting different damage states for different stacking sequences. Third, because the same stacking sequence could undergo different damage states for differing load histories, the model must be capable of reflecting the effects of load history. Fourth, because different crack orientations produce widely varying stiffness reductions, the model must be tensorial in nature. Finally, it was found that the geometry of cracking in quasi-isotropic laminates with both matrix cracks and delaminations was so complex as to preclude an accurate micromechanics solution.
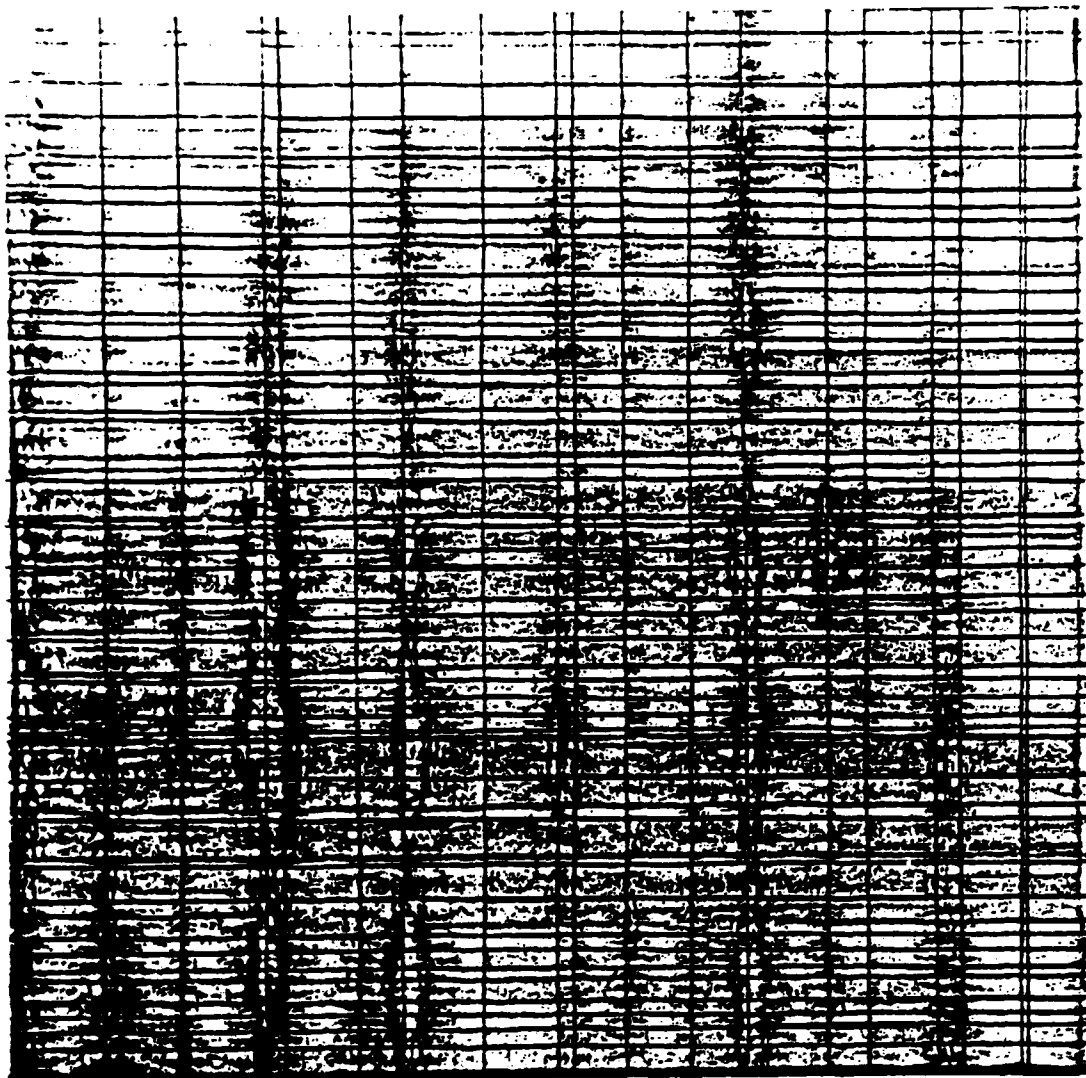
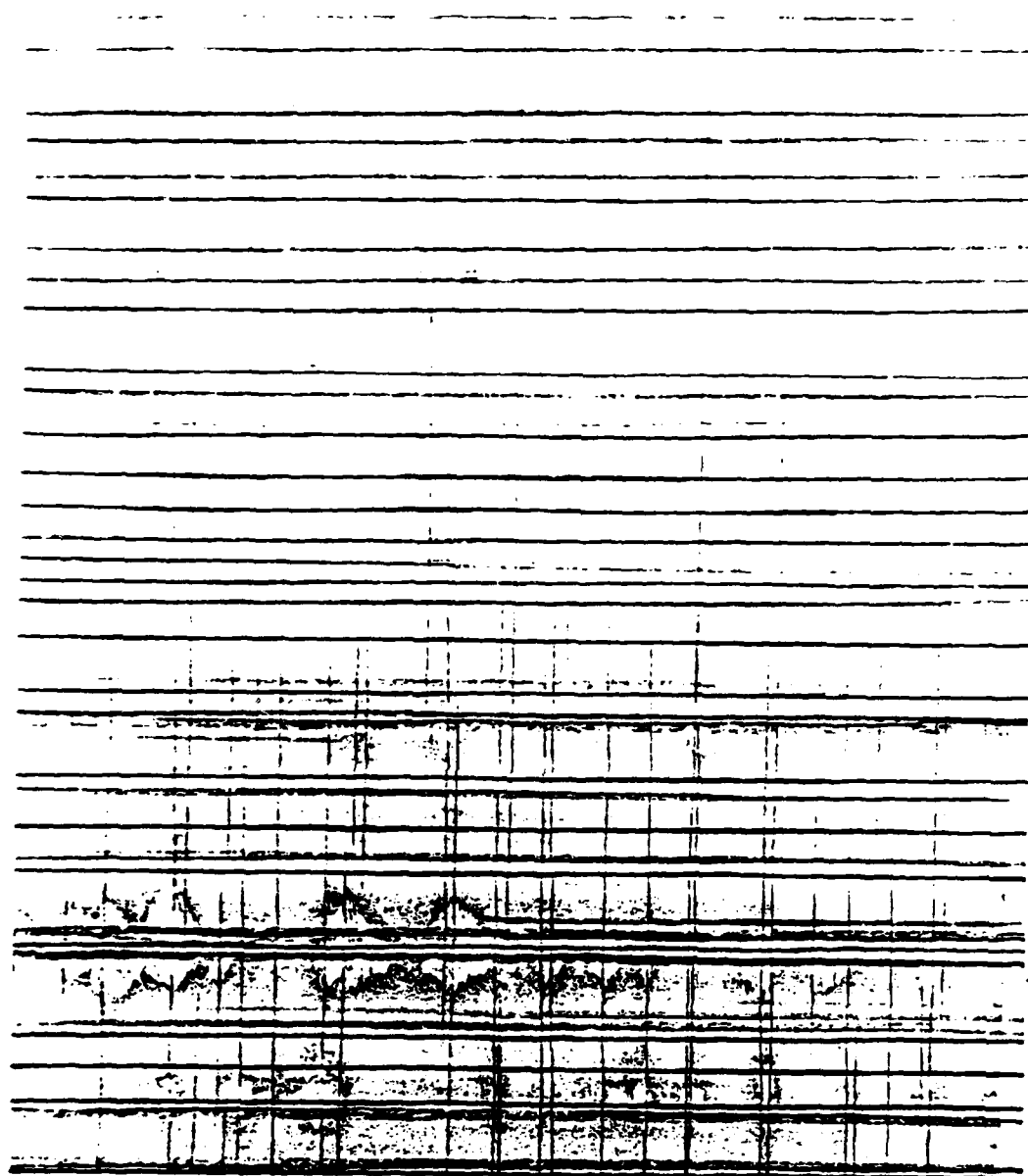FIG. 9. DELAMINATION PATTERN IN A $[0_2/90_2]_s$ AT 300,000 CYCLES, R=0.1

FIG. 10. DELAMINATION PATTERN IN A $[0/90_3]_s$ AT 200,000 CYCLES AND R=0.1

2.3 General Framework of the Damage Model

The experimental program elucidated the need to develop a theoretical damage model which was capable of accounting for the effects of microcracks on component strength and life without resorting to a detailed analysis of each crack. Therefore, a technique was sought which would accomplish this as rigorously as possible.

In 1958, L. Kachanov proposed a novel approach to modelling the effect of microcracks on the overall response of homogeneous and isotropic media [5]. In this approach, the effect of microcracks is reflected in thermomechanical constitutive equations rather than by including numerous time-dependent internal boundary conditions. Because the resulting procedure produces a simply-connected, or continuous boundary value problem which is considered to be "equivalent" to the actual domain with microcracks, the methodology has been termed continuum damage mechanics. Although Kachanov's approach was initially heuristic, a broad field of study has developed from that embryonic state [6,7]. However, until recently most efforts have been empirical and confined to initially isotropic media.

In the current research effort it was decided to attempt to produce a stronger theoretical footing for the continuum damage mechanics approach, and, in so doing, hopefully simultaneously developed an extension to layered and orthotropic media. This was initially accomplished for the case of laminates with matrix cracks and its usefulness was demonstrated by comparing to experimental evidence [8,9].

A continuum damage model must contain four essential ingredients in order to be complete: 1) stress-strain-damage equations; 2) damage evolution laws for the damage ISV's; 3) a failure function describing local failure in terms of the damage ISV's and observable state variables; and 4) an algorithm for solving boundary value problems in which the state is nonhomogeneous. If steps one through three can be accomplished accurately, then step four is relatively straightforward, involving a procedure not unlike extending an elastic algorithm to include plasticity.
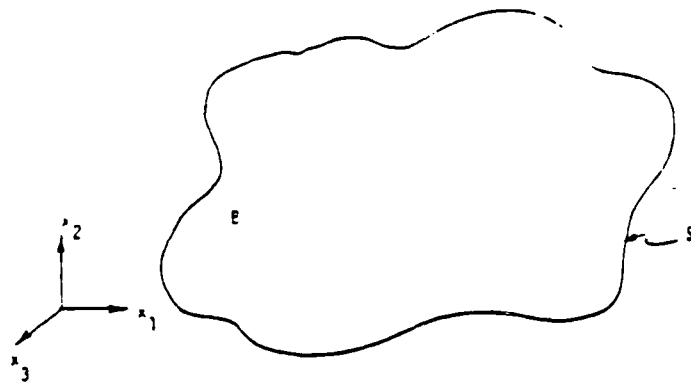
At this point in the model development steps 1 and 4 are essentially completed, and step 2 is well underway. Step 1 for the case of matrix cracking is discussed in this section, and the extension to include

delamination is summarized in Section 2.6. Step 2 is developed in Section 2.9, and step 4 is discussed in Section 2.10.
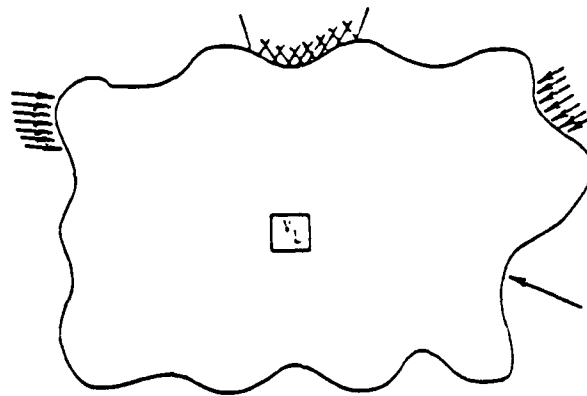
To proceed with the model development, consider an initially unloaded and undamaged composite structural component, denoted B, as shown in Fig. 11a, where undamaged is defined here to mean that the body may be considered to be continuous (without cracks) on a scale several orders of magnitude smaller than the smallest external dimension of the component. Although cracks may exist in the initial state, their total surface area is assumed to be small compared to the external surface area of the component. Under this assumption the body is assumed to be simply connected and we call the initial boundary surface the external boundary S. Although the component is undamaged, there may exist local heterogeneity caused by processing and second phase materials including fibers, matrix tougheners and voids. In addition, the body may be subjected to some residual stress state due to processing, cool down, etc.

Now suppose that the component is subjected to some traction and/or deformation history, as shown in Fig. 11b. The specimen will undergo a thermodynamic process which will in general be in some measure irreversible. This irreversibility is introduced by the occurrence of such phenomena as material inelasticity (even in the absence of damage), fracture (both micro- and macroscale), friction (due to rubbing and/o slapping of fractured surfaces), temperature flux, and chemical change. While all of these phenomena can and do commonly occur in composites, in the present research it will be assumed that all irreversible phenomena of significance occur in small zones near crack surfaces. Outside these zones, the behavior will be considered to be elastic and therefore reversible under constant temperature conditions. All fracture events will be termed damage. Due to these fracture events, the body will necessarily become multiply connected, and all newly created surfaces not intersecting the external boundary will be termed internal boundaries. Because of the above assumptions the model may be limited to polymeric and ceramic matrix composites at temperatures well below the glass transition temperature T_g or melting temperature, where viscoelasticity in matrix materials is small. Metal matrix composites may have to be excluded due to complex post-yield behavior of the matrix.
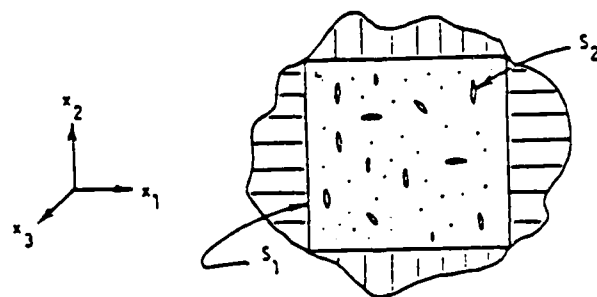
While fracture involves changes in the boundary conditions governing a complex field problem, it is hypothesized that one may neglect boundary

FIG. 11. Structural Component Labelled B
   a) Undamaged State
   b) With Applied Tractions
   c) Local Volume Element

21

condition changes caused by creation and alteration of both internal and external surfaces created during fracture as long as the resulting damage in the specimen is statistically homogeneous on a local scale which is small compared to the scale of the body of interest. However, the total newly created surface area (which includes internal surfaces) may be large compared to the original external surface area. Under the condition of small scale statistical homogeneity all continuum based conservation laws are assumed to be valid on a global scale in the sense that all changes in the continuum problem resulting from internal damage are reflected only through alterations in constitutive behavior. Typical microstructural events which may qualify as damage are matrix cracking in lamina, fiber/matrix debonding, localized interlaminar delamination and fiber fracture.

Now consider some local element labelled V_L and with external surface faces S_1 arbitrarily chosen normal to a set of Cartesian coordinate axes (x_1, x_2, x_3), as shown in Fig. 11c. The element V_L extracted from B and the newly created surfaces, denoted S_2 and with volume V_c, are subjected to appropriate boundary conditions so that the element response is identical to that when it is in B. Furthermore, the volume of the element is defined to be V_L, which includes the volume of any initial voids. The scale of V_L is chosen so that its dimensions are small compared to the dimensions of B, but at the same time, the dimensions of V_L are large enough to guarantee statistical homogeneity of the material heterogeneities and defects in V_L even though the total surface area of defects may be of the same order of magnitude as S_1. Suppose furthermore that in the absence of defects or at constant damage state the material behavior is linearly thermoelastic. Now consider the local volume element V_L. For the case where tractions or displacements are applied uniformly to the external boundary of V_L, the average stresses and strains in V_L will be determinable from the external boundary tractions or displacements.

Although the damage process actually involves the conversion of strain energy to surface energy, the fact that the damage is reflected in the local constitutive equations rather than boundary conditions suggests that it be treated as a set of energy dissipative internal state variables which are not discernible on the external boundary of the local element.

Under the conditions described above the pointwise Helmholtz free energy per unit volume h of the undamaged linear elastic medium may be expressed as a second order expansion in terms of strain ϵ_{ij} and temperature T as follows:

22

$$h \equiv u - Ts = h(\epsilon_{ij}, T) =$$

$$A + B_{ij}\epsilon_{ij} + \frac{1}{2} C_{ijkl}\epsilon_{ij}\epsilon_{kl} + D\Delta T + E_{ij}\epsilon_{ij}\Delta T + \frac{1}{2} F\Delta T^2 \qquad (1)$$

where u and s are the internal energy and entropy per unit volume, respectively, and A, B_{ij}, C_{ijkl}, D, E_{ij} and F are material parameters which are independent of strain and temperature and $\Delta T \equiv T-T_R$, where T_R is the reference temperature at which the strains are zero at zero external loads.

It is our intention to construct locally averaged field equations which are similar in form to the pointwise field equations. In performing this averaging process the pointwise Helmholtz free energy described in equation (1) will undergo a natural modification to include the energy conversion due to crack formation.

Now consider the local element shown in Fig. 11c with traction boundary conditions on the external surface S_1. In addition, the interior of V_L is assumed to be composed entirely of linear elastic material and cracks (which may include thin surface layers of damage). Integrating pointwise equation (1) and the conservation laws over the local volume will result in

$$h_{EL} = A_L + B_{Lij}\epsilon_{Lij} + \frac{1}{2} C_{Lijkl}\epsilon_{Lij}\epsilon_{Lkl} + D_L\Delta T_L + E_{Lij}\epsilon_{Lij}\Delta T_L + \frac{1}{2} F_L\Delta T_L^2 \quad (2)$$

where A_L, B_{Lij}, C_{Lijkl}, D_L, E_{Lij}, and F_L are locally averaged material constants, and the subscript L implies local averaging. Also,

$$\sigma_{Lji,j} = 0 \qquad (3)$$

$$\sigma_{Lij} = \sigma_{Lji} \qquad (4)$$

$$\dot{u}_L' - \sigma_{Lij}\dot{\epsilon}_{Lij} + q_{Lj,j} = r_L \qquad (5)$$

$$\dot{s}_L - \frac{r_L}{T_L} + (\frac{q_{Lj}}{T}), j \geq 0 \qquad (6)$$

where u_L', called the effective local internal energy, is given by

$$\dot{u}_L' \equiv \dot{u}_{EL} + \dot{u}_L^C \qquad (7)$$

u_{EL} represents the internal energy of the equivalent uncracked body, given by

$$\dot{u}_{EL} \equiv \frac{1}{V_L} \int_{V_L} \dot{u}dV - \frac{1}{V_L} \int_{S_2} T_i^E \dot{u}_i dS \qquad (8)$$

where T_i^E are called equivalent tractions, representing tractions in the uncracked body acting along fictitious crack faces, as described in detail in Appendix 7.1, and u_L^C is the mechanical power output due to cracking, given by

$$\dot{u}_L^C \equiv - \frac{1}{V_L} \int_{S_2} T_i^C \dot{u}_i dS \qquad (9)$$

where T_i^C are fictitious tractions applied to the crack faces which represent the difference between the actual crack face tractions and T_i^E. Furthermore, the locally averaged stress is given by

$$\sigma_{Lij} \equiv \frac{1}{V_L} \int_{V_L} \sigma_{ij} dV \qquad (10)$$

and the locally averaged strain is given by

$$\varepsilon_{Lij} \equiv \frac{1}{V_L} \int_{S_1} \frac{1}{2} (u_i n_j + u_j n_i)dS \qquad (11)$$

where n_i are components of the unit outer normal vector to the surface S_1. Equations (2) through (6) are identical in form to the standard pointwise conservation laws.

On the basis of this similarity we now define the locally averaged Helmholtz free energy:

$$h_L \equiv u_L' - T_L s_L = u_{EL} - T_L s_L + u_L^C = h_{EL} + u_L^C \qquad (12)$$

where it can be seen from definition (8) that h_{EL} is the locally averaged elastic Helmholtz free energy for which residual damage is zero.

The similarity between the pointwise and local field equations leads to the conclusion that

$$s_L = -\frac{\partial h_L}{\partial T_L} \qquad (13)$$

$$\sigma_{Lij} = \frac{\partial h_L}{\partial \varepsilon_{Lij}} = \frac{\partial h_{EL}}{\partial \varepsilon_{Lij}} + \frac{\partial u_L^C}{\partial \varepsilon_{Lij}} \qquad (14)$$

Equations (14) serve as the basis for thermomechanical stress-strain relations in damaged composites. All damage is reflected through the local energy due to cracking u_L^C. This term is modelled with internal state variables characterizing the various damage modes.

In order to describe the internal state, we first consider the kinematics of a typical point O with neighboring points A and B, as shown in Fig. 12. Before deformation lines OA and OB are orthogonal, as shown in (a). After deformation we image that lines joining O', A', and B' are as shown in (b), and just at the instant that deformation is completed, a crack forms normal to the plane of AOB through point O', as shown in (c). Furthermore, point O' becomes two material points O' and O" on opposite crack faces and points A' and B' deform further to points A" and B". It is assumed that all displacements, including displacement jumps across crack faces, are infinitesimal, so that strain gages attached at points O, A, and B record only the deformation A"O'B". However, the actual strain is associated with A"O"B". Therefore, it is essential to construct an internal state variable which will relate these two strain descriptions. We therefore construct the vectors $\vec{u}^C$ connecting O' and O" and $\vec{n}^C$ describing the normal to the crack face at O', as shown in (c). It should be noted that $\vec{u}^C$ can be used to construct a pseudo-strain representing the difference in rotation and extension of lines A"O'B" and A"O"B".

Now recall that the mechanical power output during cracking is given by equation (9). We assume that at any point in time t_1 tractions T_i can be applied along the crack faces which will result in an energy equivalent to that produced by the damage process:

$$u_L^C(t_1) = -\frac{1}{V} \int_{S_2(t_1)} T_i u_i^C dS \qquad (15)$$

25
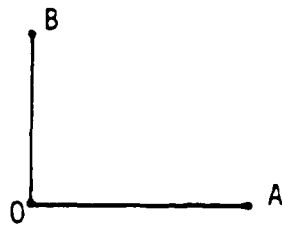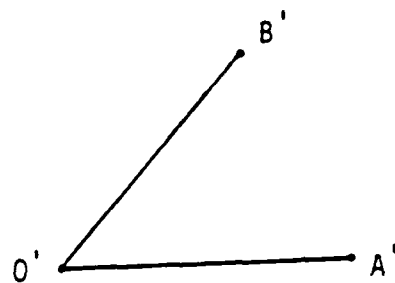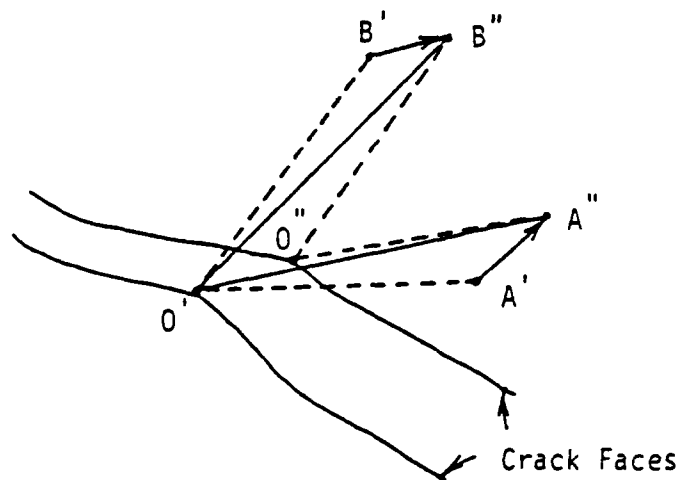
FIG. 12. Kinematics of the Damage Process
        a) Point "O" Prior to Deformation,
        b) Point "O" After Deformation and Prior to Fracture,
        c) Point "O" After Fracture.

The quantities T_i do not necessarily coincide with the terms in the integrand of (9) since the process is in some measure irreversible. However, we define them such that the total energies in equations (9) and (27) are equivalent. For convenience we will call them crack closure tractions, although they do not necessarily result in complete crack closure.

Guided by the fact that $\vec{u}^C$ and $\vec{n}^C$ describe the kinematics of the cracking process at point 0, we now define the following second order tensor valued internal state variable:

$$\alpha_{ij} \equiv \frac{1}{V_L} \int_{S_2} u_i^C n_j^C dS \tag{16}$$

The above description has been previously proposed by M.L. Kachanov [10]. Substituting the above into (15) and utilizing Cauchy's formula gives

$$u_L^C = \frac{1}{V_L} \int_{S_2} \sigma_{ij}^C \alpha_{ij} dS \tag{17}$$

Therefore, if we define $\sigma_{Lij}^{C\eta}$ to be the average crack closure stress for the ηth damage mode such that

$$\sigma_{Lkl}^{C\eta} \alpha_{Lkl}^{\eta} \equiv \frac{1}{V_L} \int_{S_2} \sigma_{ij}^C \alpha_{ij} dS \tag{18}$$

It follows that

$$u_L^C = - \sigma_{Lij}^{C\eta} \alpha_{Lij}^{\eta} \tag{19}$$

It is now proposed that u_L^C be expanded in a Taylor series which is second order in each of its arguments. Substituting this result and (2) into equation (14) and neglecting higher order terms results in

$$\sigma_{Lij} = B_{Lij} + E_{Lij} \Delta T_L + C_{Lijkl} \epsilon_{Lkl} + I_{ijkl}^{\eta} \alpha_{Lkl}^{\eta} \tag{20}$$

Equations (20) are interpreted as the ply level equations governing the response of plies with matrix cracks.

Equations (20) have been implemented to a laminate analysis code to produce predictions of stiffness loss as a function of matrix crack damage in

crossply laminates [9]. Because this procedure is fairly cumbersome to review here, the interested reader is referred to Appendix 7.2 for the details of this implementation. The results shown in Figs. 13-15, originally obtained in 1985, gave cause for optimism that the model might be a useful tool for predicting damage dependent stiffness components. As will be shown in further sections, these initial results have been substantiated by numerous further predictions.

2.4 Study of the Tensorial Nature of Damage

Experimental evidence indicates that curved matrix cracks can occur in significant quantities in cross-ply laminates [2]. As a measure of the capability of the model to predict stiffness loss components other than the axial stiffness, it was decided to use the model to predict out-of-plane stiffness loss due to the curved cracks. The procedure will be briefly reviewed here.

Consider now a local volume element with n_c cracks as shown in Fig. 16. The damage ISV for matrix cracking may be written in the following form

$$\alpha_{ij}^1 = \frac{1}{twL} \sum_{k=1}^{n_c} \int_{S_{2k}^1} u_i n_j dS \tag{21}$$

where matrix cracking is designated by the superscript 1. Now define

$$\alpha_{ij}^{1k} = \frac{1}{twL} \int_{S_{2k}^1} u_i n_j dS \tag{22}$$

so that equation (21) may be written

$$\alpha_{ij}^1 = \sum_{k=1}^{n_c} \alpha_{ij}^{1k} \tag{23}$$

28
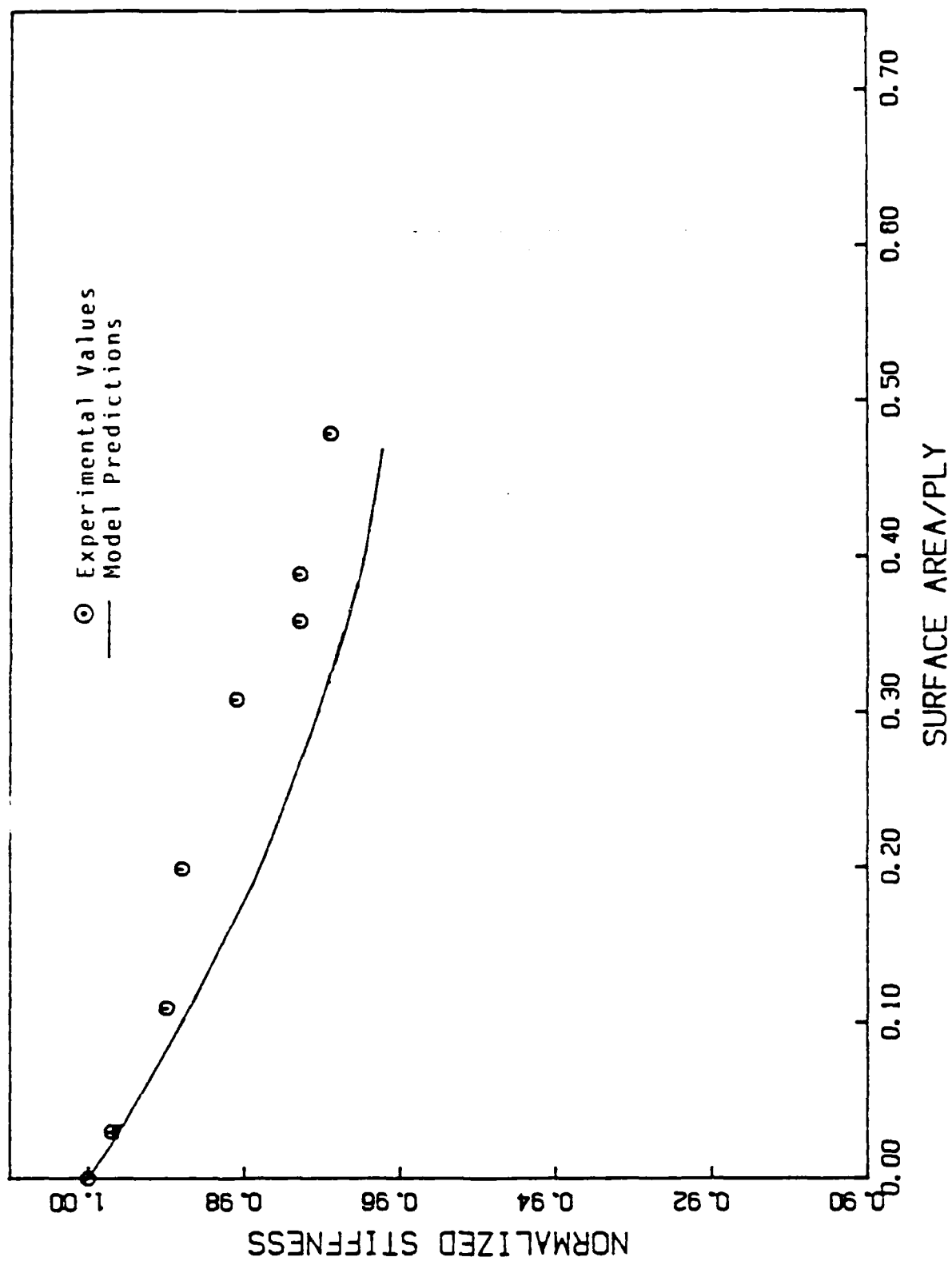
FIG. 13. Model vs. Experiment for $[0,90]_s$ Laminate
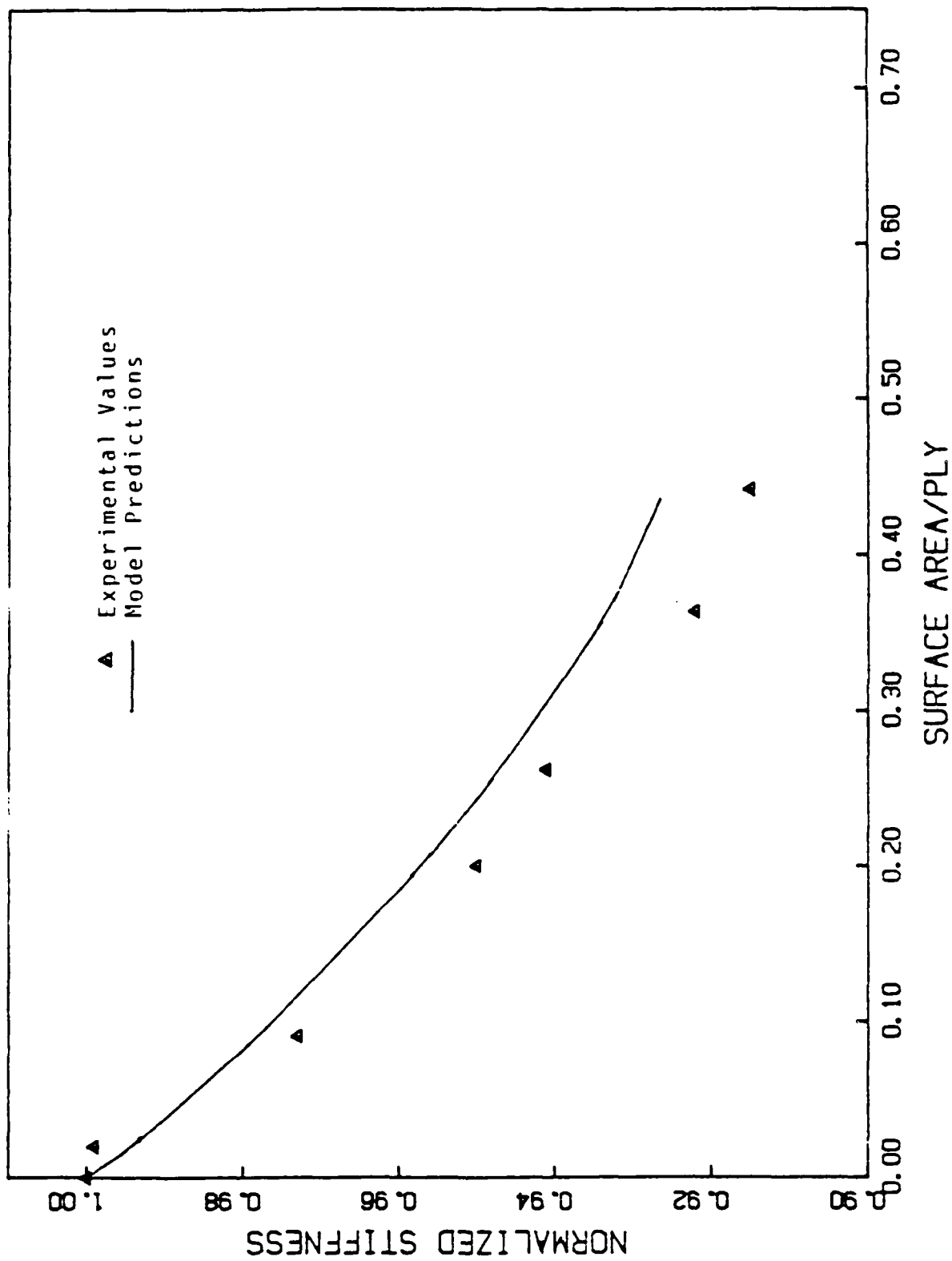
FIG. 14. Model vs. Experiment for $[0, 90_2]_s$ laminate
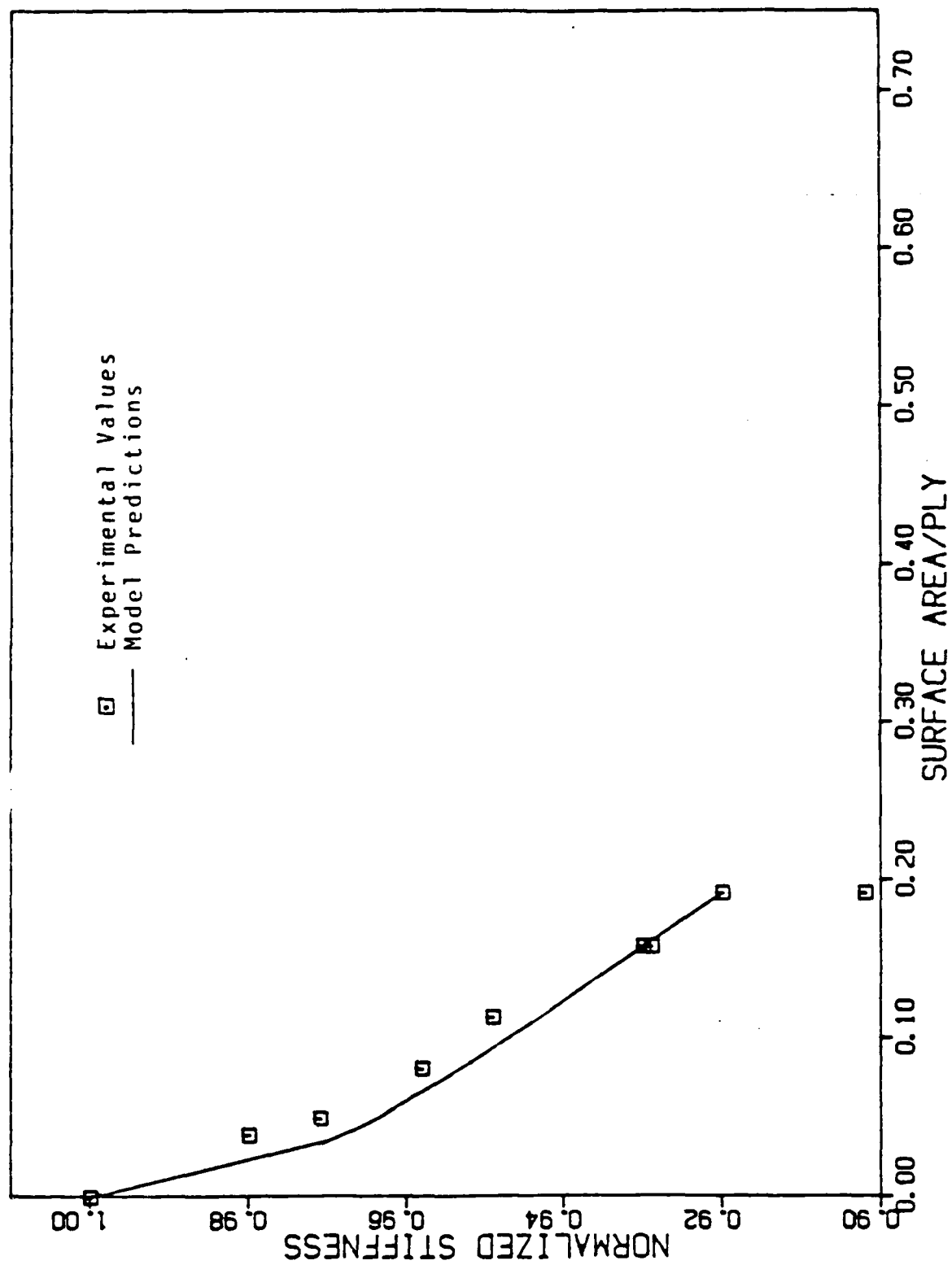
FIG. 15. Model vs. Experiment for $[0,90_3]_s$ Laminate
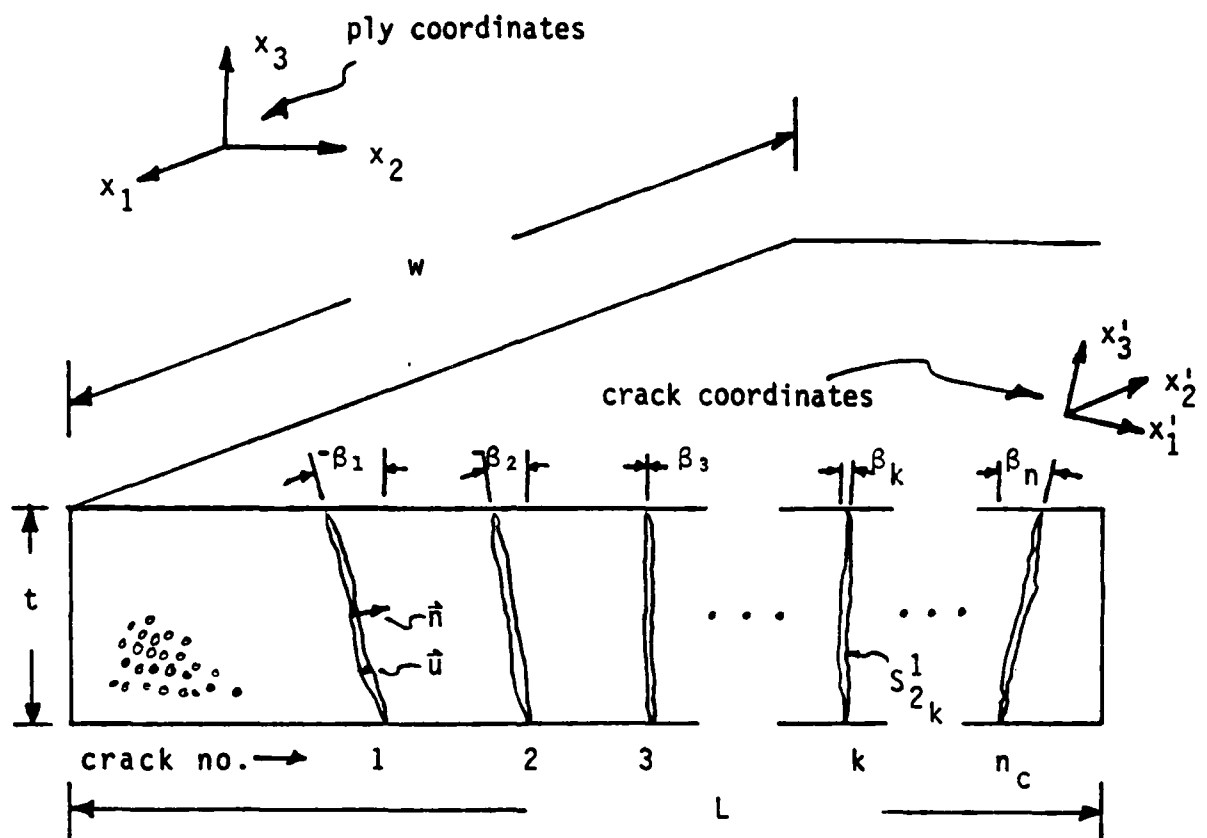
FIG. 16. Description of Curved Crack Geometry in a
Single Crossply

Now, since α_{ij}^1 is a second order tensor,

$$\bar{\alpha}_{ij}^{-1} = \sum_{k=1}^{n_c} a_{ip'}^k \, a_{jq'}^k \, \alpha_{p'q'}^{1k} \tag{24}$$

where $a_{ip'}^k$ are the direction cosines relating the coordinates of the kth crack to the laminate coordinates. Differentiating (24) with respect to the midplane strain components gives

$$\frac{\partial \bar{\alpha}_{ij}^{-1}}{\partial \epsilon_{mn}} = \sum_{k=1}^{n_c} a_{ip'}^k \, \frac{\partial \alpha_{p'q'}^{1k}}{\partial \epsilon_{mn}} \tag{25}$$

Transforming to the coordinates of the crack gives

$$\frac{\partial \bar{\alpha}_{ij}^{-1}}{\partial \epsilon_{mn}} = \sum_{k=1}^{n_c} a_{ip'}^k a_{jq'}^k \, \frac{\partial \alpha_{p'q'}^{1k}}{\partial \epsilon_{r's'}^k} \frac{\partial \epsilon_{r's'}^k}{\partial \epsilon_{mn}}$$

$$= \sum_{k=1}^{n_c} a_{ip'}^k a_{jq'}^k a_{mn'}^k a_{ns'}^k \, \frac{\partial \alpha_{p'q'}^{1k}}{\partial \epsilon_{r's'}} \tag{26}$$

However, since it is assumed that $\partial \alpha_{22}/\partial \epsilon_{22}$ is the only non-zero component, the above reduces to

$$\frac{\partial \bar{\alpha}_{ij}^{-1}}{\partial \alpha_{mn}} = \sum_{k=1}^{n_c} a_{i2'}^k a_{j2'}^k a_{m2'}^k a_{n2'}^k \frac{\partial \alpha_{2'2'}^1}{\partial \epsilon_{2'2'}^1} \tag{27}$$

The above equations may be utilized to obtain the last term in the reduced stiffness equations, where it is assumed that $\partial \alpha_{2'2'}/\partial \epsilon_{2'2'}$ is independent of crack orientation and is obtained from [0,90,0] experimental data [2]:

33

$$S'_{im} = \sum_{k=1}^{n} (\overline{C}_{ij})_k t_k + \sum_{k=1}^{n} \sum_{j=1}^{9} (\overline{T}_{ij})_k (z_k - z_{k-1}) \ (\partial\overline{\alpha}_j / \partial\epsilon_m^o)_k \tag{28}$$

where S'_{im} are the components of the effective laminate stiffness, n is the number of plies, and overbars denote quantities measured in laminate coordinates.

Comparison of the model prediction to experimental results for axial stiffness loss in a $[0,90_2]_s$ laminate is shown in Fig. 17. Although these results are encouraging, the truly exceptional results are shown in Fig. 18. In this figure out-of-plane stiffness predictions are compared to finite element calculations. It was necessary to compare to FEM results for the out-of-plane component because experimental techniques are not yet available for accurately predicting out-of-plane stiffness. The results indicate that the model is erroneous without the curved crack correction, but are quite accurate when the second order tensor transformation is included for the curved cracks. This result supports the use of the second order tensor damage parameter, as opposed to a vectorial representation [11].

2.5. Theoretical Development of Energy Release Rates For Interior Delaminations

A fracture mechanics approach has been used to develop an expression relating the ISV's to the surface area of delaminations. During loadup when the delamination surface area is growing, an energy formulation may be employed to relate the ISV to the strain energy release rate of delaminations. The energy loss in the local volume due to delamination, $(u_L^C)^d$, is related to the strain energy release rate of delaminations, G_d, as follows

$$(u_L^C)^d = \frac{1}{V_L} \int_{S_d} G_d dS \tag{29}$$

where S_d is the surface area of delaminations. Following the constitutive model development, the local energy loss may also be expressed as
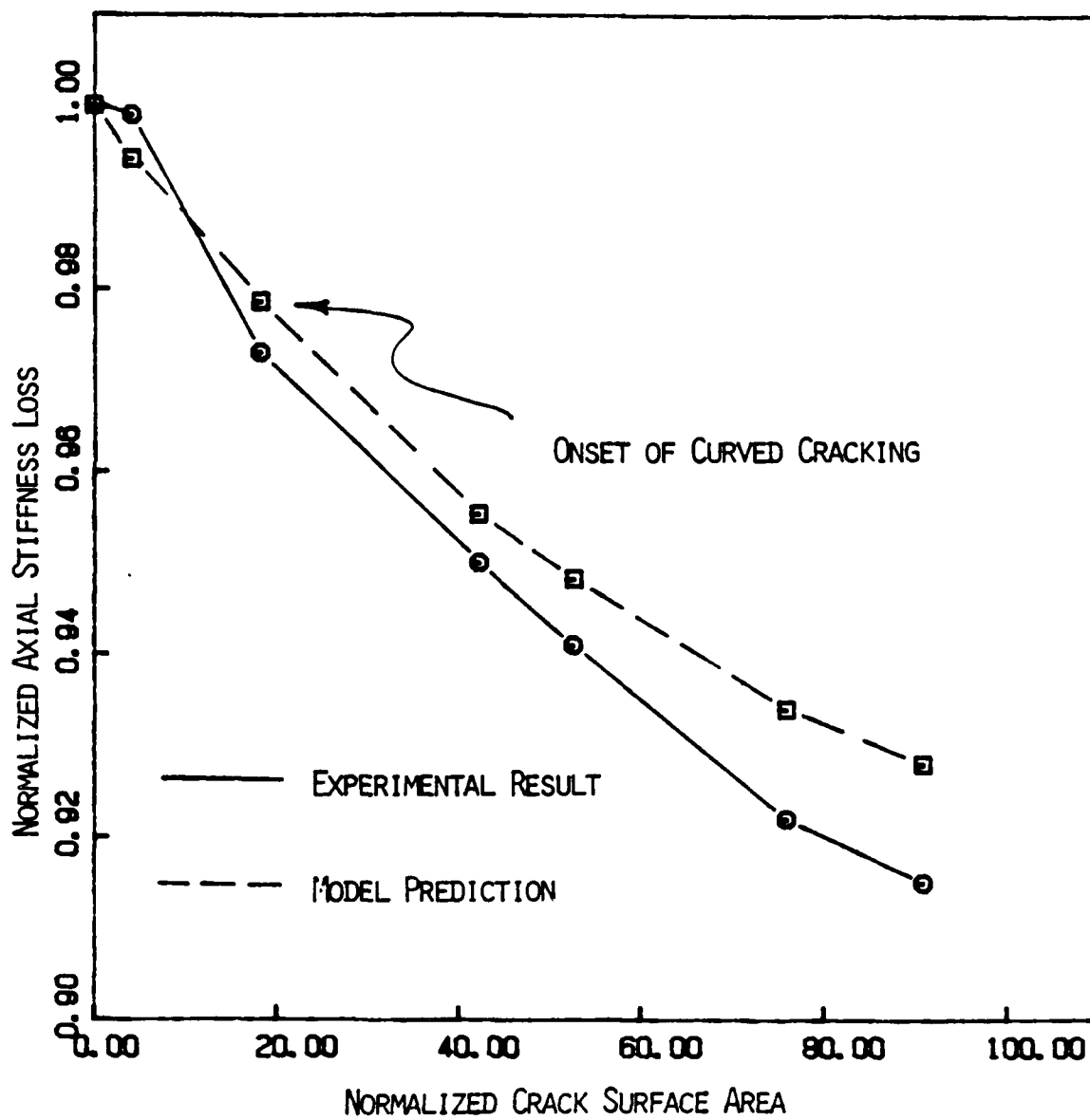
FIG. 17.Model Comparison to Experiment for Axial Stiffness Loss
in a $[0,90_2]_s$ Laminate

35
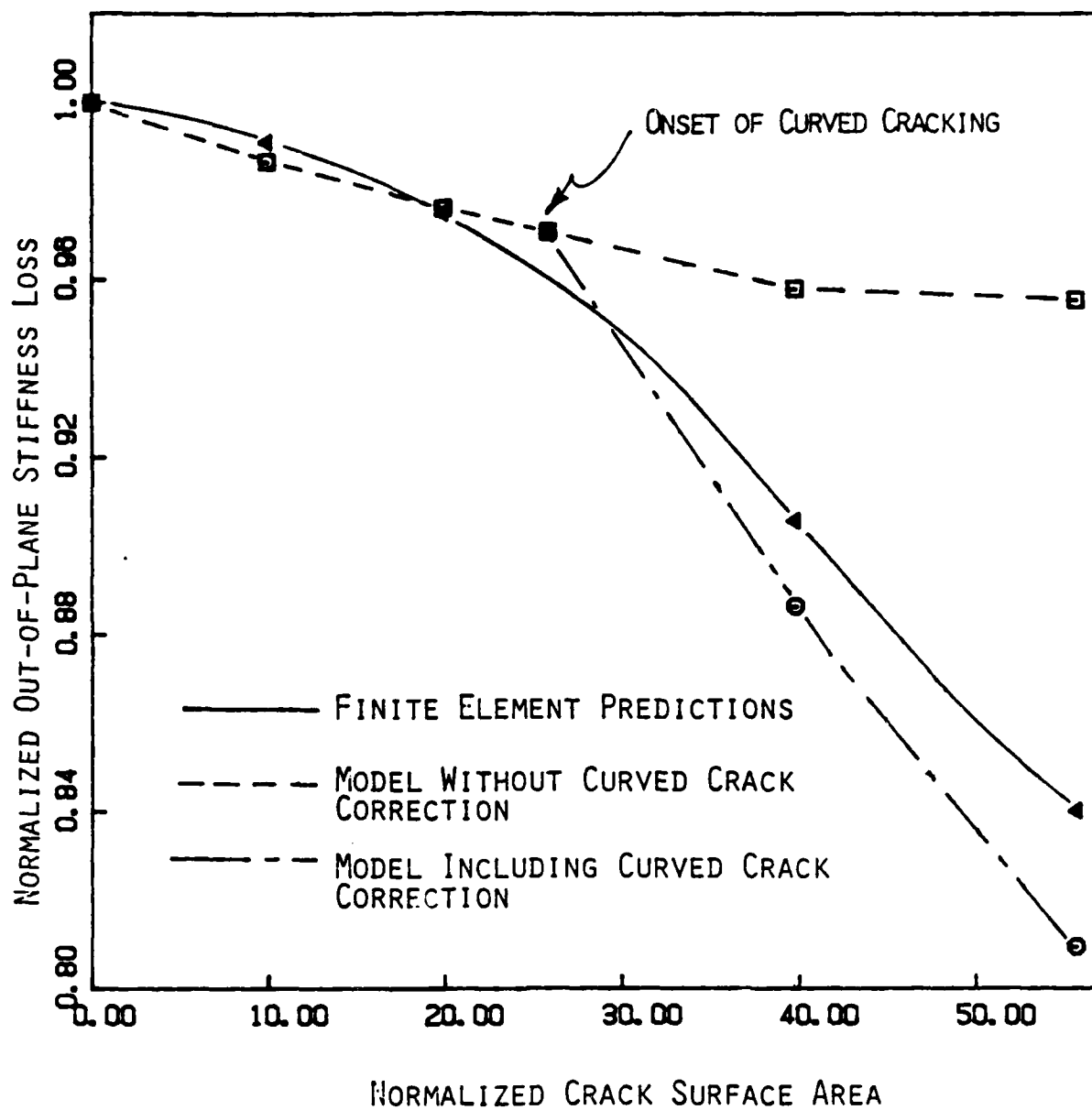
FIG. 18. Model Comparison to Finite Element Results for Out-of-Plane Stiffness Loss in a $[0,90_2]_s$ Laminate

36

$$(u_L^C)^d = I_{ij}^d \varepsilon_{Li} \alpha_j^d \qquad (30)$$

where α_j^d are the ISV's for delamination damage.

For the case of symmetric damage in symmetric laminates, the damage-dependent longitudinal modulus is obtained by differentiating the damage dependent laminate equations with respect to ε_x. Furthermore, considering only one delamination interface location, the longitudinal modulus is given by

$$E_x = E_{xo} - \frac{1}{t} \sum_{k=1}^{n} (Q_{11})_k (z_k - z_{k-1}) \left(\frac{\partial \alpha^M}{\partial \varepsilon_x}\right)_k + \frac{\overline{Q}_1 (z_1 - z_0)}{t} \frac{\partial \alpha_3^D}{\partial \varepsilon_x} \qquad (31)$$

where E_{xo} is the initial undamaged modulus and t is the laminate thickness.

Now considering only a single symmetric delamination site and only that part of the energy associated with crack-opening displacements in the x direction, we may equate (29) and (30) to obtain

$$\alpha_3^D = \frac{1}{V_L \overline{Q}_1 \varepsilon_x} \int_{S_d} G_d dS \qquad (32)$$

where I_{ij}^d has been set equal to $\overline{Q}_1$ for a single delamination site. As a first approximation, the O'Brien [12] strain energy release rate model for free edge delaminations will be assumed to be valid for internal delaminations and is expressed as

$$G_d = \frac{\varepsilon_x^2 t}{2} (E_x - E^*) \qquad (33)$$

where t is the laminate thickness and

$$E^* = \frac{\sum_{i=1}^{m} E_i t_i}{t} \tag{34}$$

where m is the number of sublaminates formed by the delamination and E_i is the longitudinal modulus of each sublaminate. Substituting (33) into (32), and integrating the delamination ISV results in

$$\alpha_3^D = \frac{\varepsilon_x t}{2 V_L \overline{Q}_1} (E_x - E^*) S_d \tag{35}$$

For the single delamination site,

$$V_L = t_1 S \tag{36}$$

where S is the total interface surface area and t_1 is the thickness of the two layers adjacent to the delamination. Substituting equation (36) into (35) results in

$$\alpha_3^D = \frac{1}{2} \varepsilon_x (\frac{t}{t_1}) \frac{(E_x - E^*)}{\overline{Q}_1} (\frac{S_d}{S}) \tag{37}$$

Now differentiating with respect to ε_x, we obtain

$$\frac{\partial \alpha_3^D}{\partial \varepsilon_x} = \frac{1}{2} (\frac{t}{t_1}) (\frac{E_x - E^*}{\overline{Q}_1}) (\frac{S_d}{S}) \tag{38}$$

Therefore, to predict the degraded axial modulus of a laminate we need standard laminate analysis data, the delamination site, and the fraction of the total delaminated area in the local volume. Equation (38) analytically addresses the influence of laminate stacking sequence and delamination site on the degraded modulus and requires only an experimental measurement of the delamination surface area.

38

2.6 Extension of the Model to Account for Delaminations

Research is underway to extend the current model to predict the response of laminates with both matrix cracks and interior delaminations, as shown in Fig. 19. This problem is complicated by two factors. First, because these two damage mechanisms are oriented differently, they require two separate tensor-valued damage parameters. Furthermore, the mechanics of these two damage modes are substantially different. The matrix cracks may be assumed to be statistically homogeneous over each ply in a small local volume element. Therefore, classical local volume averaging may be used to obtain this damage parameter. On the other hand, delaminations are not statistically homogeneous in the z coordinate direction. This requires that a modification be made to statistical averaging techniques. Although statistical homogeneity is assumed in the x and y coordinate directions, a kinematic constraint similar to the Kirchhoff-Love hypothesis is employed in the z direction. The resulting damage parameter is a weighted measure of damage, with cracks farther away from the neutral surface causing a greater effect on material properties.

The ply level stress-strain relations are given by

$$\sigma_{ij} = C_{ijk\ell}(\epsilon_{k\ell} - \alpha_{k\ell}^M) \tag{39}$$

In order to account for interply delamination the following kinematic assumption is made (See Fig. 20.):

$$u(x,y,z) = u^0(x,y) - z[\beta^0 + H(z-z_k)\beta_k^D] + H(z-z_k)u_k^D \tag{40}$$

and

$$w(x,y,z) = w^0(x,y) - H(z-z_k)w_k^D \tag{41}$$

where u is the in-plane displacement and w is the out-of-plane displacement. Furthermore, β represents rotations of the midplane. The quantities with superscripts o are midsurface values, and quantities with superscripts D are caused by interlaminar cracking.

39
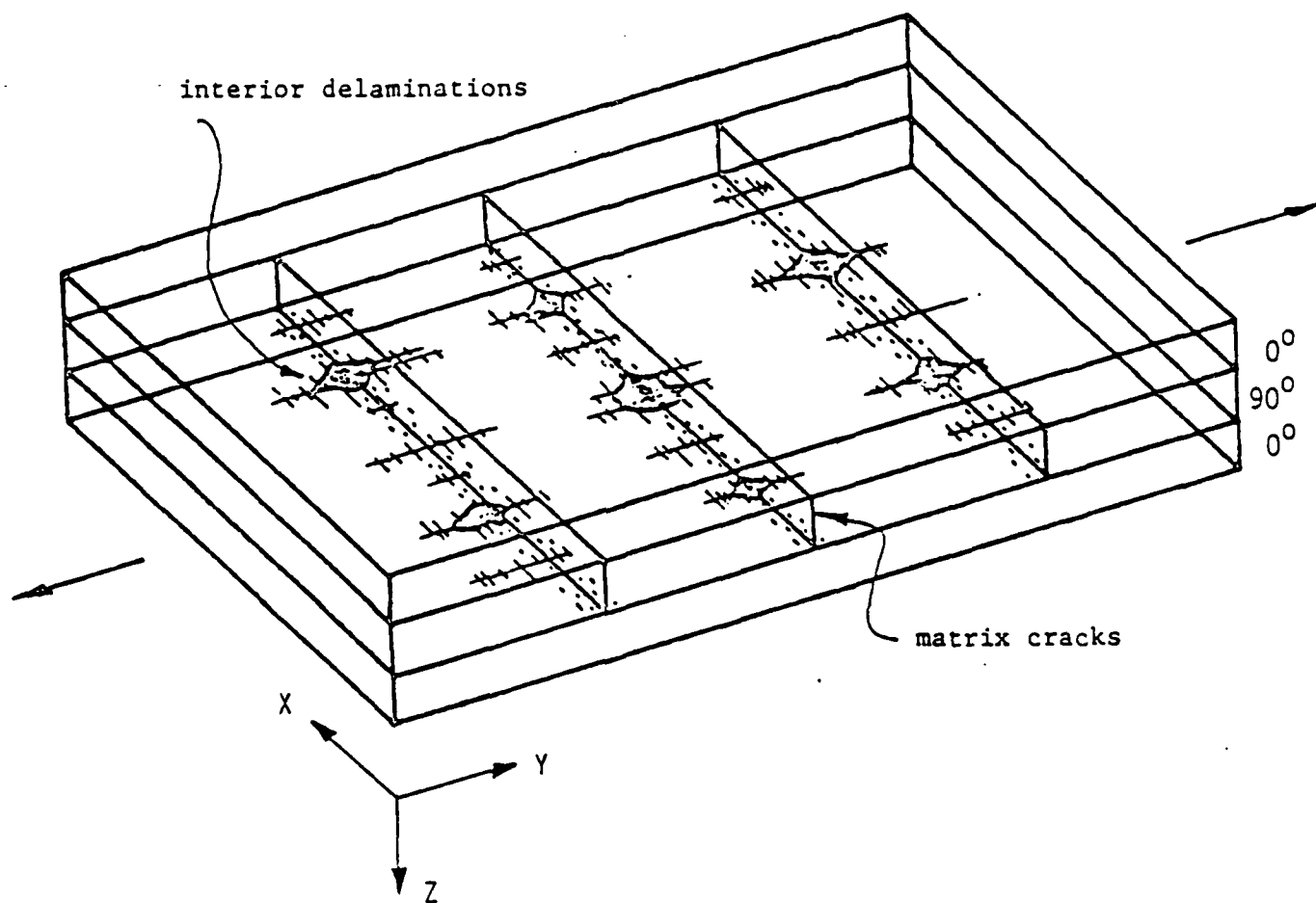
FIG. 19. Crossply Laminate Showing Combined Matrix
Cracking and Interior Delaminations
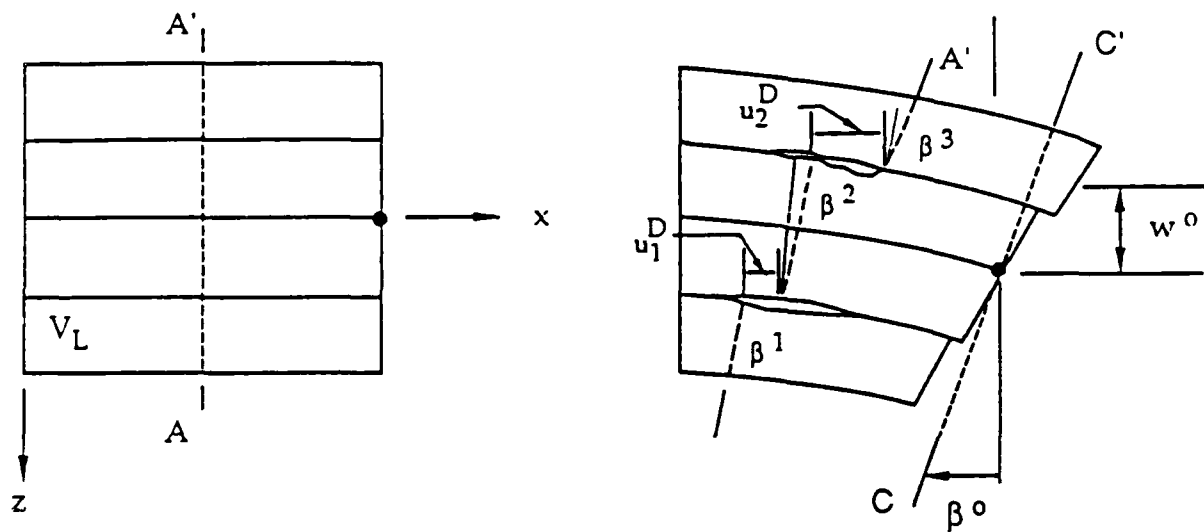
FIG. 20. KINEMATICS OF INTERIOR DELAMINATIONS

Employing standard laminate averaging techniques will result in the following laminate equations

$$\{N\} = \sum_{k=1}^{n} [Q]_k (z_k - z_{k-1}) \{\epsilon_L^0\} - \frac{1}{2} \sum_{k=1}^{n} [Q]_k (z_k^2 - z_{k-1}^2) \{\kappa_L\}$$

$$+ \sum_{i=1}^{d} [\bar{Q}]_i (z_i - z_{i-1}) \{\alpha_L^D\}_i - \sum_{k=1}^{n} [Q]_k (z_k - z_{k-1}) \{\alpha^M\}_k \qquad (42)$$

$$\{M\} = \frac{1}{2} \sum_{k=1}^{n} [Q]_k (z_k^2 - z_{k-1}^2) \{\epsilon_L^0\} - \frac{1}{3} \sum_{k=1}^{n} [Q]_k (z_k^3 - z_{k-1}^3) \{\kappa_L\}$$

$$+ \frac{1}{2} \sum_{i=1}^{d} [\bar{Q}]_i (z_i^2 - z_{i-1}^2) \{\alpha_L^D\}$$

$$- \frac{1}{2} \sum_{k=1}^{n} [Q]_k (z_k^2 - z_{k-1}^2) \{\alpha^M\}_k \qquad (43)$$

where $\{N\}$ and $\{M\}$ are the resultant forces and moments per unit length, respectively, and $\{\alpha^M\}_k$ and $\{\alpha_L^D\}_i$ represent the damage due to matrix cracking and interply delamination, respectively. Details of this development are given in Appendix 7.3.

Utilizing the procedure outlined in Section 2.5, the model has been compared to experimental results for both cross-ply and quasi-isotropic laminates with both matrix cracks and delaminations.

While the damage-dependent laminate analysis model may be used to predict any of the effective engineering moduli of a laminate, experimental results are only available for the axial modulus and Poisson's ratio. Therefore, the general utility of the model will be demonstrated by comparing model

42

predictions to experimental results for E_x and ν_{xy} for only the fully developed damage states. A typical x-ray radiograph is shown in Fig. 21. The delamination interface location was determined experimentally and the delamination area was estimated from the x-ray radiographs using an optical planimeter procedure. In both the model analysis and data reduction, it was assumed that the delamination sites were symmetrically located about the laminate midplane and contained the same delamination surface area.

The bar chart in Fig. 22 compares the model predictions to the experimental values of the engineering modulus, E_x, for combined matrix cracking and delamination. The delamination interface location and percent of delamination area are listed in the figure underneath the laminate stacking sequence. As can be seen, the comparison between model results and the experimental results is quite good. Some limited results for Poisson's ratio are given in Fig. 23 using the same bar chart format. With the exception of the $[0/90_2]_s$ laminate, these results are also quite good. The experimental value for the $[0/90_2]_s$ laminate is quite suspicious since this laminate exhibits a much larger change in Poisson's ratio than the other laminates without a corresponding difference in the delamination surface area. It should be noted that values of Poisson's ratio for the quasi-isotropic laminates are not available.

2.7 Micromechanics Model Verification

Because the ISV definition given by equation (16) is locally averaged, it represents a quantity which is not exact under certain circumstances. Furthermore, since the geometry of many cracked laminates is so complex as to preclude an exact micromechanics analysis, the author has utilized the phenomenological approach for measuring the damage state described in Section 2.5. Finally, the model has previously been compared only to experimental results. For these reasons it was felt that some research was warranted to place the ISV formulation on a stronger theoretical footing. This was accomplished by formulating a micromechanics solution for a single ply with matrix cracks and incorporating this into a laminate analysis scheme. This research is summarized in this section, and a detailed discussion is contained in Appendix 7.10.

43
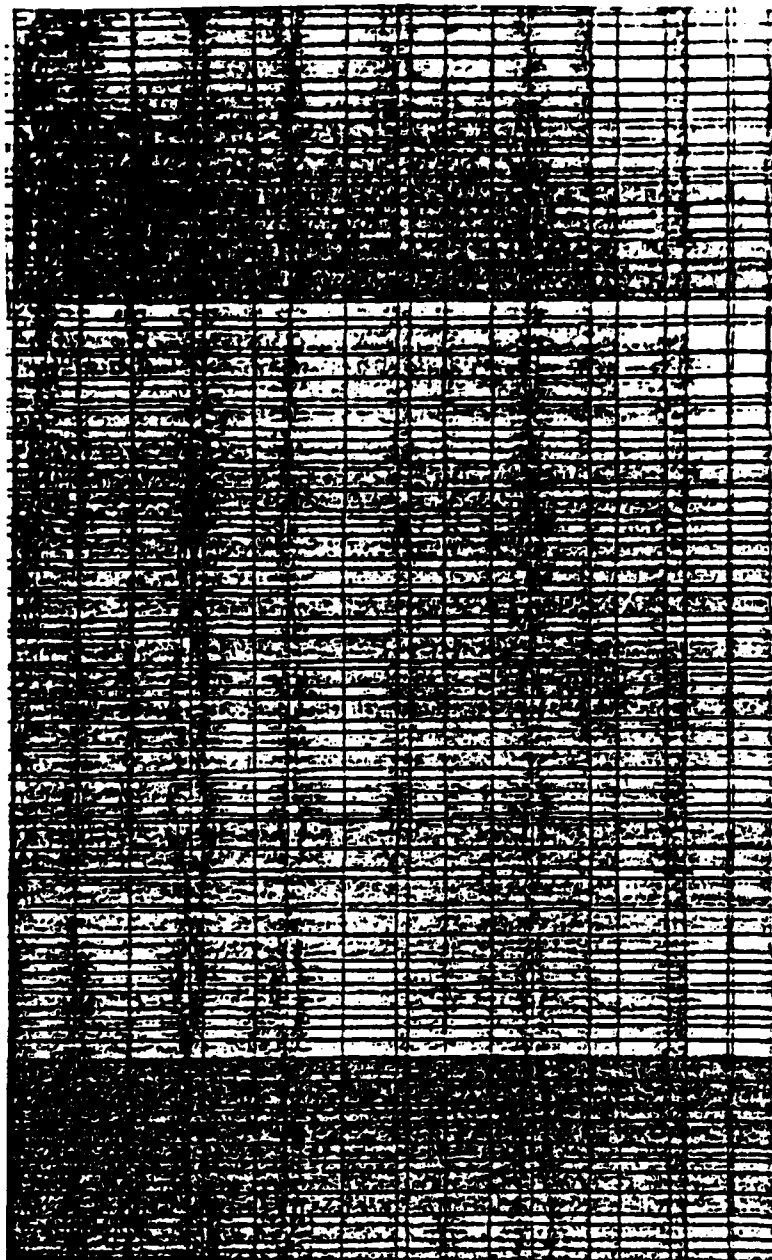
Fig. 21. Enlarged X-ray Radiograph of Damage in a $[0_2/90_2]_s$ Laminate at 400,000 Cycles with S_{max} = 75% of S_{ULT}

44

Fig. 22. Comparison of Experimental Results and Model Predictions of the Laminate Engineering Modulus, E_x Degraded by Both Matrix Cracking and Delamination Damage.

Damage-Dependent Laminate υ_{xy}
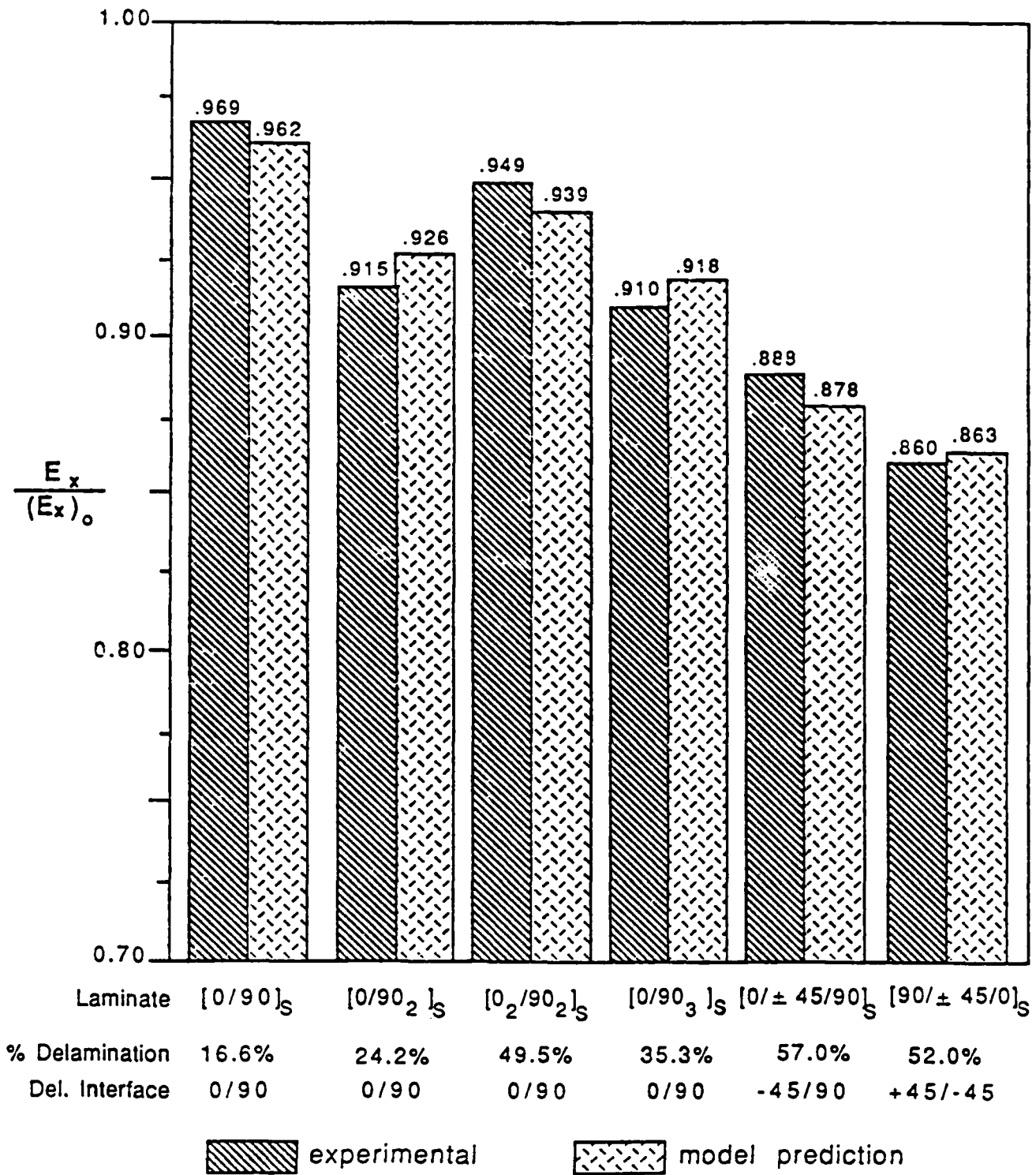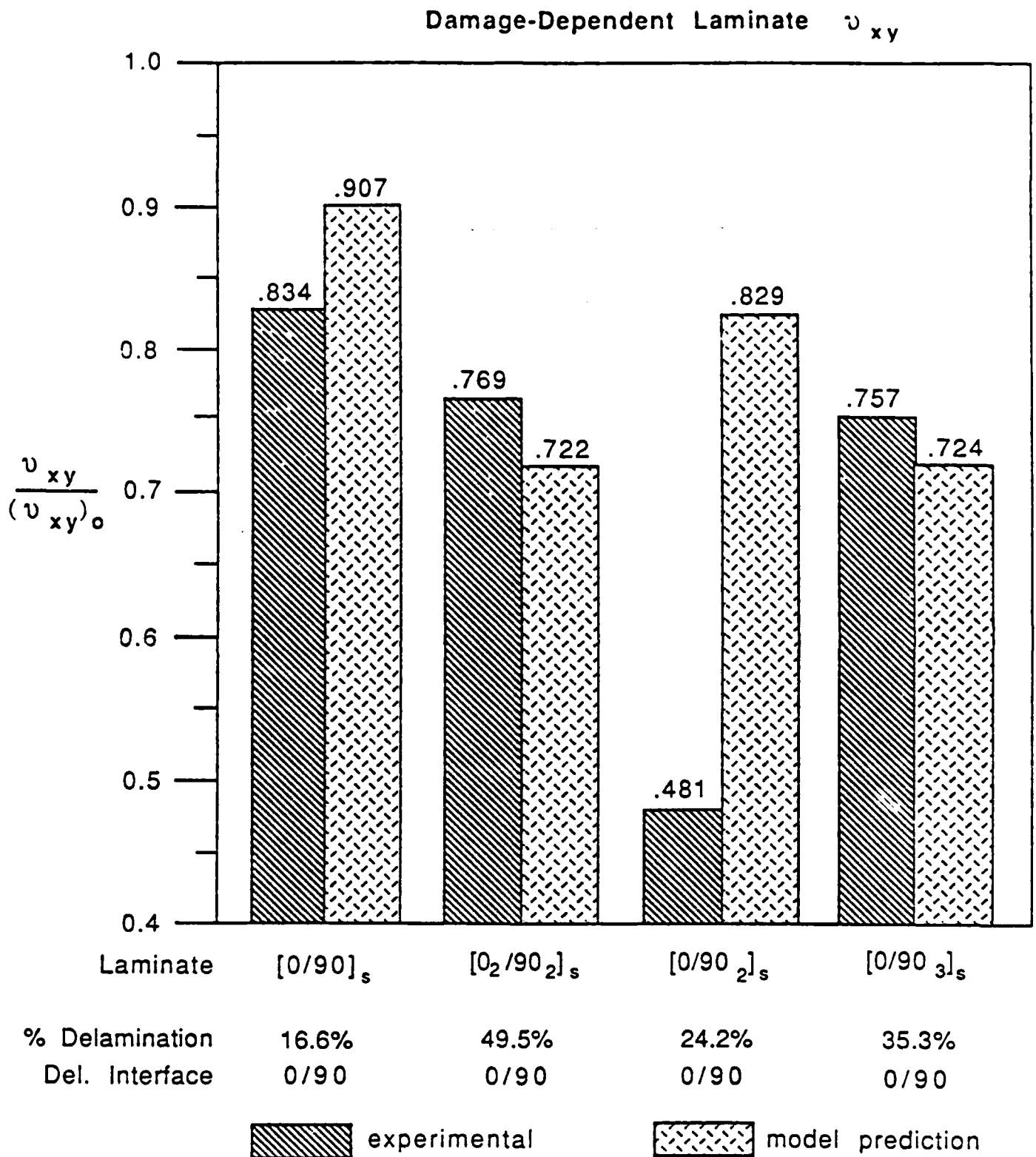
Fig. 23. Comparison of Experimental Results and Model Predictions of the Laminate Engineering Poisson's Ratio, υ_{xy}, Degraded by Both Matrix Cracking and Delamination Damage.

Consider a laminated composite material with an infinite number of 0 and 90 degree layers as illustrated in Fig. 24a. Since the crack patterns in 90 degree layers may be random, displacement fields in each crack element surrounded by two adjacent crack surfaces and two material interfaces are different. It is apparent from Fig. 24a that a solution to the boundary value problem for all possible displacement boundary conditions is impractical, or at least very cumbersome to obtain. A relatively simple solution may be obtained by postulating a fictitious boundary value problem which represents a statistically arranged volume element shown in Fig. 24b. The mutual influence between cracks in different 90 degree layers may be implicitly taken into account by assuming the y and z plane to remain plane throughout deformation under the axial tensile loading, P, at far-field. The displacement fields may then be assumed as

$$u = (u_0/a)x + \sum_m \sum_n a_{mn} \sin\alpha x \cos\beta y$$

$$v = -(v_0/t)y$$

$$w = -(w_0/b)z$$

(44)

where m, n = 1, 2, 3, ..., k

$$\alpha = (2m-1)\pi/2a$$
$$\beta = (2n-1)\pi/2t$$

(45)

Using the minimum potential energy theorem, it can be determined that

$$w_0/a = (p/2t) \left[\frac{C_{yy}C_{zz} - C_{yz}^2}{\det[C_{ij}]} + \frac{1}{\frac{\pi^4}{64\xi} - C_{xx}} \right]$$

(46)

and the axial component of the damage tensor is

$$\alpha_{xx} = \frac{(-1)p/2t}{\frac{\pi^4}{64\xi} - C_{xx}}$$

(47)

47

(a)

0 degree layer

90 degree layer

matrix crack

(b)

P

P

y   material
interface

t

-a

0

x

a

-t

undeformed
crack surface

width = 2b
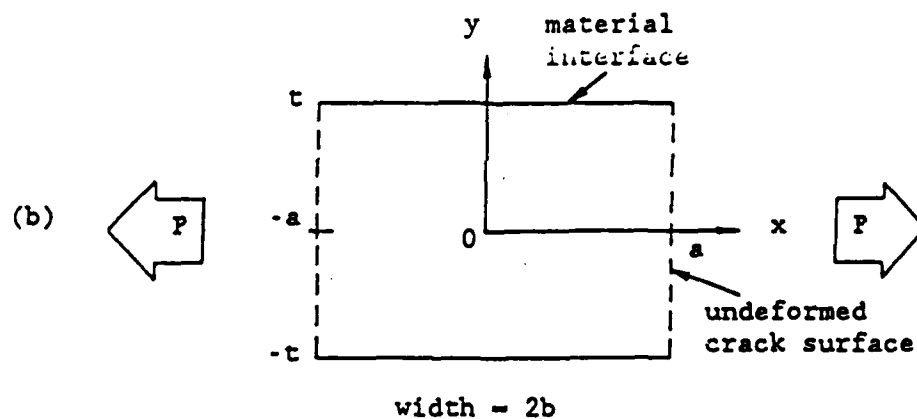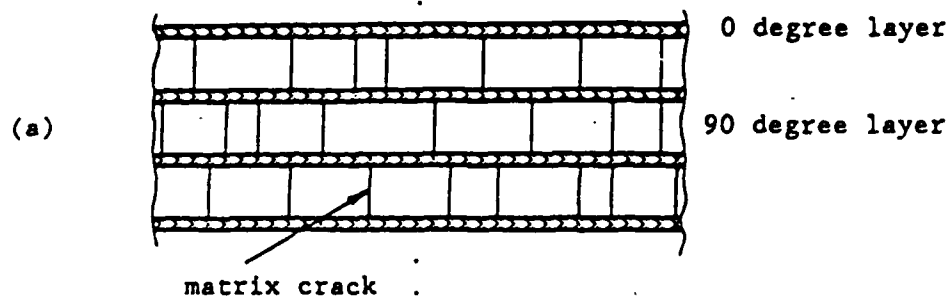
Fig. 24. $[0_q/90_r]_{n,s}$ Type Laminate with Matrix Cracks

(a) Overall Configuration

(b) One Representing 90 Degree Layer Element

48

where

$$\xi - \sum_m \sum_n \frac{1}{C_{xx}(2m-1)^2(2n-1)^2 + G_{xy}(a/t)^2(2n-1)^4} \qquad (48)$$

All other components of α_{ij} are zero.

The effective stiffness matrix for a $[0_q/90_r]_s$ laminate under in-plane biaxial tensile loading becomes

$$[\overline{C}_{ij}] = \begin{matrix} qC_{LL} + r(1-\zeta_2)C_{TT} & [q(1-\zeta_1) + r]C_{LT} \\ [q+r(1-\zeta_2)]C_{LT} & q(1-\zeta_1)C_{TT} + r\,C_{LL} \end{matrix} \qquad (49)$$

where

$$\zeta = \frac{1}{\dfrac{C_{yy}C_{zz} - C_{yz}^2}{\det[C_{ij}]}\,\dfrac{\pi^4}{64\xi} - C_{xx}} \qquad (50)$$

The comparisons illustrated in Fig. 25 and Fig. 26 verify that the present model gives a fairly accurate prediction of the degraded axial stiffness as a function of the crack density for two commonly used material systems. Furthermore, it should be noticed that the crack density (number of cracks per unit length) is not appropriate for representing the matrix crack characteristics. As an example, consider $[0_n/90_n]_s$ specimens. If the crack density is utilized as an independent parameter, the normalized stiffnesses of $[0/90]_s$ and $[0_2/90_2]_s$ will be different at the same crack density as shown in Figs. 7-a and 7-b. This violates the most important assumption in continuum mechanics, i.e., observable state variable are independent of the size of the domain of interest. On the contrary, the ratio of the crack length to the distance between two adjacent cracks, t/a, eliminates this inconsistency as illustrated in the same figures.

The analytical solution to the crack parameter, ζ_2, includes the crack interaction in an explicit form. Furthermore, the internal state variable, α_{xx}, results directly from the strain energy loss due to matrix cracks [8]. By combining the present problem solving technique with the study of Allen, et al. [8], the strain energy release rate at a given matrix crack damage state can be predicted analytically. However, the internal state variable presented

49

(a)

(b)
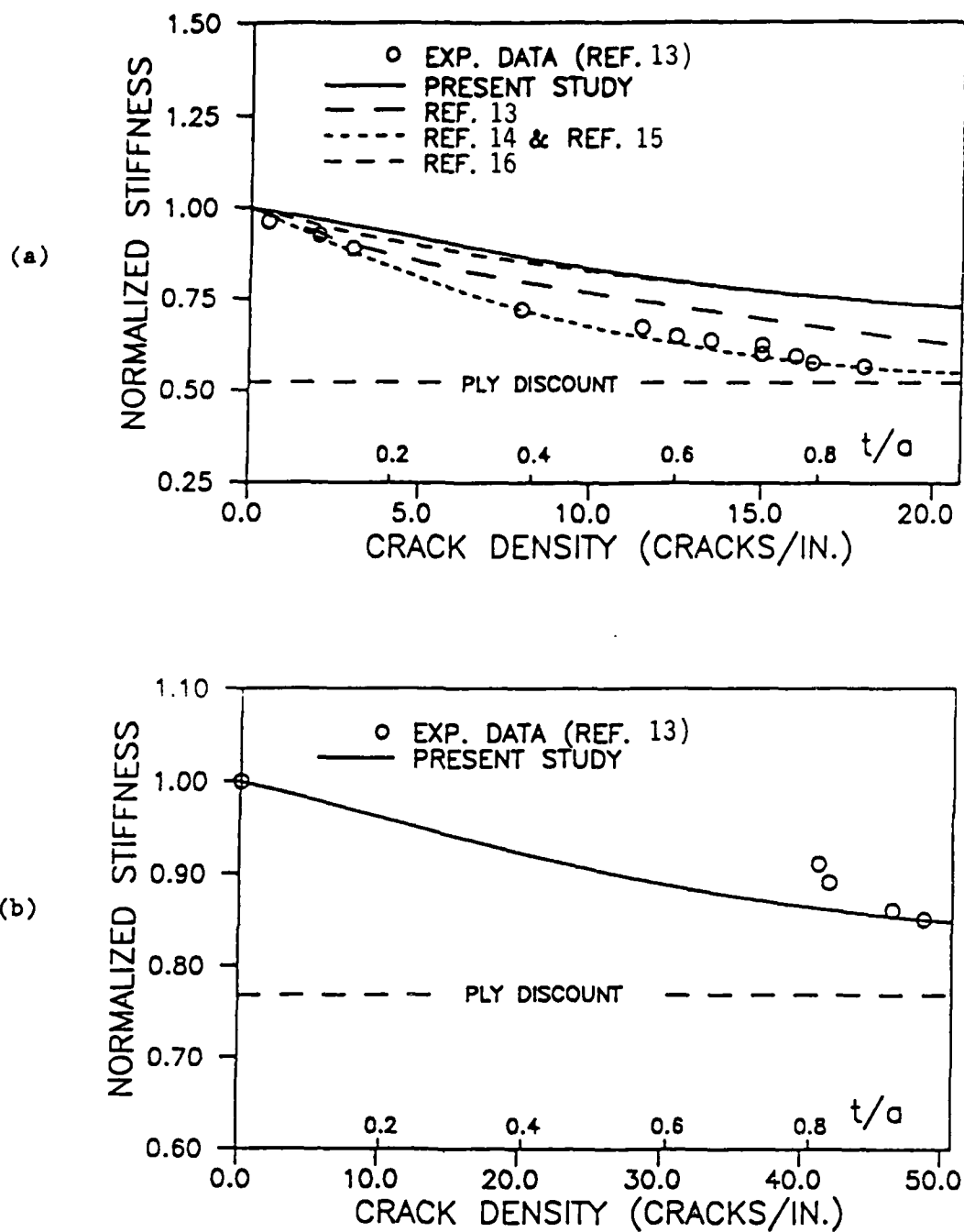
Fig. 25. Stiffness Reduction in Glass/Epoxy Specimens

(a) $[0/90_3]_s$ laminate
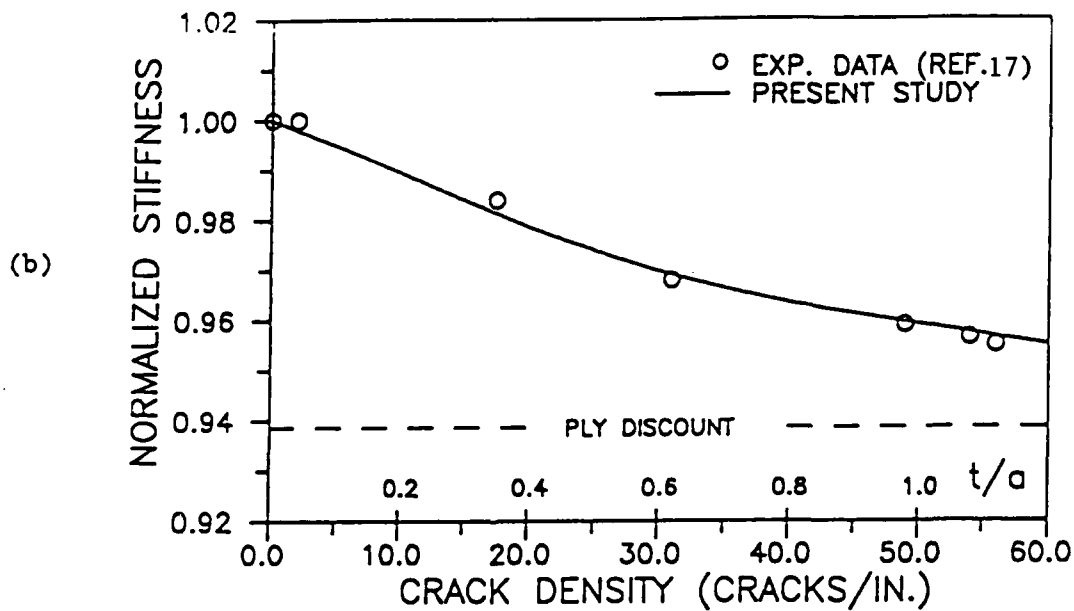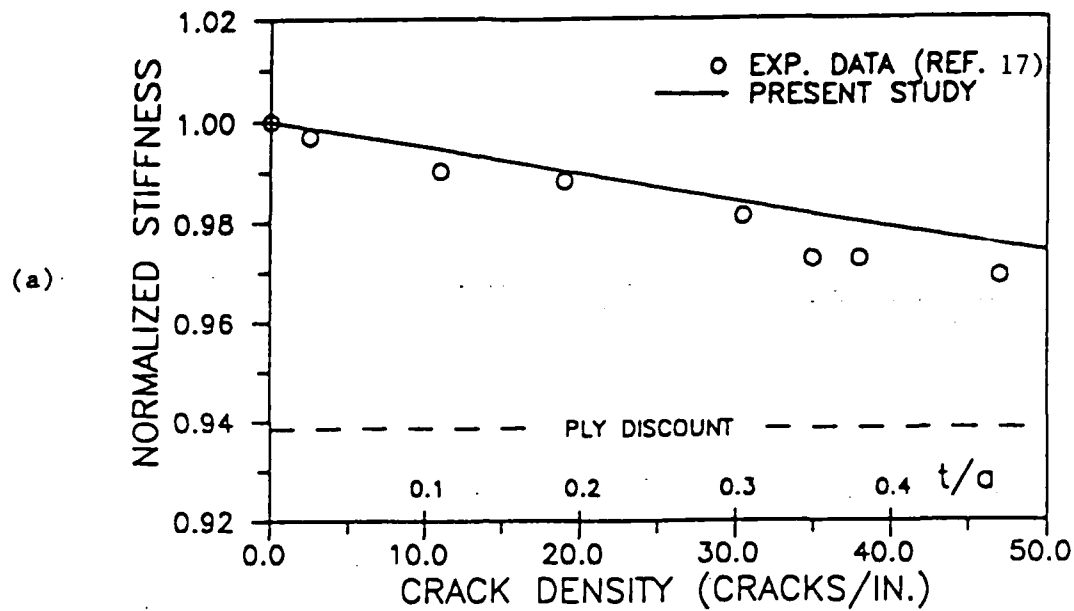
(b) $[0/90]_s$ laminate

Fig. 26. Stiffness Reduction in Graphite/Epoxy Specimens

(a) $[0/90]_s$ laminate

(b) $[0_2/90_2]_s$ laminate

(c) $[0/90_2]_s$ laminate

(d) $[0/90_3]_s$ laminate   (continued to next page)

51

herein may not be exact under the following conditions.

(1) When the matrix crack size and spacing cannot be assumed to be homogeneous.

(2) When the matrix material is viscoelastic.

(3) When the matrix cracks are dominated by microcracks rather than by those that cross the entire specimen width.

2.8 Determination of Ply Level Stresses

It is gen_.ally hypothesized that the growth of damage is driven by local stresses, which are in turn affected by the damage process. Therefore, although damage may not profoundly affect stiffness, it cannot be ignored in the prediction of failure.

In this section, the model is used to predict the effects of both matrix cracks and delaminations on ply level stresses. It is shown that the stress distribution is substantially altered by the damage state. Furthermore, the predicted stresses are significantly affected by stacking sequence. The outcome of the research is to show how the development of damage causes stress redistribution which drives the development of new damage modes.

It is assumed that the effects of matrix cracking are reflected in the ply level stress-strain relations [9]:

$$
\left\{
\begin{array}{c}
\sigma_{L_x} \\
\sigma_{L_y} \\
\sigma_{L_z} \\
\sigma_{L_{yz}} \\
\sigma_{L_{xz}} \\
\sigma_{L_{xy}}
\end{array}
\right\}
=
\begin{bmatrix}
Q_{11} & Q_{12} & Q_{13} & Q_{14} & Q_{15} & Q_{16} \\
Q_{12} & Q_{22} & Q_{23} & Q_{24} & Q_{25} & Q_{26} \\
Q_{13} & Q_{23} & Q_{33} & Q_{34} & Q_{35} & Q_{36} \\
Q_{14} & Q_{24} & Q_{34} & Q_{44} & Q_{45} & Q_{46} \\
Q_{15} & Q_{25} & Q_{35} & Q_{45} & Q_{55} & Q_{56} \\
Q_{16} & Q_{26} & Q_{36} & Q_{46} & Q_{56} & Q_{66}
\end{bmatrix}
\left\{
\begin{array}{c}
\varepsilon_{L_x} - \alpha^{M}_{xx} \\
\varepsilon_{L_y} - \alpha^{M}_{yy} \\
\varepsilon_{L_z} - \alpha^{M}_{zz} \\
\gamma_{L_{yz}} - 0 \\
\gamma_{L_{xz}} - 0 \\
\gamma_{L_{xy}} - \alpha^{M}_{xy}
\end{array}
\right\}
\tag{51}
$$

where the locally averaged strains are given by

$$\epsilon_{L_x} = \epsilon_{L_x}^0 - z \, [\kappa_{L_x} + H(z-z_i) \, \alpha_{5i}^D] + H(z-z_i) \, \alpha_{3i}^D$$

$$\epsilon_{L_y} = \epsilon_{L_y}^0 - z \, [\kappa_{L_y} + H(z-z_i) \, \alpha_{4i}^D] + H \, (z-z_i) \, \alpha_{2i}^D$$

$$\epsilon_{L_z} = \epsilon_{L_z}^0 + H(z-z_i) \, \alpha_{1i}^D$$

$$\epsilon_{L_{yz}} = \epsilon_{L_{yz}}^0 - z \, [\kappa_{L_{yz}} + H(z-z_i) \, \alpha_{4i}^D]$$

$$\epsilon_{L_{xz}} = \epsilon_{L_{xz}}^0 - z \, [\kappa_{L_{xz}} + H(z-z_i) \, \alpha_{5i}^D]$$

$$\epsilon_{L_{xy}} = \epsilon_{L_{xy}}^0 - z \, \kappa_{L_{xy}} \tag{52}$$

The observable quantities on the right hand side of the above equations are the midsurface strains, ϵ_{Lj}^0, and rotations, κ_{Lj}. These quantities normally come from the solution of the associated boundary value problem, as described in Section 2.10. The internal state variables are obtained from evolution laws of the general form

$$\dot{\alpha}_{ij}^M = \dot{\alpha}_{ij}^M(\epsilon_{k\ell}, T, \, \alpha_{k\ell}^M \, \alpha_{k\ell}^D) \tag{53}$$

and

$$\dot{\alpha}_{ij}^D = \dot{\alpha}_{ij}^D(\epsilon_{k\ell}, \, T, \, \alpha_{k\ell}^M, \, \alpha_{k\ell}^D) \tag{54}$$

Thus, equations (51) may be utilized to evaluate the "far-field" damage dependent stresses in each ply.

A computer code has been constructed to determine the effect of damage on the "far field" ply stresses in composite laminates. Results presented are for a given laminate strain $\epsilon_{xo} = .01$ (all other strains assumed to be zero). Damage variables have been calculated for matrix cracks in a saturated damage state assuming $u_0^M = .0001"$. The off-axis and 90° plies use the matrix crack damage terms of α_8^M and α_2^M, respectively. No damage is assumed in the 0° plies. Since the laminate is subjected only to ϵ_{xo}, α_3^D is assumed to be the only delamination damage component. This term is calculated for an equivalent delamination area with $u_0^D = .00001"$.

The results obtained from the model are shown in Table 1 and Figs. 27 and 28. As evidenced from the result, the damage significantly affects the far-field ply stresses. Matrix cracks have a significant effect on ply stresses in the 90° plies in cross-ply laminates. The largest number of matrix cracks is evident in the 90° plies of the $[0_2/90_2]_s$ laminate resulting in a thirty-four percent far-field ply stress reduction. The two quasi-isotropic laminates develop different damage resulting in dissimilar far-field ply stresses. The $[90/\pm45/0]_s$ laminate exhibit little matrix cracking and corresponding reduction of ply stress in both 90° and ±45 plies. The $[0/\pm45/90]$ laminate exhibit a similar stress reduction in the ±45° plies, but shows a substantial stress reduction (fifteen percent verses one percent) in the 90° plies when compared to the $[90/\pm45/0]_s$ laminate. It should be noticed that only the stresses in plies between delaminations are affected by the delamination. This is a result of symmetric delamination damage about the midplane of the laminate. For this damage state, the resulting α_3^D terms are equal in magnitude, yet opposite in sign. It is apparent that for fixed strain and a symmetric damage state, the laminate strains are affected only in the region between the delaminations. The matrix cracks are shown to alter the constitutive nature of the plies, and delamination effects are incorporated into the laminate through the laminate equations. This alteration in ply stresses will significantly affect the growth of new damage in the composite.

Results of this work illustrate that the stress state in the laminate is substantially influenced by damage. In the $[0_2/90_2]_s$ laminate, matrix cracks and delaminations reduce the stress in the 90° plies by almost sixty percent. For cross-ply laminates, the damage induced ply stress reduction varies from about forty to sixty percent of undamaged stress in the 90° plies. Stress reduction in angle-ply laminates is less dramatic (depending on location and size of the delamination). This alteration in stress state is critical in determining both the magnitude and location of damage development.

2.9 Development of Damage Evolution Laws

The prediction of damage evolution can be likened to the development of equations predicting S-N curves in metals (such as Miner's rule [18]). However, in the case of laminated composites, this phenomenological approach

Table 1. PLY STRESSES RESULTING FROM MATRIX CRACKING AND DELAMINATION

LAMINATE	PLY	INITIAL PLY STRESS σ (ksi)	STRESS W/MATRIX CRACKS σ (ksi)	STRESS W/MATRIX CRACKS & DELAM. σ (ksi)	DELAMINATION LOCATION AND MAGNITUDE α_3^D	MATRIX DAMAGE VARIABLES α_2^M	α_8^M
$[0/90]_s$	0	211.4	211.4	211.4	0/90	0	0
	90	14.0	9.6	8.5	16.6%	.00318	0
					.00076		
$[0/90_2]_s$	0	211.4	211.4	211.4	0/90	0	0
	90	14.0	9.5	7.9	24.2%	.00326	0
	90	14.0	9.5	7.9	.001109	.00326	0
$[0_2/90_2]_s$	0	211.4	211.4	211.4		0	0
	0	211.4	211.4	211.4	0/90	0	0
	90	14.0	9.2	6.0	49.5%	.00344	0
	90	14.0	9.2	6.0	.002267	.00344	0
$[0/90_3]_s$	0	211.4	211.4	211.4		0	0
	90	14.0	10.6	8.3	0/90	.00247	0
	90	14.0	10.6	8.3	35.3%	.00247	0
	90	14.0	10.6	8.3	.001617	.00247	0
$[0/\pm45/90]_s$	0	211.4	211.4	211.4		0	0
	45	64.4	64.0	64.0	-45/90	0	.00067
	-45	64.4	64.0	64.0	57%	0	-.00067
	90	14.0	11.8	8.2	.002611	.00157	0
$[90/\pm45/0]_s$	90	14.0	13.9	13.9	.00060	.00060	0
	+45	64.4	64.0	64.0	+45/-45	0	.00067
	-45	64.4	64.0	48.7	52%	0	-.00067
	0	211.4	211.4	161.0	.002382	0	0

$\varepsilon = 0.01$

▦ initial ply stress
☐ ply stress with matrix cracks
▨ ply stress with matrix cracks and delamination

Fig. 27.   Far Field Stresses in a $[0_2/90_2]s$ Laminate

Fig. 28. Far Field Ply Stresses in a [90/±45/0]s Laminate

possesses the distinct disadvantage that a new evolution law must be hypothesized for each stacking sequence because there is no underlying physical interpretation of the mechanics in the problem. The current model is independent of stacking sequence because it utilizes the damage parameters in each ply to determine the far-field ply stresses in each ply, so that damage evolution in each ply depends directly only on the state within that ply. Thus, the effects of adjacent plies are accounted for via the dependence of the ply stresses on stacking sequence as reflected in the laminate equations.

Since the ply stresses determined by this procedure represent locally averaged values, they must be considered to be far-field stresses, so that equations (53) and (54) may more properly be written:

$$\dot{\alpha}_{ij}^{M} = \dot{\alpha}_{ij}^{M} \left(\epsilon_{k\ell}, \ T, \ \alpha_{k\ell}^{M}, \ \alpha_{k\ell}^{D}, \ K_{I}, \ K_{II}, \ K_{III} \right) \tag{55}$$

and

$$\dot{\alpha}_{ij}^{D} = \dot{\alpha}_{ij}^{D} \left(\epsilon_{k\ell}, \ T, \ \alpha_{k\ell}^{M}, \ \alpha_{k\ell}^{D}, \ K_{I}, \ K_{II}, \ K_{III} \right) \tag{56}$$

where K_{I}, K_{II}, and K_{III} are the stress intensity factors, which relate the far-field stresses to the crack tip stresses for a given crack geometry. However, it is assumed that the geometry of both matrix cracking and delaminations is sufficiently independent of stacking sequence that the stress intensity factors may be treated as "material properties" and thus possess the same stress intensity factor dependence for all stacking sequences. Thus, they are encompassed implicitly in the material constants required to characterize damage evolution laws (55) and (56).

It is important to note that the above equations are independent of stacking sequence. Thus, the growth of matrix crack damage in each ply depends explicitly only on the stresses in the plies immediately above and below the delamination. Therefore, it can be seen that equations (55) and (56) can be developed generically from a single [0,90,0] specimen (or any other layup), and the same damage evolution law will apply to every ply in a complex stacking sequence. The rate of growth of damage will depend only on the stresses determined in each ply by equations (55). Herein lies the most important aspect of the current model: it may be characterized using simple layups and then applied to any other stacking sequence.

Several first generation evolution laws have already been proposed in the literature for matrix cracks [19-21] and these are being incorporated into the model in order to obtain a precise form for equations (55). Furthermore, O'Brien [12] has proposed some evolution laws for delamination, and these are being considered for equations (56).

The tensorial nature of equations (55) and (56) poses some difficulties since uniaxial testing will produce only scalar forms of these equations. Therefore, we are seeking to obtain constraints on the tensorial nature of these laws (not unlike Drucker's postulate for plastic strain [22]). Accordingly, we have determined that under isothermal conditions

$$\frac{\partial h}{\partial \alpha_{ij}^{\eta}} \dot{\alpha}_{ij}^{\eta} \geq 0 \qquad (57)$$

follows from the second law of thermodynamics. We are now seeking to show that h is a stable damage potential not unlike that proposed in the damage models of Dragon and Mroz [23] and Krajcinovic and Fonseka [24] for geologic media. If such can be shown then significant constraints can be applied, so that the tensorial nature of equations (55) and (56) can be identified from uniaxial tests.

2.10 Finite Element Plate Computer Code

In order to develop the capability to analyze structural components with spatially variable stresses such as plates with holes, equations (42) and (43) have been incorporated in a plate finite element computer code. The formulation of the governing differential equations for a laminated composite with damage follows the same procedure as that used for the formulation for a laminated composite plate with no damage [25]. The difference between the two formulations becomes apparent when the constitutive displacement equations are examined. To see how these changes affect the overall formulation, first consider the equilibrium equations for a plate.

$$\frac{\partial N_x}{\partial x} + \frac{\partial N_{xy}}{\partial y} = p_x \qquad (58)$$

$$\frac{\partial N_{xy}}{\partial x} + \frac{\partial N_y}{\partial y} = p_y \qquad (59)$$

$$\frac{\partial^2 M_x}{\partial x^2} + 2 \frac{\partial^2 M_{xy}}{\partial x \partial y} + \frac{\partial^2 M_y}{\partial y^2} = - p_z \tag{60}$$

It is now advantageous to express equations (42) and (43) in matrix form.

$$\{N\} = [A] \{\varepsilon_L^o\} + [B] \{\kappa_L\} + \{f^M\} + \{f^D\} \tag{61}$$

$$\{M\} = [B] \{\varepsilon_L^o\} + [D] \{\kappa_L\} + \{g^M\} + \{g^D\} \tag{62}$$

where

$$[A] = \sum_{k=1}^{n} (z_k - z_{k-1}) [Q_1]_k \tag{63}$$

$$[B] = \frac{1}{2} \sum_{k=1}^{n} (z_k^2 = z_{k-1}^2) [Q_1]_k \tag{64}$$

$$[D] = \frac{1}{3} \sum_{k=1}^{n} (z_k^3 - z_{k-1}^3) [Q_1]_k \tag{65}$$

$$\{f^M\} = -\sum_{k=1}^{n} (z_k - z_{k-1}) [Q_2]_k \{\alpha^M\}_k \tag{66}$$

$$\{g^M\} = -\frac{1}{2} \sum_{k=1}^{n} (z_k^2 - z_{k-1}^2) [Q_2]_k \{\alpha^M\}_k \tag{67}$$

$$\{f^D\} = \sum_{i=1}^{d} t_i [\bar{Q}_1]_i \{\alpha_1^D\}_i + \sum_{i=1}^{d+1} (z_i - z_{i-1}) [\bar{Q}_2]_i \{\alpha_2^D\}_i \tag{68}$$

$$\{g^D\} = \sum_{i=1}^{d} t_i^2 [\bar{Q}_3]_i \{\alpha_1^D\}_i + \sum_{i=1}^{d+1} (z_i^2 - z_{i-1}^2) [\bar{Q}_4]_i \{\alpha_2^D\}_i \tag{69}$$

In order to simplify the formulation of the finite element model considerably, it is expedient to consider the special case of symmetric laminates. Making this assumption effectively sets the [B] matrix equal to zero, resulting in a decoupling of the in-plane and out-of-plane laminate

60

equations. Since all laminates are not symmeric, later work will be involved in the incorporation of the [B] matrix into the formulation.

Substituting equation (61) into equations (58) and (59) results in the governing differential equations for the in-plane deformations of the plate:

$$A_{11} \frac{\partial^2 u_L^0}{\partial x^2} + 2 A_{16} \frac{\partial^2 u_L^0}{\partial x \partial y} + (A_{12} + A_{66}) \frac{\partial^2 v_L^0}{\partial x \partial y} + A_{26} \frac{\partial^2 v_L^0}{\partial y^2}$$

$$+ A_{66} \frac{\partial^2 u_L^0}{\partial y^2} + A_{16} \frac{\partial^2 v_L^0}{\partial x^2} + \frac{\partial}{\partial x} (f_1^M + f_1^D)$$

$$+ \frac{\partial}{\partial y} (f_3^M + f_3^D) = - p_x \qquad (70)$$

$$A_{16} \frac{\partial^2 u_L^0}{\partial x^2} + (A_{12} + A_{66}) \frac{\partial^2 u_L^0}{\partial x \partial y} + 2 A_{26} \frac{\partial^2 v_L^0}{\partial x \partial y} + A_{22} \frac{\partial^2 v_L^0}{\partial y^2}$$

$$+ A_{26} \frac{\partial^2 u_L^0}{\partial y^2} + A_{66} \frac{\partial^2 v_L^0}{\partial x^2} + \frac{\partial}{\partial x} (f_3^M + f_3^D)$$

$$+ \frac{\partial}{\partial y} (f_2^M + f_2^D) = - p_y \qquad (71)$$

Similarly, substituting equation (62) into equation (60) results in the governing differential equation for the out-of-plane deformations.

$$D_{11} \frac{\partial^4 w_L^0}{\partial x^4} + 4 D_{16} \frac{\partial^4 w_L^0}{\partial x^3 \partial y} + 2 (D_{12} + 2 D_{66}) \frac{\partial^4 w_L^0}{\partial x^2 \partial y^2}$$

$$+ 4 D_{26} \frac{\partial^4 w_L^0}{\partial x \partial y^3} + D_{22} \frac{\partial^4 w_L^0}{\partial y^4} - \frac{\partial^2}{\partial x^2} (g_1^M + g_1^D)$$

$$- \frac{\partial^2}{\partial y^2} (g_2^M + g_2^D) - 2 \frac{\partial^2}{\partial x \partial y} (g_3^M + g_3^D) = p_z \qquad (72)$$

Integrating the governing differential equations, (70), (71) and (72) against a test function and employing Green's Theorem results in the weak formulation of the laminated plate equilibrium equaitons. Equilibrium in the x-direction is given by:

61

$$\int_{\Omega^e} \{\frac{\partial(\delta u_L^o)}{\partial x} P_1 + \frac{\partial(\delta v_L^o)}{\partial y} P_2 \ dydx = \int_{\Gamma^e} \delta u_L^o (N_x n_x + N_{xy} n_y) \ d\Gamma$$

$$- \int_{\Omega^e} [\frac{\partial(\delta u_L^o)}{\partial x} (f_1^M + f_1^D) + \frac{\partial(\delta v_L^o)}{\partial y} (f_3^M + f_3^D)] \ dydx \qquad (73)$$

where

$$P_1 = A_{11} \frac{\partial u_L^o}{\partial x} + A_{12} \frac{\partial v_L^o}{\partial y} + A_{16} \frac{\partial u_L^o}{\partial y} + A_{16} \frac{\partial v_L^o}{\partial x} \qquad (74)$$

$$P_2 = A_{16} \frac{\partial u_L^o}{\partial x} + A_{26} \frac{\partial v_L^o}{\partial y} + A_{66} \frac{\partial u_L^o}{\partial y} + A_{66} \frac{\partial v_L^o}{\partial x} \qquad (75)$$

Equilibrium in the y-direction is given by

$$\int_{\Omega^e} \{\frac{\partial(\delta v_L^o)}{\partial x} P_2 + \frac{\partial(\delta v_L^o)}{\partial y} P_3\} \ dydx = \int_{\Gamma^e} \delta v_L^o (N_{xy} n_x + N_y n_y) \ d\Gamma$$

$$- \int_{\Omega^e} [\frac{\partial(\delta v_L^o)}{\partial x} (f_3^M + f_3^D) + \frac{\partial(\delta v_L^o)}{\partial y} (f_2^M + f_2^D)] \ dydx \qquad (76)$$

where

$$P_3 = A_{12} \frac{\partial u_L^o}{\partial x} + A_{22} \frac{\partial v_L^o}{\partial y} + A_{26} \frac{\partial u_L^o}{\partial y} + A_{26} \frac{\partial v_L^o}{\partial x} \qquad (77)$$

Equilibrium in the z-direction is given by:

$$\int_{\Omega^e} \{\frac{\partial^2(\delta w_L^o)}{\partial x^2} P_4 + \frac{\partial^2(\delta w_L^o)}{\partial y^2} P_5 + 2 \frac{\partial^2(\delta w_L^o)}{\partial x \partial y} P_6\} \ dxdy$$

$$= \int_{\Omega^e} \delta w_L^o \ p_z \ dydx + \int_{\Gamma^e} \delta w_L^o (Q_x n_x + Q_y n_y) \ d\Gamma$$

$$- \int_{\Gamma^e} [\frac{\partial(\delta w_L^o)}{\partial x} (M_x n_x + M_{xy} n_y) + \frac{\partial(\delta w_L^o)}{\partial y} (M_{xy} n_x + M_y n_y)] \ d\Gamma$$

62

$$+ \int_{\Omega^e} [\frac{\partial^2(\delta w_L^o)}{\partial x^2} (g_1^M + g_1^D) + \frac{\partial^2(\delta w_L^o)}{\partial y^2} (g_2^M + g_2^D)$$

$$2 \frac{\partial^2(\delta w_L^o)}{\partial x \partial y} (g_3^M + g_3^D)] \ dxdy \qquad (78)$$

where

$$P_4 \quad D_{11} \frac{\partial^2 w_L^o}{\partial x^2} + D_{12} \frac{\partial^2 w_L^o}{\partial y^2} + 2 D_{16} \frac{\partial^2 w_L^o}{\partial x \partial y} \qquad (79)$$

$$P_5 = D_{12} \frac{\partial^2 w_L^o}{\partial x^2} + D_{22} \frac{\partial^2 w_L^o}{\partial y^2} + 2 D_{26} \frac{\partial^2 w_L^o}{\partial x \partial y} \qquad (80)$$

$$P_6 = D_{16} \frac{\partial^2 w_L^o}{\partial x^2} + D_{26} \frac{\partial^2 w_L^o}{\partial y^2} + 2 D_{66} \frac{\partial^2 w_L^o}{\partial x \partial y} \qquad (81)$$

In equations (73), (76) and (78), Ω^e represents the element area and Γ^e represents the external boundary of the element.

It is assumed in the formulation of this finite element model that a total of five degrees of freedom exist at each node. The components of deformation at a node, k, consist of two in-plane displacements, u_k^o and v_k^o, one out-of-plane displacement, w_k^o, and two rotational terms θ_k^x and θ_k^y. The rotations can be described as the slope of the normal to the mid-plane after deformation and are described in terms of the out-of-plane displacement by:

$$\theta_k^x = \frac{\partial w_L^o}{\partial y} \qquad (82)$$

$$\theta_k^y = - \frac{\partial w_L^o}{\partial x} \qquad (83)$$

The following displacement fields are assumed to represent the components of deformation within the element:

$$u_L^o = \sum_{j=1}^{m} \psi_j^e u_j^e \qquad (84)$$

63

$$v_L^o = \sum_{j=1}^{m} \psi_j^e \, v_j^e \tag{85}$$

$$w_L^o = \sum_{k=1}^{p} \phi_k^e \, \delta_k^e \tag{86}$$

where $\{\delta\}_j = \{w_j, \theta_j^x, \theta_j^y\}$, ψ_j^e and ϕ_k^e represent the shape functions for the element, m is the number of nodes the element contains and p is three times the number of nodes.

Also,

$$\delta u_L^o = \psi_i^e \qquad i = 1, \cdots, m \tag{87}$$

$$\delta u_L^o = \psi_i^e \qquad i = 1, \cdots, m \tag{88}$$

$$\delta u_L^o = \phi_k^o \qquad k = 1, \cdots, p \tag{89}$$

Substitution of equations (84)-(89) into the weak formulation of the plate equilibrium equations, (73), (76), and (78) results in the following system of equations:

$$\begin{bmatrix} K^{11} & K^{12} & 0 \\ K^{21} & K^{22} & 0 \\ 0 & 0 & K^{33} \end{bmatrix} \begin{Bmatrix} u \\ v \\ \delta \end{Bmatrix} = \begin{Bmatrix} F_A^1 \\ F_A^2 \\ F_A^3 \end{Bmatrix} + \begin{Bmatrix} F_M^1 \\ F_M^2 \\ F_M^3 \end{Bmatrix} + \begin{Bmatrix} F_D^1 \\ F_D^2 \\ F_D^3 \end{Bmatrix} \tag{90}$$

$$\text{5m x 5m} \qquad \text{5m x 1} \qquad \text{5m x 1} \quad \text{5m x 1} \quad \text{5m x 1}$$

where the [K] matrix is the standard linear stiffness matrix, $\{F_A\}$ is the external forcing function, and $\{F_M\}$ and $\{F_D\}$ are pseudo - force vectors resulting from matrix cracks and delaminations, respectively. Assembly of the above element equations into a global set may be accomplished in the standard way.

64

Preliminary results have been obtained with the finite element code for the [0/90]$_s$ tapered specimen shown in Fig. 29. The specimen was loaded to produce the damage state shown in Fig. 30, and the code was utilized to simulate the response of the specimen. The code produced a prediction of the axial stiffness loss which compares well with the experiment. More importantly, the computer code produced predictions for the stress components (as a function of damage) in the 90 degree plies, as shown in Figs. 31 and 32. Since these stresses cannot be practically obtained experimentally, no comparison is available. However, the close agreement between the predicted and experimentally observed strains lends support to the contention that the stress predictions are also believable. Further test cases, such as a plate with a circular cutout, are now being investigated with the computer code.

2.11 Conclusion

It is now well known that laminated composite structures undergo substantial microstructural damage which is both load history and stacking sequence dependent. Because this damage ultimately may lead to component failure, it is essential to develop a model capable of predicting component response in the presence of damage in order to design away from failure. If this can be achieved, then structures can be designed to operate with non-catastrophic damage (just as metals are allowed to yield) and thus achieve greater design efficiency.

Toward the goal of achieving such a model, the author has proposed a particular methodology within the framework of continuum damage mechanics. This methodology is supported by the following framework: 1) development of a physically based set of internal state variables representing damage (Section 2.3); 2) construction of a set of stress-strain-damage constitutive equations (Section 2.3); 3) integration of the model in a lamination scheme which accounts for interply delamination (Section 2.4); 4) application of the procedure to calculate "far-field" damage dependent ply stresses (Section 2.8); 5) development of damage evolution laws (Section 2.9); 6) construction of an analytical procedure for predicting the response of structural components (Section 2.10); and 7) development of a failure function.

While this author will be the first to admit that the results given herein do not fulfill all of the steps outlined above, substantial progress

65
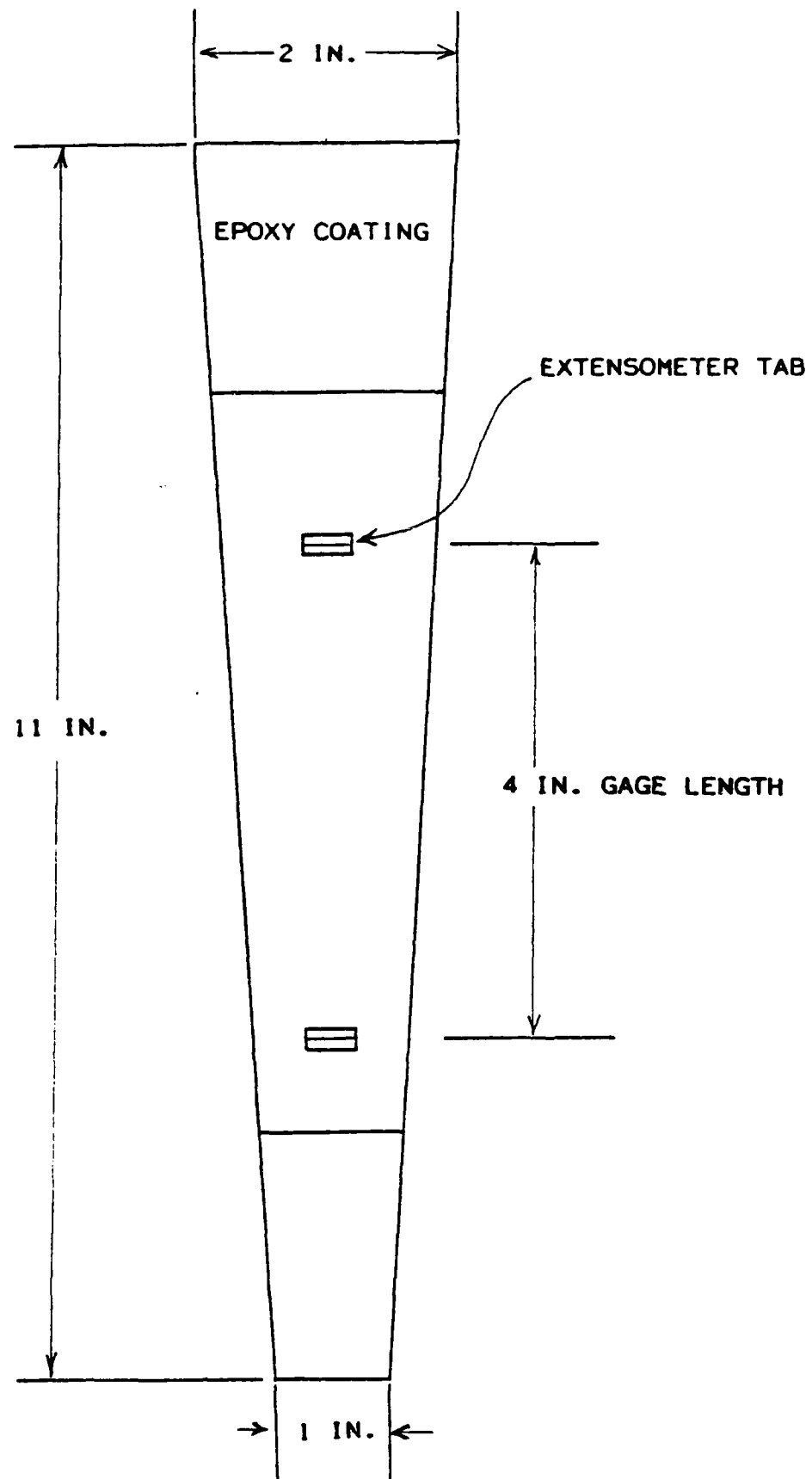
Fig. 29. Tapered Specimen Geometry
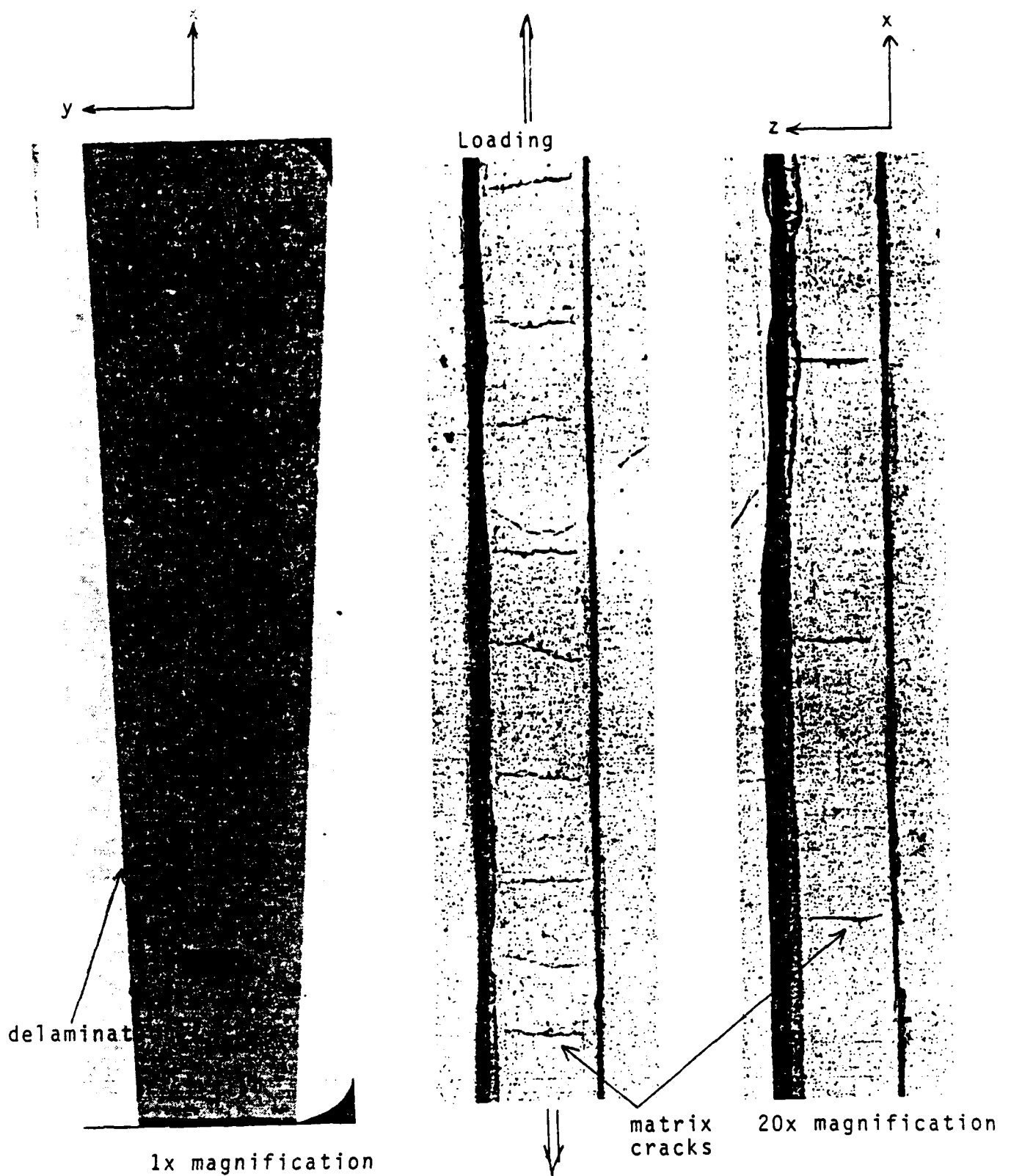
Fig. 30. Tapered Specimen X-ray and Edge Replicas

67
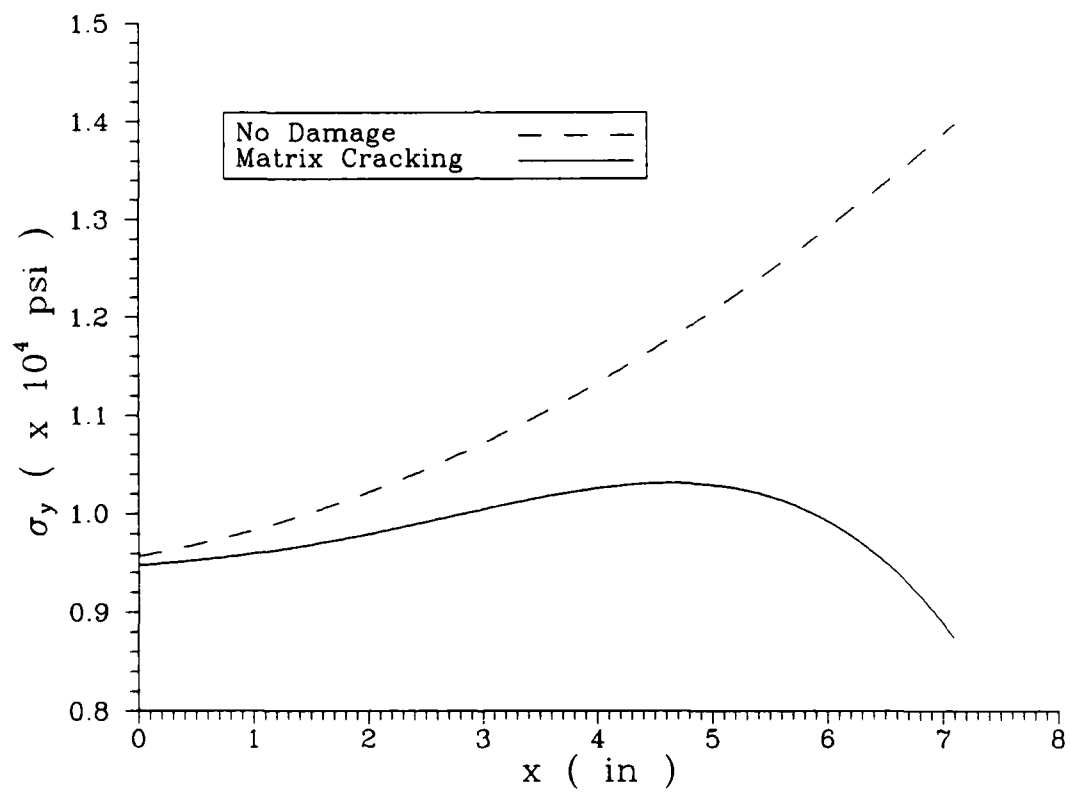
Fig. 31. σ_x in the 90° plies of the laminated tapered beam
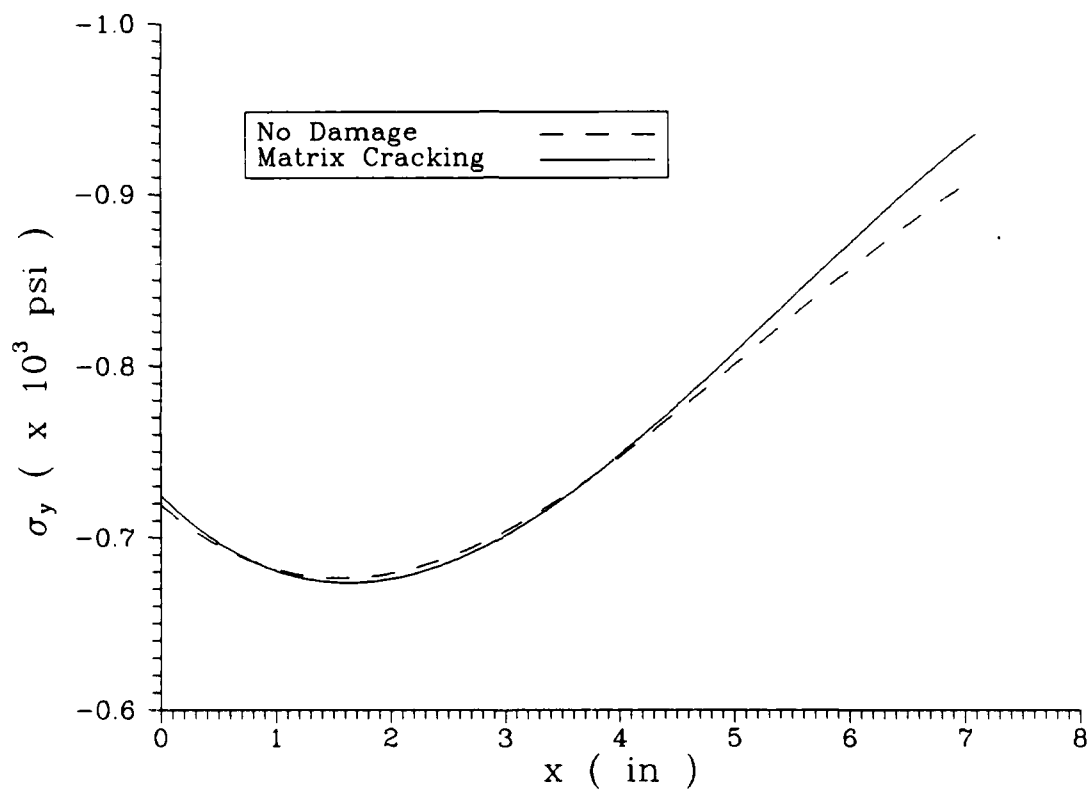
Fig. 32. σ_y in the 90° plies of the laminated tapered beam

has been made. Steps 1 through 4 and 6 are complete at this time, and step 5 is well underway. More importantly, the groundwork has been properly laid for a "mechanistic" approach to step 7. For example, the model is capable of predicting ply level stresses in the presence of damage regardless of the laminate stacking sequence and for any load history. So far as this author is aware, no other currently available analytical technique possesses this capability. In short, it is believed by this author that the basic features are now in place for predicting the response of damaged laminated composite structural components.

The ultimate goal of this research is to develop a model capable of predicting failure of a component subjected to loads resulting in stress gradients. Toward this end, the essential ingredients are now available in the current model for constructing a failure criterion which describes fiber fracture as a function of matrix cracking and delamination.

2.12 References

1. Groves, S.E., and Allen, D.H., "A Survey of Damage in Continuous Fiber Composites," Texas A&M University Mechanics and Materials Center, MM-5023-84-6, March, 1984.

2. Norvell, R.G., "An Investigation of Damage Accumulation in Graphite/Epoxy Laminates," Texas A&M University Thesis, August, 1985.

3. Georgiou, I.T., "Initiation Mechanisms and Fatigue Growth of Internal Delaminations in Graphite/Epoxy Cross-Ply Laminates," Texas A&M University Thesis, December, 1986.

4. Groves, S.E., Harris, C.E., Highsmith, A.L., Allen, D.H., and Norvell, R.G., "An Experimental and Analytical Treatment of Matrix Cracking in Cross-ply Laminates," Experimental Mechanics, Vol. 27, No. 1, pp. 73-79, 1987.

5. Kachanov, L.M., "Introduction to Continuum Damage Mechanics," Martinus Nijhoff, Dordrecht, 1986.

6. Krajcinovic, D., "Continuum Damage Mechanics," Applied Mechanics Update 1986, Steele, C.R., and Springer, G.S., Eds., The American Society of Mechanical Engineers, pp. 403-406, 1986.

7. Bazant, Z.P., "Mechanics of Distributed Cracking," Applied Mechanics Reviews, Vol. 39, pp. 675-705, 1986.

8. Allen, D.H., Harris, C.E., and Groves, S.E., "A Thermomechanical Constitutive Theory for Elastic Composites with Distributed Damage - Part I: Theoretical Development," Int. J. Solids Structures, Vol. 23, No. 9, pp. 1301-1318, 1987.

9. Allen, D.H., Harris, C.E., and Groves, S.E., "A Thermomechanical Constitutive Theory for Elastic Composites with Distributed Damage - Part II.: Application to Matrix Cracking in Laminated Composites," Int. J. Solid Structures, Vol. 23, No. 9, pp. 1319-1338, 1987.

10. Kachanov, M.L., "Continuum Theory of Media with Cracks," Izv. AN SSSR, Mekhanika Tverdogo Tela, Vol. 7, No. 2, pp. 54-59, 1972.

11. Talreja, R., "A Continuum Mechanics Characterization of Damage in Composite Materials," Proc. R. Soc. London, Vol. 399A, 1985, pp. 195-216.

12. O'Brien, T.K., "Characterization of Delamination Onset and Growth in a Composite Laminate," Damage in Composite Materials, ASTM STP 775, K.L. Reifsnider, Ed., American Society for Testing and Materials, 1982, pp. 140-167.

13. Highsmith, A.L. Reifsnider, K.L., "Stiffness-Reduction Mechanisms in Composite Laminates," Damage in Composite Materials, ASTM STP 775, K.L. Reifsnider, Ed., American Society for Testing and Materials, 1982, pp. 103-117.

14. Dvorak, G.J., "Analysis of Progressive Matrix Cracking in Composite Laminates," AFOSR-82-0308, Rensselaer Polytechnic Institute, March 1985.

15. Hashin, Z., "Analysis of Cracked Laminates: A Variational Approach," Mechanics of Materials 4, North Holland, pp. 121-136, 1985.

16. Aboudi, J., "Stiffness Reduction of Cracked Solids," Engineering Fracture Mechanics, Vol. 26, No. 5, pp. 637-650, 1987.

17. Groves, S.E., "A Study of Damage Mechanics in Continuous Fiber Composite Laminates with Matrix Cracking and Interply Delaminations," Dissertation, Texas A&M University, 1986.

18. Miner, M.A., "Cumulative Damage in Fatigue," J. Appl. Mech., Vol. 12, p. 159, 1945.

19. Wang, A.S.D. and Bucinell, R.B., "Cumulative Damage Model for Advanced Composite Materials," Drexel University Interim Report No. 6, Feb., 1984

20. Hashin, Z., "Cumulative Damage Theory for Composite Materials: Residual Life and Residual Strength Methods," Composite Science and Technology, Vol. 23, pp. 1-9, 1985.

21. Hashin, Z. and Rotem, A., "A Cumulative Damage Theory of Fatigue Failure," Materials Science and Engineering, Vol. 34, pp. 147-160, 1978.

22. Drucker, D.C., "A More Fundamental Approach to Plastic Stress-Strain Relations," Proc. for U.S. Natl. Congr. Appl. Mech., ASME, pp. 487-491, 1951.

23. Dragon, A. and Mroz, Z., "A Continuum Model for Plastic-Brittle Behaviour of Rock and Concrete," Int. J. Eng. Sci., Vol. 17, pp. 121-137, 1979.

24. Krajcinovic, D. and Fonseka, G.U., "The Continuous Damage Theory of Brittle Materials - Part I - General Theory," J. Appl. Mech., Vol. 48, pp. 809-815, 1981.

3. PUBLICATION LIST

3.1 Journal Publications

1. Allen, D.H., Harris, C.E., and Groves, S.E., "A Thermomechanical Constitutive Theory for Elastic Composites with Distributed Damage - Part I: Theoretical Development," International Journal of Solids and Structures, Vol. 23, No. 9, pp. 1301-1318, 1987 (Appendix 7.1).

2. Allen, D.H., Harris, C.E., and Groves, S.E., "A Thermomechanical Constitutive Theory for Elastic Composites with Distributed Damage - Part II: Application to Matrix Cracking in Laminated Composites," International Journal of Solids and Structures, Vol. 23, No. 9, pp. 1319-1338, 1987 (Appendix 7.2).

3. Allen, D.H., Harris, C.E., Groves, S.E., and Norvell, R.G., "Characterization of Stiffness Loss in Cross-ply Laminates with Curved Matrix Cracks," Journal of Composite Materials, Vol. 22, No. 1, pp. 71-80, 1988 (See the Third Annual Report).

4. Groves, S.E., Harris, C.E., Highsmith, A.L., Allen, D.H. and Norvell, R.G., "An Experimental and Analytical Treatment of Matrix Cracking in Cross-ply Laminates," Experimental Mechanics, Vol. 27, No. 1, pp. 73-79, 1987 (See the Third Annual Report).

5. Allen, D.H., Groves, S.E., Allen D.H., and Harris, C.E., "A Cumulative Damage Model for Continuous Fiber Composite Laminates with Matrix Cracking and Interply Delaminations," Composite Materials: Testing and Design (8th Conference, ASTM STP 972, J.D. Whitcomb, Ed., American Society for Testing and Materials, pp. 57-79, 1988 (Appendix 7.3).

6. Harris, C.E., Allen, D.H., Nottorf, E.W., and Groves, S.E., "Modelling Stiffness Loss in Quasi-Isotropic Laminates Due to Microstructural Damage," Journal of Engineering Materials Technology, American Society of Mechanical Engineers, Vol. 110, No. 2, pp. 128-133, 1988 (Appendix 7.4).

7. Harris, C.E. and Allen, D.H. "A Continuum Damage Model of Fatigue-Induced Damage in Laminated Composites," to appear in Encyclopedia of Composites, 1988 (Appendix 7.5).

3.2 Conference Proceedings

1. Allen, D.H., Harris, C.E., and Groves, S.E., "Damage Modelling in Laminated Composites," Proceedings IUTAM/ICM Symposium on Yielding, Damage and Failure of Anisotropic Solids, Grenoble, France, 1987 (peer reviewed - Appendix 7.6).

2. Harris, C.E., Allen, D.H., and Nottorf, E.W., "Damaged Induced Changes in the Poisson's Ratio of Cross-Ply Laminates: An Application of a Continuum Damage Mechanics Model for Laminated Composites," Damage Mechanics in Composites, A.S.D. Wang and G.K. Haritos, Eds., American Society of Mechanical Engineers, AD-Vol. 12, pp. 17-24, 1987 (also submitted to Journal of Composites Technology and Research - Appendix 7.7).

3. Allen, D.H., Nottorf, E.W., and Harris, C.E., "Effect of Microstructural Damage on Ply Stresses in Laminated Composites," Proceedings ASME Winter Annual Meeting, Chicago, 1988 (to appear - Appendix 7.8).

3.3 Chapters in Textbooks

1. Allen, D.H. and Harris, C.E., "A Damage Dependent Constitutive Model for Laminated Composites," Mechanical Behaviour of Materials, A. Aladjem, Ed., Freund Publishing, Tel Aviv, 1988 (Appendix 7.9).

3.4 Papers in Review

1. Lee, J.W., Allen, D.H., and Harris, C.E., "Internal State Variable Approach for Predicting Stiffness Reductions in Fibrous Laminated Composites with Matrix Cracks," submitted to _Journal of Composite Materials_, 1988 (Appendix 7.10).

3.5 Future Papers

We expect perhaps three additional papers to result from the theses discussed in Section 4.2.

4. GRADUATE RESEARCH ASSISTANT ACTIVITIES

4.1 Degrees Completed

1. R.G. Norvell - M.S., August, 1985.
2. S.E. Groves - Ph.D., December, 1986.
3. I.T. Georgiou - M.S., December, 1986.
4. D. Lo - M.S., August, 1988 (expected).
5. K. Buie - M.S., July, 1988.
6. E.W. Nottorf - Ph.D., September, 1988 (expected).

4.2 Thesis Abstracts

ABSTRACT

A Study of Damage Mechanics in Continuous Fiber Composite
Laminates with Matrix Cracking and Internal Delaminations

Scott Eric Groves, B.S., Texas A&M University;
M.S., Virginia Polytechnic Institute
Chairman of Advisory Committee: Dr. David H. Allen

A cumulative damage model for predicting the stiffness loss in cross-ply graphite/epoxy laminates is obtained by applying a thermomechanical constitutive theory for elastic composites with distributed damage. The model proceeds from a continuum mechanics and thermodynamics approach wherein the distributed damage is characterized by a set of second order tensor valued internal state variables. The internal state variables represent globally averaged measures of matrix cracking and internal delaminations. The resulting model represents a set of damage dependent laminate plate equations. These are developed by modifying the classical Kirchhoff plate theory. The effect of internal delamination enters the formulation through modifications of the Kirchhoff displacements. The corresponding internal state variable is defined utilizing the kinematics of the internal delaminated region and the divergence theorem. This internal state variable represents the components of the out-of-plane displacement modes created by the delamination. A local anisotropic stiffness is then defined to couple these out-of-plane displacements with the in-plane forces. The effect of the matrix cracking enters the formulation through alteration in the individual lamina constitution. The internal state variable is related to the surface area of delamination by employing linear elastic fracture mechanics. This leads to a relation between the strain energy release rate and the internal state variable. Thus, as long as the strain energy release rate can be defined, the model is applicable of predicting the response of general laminate plate behavior. The model is demonstrated by predicting the relative axial stiffness loss due to internal delamination in cross-ply laminates with very good results.

ABSTRACT

Initiation Mechanisms and Fatigue Growth of Internal Delaminations
in Graphite/Epoxy Cross-Ply Laminates. (December (1986)

Ioannis Theodorou Georgiou, B.S., Aerospace Engineering Texas A&M University
Co-Chairmen of Advisory Committee: Dr. C.E. Harris
Dr. D.H. Allen

An experimental investigation has documented the initiation and growth of internal delaminations in laminated fiber-reinforced composites made of AS4/3502 graphite/epoxy. Cross-ply laminates of the general type $(0_n/90_m)_s$ were subjected to a tension-tension cyclic load at 2.0 Hz and R=0.1 to develop internal delaminations. Isolation of internal delaminations from other major matrix fracture phenomena was the main reason for selecting cross-ply laminates for this study.

The X-ray radiography nondestructive method was used to record the internal delaminations at specified load cycles. In addition, Scanning Electron Microscopy was used to examine the damage state in the interior of the laminates. Also, the residual mechanical properties E_{xx} and ν_{yx} were measured at the cycles where the damage was recorded.

The experimental results were interpreted by using force and moment equilibrium conditions and compatibility of deformations. The conditions leading to the fracture phenomenon of internal delaminations were delineated. The factors leading to distinct patterns of internal delamination initiation and growth were identified.

78

ABSTRACT

An Investigation of Damage Accumulation in
Graphite/Epoxy Laminates. (August 1985)

Robert Gerald Norvell, B.S., Texas A&M University
Co-Chairmen of Advisory Committee: Dr. David H. Allen
Dr. Richard A. Schapery

The objective of this investigation has been to identify the mechanisms of initiation and growth of matrix cracks in graphite/epoxy laminates and to identify the effect of matrix cracking on material response. An extensive experimental data base was produced for use in the development of a damage model and for model verification.

An as yet unreported form of transverse cracking has been observed. Two distinct forms of transverse cracks were found, each clearly having its own mechanisms of initiation and growth. Subsequent damage modes associated with transverse cracks, such as longitudinal splitting and delamination, also developed separate forms corresponding to the transverse crack variations.

.ABSTRACT

An Investigation Into the Effects of Damage on the

Stresses in a Composite Laminate. (December 1988)

Eric Walter Nottorf, B. S. Aeronautical and Astronautical Engineering,

Purdue University, M. S. Aerospace Engineering, Texas A & M University.

Co-Chairmen of Advisory Committee: Dr. D. H. Allen and Dr. C. E. Harrris

A general constitutive framework for composite laminates with damage is
reviewed. This constitutive framework is based on continuum damage
mechanics with constraints imposed by thermodynamics.

Factors that effect the ply stresses and thus delamination initiation and
growth in composite laminates are investigated and presented within. It is
postulated that adjacient ply "effective stresses" are crucial in influencing the
initiation and growth of delaminations in composite laminates. In particular,
adjacient ply normal stresses have been used in the determination and
postulated growth of delaminations.

A method for determining the "effective stresses" in the adjacent plies is
presented along with calculated stress changes due to various types of damage.
The specific damage is incorporated into the model by two tensor-valued
internal state variables for both matrix cracking and delaminations,
respectively.

Along with this stress calculation method, a general framework for the
determination of delamination initiation and growth using the concepts of
fracture mechanics and stress states is presented.

Abstract

A Matrix Crack Damage Accumulation

Model for Laminated Composites

David C. Lo, B.S., Texas A&M University

Directed by: Drs. D.H. Allen and C.E. Harris

A damage accumulation relationship in the framework of *Continuum Damage Mechanics* is proposed for the growth of matrix cracks in brittle-elastic continuous fiber reinforced laminated composites. The effects of the matrix cracks are represented by the local volume average of the diadic product of the crack opening displacement vector and the crack face normal. The local volume under consideration is assumed to be statistically homogeneous. The concept of flow potentials are adopted to determine the lamina damage evolution equations. The stability of the matrix crack growth, when viewed from the level of the local volume, is assumed in the formulation.

The damage evolution equations are incorporated into a continuum damage model for laminated composites. This model takes the form of laminate analysis equations modified by internal state variables. Stacking sequence independence is exhibited by the damage evolution equations because the local ply response, used in the equations, reflects the global laminate behavior through averaging over the entire laminate thickness. The model is then implemented in a laminate analysis computer code. Model predictions are compared with published experimental data for graphite/epoxy laminates with different stacking sequences. The ability of the model to account for the effects of adjacent ply constraints and damage interaction by global averaging is examined. Finally, further developments for this damage accumulation relationship are discussed.

ABSTRACT

A Finite Element Model for Laminated Composite Plates

with Matrix Cracks and Delaminations.   (December 1988)

Kevin Daniel Buie, B.S., Texas A&M University

Chair of Advisory Committee: Dr. David H. Allen

A finite element model is developed herein for the analysis of laminated composite plates experiencing microstructural damage in the forms of matrix cracking and interply delaminations.   The idea of representing the formation of damage within a laminated composite plate with strain-like internal state variables is utilized to obtain the weak form of the equilibrium equations.   From these equations the necessary stiffness and force matrices are formulated for the three node, fifteen degree of freedom triangular element used by the model. A FORTRAN program capable of predicting the response of symmetric laminated composite plates, having the same lamina material properties, to any combination of force and moment loadings is generated from the finite element model.   Finally, the program is used to examine the effects of matrix cracking and delamination on the lamina stresses in two example cases.

5.0 PROFESSIONAL PERSONNEL INFORMATION

5.1 Faculty Research Assignments

1. Dr. D.H. Allen (Co-principal Investigator) - overall program coordination; development of stiffness relationships; construction of ISV growth laws; mechanical testing.

2. Dr. C.E. Harris (Co-principal Investigator) - overall experimental coordination; mechanical testing; nondestructive evaluation; stiffness modelling; fracture mechanics (now Branch Head, Fatigue and Fracture Branch, NASA Langley Research Center).

5.2 Additional Staff and Students

1. Ms. C. Rice (Secretary) - secretarial support.

2. Mr. S.E. Groves (Lecturer, Research Assistant, and Ph.D. Candidate) - ISV growth laws; laminate analysis; finite element modelling; mechanical testing (completed Ph.D., December, 1986 - now at Lawrence Livermore Labs).

3. Mr. I. Georgiou (Research Assistant and M.S. Candidate) - mechanical testing; nondestructive evaluation; ISV growth laws (completed M.S., December, 1986 - now Ph.D. candidate at Purdue University).

4. Mr. E.W. Nottorf (Research Assistant and Ph.D. candidate) - modelling of stiffness loss; mechanical testing.

5. Mr. David Lo (Research Assistant and M.S. Candidate) - ISV growth laws.

6. Mr. Kevin Buie (Research Assistant and M.S. Candidate) - modelling combined damage modes (completed M.S., July, 1988).

7. Mr. C. Fredericksen (Lab Technician) - experimental lab support.

8. Mr. R.G. Norvell (Research Assistant and M.S. Candidate) - experimental damage observation (now at General Dynamics - Fort Worth).

6.0 INTERACTIONS

6.1 Papers Presented

6.1.1 Conference Presentations

1. S.E. Groves, D.H. Allen, and C.E. Harris, "A Cumulative Damage Model for Continuous Fiber Composite Laminates with Matrix Cracking and Interply Delaminations," American Society for Testing and Materials Conference, Charleston, S.C., April, 1986.

2. D.H. Allen, C.E. Harris, S.E. Groves, and R.G. Norvell, "Characterization of Stiffness Loss in Cross-ply Laminates with Curved Matrix Cracks," Third Japan - United States Conference on Composite Materials, Tokyo, June, 1986.

3. C.E. Harris and D.H. Allen, "The Application of Fracture Mechanics to Specify the Internal State Variable for Matrix Crack Damage in Laminated Composites," 23rd Annual Meeting of the Society of Engineering Science, Buffalo, August, 1986.

4. Allen, D.H., Groves, S.E., and Schapery R.A., "A Damage Model for Continuous Fiber Composite," Society of Engineering Science 21st Annual Meeting, Blacksburg, VA, October, 1984.

5. Allen, D.H., Groves, S.E., and Schapery, R.A., "A Damage Model for Continuous Fiber Composites," Tenth Annual Composites Review, Dayton, October, 1984 (Invited).

6. Allen, D.H., Harris, C.E., Norvell, R.G., and Groves, S.E., "Modelling of Stiffness Reduction Due to Matrix Cracks in Graphite/Epoxy Laminates," Society of Engineering Science 22nd Annual Meeting, State College, PA, October, 1985 (Invited).

7. Allen, D.H., Harris, C.E., and Groves, S.E., "Damage Modelling in Laminated Composites," IUTAM/ICM Symposium on Yielding, Damage and Failure in Anisotropic Solids, Grenoble, France, August, 1987 (Invited).

8. Harris, C.E., Allen, D.H., Nottorf, E.W., and Groves, S.E., "Modelling Stiffness Loss in Quasi-Isotropic Laminated Composites Due to Microstructural Damage," ASME Winter Annual Meeting, Boston, December, 1987 (Invited).

9. Harris, C.E., Allen, D.H., and Nottorf, E.W., "Damage-Induced Changes in the Poisson's Ratio of Cross-Ply Laminates: An Application of a Continuum Damage Mechanics Model for Laminated Composites," ASME Winter Annual Meeting, Boston, December, 1987.

10. Allen, D.H., Nottorf, E.W., and Harris, C.E., "Effect of Microstructural Damage on Ply Stresses in Laminated Composites," ASME Winter Annual Meeting, Chicago, December, 1988.

6.1.2 Invited Lectures

1. Damage Modelling in Laminated Composites," Technical University of Denmark, Lyngby, Denmark, September, 1987.

2. "Modelling Damage in Composites," Lawrence Livermore National Labs, July, 1988.

7.0 APPENDIX
INTERIM TECHNICAL REPORTS

Appendix 7.1

A THERMOMECHANICAL CONSTITUTIVE THEORY FOR ELASTIC
COMPOSITES WITH DISTRIBUTED DAMAGE

PART I: Theoretical Development

by

D.H. Allen

S.E. Groves

and

C.E. Harris

Aerospace Engineering Department
Texas A&M University
College Station, Texas 77843

A THERMOMECHANICAL CONSTITUTIVE THEORY FOR ELASTIC COMPOSITES WITH DISTRIBUTED DAMAGE

PART I: Theoretical Development

by

D.H. Allen
C.E. Harris

Aerospace Engineering Department
Texas A&M University
College Station, Texas 77843

and

S.E. Groves

Lawrence Livermore Laboratories
Livermore, CA 94550

ABSTRACT

A continuum mechanics approach is utilized herein to develop a model for predicting the thermomechanical constitution of elastic composites subjected to both monotonic and cyclic fatigue loading. In this model the damage is characterized by a set of second order tensor valued internal state variables representing locally averaged measures of specific damage states such as matrix cracks, fiber-matrix debonding, interlaminar cracking, or any other damage state. Locally averaged history dependent constitutive equations are posed utilizing constraints imposed from thermodynamics with internal state variables.

In Part I the thermodynamics with internal state variables is constructed and it is shown that suitable definitions of the locally averaged field variables will lead to useful thermodynamic constraints on a local scale containing statistically homogeneous damage. Based on this result the Helmholtz free energy is then expanded in a Taylor series in terms of strain, temperature, and the internal state variables to obtain the stress-strain relation for composites with damage. In Part II the three dimensional tensor equations developed in Part I are simplified using material symmetry constraints and are written in engineering notation. The resulting constitutive model is then cast into laminate equations and an example problem is solved and compared to experimental results.

It is concluded that although the model requires further development and extensive experimental verification it may be a useful tool in characterizing the thermomechanical constitutive behavior of continuous fiber composites with damage.

INTRODUCTION

A model for predicting the effect of microstructural damage on the constitutive behavior of continuous fiber-reinforced laminated composites is presented in this two part paper. In Part I, the general model is developed from a theoretical treatment of damage mechanics using continuum mechanics and thermodynamic principles. In Part II, the constitutive model is specialized for the case of matrix crack damage confined to the 90° plies of cross-ply laminates. Predicted values of the damage-degraded axial modulus of cross-ply laminates with a variety of stacking sequences are compared to experimental values.

While the motivation for the research is to model laminated composites, the general model formulated in Part I is applicable to a broad class of media. Therefore, the following literature review discusses the general field of damage mechanics, whereas developments specifically related to laminated composites are discussed in more detail in the introduction to Part II.

The research fields of fracture mechanics and damage mechanics are often related and in some cases contain significant commonality. For the purpose of the current research we define fracture mechanics to be that branch of mechanics wherein a crack is treated as a boundary of the body of interest, whereas damage mechanics is considered to be that branch of mechanics wherein the effects of cracks are included in constitutive equations rather than in boundary conditions. The usefulness of damage mechanics is apparent when one considers a body containing numerous microcracks for which an exact analytic solution is often untenable. Since in many cases internal cracking is noncatastrophic, it is pragmatic to consider the locally averaged effect of the cracks on the response of the body. This approach was first utilized by Kachanov in 1959 [1]. Since that time the field of damage mechanics has grown rapidly to the current state of development [2]. However, the predominant body of research to date has centered on the application of the method to statistically isotropic media.

Microcrack damage has been observed in a wide variety of media, including metals [3], concrete [4], geologic media [5], and composites [6-12]. The significance of this damage lies in the fact that numerous global material properties such as stiffness, damping and residual strength may be substantially altered during the life of the component, as shown in Fig. 1 [13].

Attempts to model damage initially were somewhat phenomenological in nature [1,3]. However, considerable research has shown that this approach can often be justified by micromechanics [14-18] for initally isotropic materials [2]. Fracture based concepts have recently been utilized to model damage development [19-22]. Although the first of these studies [19] contains a general theory which may be applied to fibrous composites, it has so far only been utilized for quasi-isotropic random particulate composites such as solid rocket propellant [20], and as such has not been applied to continuous fiber composites. The theory in the latter two [21,22] has been

1

utilized to develop fatigue matrix crack growth laws for
laminated composites. Kachanov's technique [1] has also been
applied to fibrous composites [23] and although promising results
were obtained, the model was utilized in uniaxial form only.

The concept of damage as an internal state variable has been
previously utilized in continuum mechanics/thermodynamics based
theories for crystalline and/or brittle materials [24-31], as
well as for nonlinear viscoelastic materials [18]. A study has
been made of the effect of vector-valued damage parameters on
various compliance terms [32], and this methodology is currently
undergoing further development [33, 34].

The foregoing discussion indicates that important progress
has been made in characterizing damage in a variety of media.
However, with a few notable exceptions [16,21-23,25,35-38],
applications have been made only to initially isotropic media.
Therefore, it is the contention of these authors that substantial
and continued research is warranted to develop a model of damage
in laminated continuous fiber composites. In this paper an
attempt will be made to utilize many of the concepts embodied in
the previously referenced research efforts to develop a
thermomechanical constitutive model for damage in composites
which is rigorously based in continuum mechanics/thermodynamics
and is generic with regard to material type, load spectrum, and
specimen geometry.

The model will utilize the concept of a local volume element
with statistically homogeneous damage to construct constitutive
equations relating stress, strain, and damage. Unlike methods
which model the local volume analytically (called
microcmechanics), the current research will model the local
volume element experimentally (called phenomenological). The
model will therefore not be restricted to linear elastic media
with homogeneous elastic properties. Furthermore, the model will
be applicable to cracks which are oriented and of heterogeneous
and irregular size and shape. The effect of the cracks will be
reflected through locally averaged quantities describing the
kinematics of the cracks. The output of the model will be a set
of constitutive equations which apply on a scale that is small
compared to the boundary value problem of interest. Therefore,
it will be applicable to the analysis of bodies with stress
gradients and heterogeneous damage states.

CHARACTERIZATION OF DAMAGE AS A
SET OF INTERNAL STATE VARIABLES

Consider an initially unloaded and undamaged composite
structural component, denoted B, as shown in Fig. 2a, where
undamaged is defined here to mean that the body may be
considered to be continuous (without cracks) on a scale several
orders of magnitude smaller than the smallest external dimension
of the component. Although cracks may exist in the initial
state, their total surface area is assumed to be small compared
to the external surface area of the component. Under this
assumption the body is assumed to be simply connected and we call
the initial bounding surface the external boundary S. Although

2

the component is undamaged, there may exist local heterogeneity caused by processing and second phase materials including fibers, matrix tougheners and voids. In addition, the body may be subjected to some residual stress state due to processing, cool down, etc.

Now suppose that the component is subjected to some traction and/or deformation history, as shown in Fig. 2b. The specimen will undergo a thermodynamic process which will in general be in some measure irreversible. This irreversibility is introduced by the occurrence of such phenomena as material inelasticity (even in the absence of damage), fracture (both micro- and macroscale), friction (due to rubbing and/or slapping of fractured surfaces), temperature flux, and chemical change. While all of these phenomena can and do commonly occur in composites, in the present research it will be assumed that all irreversible phenomena of significance occur in small zones near crack surfaces. Outside these zones, the behavior will be considered to be elastic and therefore reversible under constant temperature conditions. All fracture events will be termed damage. Due to these fracture events, the body will necessarily become multiply connected, and all newly created surfaces not intersecting the external boundary will be termed internal boundaries. Because of the above assumptions the model may be limited to polymeric and ceramic matrix composites at temperatures well below the glass transition temperature T_g or melting temperature, where viscoelasticity in matrix materials is small. Metal matrix composites may have to be excluded due to complex post-yield behavior of the matrix.

While fracture involves changes in the boundary conditions governing a complex field problem, it is hypothesized that one may neglect boundary condition changes caused by creation and alteration of both internal and external surfaces created during fracture as long as the resulting damage in the specimen is statistically homogeneous on a local scale which is small compared to the scale of the body of interest. However, the total newly created surface area (which includes internal surfaces) may be large compared to the original external surface area. Under the condition of small scale statistical homogeneity all continuum based conservation laws are assumed to be valid on a global scale in the sense that all changes in the continuum problem resulting from internal damage are reflected only through alterations in constitutive behavior. Typical microstructural events which may qualify as damage are matrix cracking in lamina, fiber/matrix debonding, localized interlaminar delamination and fiber fracture. Large scale changes in the external surface such as edge delaminations, however, are treated as boundary effects which must be reflected in conservation laws via changes in the external boundary conditions rather than in constitutive equations [36,39].

THERMODYNAMICS OF MEDIA
WITH DAMAGE

We now proceed to construct a concise model of the

3

composite with damage. To do this, consider once again the structural component, denoted B in Fig. 2a. The body B is assumed to be of the scale of some appropriate boundary value problem of interest. Now consider some local element labelled V_L and with external surface faces S_1 arbitrarily chosen normal to a set of Cartesian coordinate axes (x_1, x_2, x_3), as shown in Fig. 2c. The element V_L extracted from B and the newly created surfaces, denoted S_2 and with volume V_c, are subjected to appropriate boundary conditions so that the element response is identical to that when it is in B. Furthermore, the volume of the element is defined to be V_L, which includes the volume of any initial voids. The scale of V_L is chosen so that its dimensions are small compared to the dimensions of B, but at the same time, the dimensions of V_L are large enough to guarantee statistical homogeneity of the material heterogeneities and defects in V_L even though the total surface area of defects may be of the same order of magnitude as S_1 [40]. Suppose furthermore that in the absence of defects or at constant damage state the material behavior is linearly thermoelastic. Now consider the local volume element V_L. For the case where tractions or displacements are applied uniformly to the external boundary of V_L, the average stresses and strains in V_L will be determinable from the external boundary tractions or displacements.

Although the damage process actually involves the conversion of strain energy to surface energy, the fact that the damage is reflected in the local constitutive equations rather than boundary conditions suggests that it be treated as a set of energy dissipative internal state variables which are not discernible on the external boundary of the local element.

Review of Thermodynamic Constraints on Linear Thermoelastic Media

The following notation is adopted. Quantities without capitalized subscripts denote pointwise quantities. Those with subscripts L denote quantities which are averaged over the local element V_L. Finally, the subscript E denotes linear thermoelastic properties.

Under the conditions described in the previous section the pointwise Helmholtz free energy per unit volume h of the undamaged linear elastic medium may be expressed as a second order expansion in terms of strain ϵ_{ij} and temperature T as follows [41]:

$$h \equiv u - Ts = h(\epsilon_{ij}, T) =$$

$$A + B_{ij}\epsilon_{ij} + \frac{1}{2} C_{ijkl}\epsilon_{ij}\epsilon_{kl} + D\Delta T + E_{ij}\epsilon_{ij}\Delta T + \frac{1}{2} F\Delta T^2 \qquad , \quad (1)$$

where u and s are the internal energy and entropy per unit volume, respectively, and A, B_{ij}, C_{ijkl}, D, E_{ij} and F are material parameters which are independent of strain and temperature and $\Delta T \equiv T - T_R$, where T_R is the reference temperature at which the strains are zero at zero external loads. In addition, we assume here that all motions are associated with

4

small deformations. Furthermore, inertial effects and electromagnetic coupling are assumed to be negligible.

Pointwise conservation laws appropriate to the body are as follows:

1) conservation of linear momentum

$$\sigma_{ji,j} = 0 \qquad\qquad ; \qquad\qquad (2)$$

where σ_{ij} is the work conjugate stress tensor to the strain tensor ε_{ij} and body forces are assumed to be negligible;

2) conservation of angular momentum (assuming body moments may be neglected)

$$\sigma_{ij} = \sigma_{ji} \qquad\qquad ; \qquad\qquad (3)$$

3) balance of energy

$$\dot{u} - \sigma_{ij}\dot{\varepsilon}_{ij} + q_{j,j} = r \qquad\qquad ; \qquad\qquad (4)$$

where q_j are the components of the heat flux vector, and r is the heat source per unit volume. In addition, dots denote time differentiation and $_{,j} \equiv \partial/\partial x_j$;

4) the second law of thermodynamics

$$\dot{s} - \frac{r}{T} + (\frac{q}{T}j)_{,j} \geq 0 \qquad\qquad . \qquad\qquad (5)$$

Furthermore,

$$\varepsilon_{ij} \equiv \frac{1}{2}(u_{i,j} + u_{j,i}) \qquad\qquad , \qquad\qquad (6)$$

where u_i are the components of the displacement vector. Constraints imposed by the second law of thermodynamics will result in [41]

$$s = s_E = -\frac{\partial h_E}{\partial T} = -D - E_{ij}\varepsilon_{ij} - F\Delta T \qquad , \qquad (7)$$

and

$$\sigma_{ij} = \sigma_{Eij} = \frac{\partial h_E}{\partial \varepsilon_{ij}} = B_{ij} + C_{ijkl}\varepsilon_{kl} + E_{ij}\Delta T \qquad , \qquad (8)$$

where B_{ij} are interpreted as components of residual stresses at the reference temperature at which $\Delta T=0$, and [41]

$$q_i \cong -k_{ij}g_j \qquad , \qquad (9)$$

where

$$g_j \cong T_{,j} \qquad , \qquad (10)$$

and k_{ij} is the thermal conductivity tensor.

Thermodynamic Constraints with Local Damage

It is our intention to construct locally averaged field equations which are similar in form to the pointwise field equations discussed above. In performing this averaging process the pointwise Helmholtz free energy described in equation (1) will undergo a natural modification to include the energy conversion due to crack formation.

Now consider the local element shown in Fig. 2c with traction boundary conditions on the external surface S_1. In addition, the interior of V_L is assumed to be composed entirely of linear elastic material and cracks (which may include thin surface layers of damage). Integrating pointwise equations (1) through (6) over the local volume will result in

$$h_{EL} = A_L + B_{Lij}\varepsilon_{Lij} + \frac{1}{2}C_{Lijkl}\varepsilon_{Lij}\varepsilon_{Lkl} + D_L\Delta T_L + E_{Lij}\varepsilon_{Lij}\Delta T_L + \frac{1}{2}F_L\Delta T_L^2 \quad ,(11)$$

where A_L, B_{Lij}, C_{Lijkl}, D_L, E_{Lij}, and F_L are locally averaged material constants. Also,

$$\sigma_{Lji,j} = 0 \qquad , \qquad (12)$$

$$\sigma_{Lij} = \sigma_{Lji} \qquad , \qquad (13)$$

$$\dot{u}_L' - \sigma_{Lij}\dot{\varepsilon}_{Lij} + q_{Lj,j} = r_L \qquad , \qquad (14)$$

and

$$\dot{s}_L - \frac{\Gamma_L}{T_L} + \left(\frac{q_{Lj}}{T_L}\right)_{,j} \geq 0 \qquad (15)$$

where u'_L, called the effective local internal energy, is given by

$$\dot{u}'_L \equiv \dot{u}_{EL} + \dot{u}^C_L \qquad (16)$$

u_{EL} represents the internal energy of the equivalent uncracked body, given by

$$\dot{u}_{EL} \equiv \frac{1}{V_L}\int_{V_L} \dot{u}\,dV - \frac{1}{V_L}\int_{S_2} T^E_i \dot{u}_i\,dS \qquad (17)$$

where T^E_i are called equivalent tractions, representing tractions in the uncracked body acting along fictitious crack faces, as described in detail in the appendix, and u^C_L is the mechanical power output due to cracking, given by

$$\dot{u}^C_L \equiv -\frac{1}{V_L}\int_{S_2} T^C_i \dot{u}_i\,dS \qquad (18)$$

where T^C_i are fictitious tractions applied to the crack faces which represent the difference between the actual crack face tractions and T^E_i. Furthermore, the locally averaged stress is given by

$$\sigma_{Lij} \equiv \frac{1}{V_L}\int_{V_L}\sigma_{ij}\,dV \qquad (19)$$

and the locally averaged strain is given by

$$\varepsilon_{Lij} \equiv \frac{1}{V_L}\int_{S_1}\frac{1}{2}(u_i n_j + u_j n_i)\,dS \qquad (20)$$

where n_i are components of the unit outer normal vector to the surface S_1. Equations (11) through (15) are identical in form to equations (1) through (5), respectively. Further details on this similarity are given in the appendix.

7

On the basis of this similarity we now define the locally averaged Helmholtz free energy [19,39]:

$$h_L \equiv u'_L - T_L s_L = u_{EL} - T_L s_L + u_L^C = h_{EL} + u_L^C \quad , \tag{21}$$

where it can be seen from definition (17) that h_{EL} is the locally averaged elastic Helmholtz free energy for which residual damage is zero.

The similarity between the pointwise and local field equations leads to the conclusion that

$$s_L = - \frac{\partial h_L}{\partial T_L} \quad , \tag{22}$$

$$\sigma_{Lij} = \frac{\partial h_L}{\partial \varepsilon_{Lij}} = \frac{\partial h_{EL}}{\partial \varepsilon_{Lij}} + \frac{\partial u_L^C}{\partial \varepsilon_{Lij}} \quad , \tag{23}$$

$$q_{Li} \equiv - k_{Lij} g_{Lj} \quad , \tag{24}$$

and

$$g_{Lj} \equiv T_{L,j} \quad , \tag{25}$$

where

$$k_{Lik} \equiv \frac{1}{g_{Lk} V_L} \int_{V_L} k_{ij} g_j dV \quad , \tag{26}$$

Note the similarity between equations (7) through (10) and (22) through (25), respectively.

Equations (23) will serve as the basis for thermomechanical stress-strain relations in damaged composites. All damage will be reflected through the local energy due to cracking u_L^C. This term will be modelled with internal state variables characterizing the various damage modes.

Description of the Internal State

In order to describe the internal state, we first consider the kinematics of a typical point 0 with neighboring points A and B, as shown in Fig. 3. Before deformation lines 0A

and OB are orthogonal, as shown in (a). After deformation we imagine that lines joining O', A', and B' are as shown in (b), and just at the instant that deformation is completed, a crack forms normal to the plane of AOB through point O', as shown in (c). Furthermore, point O' becomes two material points O' and O" on opposite crack faces and points A' and B' deform further to points A" and B". It is assumed that all displacements, including displacement jumps across crack faces, are infinitesimal, so that strain gages attached at points O, A, and B record only the deformation A"O'B". However, the actual strain is associated with A"O"B". Therefore, it is essential to construct an internal state variable which will relate these two strain descriptions. We therefore construct the vectors $\vec{u}^c$ connecting O' and O" and $\vec{n}^c$ describing the normal to the crack face at O', as shown in (c). It should be noted that $\vec{u}^c$ can be used to construct a pseudo-strain representing the difference in rotation and extension of lines A"O'B" and A"O"B".

Now recall that the mechanical power output during cracking is given by equation (18). We assume that at any point in time t_1 tractions T_i can be applied along the crack faces which will result in an energy equivalent to that produced by the damage process:

$$u_L^c(t_1) = - \frac{1}{V_L} \int_{S_2(t_1)} T_i u_i^c dS \quad . \tag{27}$$

The quantities T_i do not necessarily coincide with the terms in the integrand of (18) since the process is in some measure irreversible. However, we define them such that the total energies in equations (18) and (27) are equivalent. For convenience we will call them crack closure tractions, although they do not necessarily result in complete crack closure.

Guided by the fact that $\vec{u}^c$ and $\vec{n}^c$ describe the kinematics of the cracking process at point O, we now define the following second order tensor valued internal state variable:

$$\alpha_{ij} \equiv u_i^c n_j^c => [\alpha_{ij}] = \begin{bmatrix} u_1^c n_1^c & u_1^c n_2^c & u_1^c n_3^c \\ u_2^c n_1^c & u_2^c n_2^c & u_2^c n_3^c \\ u_3^c n_1^c & u_3^c n_2^c & u_3^c n_3^c \end{bmatrix} \quad . \tag{28}$$

The above description has been previously proposed by M. Kachanov[42]. Substituting the above into (27) and utilizing Cauchy's formula gives

$$u_L^c = - \frac{1}{V_L} \int_{S_2} \sigma_{ij}^c \alpha_{ij} dS \quad , \tag{29}$$

where it should be pointed out that integration is performed with respect to undeformed coordinates.

Note that the components of $\vec{u}^C$ can be recovered from (28) by using simple row multiplication on α_{ij}:

$$u_i^2 = u_i^C n_j^C u_i^C n_j^C \qquad \text{(no sum on i)} \qquad . \qquad (30)$$

Similarly, $\vec{n}^C$ can be recovered by using column multiplication on α_{ij}:

$$n_i^2 = u_i^C n_j^C u_i^C n_j^C / (\vec{u}^C)^2 \qquad \text{(no sum on j)} \qquad . \qquad (31)$$

Therefore, although it would not be necessary to actually perform the operations described in equations (30) and (31), the normal and shear modes of crack displacement can be recovered from α_{ij}.

Note furthermore that α_{ij} is generally an asymmetric tensor, and that a symmetric alternative to equations (28) could not be utilized to recover normal and shear modes as described in (30) and (31). As an example, consider the following decomposition of (28) into symmetric and anti-symmetric components

$$\alpha_{ij} = \omega_{1ij} + \omega_{2ij} \qquad , \qquad (32)$$

where

$$\omega_{1ij} \equiv \tfrac{1}{2}(u_i^C n_j^C + u_j^C n_i^C) \qquad , \qquad (33)$$

and

$$\omega_{2ij} \equiv \tfrac{1}{2}(u_i^C n_j^C - u_j^C n_i^C) \qquad . \qquad (34)$$

In order for the anti-symmetric tensor ω_{2ij} to be zero, $\vec{u}^C$ and $\vec{n}^C$ must be parallel vectors, implying pure mode I fracture. In this case ω_{1ij} could be decomposed into a vector (in local coordinates), thus resulting in vector-valued internal state variables. For the case where the cracks in the local volume V_L are randomly oriented and of statistically homogeneous shape and size, the surface integral in equation (29) may be carried out over all cracks. However, if various groups of cracks in the local volume V_L are distinguished by markedly different crack normals $\vec{n}^C$ or geometries, then it will be necessary to distinguish between the damage modes in order to retain the kinematic features of the damage process. Therefore, define the locally averaged internal state variable α_{Lij}^n for the nth damage mode as follows:

$$\alpha_{Lij}^n \equiv \frac{1}{V_L} \int\limits_{S_2^n} u_i^c n_j^c dS = \frac{1}{V_L} \int\limits_{S_2^n} \alpha_{ij} dS \qquad , \qquad (35)$$

where

$$S_2 = \sum_{\eta=1}^{N} S_2^\eta \qquad , \qquad (36)$$

and N is the number of damage modes. For a continuous fiber laminated composite, the modes might be represented by matrix cracks, interply delamination, fiber fracture, and fiber-matrix debond (N=4). For a quasi-isotropic chopped-fiber metal matrix composite, a single isotropic damage tensor might suffice for randomly oriented matrix cracking (N=1).

Therefore, if we define σ_{Lij}^{cn} to be the average crack closure stress for the ηth damage mode such that

$$\sigma_{Lkl}^{cn} \alpha_{Lkl}^n \equiv \frac{1}{V_L} \int\limits_{S_2} \sigma_{ij}^c \alpha_{ij} dS \qquad , \qquad (37)$$

it follows from equations (29), (35), (36), and (37) that

$$u_L^c = - \sigma_{Lij}^{cn} \alpha_{Lij}^n \qquad , \qquad (38)$$

where we have assumed that repeated indeces η imply summation over the range N. It is clear from the above discussion that the value of N must be sufficiently large to recover the essential physics of the damage process. In a mathematical sense, this implies that, whereas the mapping from α_{ij} to α_{Lij}^n is unique, the inverse should also be true in an approximate sense. However, there is no clearcut definition for the range N which will lead to an accurate description of the internal damage state. Note also that both u_i and n_i in equations (35) will be affected by crack interaction in the local volume.

As an example, consider the case of mode I opening of an elliptic crack. For this case, equation (35) will result in dependence of α_{Lij}^n on the volume of the inclusion. Although analytic models for linear elastic bodies with cracks result in response which is dependent on the surface area of cracks only [15-17], it should be pointed out that they also require the average crack diameter. This quantity is replaced herein by the crack opening displacement, which is proportional to the crack

11

diameter in a linear elastic body. Therefore, specifying the crack opening displacement is equivalent to specifying the crack diameter.

Now consider equation (38) in further detail. The kinetic quantities σ_{Lij}^{Cn} may be interpreted as generalized stresses which are energy conjugates to the kinematic strain-like internal state variables α_{Lij}^{n}. We infer from this that there exists a constitutive relation between these variables of the form

$$\sigma_{Lij}^{Cn} = \sigma_{Lij}^{Cn}(\varepsilon_{Lkl}, T_L, \alpha_{Lkl}^{u}) \qquad . \qquad (39)$$

which is history dependent via the explicit dependence on the internal state variables.

Therefore, substituting (39) into (38) will give

$$u_L^C(t_1) = \int_{-\infty}^{t_1} \dot{u}_L^C(t)dt = u_L^C(\varepsilon_{Lkl}(t_1), T_L(t_1), \alpha_{Lkl}^{u}(t_1)) \qquad . \quad (40)$$

It is now proposed that u_L^C be expanded in a Taylor series which is second order in each of the arguments in equation (40) as follows:

$$u_L^C = G_{ij}^{n}\alpha_{Lij}^{n} + H_{ij}^{n}\alpha_{Lij}^{n}\Delta T_L + I_{ijkl}^{n}\varepsilon_{Lij}\alpha_{Lkl}^{n} + J_{ijkl}^{n\zeta}\alpha_{Lij}^{n}\alpha_{Lkl}^{\zeta}\Delta T_L$$

$$+ L_{ijklmn}^{n\zeta}\varepsilon_{Lij}\alpha_{Lkl}^{n}\alpha_{Lmn}^{\zeta} + \tfrac{1}{2}M_{ijklmn}^{n}\varepsilon_{Lij}\varepsilon_{Lkl}\alpha_{Lmn}^{n}$$

$$+ N_{ijkl}^{n}\varepsilon_{Lij}\alpha_{Lkl}^{n}\Delta T_L + P_{ij}^{n}\alpha_{Lij}^{n}\Delta T_L^2 + \tfrac{1}{2}Q_{ijklmnpq}^{n\zeta}\varepsilon_{Lij}\varepsilon_{Lkl}\alpha_{Lmn}^{n}\alpha_{Lpq}^{\zeta}$$

$$+ R_{ijklmn}^{n\zeta}\varepsilon_{Lij}\alpha_{Lkl}^{n}\alpha_{Lmn}^{\zeta}\Delta T_L + S_{ijkl}^{n\zeta}\alpha_{Lij}^{n}\alpha_{Lkl}^{\zeta}\Delta T_L^2$$

$$+ T_{ijklmn}^{n}\varepsilon_{Lij}\varepsilon_{Lkl}\alpha_{Lkl}^{n}\Delta T_L + U_{ijkl}^{n}\varepsilon_{Lij}\varepsilon_{Lkl}\alpha_{Lkl}^{n}\Delta T_L^2$$

$$+ V_{ijklmnop}^{n\zeta}\varepsilon_{Lij}\varepsilon_{Lkl}\alpha_{Lmn}^{n}\alpha_{Lop}^{\zeta}\Delta T_L + W_{ijklmn}^{n}\varepsilon_{Lij}\varepsilon_{Lkl}\alpha_{Lmn}^{n}\Delta T_L^2$$

$$+ X_{ijklmn}^{n\zeta}\varepsilon_{Lij}\alpha_{Lkl}^{n}\alpha_{Lmn}^{\zeta}\Delta T_L^2 + \tfrac{1}{2}Y_{ijklmn}^{n\zeta}\varepsilon_{Lij}\alpha_{Lkl}^{n}\alpha_{Lmn}^{\zeta}\Delta T_L$$

$$+ Z_{ijklmnpq}^{n\zeta}\varepsilon_{Lij}\varepsilon_{Lkl}\alpha_{Lmn}^{n}\alpha_{Lpq}^{\zeta}\Delta T_L^2 \qquad\qquad , \quad (41)$$

where all terms are at least linear in α_{Lij}^{n} due to the fact

12

that u_L^c depends explicitly on damage, and $\Delta T_L \equiv T_L - T_R$. Thus, substituting (11) and (41) into equations (23) and neglecting higher order terms yields:

$$\sigma_{Lij} = B_{Lij} + E_{Lij}\Delta T_L + C_{Lijkl}\epsilon_{Lkl} + I^\eta_{ijkl}\alpha^\eta_{Lkl} \qquad . \ (42)$$

Restricting the damage to small quantities constitutes a sufficient but not a necessary condition for dropping the higher order terms. Equations (42) may be written in the following alternate form for isothermal conditions

$$\sigma_{Lij} = \sigma^R_{Lij} + C'_{Lijkl}\epsilon_{Lkl} \qquad , \ (43)$$

where

$$\sigma^R_{Lij} \equiv B_{Lij} \qquad , \qquad (44)$$

is the residual stress tensor; and

$$C'_{Lijkl}\epsilon_{kl} \equiv C_{Lijkl}\epsilon_{Lkl} + I^\eta_{Lijkl}\alpha^\eta_{Lkl} \qquad , \qquad (45)$$

defines the effective modulus tensor C'_{Lijkl} for any damage state. Note that although equations (43) are similar to Kachanov's model [1], the stiffness reduction is a first order effect of damage. Note also that the inclusion of higher order terms will result in damage dependent residual and thermal stresses, as well as nonlinear stiffness loss as a function of damage.

Equations (42) are the completed description of the stress-strain relationship. Note that these equations reduce to the standard linear thermoelastic equations in the absence of damage ($\alpha^\eta_{Lij}=0$).

Damage Growth Laws

The model is completed with the construction of the damage growth laws, which may be described in the following differential equation form:

$$\dot{\alpha}^\eta_{Lij} = \Omega^\eta_{ij}(\epsilon_{Lkl}, \dot{\epsilon}_{Lkl}, T_L, \alpha^u_{Lkl}) \qquad , \ (46)$$

or equivalently, when Ω^η_{ij} are single valued functions of time,

$$\alpha_{Lij}^{n}(t_1) = \int_{-\infty}^{t_1} \Omega_{ij}^{n}(\varepsilon_{Lkl}(t), T_L(t), \alpha_{Lkl}^{\mu}(t)) dt \quad . \quad (47)$$

Although the above equations are called "growth" laws they have the more general capability to model such phenomena as healing.

The precise nature of equations (47) is determinable only through a concise experimental program coupled with an understanding of the micromechanics of the medium. Indeed, these growth laws constitute the single most complex link in the model development.

In this section an example of a first generation growth law will be constructed for predicting damage up to the CDS in continuous fiber composites. Experimental evidence suggests that matrix cracks dominate the first phase of damage development in laminated composites [9-11]. Guided by this observation, a single damage tensor is considered in this section: α_{Lij}^{1} representing matrix cracking.

In order to completely define equations (47), it is necessary to construct indicators of both the magnitude and direction of the damage tensor. In this first generation model *it is assumed that the direction of the damage tensor is known a priori and does not vary as the damage state changes.* Specifically, in a typical laminate, it is assumed that, for this simple example, in accordance with equation (35), the locally averaged resultants of $\vec{u}^{c}$ and $\vec{n}^{c}$ are normal to the fiber direction in each ply, as shown in Fig. 4. Thus, for example, in a $0°$ ply $\alpha_{L22}^{1} \neq 0$, and all other components are zero, whereas in a $90°$ ply, $\alpha_{L11}^{1} \neq 0$, and all other components are zero (in global coordinates). In Part II a somewhat more general case of the damage state for matrix cracking will be considered.

Under the above assumptions, the magnitude of the damage tensor is the sole repository for history dependence in each ply. Experimental evidence indicates that for matrix cracking in randomly oriented particulate composites [43] and matrix cracks in fibrous composites [21,22] the growth of damage surface area is related to the energy release rate G by

$$\frac{dS}{dN}2 \propto G^{n} \qquad , \quad (48)$$

where S_2 represents crack area, N represents the number of cycles in a fatigue test, and n is some material parameter. Guided by these results, a similar law is constructed here. Equation (48) may be rewritten in the following form:

$$\frac{dS}{dt}2 = KG^{n} \cdot \frac{dN}{dt} \qquad , \quad (49)$$

14

so that it follows that

$$\dot{\alpha}^1_{L22} = \frac{d\alpha^1_{L22}}{dS_2} \cdot \frac{dS_2}{dt} = \frac{d\alpha^1_{L22}}{dS_2} \cdot KG^n \cdot \frac{dN}{dt} \qquad . \quad (50)$$

Assuming that the energy release rate is essentially mode I and therefore depends on the maximum normal strain, the damage growth law for matrix cracking is thus hypothesized to be of the form

$$\dot{\alpha}^1_{L22} = k_1 \left(\frac{\varepsilon_n - \varepsilon_{nmin}}{\alpha^1_{L22}} \right)^{n_1} \cdot \frac{d\varepsilon}{dt}_n \quad \text{if} \quad \varepsilon_{nmin} < \varepsilon_n \qquad , \text{ and}$$

$$\dot{\alpha}^1_{L22} = k_2 \dot{\varepsilon}_n \qquad \qquad \text{if} \quad \varepsilon_{nmin} \geq \varepsilon_n \qquad , \qquad (51)$$

where ε_n is the local normal strain component which is normal to the fibers. Furthermore, ε_{nmin} is the value of ε_n at which matrix cracking initiates. k_1, k_2, and n are experimentally determined material parameters which may depend on the initial damage state or on history dependent damage other than matrix cracks. The use of ε_n presupposes that the fracture mode is predominantly mode I in nature, which may not be the case in some complex layups. In these cases, mode II and mode III terms may be required. Note that all components of α^1_{Lij} are zero except α^1_{L22}, which is nonzero in the local ply coordinate system wherein the fibers are aligned parallel to the local x_1 axis.

Experimental evidence [44] indicates that in crossply laminates with multiple adjacent crossplies in sequence, it is not uncommon to observe matrix cracks which are curved rather than normal to the plane of the ply. For these cases it is necessary to carry components of α^1_{Lij} in both the x_2 and x_3 coordinate directions. Although it is hypothesized that these components may perhaps be determinable from the orientation of the maximum normal strain, ε_n, this issue is under further investigation by the authors.

Equations (51) complete the description of the damage model for the case of matrix cracking. Integration of these equations in time will lead to current values of the damage tensor which is input to constitutive equations (42). Fig. 5 shows a typical growth history for a specimen subjected to monotonically increasing deformation u(L). It should be pointed out, however, that these equations may be extremely nonlinear and as such must in some cases be integrated numerically with stiff integration schemes [45].

CONCLUSION

Stress-strain relations have been developed herein which account for various forms of damage in continuous fiber composites. Furthermore, a damage growth law has been proposed for matrix cracking in fibrous composites. The model developed herein is thus a complete description necessary to characterize the thermomechanical constitution of a fibrous composite with matrix cracks (excluding failure).

The actual use of this model is complicated by the requirement for numerous experimentally determined quantities, as well as the necessity to determine locally based observable state variables by analytic methods. The construction of these parameters constitutes an entire separate research effort which is considered in Part II.

Finally, it should be pointed out that although an internal state variable growth law has been proposed herein only for matrix cracks, the model is in principle applicable to more complex damage states in laminated composites, and research is underway to consider other damage modes [45].

ACKNOWLEDGEMENT

REFERENCES

1. Kachanov, L.M., 'On the Creep Fracture Time," _Izv. AN SSR, Otd. Tekhn. Nauk_, No. 8, pp. 26-31, 1958 (in Russian).

2. Chaboche, "How to Use Damage Mechanics," _Nuclear Engineering and Design_, Vol. 80, pp. 233-245, 1984.

3. Rabotnov, Y. N., _Creep Problems in Structural Members_, North-Holland, Amsterdam, 1969.

4. Bazant, Z.P., and Belytschko, T., "Strain-Softening Continuum Damage: Localization and Size Effect," _Constitutive Laws for Engineering Materials Theory and Applications_, Desai, C.S., Krempl, E., Kiousis, P.D., and Kundu, T., Eds., Elsevier, New York, Vol. 1, pp. 11-33, 1987.

5. Schapery, R.A., Riggins, M., "Development of Cyclic Non-linear Viscoelastic Constitutive Equations for Marine Sediment," _Numerical Models in Geomechanics_, Dungar, R., Pande, G.N., Studer, L.A., Eds., A.A. Balkema, Rotterdam, pp. 172-182, 1982.

6. Stinchcomb, W.W., and Reifsnider, K.L., "Fatigue Damage Mechanisms in Composite Materials: A Review", _Fatigue Mechanisms_, Proc. of ASTM-NBS-NSF Symp., Kansas City, MO., May 1978, J.J. Fong, ed., ASTM STP 679, 1979, pp. 762-787.

7. Hahn, H.T., "Fatigue Behavior and Life Prediction of Composite Laminates", _Composite Materials: Testing and Design_ (Fifth Conf.), ASTM STP 674, 1979, pp. 383-417.

8. Lehman, M.W., "An Investigation of Intra-Play Microcrack Density Development in a Cross-Ply Laminate," Texas A&M University Mechanics and Materials Research Center, MM 3724-80-11, December, 1980.

9. Stinchcomb, W.W., Reifsnider, K.L,. Yeung, P., and Masters, J., "Effect of Ply Constraint on Fatigue Damage Development in Composite Material Laminates," _Fatigue of Fibrous Composite Materials_, ASTM STP 723, 1981, pp. 65-84.

10. Highsmith, A.L., Stinchcomb, W.W., and Reifsnider, K.L., "Stiffness Reduction Resulting from Transverse Cracking in Fiber-Reinforced Composite Laminates," Virginia Polytechnic Institute and State University, VPI-E-81.33, November, 1981.

11. Reifsnider, K.L., and Jamison, R., "Fracture of Fatigue-Loaded Composite Laminates," _Int. J. Fatigue_, 1982, pp. 187-197.

12. Leichti, K.M., Masters, J.E., Ulman, D.A., and Lehman, M.W., "SEM/TEM Fractography of Composite Materials," AFWAL-TR-82-4035, September, 1982.

13. Ulman, D.A., "Cumulative Damage Model for Advanced Composite Materials," Semi-annual Report No. 3 (FZM-7070) and No. 4 (FZM-

7106), Air Force Materials Laboratory, 1983.

14. Budiansky, B. and O'Connel, R.J., "Elastic Moduli of a Cracked Body," *Int. J. of Solids Structures*, Vol. 12, 1981.

15. Horii, H. and Nemat-Nasser, S., "Overall Moduli of Solids with Microcracks: Load-Induced Anisotropy," *J. Mech. & Phys. Solids*, Vol. 31, No. 2, pp. 155-171, 1983.

16. Laws, N., Dvorak, G.J., and Hejazi, M., "Stiffness Changes in Unidirectional Composites Caused by Crack Systems," *Mechanics of Materials*, Vol. 2, 1983.

17. Margolin, L.G., "Elastic Moduli of a Cracked Body," *Int. J. Fracture*, Vol. 22, 1983.

18. Mura, T., *Micromechanics of Defects in Solids*, Martinus Nijhoff Publ., The Hague, Boston, 1982.

19. Schapery, R.A., "On Viscoelastic Deformation and Failure Behavior of Composite Materials with Distributed Flaws," *Advances in Aerospace Structures and Materials*, ASME AD-01, 1981, pp. 5-20.

20. Schapery, R.A., "Models for Damage Growth and Fracture in Nonlinear Viscoelastic Particulate Composites," *Proc. 9th U.S. National Cong. Appl. Mech.*, August, 1982.

21. Chou, P.C., Wang, A.S.D., and Miller, H., "Cumulative Damage Model for Advanced Composite Materials," AFWAL-TR-82-4-83, September, 1982.

22. Wang, A.S.D., and Bucinell, R.B., "Cumulative Damage Model for Advanced Composite Materials," Interim Report No. 6, Feb. 1984.

23. Poursartrip, A., et al., "Damage Accumulation during Fatigue of Composites," Cambridge University (England) Dept. of Engineering, Nov. 1981, p. 29.

24. Miner, M.A., "Cumulative Damage in Fatigue," *J. Appl. Mech.*, Vol. 12, 1945, p. 159.

25. Hashin, Z., and Rotem, A., "A Cumulative Damage Theory of Fatigue Failure," AFOSR-TR-77-0717, 1977.

26. Coleman, B.D., and Gurtin, M.E., "Thermodynamics with Internal State Variables," *Journal of Chemical Physics*, Vol. 47, pp. 597-613, 1967.

27. Lemaitre, J. and Chaboche, J.L., "Aspect Phenomenologique de la Rupture por Endommagement," *Journal de Mecanique Appliquee*, Vol. 2, 1978, pp. 317-365.

28. Bodner, S.R., "A Procedure for Including Damage in

Constitutive Equations for Elastic-Viscoplastic Work-Hardening Materials," *Physical Non-Linearities in Structural Analysis*, Springer-Verlag, Berlin, 1981, pp. 21-28.

29. Krajcinovic, D., and Fonseka, G.U., "The Continuous Damage Theory of Brittle Materials-Part I - General Theory," *J. Appl. Mech.*, Vol. 48, 1981, pp. 809-815.

30. Krajcinovic, D., "Continuum Damage Mechanics," *Applied Mechanics Reviews*, Vol. 37, No. 1, January 1984.

31. Krajcinovic, D., "Continuous Damage Mechanics Revisted: Basic Concepts and Definitions," To appear in *Journal of Applied Mechanics*, 1984.

32. Davidson, L., and Stevens, A.L., "Thermomechanical Constitution of Spalling Elastic Bodies," *J. Appl. Phys.*, Vol. 44, No. 2, pp. 668-674, 1973.

33. Kratochvil, J., and Dillon, O.W., Jr., "Thermodynamics of Elastic-Plastic Materials as a Theory with Internal State Variables," *J. of Applied Physics*, Vol. 40, 1969, pp. 3207-3218.

34. Kratochvil, J. and Dillon, O.W., Jr., "Thermodynamics of Crystalline Elastic-Visco-Plastic Materials," *J. of Applied Physics*, Vol. 44, 1970, pp. 1470-1478.

35. O'Brien, T.K., "An Evaluation of Stiffness Reduction as a Damage Parameter and Criterion for Fatigue Failure in Composite Materials," Ph.D. Dissertation, Virginia Polytechnic Institute and State University, October, 1978.

36. Talreja, R., "A Continuum Mechanics Characterization of Damage in Composite Materials," *Proc. R. Soc. London*, Vol. 399A, 1985, pp. 195-216.

37. Talreja, R., "Residual Stiffness Properties of Cracked Composite Laminates," Danish Center for Applied Mathematics and Mechanics, The Technical University of Denmark, Report No. 277, Feb., 1984.

38. Talreja, R., "Transverse Cracking and Stiffness Reduction in Composite Laminates," Danish Center for Appl. Mathematics and Mechanics, The Technical University of Denmark, July, 1984.

39. Arenburg, R.T., "Analysis of the Effect of Matrix Degradation of Fatigue Behavior of a Graphite/Epoxy Laminate," Texas A&M Mechanics and Materials Center (M.S. Thesis), MM 3724-82-2, May, 1982.

40. Hashin, Z., "Analysis of Composites-A Survey," *J. Appl. Mech.*, Vol. 50, pp. 481-505, 1983.

41. Coleman, B.D., and Noll, W., "The Thermodynamics of Elastic Materials with Heat Conduction and Viscosity," *Archive for*

Rational Mechanics and Analysis, Vol. 13, p. 167, 1963.

42. Kachanov, M., "Continuum Theory of Media with Cracks," Izv.
AN SSSR, _Mekhanika Tverdogo Tela_, ASCE, Vol. 7, pp. 54-59, 1972.

43. Schapery, R.A. and Riggins, M., "Development of Cyclic
Nonlinear Viscoelastic Constitutive Equations for Marine
Sediment," MM 3168-82-4, Texas A&M University, May 1982.

44. Norvell, R.G., "An Investigation of Damage Accumulation in
Graphite/Epoxy Laminates," Texas A&M University M.S. Thesis,
August, 1985.

45. Gear, C.W., "The Automatic Integration of Stiff Ordinary
Differential Equations," _Information Processing_, Vol. 1, 1969,
pp. 187-193.

45. Groves, S.E., Allen, D.H., and Harris, C.E., "A Cumulative
Damage Model for Continuous Fiber Composite Laminates with Matrix
Cracking and Interply Delaminations," Texas A&M University
Mechanics and Materials Center, MM 5023-86, August, 1986.

APPENDIX

Consider a local volume element with some damage state, where the crack faces are defined as traction free surfaces, as shown in Fig. A1 (a1). For convenience we show only one crack, although in actuality the damage must be statistically homogeneous in V_L. Now replace the actual cracks with fictitious cracks which are described by the bounding surface between elastic and inelastic response near cracks, as shown in (a2). We define this surface to be S_2. In order to insure that the total mechanical states in the two systems are identical, the fictitious case must include tractions labelled T_i^F on S_2.

Now suppose that V_L is subjected to boundary tractions on S_1 in the undamaged state as shown in (b1). We define an equivalent elastic problem in which the surface S_2 described in (a2) is cut from V_L and elastic tractions T_i^E are applied on S_2 so that the total mechanical states of systems (b1) and (b2) are equivalent.

The actual system of interest is described in (a1). However, for pragmatic reasons we wish to replace the actual system with a fictitious system with equivalent mechanical state. To do this, we first replace (a1) with (a2), which by definition has equivalent mechanical state. Next, we define a system equivalent to (a2), such that

$$T_i^C \equiv T_i^F - T_i^E \implies T_i^F = T_i^C + T_i^E \quad , \quad (A1)$$

as shown in (c). Integrating the balance of energy (4) over the local volume and dividing through by the local volume results in

$$\frac{1}{V_L}\int_{V_L} \dot{u}\,dV - \frac{1}{V_L}\int_{V_L} \sigma_{ij}\dot{\epsilon}_{ij}\,dV + \frac{1}{V_L}\int_{V_L} q_{j,j}\,dV = \frac{1}{V_L}\int_{V_L} r\,dV \quad . \quad (A2)$$

Now consider the second term in equation (A2). Recall that since σ_{ij} is a symmetric tensor

$$\sigma_{ij}\dot{\epsilon}_{ij} = \frac{1}{2}\sigma_{ij}(\dot{u}_{i,j} + \dot{u}_{j,i}) = \sigma_{ij}\dot{u}_{i,j} \quad . \quad (A3)$$

Thus, assuming that the stresses are negligible in V_c, the volume enclosed by S_2, using the divergence theorem and substituting Cauchy's formula gives

$$\frac{1}{V_L}\int_{V_L}\sigma_{ij}\dot{\varepsilon}_{ij}dV = \frac{1}{V_L}\int_{V_L-V_c}\sigma_{ij}\dot{u}_{i,j}dV = \frac{1}{V_L}\int_{S_1}T_i\dot{u}_idS + \frac{1}{V_L}\int_{S_2}T_i^F\dot{u}_idS$$

$$= \frac{1}{V_L}\int_{S_1}T_i\dot{u}_idS + \frac{1}{V_L}\int_{S_2}T_i^E\dot{u}_idS + \frac{1}{V_L}\int_{S_2}T_i^C\dot{u}_idS \qquad , \quad (A4)$$

where n_j are the components of the unit outer normal vector to the surface $S = S_1 + S_2$. Now define

$$\dot{u}_L^C \equiv -\frac{1}{V_L}\int_{S_2}T_i^C\dot{u}_idS \qquad , \quad (A5)$$

which is the effective specific mechanical power output of the continuum due to the crack surface tractions. This term contains both the mechanical power due to crack extension as well as the mechanical power due to apparent stiffness loss caused by existing cracks. For the special case of a reversible process this is the time rate of change of surface energy release per unit local volume due to cracking in V_L. Furthermore, define

$$\varepsilon_{Lij} \equiv \frac{1}{V_L}\int_{S_1}\frac{1}{2}(u_in_j+u_jn_i)dS \qquad , \quad (A6)$$

and

$$\sigma_{Lij} \equiv \frac{1}{V_L}\int_{S_1}\frac{1}{2}(\sigma_{im}n_mx_j+\sigma_{jm}n_mx_i)dS = \frac{1}{V_L}\int_{V_L}\sigma_{ij}dV \qquad . \quad (A7)$$

Therefore, for the case of either spacially uniform surface tractions or displacements which are linear in coordinates on S_1 one readily obtains

$$\sigma_{Lij}\dot{\varepsilon}_{Lij} = \frac{1}{V_L}\int_{S_1}\sigma_{ij}\dot{u}_in_jdS = \frac{1}{V_L}\int_{S_1}T_i\dot{u}_idS \qquad . \quad (A8)$$

Although it will be assumed in the remainder of this paper that the above conditions are satisfied, they need only be approximately true if V_L is statistically homogeneous. Thus,

equation (A4) becomes

$$\frac{1}{V_L} \int_{V_L} \sigma_{ij} \dot{\epsilon}_{ij} dV = \sigma_{Lij}\dot{\epsilon}_{Lij} + \frac{1}{V_L} \int_{S_2} T_i^E \dot{u}_i dS - \dot{u}_L^c \qquad . \quad (A9)$$

Define also

$$q_{Li,j} \equiv \frac{1}{V_L} \int_{S_1} q_i n_j dS \qquad , \quad (A10)$$

and

$$r_L \equiv \frac{1}{V_L} \int_{V_L} r \, dV \qquad . \quad (A11)$$

Now define

$$\dot{u}_{EL} \equiv \frac{1}{V_L} \int_{V_L} \dot{u} \, dV - \frac{1}{V_L} \int_{S_2} T_i^E \dot{u}_i dS \qquad , \quad (A12)$$

which can be seen from Fig. A1 (b) to be the equivalent internal energy rate that would be produced in the body without cracks. Note that u_{EL} is not path dependent since it represents elastic response. Substituting equations (A4), (A5),(A9), (A10), (A11), and (A12) into equation (A2) yields the following locally averaged balance of energy:

$$\dot{u}_{EL} + \dot{u}_L^c - \sigma_{Lij}\dot{\epsilon}_{Lij} + q_{Lj,j} = r_L \qquad , \quad (A13)$$

We now define the effective internal energy u_L' (which may be path dependent) such that

$$\dot{u}_L' \equiv \dot{u}_{EL} + \dot{u}_L^c \qquad , \quad (A14)$$

Substitution of (A14) into (A13) results in

$$\dot{u}_L' - \sigma_{Lij}\dot{\epsilon}_{Lij} + q_{Lj,j} = r_L \qquad , \quad (A15)$$

which can be seen to be equivalent in form to energy balance law (4).

In order to construct a similar statement for entropy production inequality (5), first multiply through by T and then integrate over the local volume V_L and divide by this quantity to obtain

$$\frac{1}{V_L} \int_{V_L} \dot{s} T dV - \frac{1}{V_L} \int_{V_L} r dV + \frac{1}{V_L} \int_{V_L} T(q_j/T)_{,j} dV \geq 0 \qquad \text{(A16)}$$

Now define

$$T_L \equiv \frac{1}{V_L} \int_{V_L} T dV \qquad \text{(A17)}$$

and

$$\dot{s}_L \equiv \frac{1}{T_L V_L} \int_{V_L} \dot{s} T dV \qquad \text{(A18)}$$

so that substitution of definitions (A11), (A17) and (A18) into (A16) will result in

$$\dot{s}_L T_L - r_L + \frac{1}{V_L} \int_{V_L} T(q_j/T)_{,j} dV \geq 0 \qquad \text{(A19)}$$

Now note that the last term in (A19) may be written as follows using the product rule:

$$\frac{1}{V_L} \int_{V_L} T(q_j/T)_{,j} dV = \frac{1}{V_L} \int_{V_L} q_{j,j} dV - \frac{1}{V_L} \int_{V_L} (q_j g_j/T) dV \qquad \text{(A20)}$$

Define now

$$T_{L,j} \equiv \frac{1}{V_L} \int_{S_1} T n_j dS \qquad \text{(A21)}$$

Thus, for the case when T is a linear function of coordinates in V_L, definitions (A10) and (A21) may be substituted into (A20) and this result into (A19) to obtain

$$\dot{s}_L - \frac{r_L}{T_L} + (\frac{q_L j}{T_L}),_j \geq \dot{s}_c \geq 0 \qquad , \text{(A22)}$$

where

$$\dot{s}_c \equiv (1/T_L V_L) \int_{V_L} (q_j g_j / T) dV - (1/T_L^2 V_L^2) \int_{V_L} q_j dV : \frac{1}{V_L} \int_{V_L} g_j dV . \text{(A23)}$$

$\dot{s}_c$ can be shown to be strictly nonnegative with the assumption that T is everywhere nonnegative, along with equation (9).

We now assume that the local volume is small enough compared to B that the standard procedure may be utilized to obtain the linear conservation of momentum equations [40]

$$\sigma_{Lji,j} = 0 \qquad , \text{(A24)}$$

similar to pointwise equations (2), and the conservation of angular momentum may also be obtained

$$\sigma_{Lij} = \sigma_{Lji} \qquad , \text{(A25)}$$

similar to equations (3). Thus, it is assumed that no body moments are introduced via material inhomogeneity or other sources. This assumption must be relaxed when the model is utilized for interply delamination, since in this case the local volume element goes through the entire laminate thickness.

Equations (A24), (A25), (A15), (A22), (A14), (A18), (A5), (A7), and (A6) are rewritten as equations (12) through (20), respectively, in the main text.
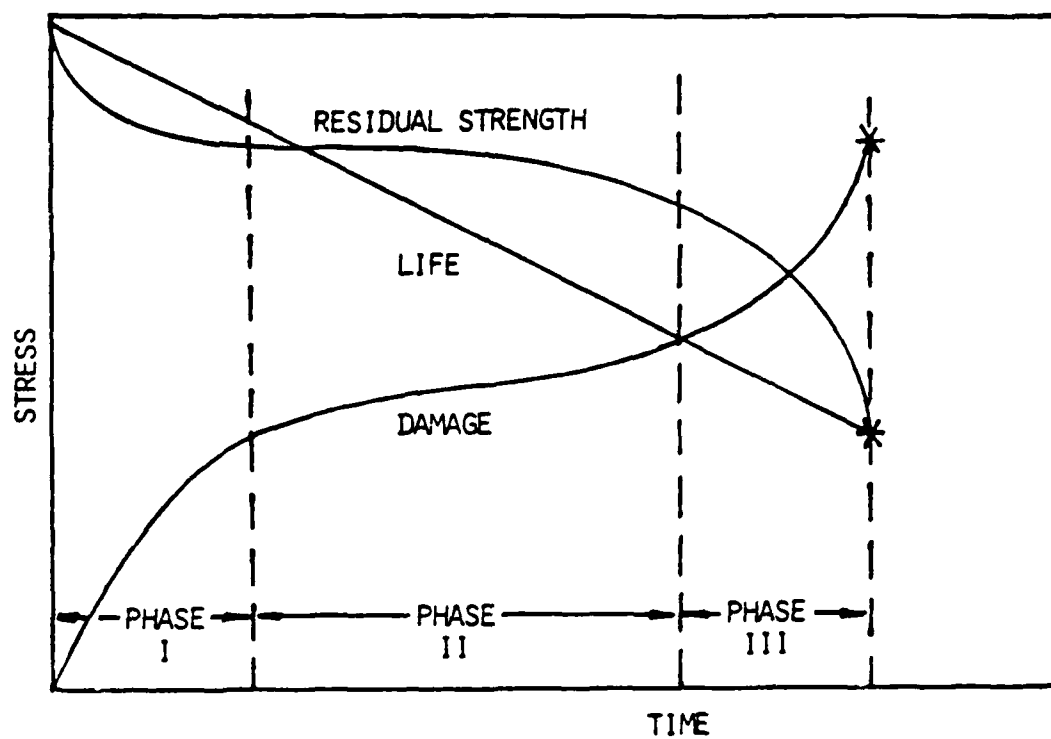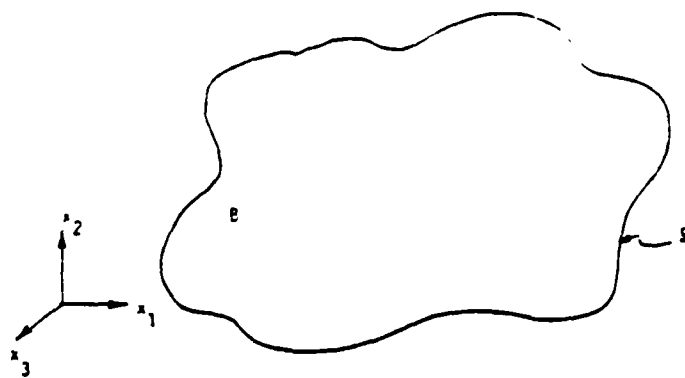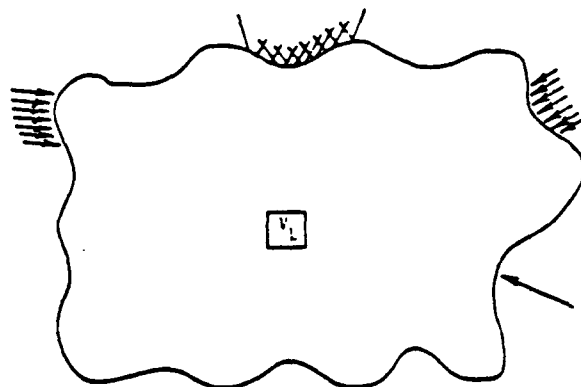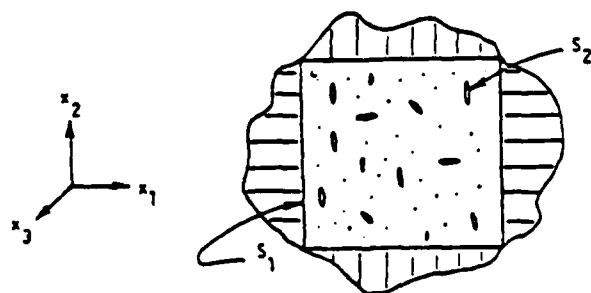
Fig. 1   Damage Accumulation in a Continuous Fiber
          Composite Subjected to Monotonic Load or
          Strain Controlled Cyclic Fatigue (from ref. 8).

(a)
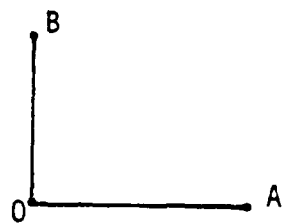
(b)

(c)

Fig. 2   Structural Component Labelled B
          a) Undamaged State
          b) With Applied Tractions
          c) Local Volume Element
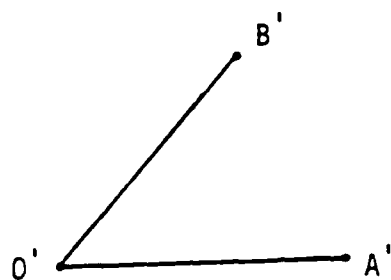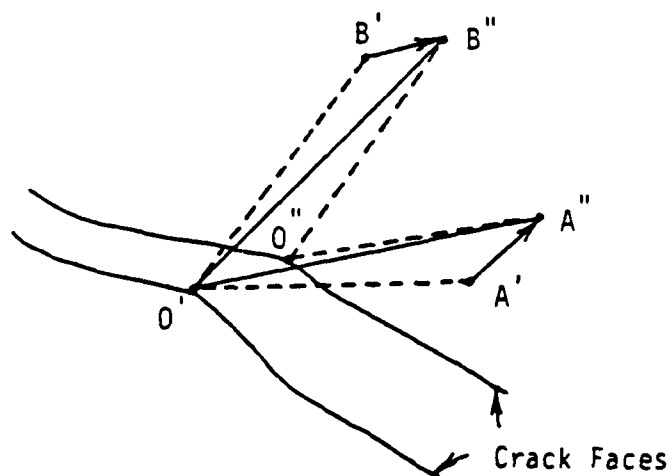
Fig. 3 Kinematics of the Damage Process
   a) Point "O" Prior to Deformation,
   b) Point "O" After Deformation and Prior to Fracture,
   c) Point "O" After Fracture.
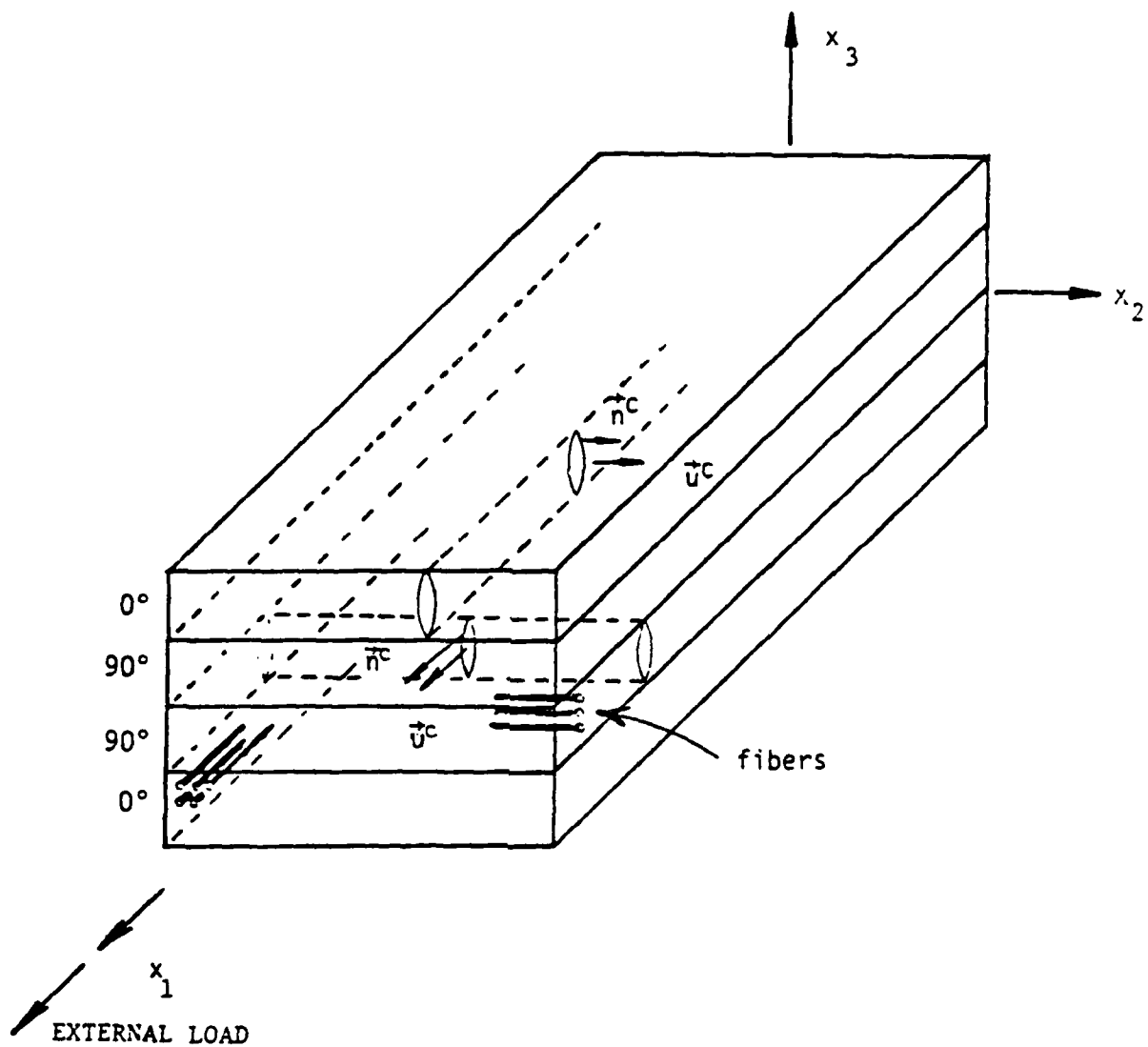
Fig. 4 Assumed Damage Vector Directions in a [0,90]$_s$ Laminate.
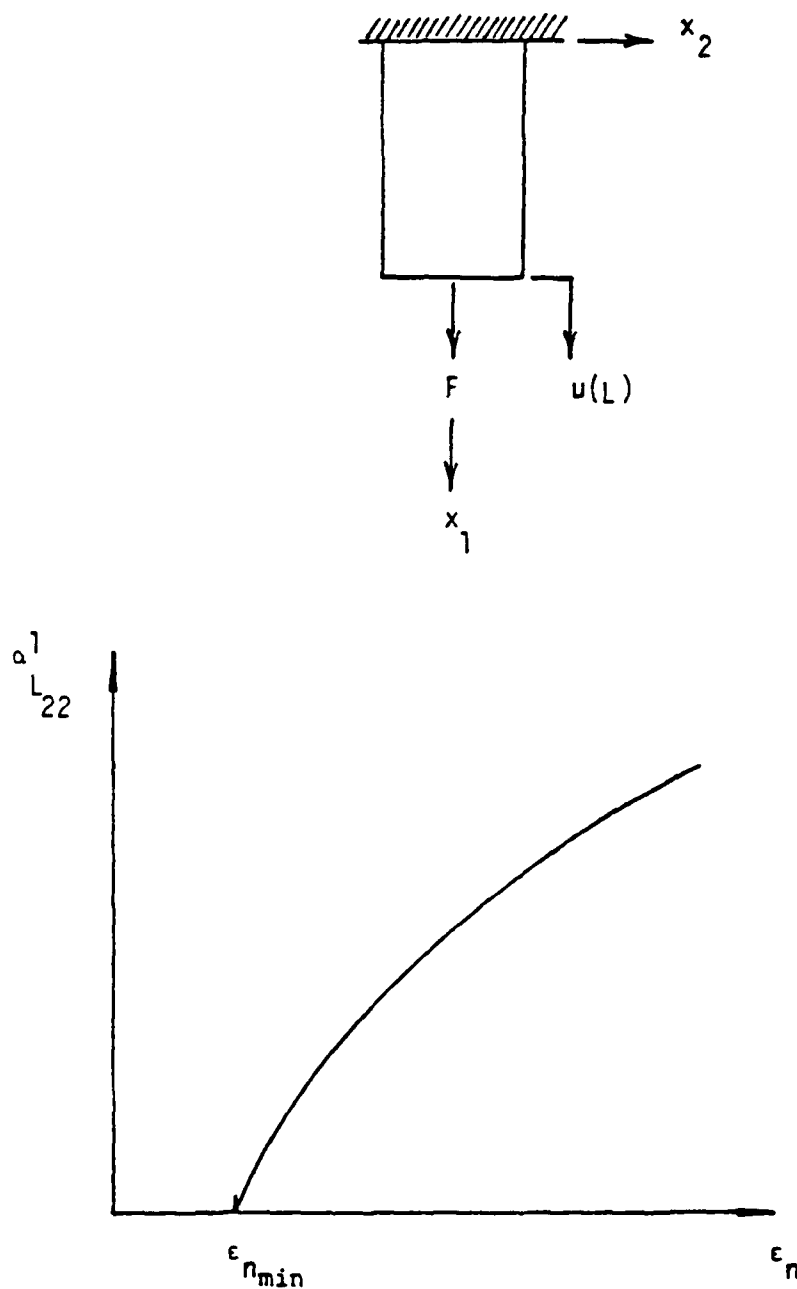
Fig. 5 Typical Growth of damage in a Specimen with Matrix Cracks.
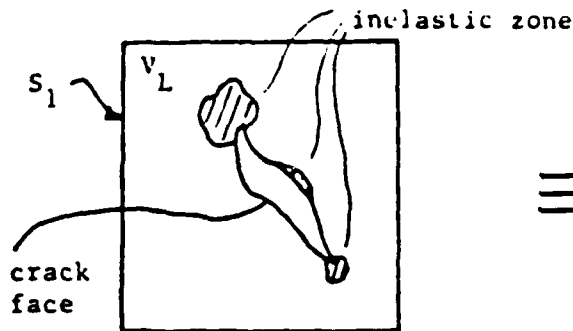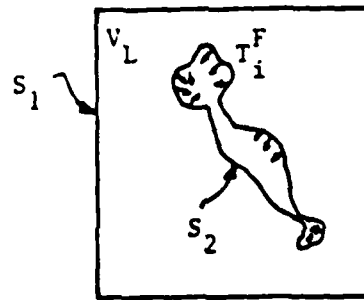
(a1) actual damage   (a2) fictitious equivalent damage

(a) Replacement of actual crack with fictitious crack
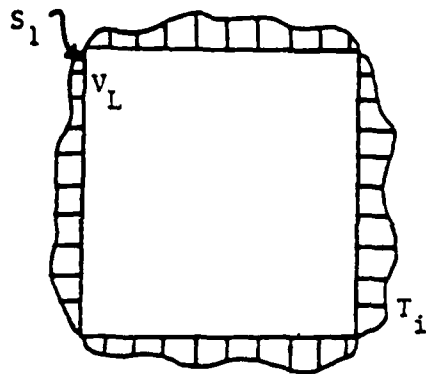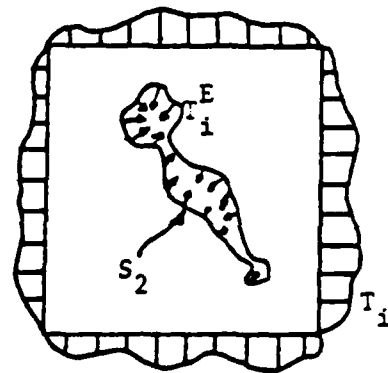
(b1) undamaged V_L (b2) equivalent V_L with internal surfaces described in (a2)

(b) V_L subjected to tractions without damage
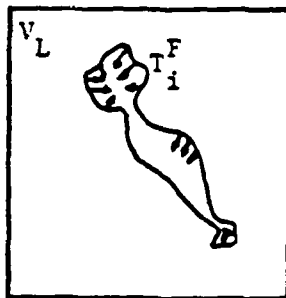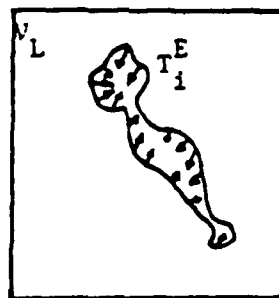
(c1) same as (a2)   (c2) same as (b2)   (c3) effective tractions

Fig. Al   Description of Local Volume Element with Damage

Appendix 7.2

A THERMOMECHANICAL CONSTITUTIVE THEORY FOR ELASTIC
COMPOSITES WITH DISTRIBUTED DAMAGE

PART II: Application to Matrix Cracking
in Laminated Composites

by

D.H. Allen

C.E. Harris

and

S.E. Groves

Aerospace Engineering Department
Texas A&M University
College Station, Texas 77843

A THERMOMECHANICAL CONSTITUTIVE THEORY FOR ELASTIC COMPOSITES WITH DISTRIBUTED DAMAGE

PART II: Application to Matrix Cracking in Laminated Composites

by

D.H. Allen
C.E. Harris

Aerospace Engineering Department
Texas A&M University
College Station, Texas 77843

and

S.E. Groves

Lawrence Livermore Laboratories
Livermore, CA 94550

ABSTRACT

A continuum mechanics approach is utilized herein to develop a model for predicting the thermomechanical constitution of initially elastic composites subjected to both monotonic and cyclic fatigue loading. In this model the damage is characterized by a set of second order tensor valued internal state variables representing locally averaged measures of specific damage states such as matrix cracks, fiber-matrix debonding, interlaminar cracking, or any other damage state. Locally averaged history dependent constitutive equations are constructed utilizing constraints imposed from thermodynamics with internal state variables. In Part I the thermodynamics with internal state variables was constructed and it was shown that suitable definitions of the locally averaged field variables led to useful thermodynamic constraints on a local scale containing statistically homogeneous damage. Based on this result the Helmholtz free energy was then expanded in a Taylor series in terms of strain, temperature, and the internal state variables to obtain the stress-strain relation for composites with damage. In Part II, the three dimensional tensor equations from Part I [1] are simplified using symmetry constraints. After introducing engineering notation and expressing the constitutive equations in the standard laminate coordinate system, a specialized constitutive model is developed for the case of matrix cracks only. The potential of the model to predict degradation of effective stiffness components is demonstrated by solving the problem of transverse matrix cracks in the 90° layer of several crossply laminates.

To solve the example problems, the undamaged moduli are determined from experimental data. The internal state variable for matrix cracking is then related to the strain energy release rate due to cracking by utilizing linear elastic fracture

mechanics. These values are then utilized as input to a modified laminate analysis scheme to predict effective stiffnesses in a variety of crossply laminates. The values of effective (damage degraded) stiffnesses predicted by the constitutive model are in agreement with experimental results. The agreement obtained in these example problems, while limited to transverse matrix cracks only, demonstrates the potential of the constitutive model to predict degraded stiffnesses.

INTRODUCTION

In Part I it was hypothesized that damage can be modeled by a set of second order tensor valued internal state variables (ISV's) which represent locally averaged measures of cracking on a scale assumed to be small compared to the boundary value problem of interest. Continuum mechanics [1] was then utilized to construct stress-strain relations in which all components of the degraded modulus tensor can be determined for a given damage state. The intent of Part II is to apply this damage model to the analysis of continuous fiber-reinforced laminated composites. The current paper seeks only to predict axial stiffness as a function of a known damage state. It therefore represents an application only of the stress-strain relations. The all-important ISV growth laws are the subject of ongoing research. Furthermore, as a long range research goal, it is hoped that the characterization of the ISV's for damage will lead to the development of a model for structural failure in terms of the internal state within any local volume in a typical structural component.

Considerable experimental research has been performed in the last decade detailing the growth of damage in laminated composites under both monotonic and cyclic loading conditions [2-8]. The significance of this damage lies in the fact that numerous global material properties such as stiffness, damping and residual strength may be substantially altered during the life of the component. It has been found that the first phase of fatigue is typified by development of a characteristic damage state (CDS) [9] which is composed primarily of matrix cracking in off-axis plies. During the second phase of damage development the CDS contributes to fiber-matrix debonding, delamination, and fiber microbuckling. These phenomena in turn contribute to a tertiary damage phase in which edge delamination and fiber fracture lead to ultimate failure of the specimen [6].

Analytical modeling of stiffness loss in laminated composites with damage appears to be only recently studied. The earliest attempts fall under the general heading of ply discount methods, in which various phenomenological models have been developed to discount ply properties in the presence of damage [10-12]. Axial stiffness reduction and stress distribution in the CDS have also been predicted using a one-dimensional shear lag concept [5]. Kachanov's modulus reduction technique [13] has also been applied to fibrous composites [14] and although promising results were obtained, the model was utilized in uniaxial form only.

Similarly, very little research has been performed to develop ISV growth laws modelling the evolution of damage in laminated composites as a function of load history. Although extended forms of Miner's rule [15] have been proposed for life prediction [16,17], they are based on simplified microphysical models at this time.

A complex interactive experiment and analysis model (called a mechanistic model) has been proposed [18] for prediction of life of damaged composites. The mechanistic model appears to require numerous experimental results for each geometric layup in

order to determine which damage mode results in failure.

Perhaps the most significant attempts to model damage in laminated composites are contained in references 19-23. The first two of these use analytical methods to model a medium with oriented cracks and thus fall under the heading of microphysical techniques. The first of these two uses variational principles to obtain effective moduli for linear elastic cracked plies [19]. The second uses the self-consistent scheme to predict stiffness loss in a single ply as a function of surface area of matrix cracks [20]. It has not to these authors knowledge been applied to general laminate analysis. Furthermore, to our knowledge no analytic microphysical technique has yet been developed for predicting stiffness loss in laminated composites when damage modes other than matrix cracking occur.

As stated in Part I, the current model is phenomenological in the sense that the local volume element is modelled experimentally. Another phenomenological model has been proposed in the literature for laminated composites [21-23], and this model has significantly influenced the current model development. Nevertheless, there exist significant differences between these two phenomenological models. The most significant difference is that the damage ISV in Talreja's model is a vector, whereas that proposed herein is a second order tensor. Support for the second order tensorial nature of the ISV has been supplied in reference 24. Recently, Talreja has modified his ISV description somewhat to include second order tensors [25]. Furthermore, the vector-valued model appears at this time to be laminate specific. Although both models have been applied to the combined modes of matrix cracking and internal delamination [26,27], these attempts must be considered embryonic at this time. It is our contention that both models warrant further study, especially in anisotropic media.

The literature review cited above and in Part I indicates that although substantial progress has been made in damage modelling, the principal results to date deal only with isotropic homogeneous media. It is the contention of these authors that the material heterogeneity and layered orthotropy encountered in laminated composites requires that a more advanced model be developed for these media. The tensorial nature of the damage ISV's proposed in Part I may provide this capability.

In this paper the general constitutive model developed in Part I is specialized for the single damage mode of matrix cracking in the 90° plies of crossply laminates. Properties of a single lamina with known damage are utilized to specify the value of the ISV as a function of damage state. This expression for the matrix crack ISV is then used to predict the damage-degraded axial stiffness of crossply laminates with a variety of stacking sequences. The validity of the constitutive model formulation is verified by comparing the predicted values of stiffness to experimentally measured values for other stacking sequences, thus demonstrating that at least for this case the model is independent of stacking sequence.
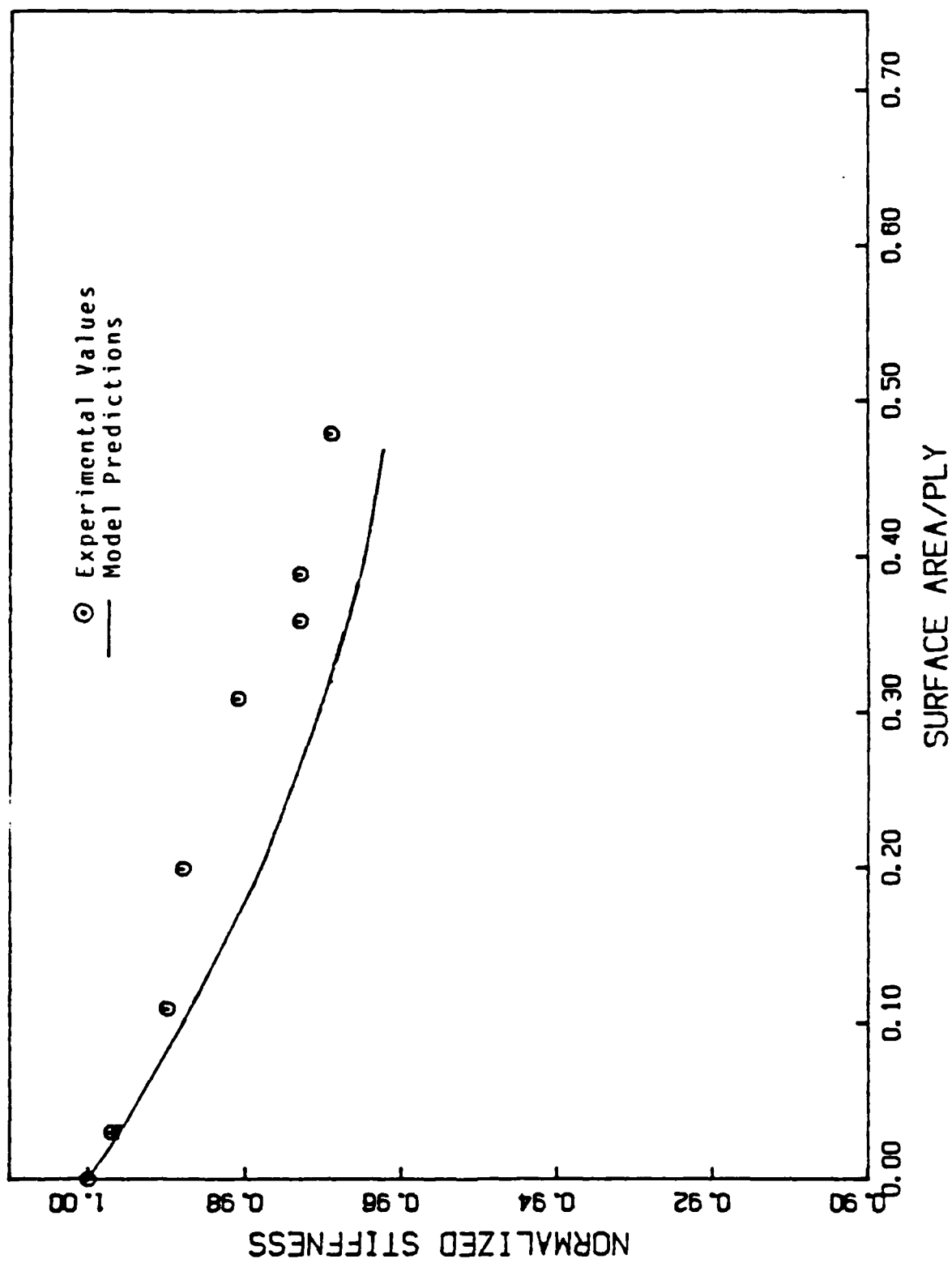
2

Fig. 5.   Model vs. Experiment for [0,90]$_s$ Laminate
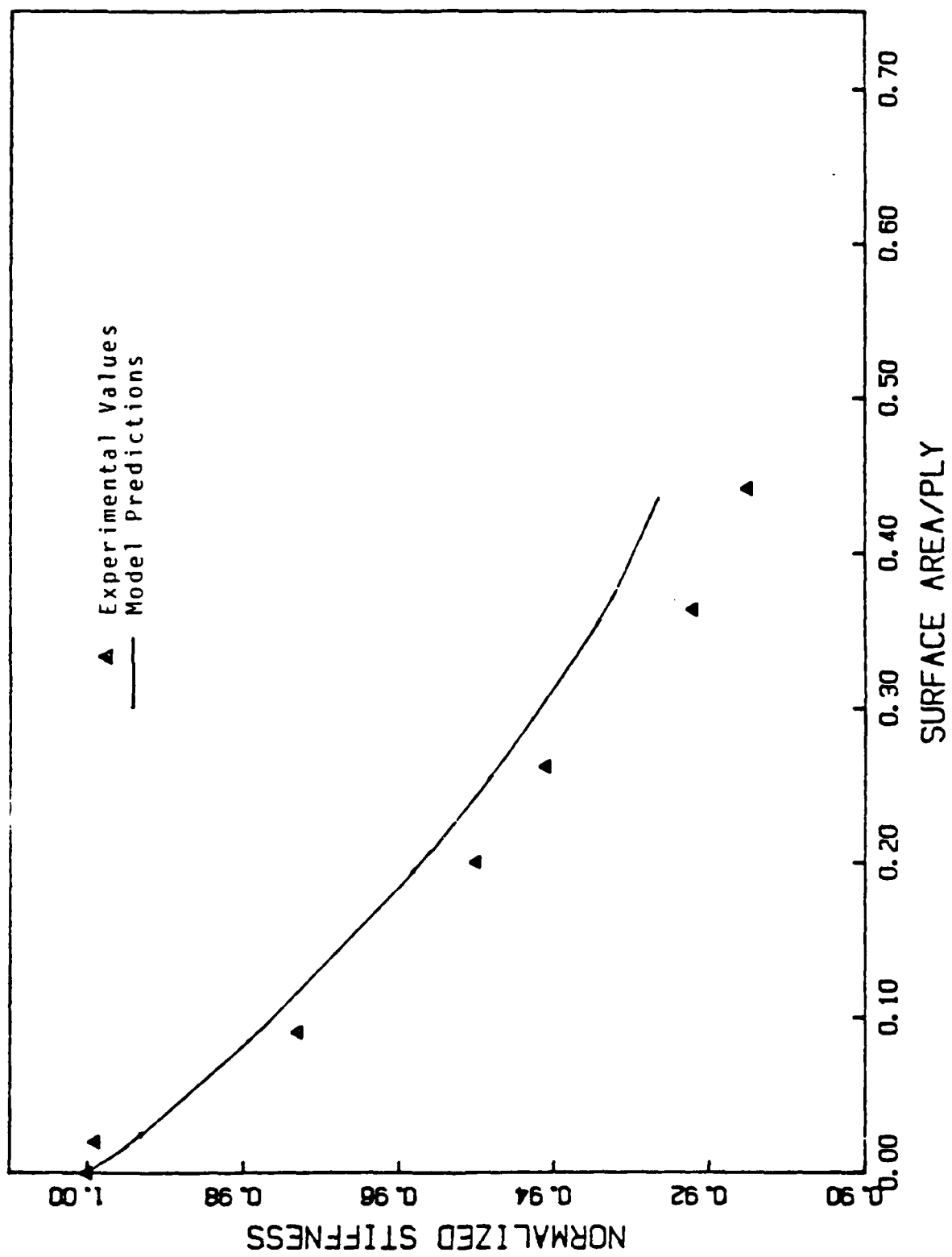
Fig. 6. Model vs. Experiment for $[0,90_2]_s$ Laminate
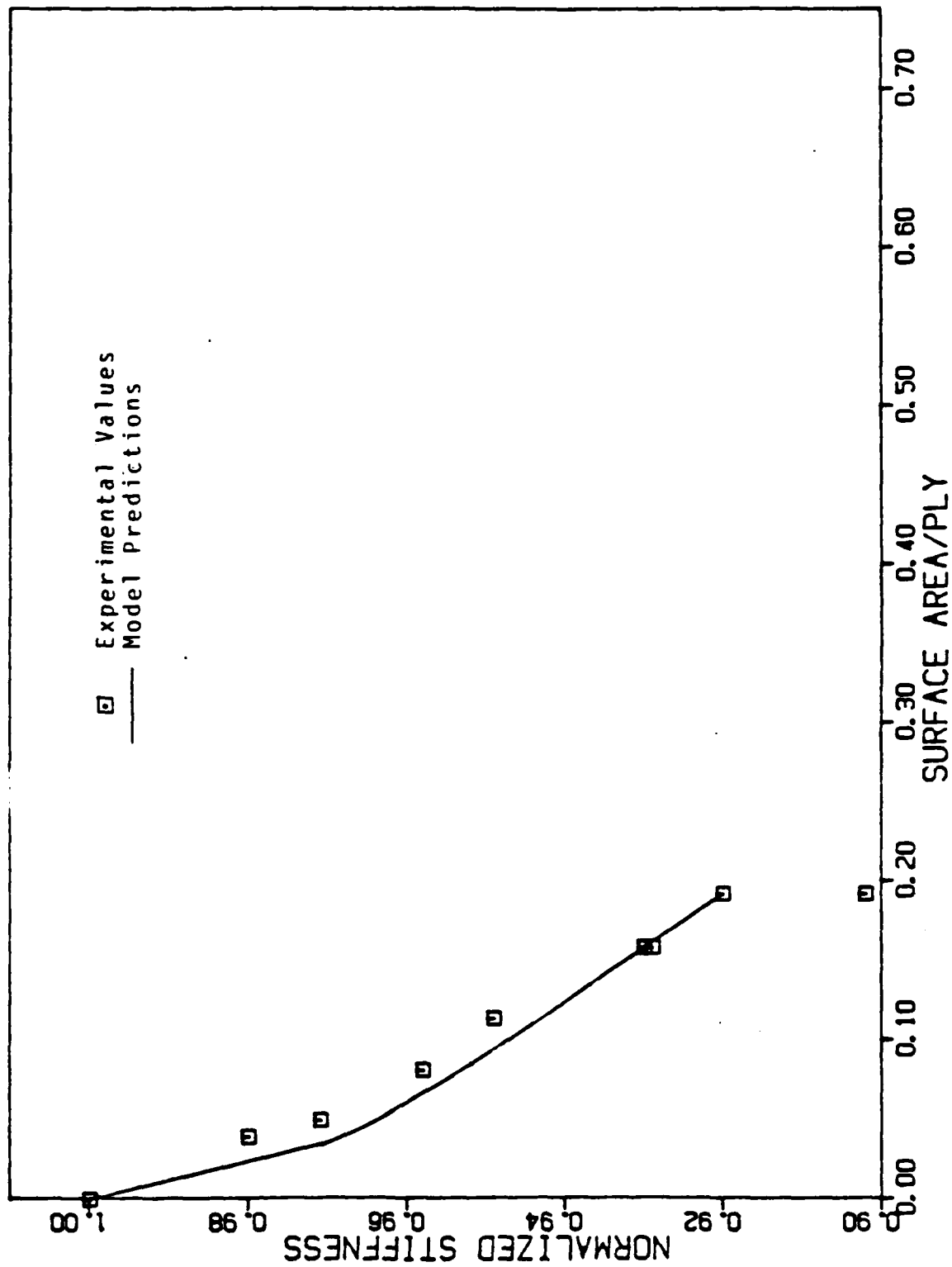
Fig. 7 Model vs. Experiment for $[0,90_3]_s$ Laminate

SIMPLIFICATION OF THE MODEL

We now consider the stress-strain relation described in equations (42) through (45) of Part I (see Appendix A). For the examples to be considered herein, it is assumed that all residual stress components are zero ($\sigma_{Lij}^R = 0$), and that there are no temperature changes ($\Delta T_L = 0$).

Reduction to Single-Index Notation

By incorporating the symmetry of the stress and strain tensors, the quadratic dependence of the Helmholtz free energy on strain, and the Voigt single index notation [28], the constitutive equations reduce to (see Appendix A)

$$\sigma_i = C_{ij}\epsilon_j + I_{ik}^{\eta}\alpha_k^{\eta} \qquad . \quad (1)$$

Although we have dropped the subscript L, all quantities in equations (1) represent locally averaged measures. The subscripts i and j range from 1 to 6, the subscript k ranges from 1 to 9, and the superscript η ranges from 1 to N, the number of damage modes.

At this point, further reductions can be made to the number of unknown constants in equations (1) only by specifying the material symmetry and specific damage modes of interest.

Material Symmetry Constraints

Material symmetries may now be utilized to further simplify the constitutive equations. The material in question is assumed to be initially transversely isotropic in the undamaged state on the local scale, where the plane of isotropy is the $x_2 - x_3$ plane shown in Fig. 1. In the undamaged state the modulus tensor C_{ij} is given by [29]

$$[C] = \begin{bmatrix} C_{11} & C_{12} & C_{12} & 0 & 0 & 0 \\ C_{12} & C_{22} & C_{23} & 0 & 0 & 0 \\ C_{12} & C_{23} & C_{22} & 0 & 0 & 0 \\ 0 & 0 & 0 & C_{44} & 0 & 0 \\ 0 & 0 & 0 & 0 & C_{55} & 0 \\ 0 & 0 & 0 & 0 & 0 & C_{55} \end{bmatrix} \qquad . \quad (2)$$

where $C_{44} = 2(C_{22} - C_{23})$.

3

It is assumed that the crack induces orthotropy in three planes: the plane of the crack, the plane in which the crack opening displacement $\bar{u}^c$ and crack normal $\bar{n}^c$ lie, and a third plane which is orthogonal to the first two. Therefore, the damage tensor I_{ik}^1 is an orthotropic tensor containing 15 unknown constants in the coordinates described by the crack geometry (see Appendix B), given by

$$[I^1] = \begin{bmatrix} I_{11}^1 & I_{12}^1 & I_{13}^1 & 0 & 0 & 0 & 0 & 0 & 0 \\ I_{21}^1 & I_{22}^1 & I_{23}^1 & 0 & 0 & 0 & 0 & 0 & 0 \\ I_{31}^1 & I_{32}^1 & I_{33}^1 & 0 & 0 & 0 & 0 & 0 & 0 \\ 0 & 0 & 0 & I_{44}^1 & I_{45}^1 & 0 & 0 & 0 & 0 \\ 0 & 0 & 0 & 0 & 0 & I_{56}^1 & I_{57}^1 & 0 & 0 \\ 0 & 0 & 0 & 0 & 0 & 0 & 0 & I_{68}^1 & I_{69}^1 \end{bmatrix} \qquad . \quad (3)$$

Thus, the complete constitutive equations (1) (assuming the damage growth law is known) require the determination of 5 independent material constants for the undamaged modulus tensor C_{Lij}, and 15 independent constants for the damage tensor, I_{ik}^1. It should be noted, however, that the planes of these symmetries will not coincide unless the crack displacement $\bar{u}^c$ is oriented parallel to the x_1, x_2, or x_3 axis in ply coordinates.

Application to Matrix Cracking in Continuous Fiber Laminates

As discussed in the introduction, the capability of the constitutive model will be demonstrated by considering the case of matrix cracking in continuous fiber laminated composites. An example of this damage state is shown schematically in Fig. 2. In order to apply the proposed constitutive model to this system we first examine the response of a single ply subjected to transverse matrix cracking, as previously shown in Fig. 1. Assuming that the crack geometry is symmetric about normals to each of the ply coordinates, the internal state variable associated with matrix cracking is represented in ply coordinates by

$$[\alpha_k^1] = [\, 0 \quad \alpha_2^1 \quad 0 \quad 0 \quad \alpha_5^1 \quad 0 \quad 0 \quad \alpha_8^1 \quad 0 \,] \qquad , \quad (4)$$

where the single subscripted notation is defined by equations (7a). This implies that the crack normal $\bar{n}^c$ in a single ply is parallel to the local x_2 coordinate. Furthermore, the crack-

opening displacement, $\hat{u}^c$, may contain three components.

Note that a second order tensor representation of the internal state variable may be insufficient if the crack displacement $\hat{u}^c$ or normal $\hat{n}^c$ rotates during the load history. In this case a higher order tensor may be required [30]. However, since the crack is matrix dominated and constrained by fibers, time dependent rotation is assumed to be negligible and the second order tensorial representation is considered adequate in the current model. Recent experimental evidence [31] indicates that cracks do indeed change planes sometimes in multi-ply laminates with several adjacent crossplies at the same orientation. However, the crack plane is essentially straight in each ply, the level at which the local volume is constructed for matrix cracks.

For the single damage mode of matrix cracking described in Fig. 2, equations (1) reduce to

$$\sigma_i = C_{ij}\varepsilon_j + I^1_{i2}\alpha^1_2 + I^1_{i5}\alpha^1_5 + I^1_{i8}\alpha^1_8 \qquad . \quad (5)$$

For relatively thin laminates it is useful to apply the conditions of generalized plane stress where the out-of-plane shear stresses σ_4 and σ_5 are neglected. Applying these conditions to equations (5), imposing the symmetry constraints described in equations (2) and (3), and using matrix notation results in

$$\begin{Bmatrix} \sigma_1 \\ \sigma_2 \\ \sigma_3 \\ \sigma_6 \end{Bmatrix} = \begin{bmatrix} C_{11} & C_{12} & C_{12} & 0 \\ C_{12} & C_{22} & C_{23} & 0 \\ C_{12} & C_{23} & C_{33} & 0 \\ 0 & 0 & 0 & C_{66} \end{bmatrix} \begin{Bmatrix} \varepsilon_1 \\ \varepsilon_2 \\ \varepsilon_3 \\ \varepsilon_6 \end{Bmatrix} + [I^1]\{\alpha^1\} \qquad , \quad (6)$$

where

$$[I^1] = \begin{bmatrix} 0 & I^1_{12} & 0 & 0 & 0 & 0 & 0 & 0 & 0 \\ 0 & I^1_{22} & 0 & 0 & 0 & 0 & 0 & 0 & 0 \\ 0 & I^1_{32} & 0 & 0 & 0 & 0 & 0 & 0 & 0 \\ 0 & 0 & 0 & 0 & 0 & 0 & 0 & I^1_{68} & 0 \end{bmatrix} \qquad . \quad (7)$$

Note that the fifth column of the coefficient matrix in equations (5) is zero due to the fact that α^1_5 does not contribute to the in-plane stresses in the generalized plane stress reduction. Furthermore, note that I^1_{12}, I^1_{22} and I^1_{32} are the coefficients of

5

the effect of loss of stiffness on the normal stresses σ_1, σ_2 and σ_3, respectively. Finally, note that I_{68}^1 is the coefficient determining the influence of stiffness loss on the in-plane shear stress σ_6. It is apparent from the above equations that for generalized plane stress conditions there are ten unknown material constants to be determined for the case of matrix cracking.

Determination of the I Matrix

Theoretically it is possible to determine the I matrix directly from experimental data. This may be accomplished by subjecting test coupons to prescribed deformation histories, removing the deformations, and nondestructively evaluating the damage state. The residual stresses will determine the I matrix. However, in graphite/epoxy laminates this procedure breaks down due to the fact that although the crack surfaces may be determined nondestructively using x-rays and edge replicas, the crack opening displacements cannot be accurately determined experimentally. Therefore, an alternative approach is used herein to evaluate the I matrix.

As described in Appendix C, for the case considered in this paper, at least to a first approximation, it can be shown that

$$I_{12}^1 = -C_{12} \qquad I_{22}^1 = -C_{22}$$

$$I_{32}^1 = -C_{23} \qquad I_{68}^1 = -C_{66} \tag{8}$$

Therefore, the number of unknown material constants is reduced to a total of six for the case considered herein.

Laminate Equations

In order to utilize single lamina equations to characterize the response of multilayered laminates, it is necessary to globally average the local ply constitutive equations. This is accomplished herein by imposing the Kirchhoff hypothesis for thin plates [31]. However, higher order plate or shell theories could be utilized also. Generalized plane strain conditions are imposed rather than plane strain because this is consistent with the stress state in equations (6) (A detailed description of the global averaging is given in Appendix D). The resulting equations are as follows:

$$\{N\} = [A]\{\varepsilon^0\} + \{D\} \tag{9}$$

or

$$\{\varepsilon^0\} = [A^{-1}](\{N\} - \{D\}) \tag{10}$$

6

where

$$A_{ij} \equiv \sum_{k=1}^{n} (\overline{C}_{ij})_k \, t_k \qquad , \quad (11)$$

and

$$[D] \equiv \sum_{k=1}^{n} t_k \, [\overline{I}^1]_k \, (\overline{a}^1)_k \qquad , \quad (12)$$

$[\overline{I}^1]_k$ and $(\overline{a}^1)_k$ are in laminate coordinates as defined in Appendix E, and $\{\varepsilon^0\}$ contains the laminate midplane strains. Furthermore, k specifies the ply and t_k is the ply thickness. For convenience, we have assumed that no moments are produced by the damage (in the absence of curvature), which is assumed to hold for symmetric laminates.

In order to determine the effective stiffness for any damage state, we evaluate the rate of change of $\{N\}$ with respect to the midsurface strains $\{\varepsilon^0\}$ during unloading, that is,

$$S'_{im} = \partial N_i/\partial \varepsilon^0_j = A_{ij} + \sum_{k=1}^{n} \sum_{j=1}^{9} t_k \, (\overline{I}_{ij})_k \, (\partial \overline{a}_j/\partial \varepsilon^0_m)_k \qquad , \quad (13)$$

where S'_{im} is defined to be the effective stiffness. Experimental work on graphite/epoxy laminates has shown that S'_{11} is very nearly a constant during unloading, implying that, at least as a first approximation for crossply laminates,

$$(\partial \overline{a}_1/\partial \varepsilon^0_1)_k \cong constant \qquad k=1,\ldots,n \qquad . \quad (14)$$

THE INTERNAL STATE VARIABLE FOR MATRIX CRACK DAMAGE

Equation (41) in Part I [1] gave the second order Taylor series expansion of the local energy per unit volume due to cracking, u^C_L, in terms of strain, ε_{Lij}, temperature, ΔT, and the internal state variable (ISV), a^n_{Lij}. For demonstration purposes, the predictions of this paper are being confined to symmetric cross-ply laminates loaded in uniaxial tension with matrix cracks extending straight through the $90°$ plies. For this case, a^1_2 is the only component of the ISV of interest and is defined (in the ply coordinate system) as

7

$$\alpha_2^1 = \frac{1}{V_L} \int_{S_2} u_2 dS \qquad , \quad (15)$$

where u_2 is the crack-opening displacement, V_L is the local element volume and S_2 is the surface area of matrix cracks. Furthermore, we will consider only the case of load-up in the fixed grip mode where matrix crack extension occurs at constant strain. Therefore, if the higher order terms in the Taylor series expansion are neglected, the local energy due to cracking reduces to

$$u_L^C = (A + I_{22}^1 \epsilon_2) \alpha_2^1 \qquad , \quad (16)$$

where A is a constant. Since equation (16) applies to load-up in the fixed grip mode, α_2^1 can be related to the strain energy release rate, G_m, for matrix cracking by noting that u_L^C is related to G_m as follows:

$$u_L^C(t) = -\frac{1}{V_L} \int_0^{S_2(t)} G_m dS \qquad , \quad (17)$$

where it is assumed that the initial matrix crack surface area is zero and $S_2(t)$ is the surface area at time t. If we make the assumption that the energy stored due to residual damage is negligible, then the constant A in equation (16) is zero, and equating (16) and (17) yields

$$I_{22}^1 \epsilon_2 \alpha_2^1 = -\frac{1}{V_L} \int_0^{S_2(t)} G_m dS \qquad , \quad (18)$$

for stable crack growth. In order to properly account for crack interaction an expression for G_m will be determined experimentally.

The strain energy release rate due to matrix cracking may be defined as

$$G_m = -\frac{\partial U}{\partial S} \qquad , \quad (19)$$

where S denotes matrix crack surface area and U is the strain energy of the laminate.

As a first approximation we will assume that all the strain energy released during matrix crack formation occurs in the 90° layer containing the cracks. The strain energy in a 90° layer is

8

defined by

$$U = \frac{1}{2} E_{22} \epsilon_2^2 \qquad , \quad (20)$$

for a uniform applied strain, ϵ_2, in an elastic material. Assuming the applied strain to be constant for the fixed grip condition, substituting (20) into (19) results in

$$G_m = -\frac{1}{2} V_L \epsilon_2^2 \frac{\partial E_{22}}{\partial S} \qquad . \quad (21)$$

This implies that the effective modulus of the 90° layer changes due to matrix crack formation. It is noted that Equation (21) is similar to the expression for strain energy release rate written in terms of test specimen compliance.

The rule of mixtures yields the following expression for the loading direction modulus of a cross-ply laminate:

$$E_x = \frac{p E_{11} + q E_{22}}{p+q} \qquad , \quad (22)$$

where p is the number of 0° plies and q is the number of 90° plies. Assuming that matrix cracks are confined to the 90° plies,

$$\frac{\partial E_x}{\partial S} = \frac{q}{p+q} \frac{\partial E_{22}}{\partial S} \qquad . \quad (23)$$

Substituting (23) into (21) gives

$$G_m = -\frac{1}{2} V_L \epsilon_2^2 \frac{p+q}{q} \frac{\partial E_x}{\partial S} \qquad . \quad (24)$$

If the right hand side of equation (24) is determined experimentally from a laminate that has a 90° layer that is one ply thick, the resulting strain energy release rate can be utilized for other layups by observing that the strain energy release rate for a ply in a layer that is n plies thick is given by (See Appendix F.)

$$(G_m)_1 = -\frac{1}{2} n \ V_L \ \epsilon_2^2 \left(\frac{p+q}{q} \right) \left[\frac{\partial E_x}{\partial S} \right]_{1 \ ply \ layer} \qquad , \quad (25)$$

where V_L is the volume of a single ply. Equation (25) can now be substituted into equation (18) to obtain the expression for the ISV of a single 90° ply for matrix crack extension during load-up. The resulting equation is

$$\alpha_2^1 = \frac{1}{2}\varepsilon_2 \; \frac{n(p+q)}{I_{22}^1 \; q} \int_0^{S_2(t)} \frac{\partial E_x}{\partial S} \, dS \qquad . \quad (26)$$

The integral term in equation (26) can be evaluated as follows:

$$\int_0^{S_2(t)} \frac{\partial E_x}{\partial S} \, dS = \int_{E_{xo}}^{E_{x1}} dE_x = E_{x1} - E_{xo} \qquad , \quad (27)$$

where E_{xo} is the undamaged elastic modulus and E_{x1} is the degraded modulus corresponding to damage state $S_2(t_1)$. Substituting (27) into (26) and rearranging, the ISV for load-up is expressed as

$$\left. \alpha_2^1 \right|_{\substack{\text{load-up} \\ \text{at } S_2(t_1)}} = \frac{1}{2}\varepsilon_2 \; n\frac{(p+q)}{q} \; \frac{E_{xo}}{I_{22}^1} \left(\left. \frac{E_{x1}}{E_{xo}} \right|_{S_2(t_1)} - 1 \right) \qquad . \quad (28)$$

Although it is possible for matrix crack surface area to increase during unloading, in the current development this effect is assumed to be negligible. Therefore, on unloading α_2^1 depends only on the crack-closure displacement, u_2 in equation (15), and would go to zero on complete crack closure. Assuming that the crack-closure displacement is linear with strain and the matrix crack surface area is constant, equation (15) can be rewritten as

$$\left. \alpha_2^1 \right|_{\text{unloading}} = c\varepsilon_2 \qquad , \quad (29)$$

where c is a constant of proportionality.

The constants in equations (28) and (29) must be determined from experimental data. Considering a tensile test with a load and unloading cycle, at the instant of load reversal the expressions for the ISV for load-up and unloading must be equal. Therefore, setting equation (28) equal to (29) and rearranging, gives the following relationship

10

$$c \Big|_{S_2(t_1)} = \frac{1}{2}n\frac{(p+q)}{q} \ \frac{E_{xo}}{I_{22}^1} \left(\frac{E_{x1}}{E_{xo}}\Big|_{S_2(t_1)} -1 \right) \qquad . \ (30)$$

It should be noted that all matrix cracking information is contained in the term E_{x1}/E_{xo}. Since equation (30) applies only to a single $90°$ ply, E_{x1} was determined from the experimental results of the $[0/90/0]_s$ laminate. The following expression was obtained from a least squares curve fit to the experimental values of E_{x1}/E_{xo} versus S_2:

$$E_{x1}/E_{xo} = 0.9969 - 0.061607 \cdot S_2(t_1) + 0.046230 \cdot S_2(t_1)^2 \qquad . \ (31)$$

Recalling equation (13), it is seen that the effective stiffness of a laminate can be obtained by specifying $\partial\alpha_2^1/\partial\epsilon_2$. On unloading this is given by equation (29) to be

$$\partial\alpha_2^1/\partial\epsilon_2 = c \qquad . \ (32)$$

Therefore, equations (30) and (31) are used with laminate equations (13) to predict the effective stiffness of any laminate.

MODEL COMPARISON TO EXPERIMENTAL RESULTS

The model has been utilized to predict the damage dependent ... ed stiffness of several crossply laminates. This has been ...plished by utilizing the laminate stiffness equations (13), in conjunction with the damage evaluation procedure described in the previous section. The reduced stiffnesses predicted by the model have been compared to experimental results obtained from graphite/epoxy coupons composed of Hercules AS4/3502.

The coupons were obtained from laminates fabricated from prepreg tape using a hot press technique in the Mechanics and Materials Center at Texas A&M University. The laminates were cured according to the procedure recommended by the prepreg tape vendor. Quasi-static tensile tests were conducted on an Instron 1128 screw driven uniaxial testing machine. Matrix crack damage states were evaluated by x-ray radiography and edge replication. Further details of these procedures are contained in reference [31]. Initial undamaged lamina properties are given in Table 1. These properties were obtained experimentally from $[0]_8$, $[90]_8$ and $\pm[45]_{2s}$ laminates and are typical for this material system. As discussed in the previous section, the strain energy release rate as a function of surface area was obtained from $[0,90,0]_s$ control coupons.

The experimental values of normalized axial stiffness versus matrix crack surface area per $90°$ ply are shown in Fig. 3. For each laminate, test coupons were quasi-statically loaded in an

11

incremental fashion to the matrix crack saturation damage state. At each load step, the matrix crack damage state was documented and the axial modulus was measured by unloading and reloading the coupon. As would be suggested by ply disount theory, the axial stiffness loss increases with increasing number of $90°$ plies. Also, as would be predicted by shear lag analysis, the number of cracks per inch at the saturation damage state decreases with increasing $90°$ layer thickness.

Values of effective stiffness for each cross-ply laminate were predicted by the constitutive model using equations (30), (31), and (13) and the experimentally determined values of matrix crack surface area. Figure 4 presents a comparison of the model predictions to the experimental results for the $[0,90,0]_s$ laminate. The excellent agreement between theory and experiment for this laminate was used to characterize the strain energy release rate as a function of matrix crack surface area. Figures 5, 6, and 7 present the comparison between the model predictions and the experimental results for the $[0,90]_s$, $[0,90_2]_s$, and $[0,90_3]_s$ laminates, respectively. As can be seen, the model predictions are in close agreement with the experimental results. The results are quite encouraging given the relatively small stiffness losses of the $[0,90,0]_s$ and $[0,90]_s$ laminates relative to the larger losses experienced by the $[0,90_2]_s$ and $[0,90_3]_s$ laminates.

SUMMARY AND CONCLUSIONS

A model for predicting the stiffness loss in laminated composites as a function of microstructural damage has been proposed in this two part paper. In part I the general theoretical framework was constructed for elastic composites with damage. In part II the model has been specialized for the case matrix cracks in crossply laminates. In this process the following key developments have been reported:

1) material symmetry constraints have been imposed on the damage constant tensor I_{ijkl};

2) the damage tensor α_{ij} has been reduced for the case of plane stress;

3) an approximate procedure has been proposed for obtaining the damage constant tensor;

4) damage dependent laminate equations have been constructed; and

5) the internal state for any crossply layup has been found to be derivable from energy release rates experimentally obtained from a single layup.

The model has been demonstrated to be accurate in predicting the damage dependent reduced stiffness of several graphite/epoxy crossply laminates with matrix cracks. While a number of simplifying assumptions were necessary for this model demonstration, most of these assumptions are the same as are typically made by classical lamination theory and do not represent a restriction or limitation to the general applicability of the model. However, the development herein is

currently limited to cross-ply laminates with symmetric damage states. The authors are addressing this limitation by developing damage dependent laminate equations which account for the curvature produced by nonsymmetric damage and the resulting coupling between extension and bending [27]. Finally, the approach described herein depends on the damage state being determined experimentally. This restriction is being addressed by developing damage growth laws which would allow the ISV, and hence the damage state, to be predicted as a function of the loading history of the coupon or structural component.

Current and future development of the model will deal with the following issues:
1) application of the model to laminates with matrix cracks that are angled or curved rather than extending straight through the 90° layer in the x_1-x_3 plane [24];
2) application of the model to laminates with both matrix cracks and interply delaminations [27];
3) application of the model to layups more complex than crossply laminates; and
4) development of internal state variable growth laws for matrix cracking and interply delamination.

ACKNOWLEDGEMENT

REFERENCES

1.   Allen, D.H., Groves, S.E., Schapery, R.A., and Harris, C.E., "A Thermomechanical Constitutive Theory for Elastic Composites with Distributed Damage - Part I: Theoretical Development," Texas A&M University Mechanics and Materials Center, MM-5023-85-17, October, 1985.

2.   Stinchcomb, W.W., and Reifsnider, K.L., "Fatigue Damage Mechanisms in Composite Materials: A Review", Fatigue Mechanisms, Proc. of ASTM-NBS-NSF Symp., Kansas City, MO., May 1978, J.J. Fong, ed., ASTM STP 679, 1979, pp. 762-787.

3.   Hahn, H.T., "Fatigue Behavior and Life Prediction of Composite Laminates", Composite Materials: Testing and Design (Fifth Conf.), ASTM STP 674, 1979, pp. 383-417.

4.   Lehman, M.W., "An Investigation of Intra-Play Microcrack Density Development in a Cross-Ply Laminate," Texas A&M University Mechanics and Materials Research Center, MM 3724-80-11, December, 1980.

5.   Stinchcomb, W.W., Reifsnider, K.L,. Yeung, P., and Masters, J., "Effect of Ply Constraint on Fatigue Damage Development in Composite Material Laminates," Fatigue of Fibrous Composite Materials, ASTM STP 723, 1981, pp. 65-84.

6.   Highsmith, A.L., Stinchcomb, W.W., and Reifsnider, K.L., "Stiffness Reduction Resulting from Transverse Cracking in Fiber-Reinforced Composite Laminates," Virginia Polytechnic Institute and State University, VPI-E-81.33, November, 1981.

7.   Reifsnider, K.L., and Jamison, R., "Fracture of Fatigue-Loaded Composite Laminates," Int. J. Fatigue, 1982, pp. 187-197.

8.   Leichti, K.M., Masters, J.E., Ulman, D.A., and Lehman, M.W., "SEM/TEM Fractography of Composite Materials," AFWAL-TR-82-4035, September, 1982.

9. Ulman, D.A., "Cumulative Damage Model for Advanced Composite Materials," Semi-annual Report No. 3 (FZM-7070) and No. 4 (FZM-7106), Air Force Materials Laboratory, 1983.

10. Hill, R., The Mathematical Theory of Plasticity, Oxford University Press, London, 1950.

11. Tsai, Stephen W., "Strength Theories of Filamentary Structures," in R.T. Schwartz and H.S. Schwartz (eds.), Fundamental Aspects of Fiber Reinforced Plastic Composites, Wiley Interscience, New York, 1968, pp. 3-11.

12. O'Brien, T.K., "An Evaluation of Stiffness Reduction as a Damage Parameter and Criterion for Fatigue Failure in Composite Materials," Ph.D. Dissertation, Virginia Polytechnic Institute and State University, October, 1978.

13. Kachanov, L.M., "On the Creep Fracture Time," *Izv. AN SSR, Otd. Tekhn. Nauk*, No. 8, pp. 26-31, 1958 (in Russian).

14. Poursartrip, A., et al., "Damage Accumulation during Fatigue of Composites," Cambridge University (England) Dept. of Engineering, Nov. 1981, p. 29.

15. Miner, M.A., "Cumulative Damage in Fatigue," *J. Appl. Mech.*, Vol. 12, 1945, p. 159.

16. Schapery, R.A., "Models for Damage Growth and Fracture in Nonlinear Viscoelastic Particulate Composites," *Proc. 9th U.S. National Cong. Appl. Mech.*, August, 1982.

17. Chou, P.C., Wang, A.S.D., and Miller, H., "Cumulative Damage Model for Advanced Composite Materials," AFWAL-TR-82-4-83, September, 1982.

18. Reifsnider, K.L., and Highsmith, A., "Characteristic Damage States: A New Approach to Representing Fatigue Damage in Composite Laminates," *Materials, Experimentation, and Design in Fatigue*, Westbury House, Surrey, England, pp. 246-260, 1981.

19. Gottesman, T., Hashin, Z., and Brull, M.A., "Effective Elastic Moduli of Cracked Fiber Composites," *Advances in Composite Materials*, Bunsell, A.R., Ed., Pergamon, Oxford, Vol. 1, pp. 749-758, 1980.

20. Laws, N., Dvorak, G.J., and Hejazi, M., "Stiffness Changes in Unidirectional Composites Caused by Crack Systems," *Mechanics of Materials*, Vol. 2, 1983.

21. Talreja, R., "A Continuum Mechanics Characterization of Damage in Composite Materials," *Proc. R. Soc. London*, Vol. 399A, 1985, pp. 195-216.

22. Talreja, R., "Residual Stiffness Properties of Cracked Composite Laminates," Danish Center for Applied Mathematics and Mechanics, The Technical University of Denmark, Report No. 277, Feb., 1984.

23. Talreja, R., "Transverse Cracking and Stiffness Reduction in Composite Laminates," Danish Center for Applied Mathematics and Mechanics, The Technical University of Denmark, July, 1984.

24. Allen, D.H., Harris, C.E., Groves, S.E., and Norvell, R.G., "Characterization of Stiffness Loss in Crossply Laminates with Curved Matrix Cracks," *COMPOSITES '86: Recent Advances in Japan and the United States*, Oct., 1986.

25. Talreja, R., "Mechanism and Models of Damage in Composite Materials," Danish Center for Applied Mathematics and Mechanics, The Technical University of Denmark, October, 1986.

26. Talreja, R., "Stiffness Properties of Composite Laminates with Matrix Cracking and Interior Delamination," Danish Center for Applied Mathematics and Mechanics, The Technical University of Denmark, March, 1986.

27. Groves, S.E., Allen, D.H., and Harris, C.E., "A Cumulative Damage Model for Continuous Fiber Composite Laminates with Matrix Cracking and Interply Delaminations," Texas A&M University Mechanics and Materials Center, MM-5023-86, August, 1986.

28. Frederick, D. and Chang, T.S., Continuum Mechanics, Scientific Publishers, Inc., Cambridge, Mass., 1972.

29. Jones, R.M., Mechanics of Composite Materials, McGraw-Hill, 1975.

30. Krajcinovic, D., "Constitutive Equations for Damaging Materials," Journal of Applied Mechanics, Transactions of the ASME, 83-APM-12, June, 1983.

31. Norvell, R.G., "An Investigation of Damage Accumulation in Graphite/Epoxy Laminates," Texas A&M University Thesis, August, 1985.

Table I. Material Properties for Hercules AS4/3502

Lamina Properties

Property	Symbol	Value
Longitudinal Modulus	E_{11}	$21.0 \times 10^6 \pm 2.0\%$ psi
Transverse Modulus	E_{22}	$1.39 \times 10^6 \pm 2.1\%$ psi
Shear Modulus	G_{12}	0.694×10^6 psi
Poisson's Ratio	ν_{12}	$0.310 \pm 3.7\%$
Longitudinal Strength	F_{tu1}	$326,000 \pm 3.5\%$ psi
Transverse Strength	F_{tu2}	$11,085 \pm 9.8\%$ psi
Long. Failure Strain	ε_{tu1}	$0.0144 \pm 4.6\%$ in/in
Tran. Failure Strain	ε_{tu2}	$0.00773 \pm 6.7\%$ in/in

APPENDIX A: APPLICATION OF SYMMETRY CONSTRAINTS

The damage-dependent constitutive model (equations (42) through (45) of Part I [1]) is defined as follows:

$$\sigma_{ij} = \sigma_{ij}^R + C_{ijkl}(\epsilon_{kl} - \epsilon_{kl}^T) + I_{ijkl}^\eta \alpha_{kl}^\eta \qquad , \quad (1a)$$

where σ_{ij} is the local stress tensor, ϵ_{kl} is the local strain tensor, σ_{ij}^R is the residual stress in the absence of strain and temperature change, C_{ijkl} is the undamaged modulus tensor, ϵ_{kl}^T is the thermal strain tensor, α_{kl}^η is the internal state variable tensor, and I_{ijkl}^η is the damage modulus tensor. Furthermore, we have dropped the subscript L (denoting locally averaged quantities) for convenience.

For demonstration purposes, the residual stress tensor and the temperature change are assumed to be negligible, resulting in

$$\sigma_{ij} = C_{ijkl}\epsilon_{kl} + I_{ijkl}^\eta \alpha_{kl}^\eta \qquad . \quad (2a)$$

Note that I_{ijkl}^η is a fourth order tensor with 81 coefficients .or each value of η. It is assumed here that the constitutive equations given by (2a) are statistically homogeneous. Therefore, the conditions of stress and strain symmetry as well as the existence of an elastic potential can be applied to equations (2a) to obtain

$$C_{ijkl} = C_{jikl} \cdot \quad C_{ijkl} = C_{ijlk} \cdot \quad C_{ijkl} = C_{klij} \qquad , \quad (3a)$$

and

$$I_{ijkl}^\eta = I_{jikl}^\eta \qquad . \quad (4a)$$

It is most convenient at this point to reindex the constitutive tensors using the Voigt notation [28] where

$$\sigma_1 \equiv \sigma_{11} \qquad \sigma_4 \equiv \sigma_{23} = \sigma_{32}$$

$$\sigma_2 \equiv \sigma_{22} \qquad \sigma_5 \equiv \sigma_{13} = \sigma_{31} \qquad , \quad (5a)$$

$$\sigma_3 \equiv \sigma_{33} \qquad \sigma_6 \equiv \sigma_{12} = \sigma_{21}$$

and

$$\epsilon_1 \equiv \epsilon_{11} \qquad \epsilon_4 \equiv 2\epsilon_{23} = 2\epsilon_{32}$$

$$\epsilon_2 \equiv \epsilon_{22} \qquad \epsilon_5 \equiv 2\epsilon_{13} = 2\epsilon_{31} \qquad . \quad (6a)$$

$$\epsilon_3 \equiv \epsilon_{33} \qquad \epsilon_6 \equiv 2\epsilon_{12} = 2\epsilon_{21}$$

Furthermore, for all values of η

$$\alpha_1 \equiv \alpha_{11} \qquad \alpha_4 \equiv \alpha_{23} \qquad \alpha_7 \equiv \alpha_{31}$$

$$\alpha_2 \equiv \alpha_{22} \qquad \alpha_5 \equiv \alpha_{32} \qquad \alpha_8 \equiv \alpha_{12} \qquad . \quad (7a)$$

$$\alpha_3 \equiv \alpha_{33} \qquad \alpha_6 \equiv \alpha_{13} \qquad \alpha_9 \equiv \alpha_{21}$$

Using the contracted notation, equations (2a) can be written as

$$\sigma_i = C_{ij}\epsilon_j + l^{\eta}_{ik}\alpha^{\eta}_k \qquad . \quad (8a)$$

where i and j range from 1 to 6, k ranges from 1 to 9, and η ranges from 1 to N, where N is the number of damage modes.

APPENDIX B: SYMMETRY CONSTRAINTS ON THE DAMAGE MODULUS TENSOR

Consider the following component of internal energy due to cracking:

$$u^c_1 \equiv I^1_{ijkl}\epsilon_{ij}\alpha^1_{kl}$$. (1b)

Since the strain tensor is symmetric

$$I^1_{ijkl}=I^1_{jikl}$$. (2b)

Therefore, there are 54 independent constants in the damage modulus tensor I^1_{ijkl}. Expanding out equation (1b) thus gives

$$u^c_1 = I^1_{1111}\epsilon_{11}\alpha^1_{11} + I^1_{1122}\epsilon_{11}\alpha^1_{22} + I^1_{1133}\epsilon_{11}\alpha^1_{33} + I^1_{1123}\epsilon_{11}\alpha^1_{23}$$

$$+ I^1_{1132}\epsilon_{11}\alpha^1_{32} + I^1_{1113}\epsilon_{11}\alpha^1_{13} + I^1_{1131}\epsilon_{11}\alpha^1_{31} + I^1_{1112}\epsilon_{11}\alpha^1_{12}$$

$$+ I^1_{1121}\epsilon_{11}\alpha^1_{21} + I^1_{2211}\epsilon_{22}\alpha^1_{11} + I^1_{2222}\epsilon_{22}\alpha^1_{22} + I^1_{2233}\epsilon_{22}\alpha^1_{33}$$

$$+ I^1_{2223}\epsilon_{22}\alpha^1_{23} + I^1_{2232}\epsilon_{22}\alpha^1_{32} + I^1_{2213}\epsilon_{22}\alpha^1_{13} + I^1_{2231}\epsilon_{22}\alpha^1_{31}$$

$$+ I^1_{2212}\epsilon_{22}\alpha^1_{12} + I^1_{2221}\epsilon_{22}\alpha^1_{21} + I^1_{3311}\epsilon_{33}\alpha^1_{11} + I^1_{3322}\epsilon_{33}\alpha^1_{22}$$

$$+ I^1_{3333}\epsilon_{33}\alpha^1_{33} + I^1_{3323}\epsilon_{33}\alpha^1_{23} + I^1_{3332}\epsilon_{33}\alpha^1_{32} + I^1_{3313}\epsilon_{33}\alpha^1_{13}$$

$$+ I^1_{3331}\epsilon_{33}\alpha^1_{31} + I^1_{3312}\epsilon_{33}\alpha^1_{12} + I^1_{3321}\epsilon_{33}\alpha^1_{21} + I^1_{2311}\epsilon_{23}\alpha^1_{11}$$

$$+ I^1_{2322}\epsilon_{23}\alpha^1_{22} + I^1_{2333}\epsilon_{23}\alpha^1_{33} + I^1_{2323}\epsilon_{23}\alpha^1_{23} + I^1_{2332}\epsilon_{23}\alpha^1_{32}$$

$$+ I^1_{2313}\epsilon_{23}\alpha^1_{13} + I^1_{2331}\epsilon_{23}\alpha^1_{31} + I^1_{2312}\epsilon_{23}\alpha^1_{12} + I^1_{2321}\epsilon_{23}\alpha^1_{21}$$

$$+ I^1_{1311}\epsilon_{13}\alpha^1_{11} + I^1_{1322}\epsilon_{13}\alpha^1_{22} + I^1_{1333}\epsilon_{13}\alpha^1_{33} + I^1_{1323}\epsilon_{13}\alpha^1_{23}$$

$$+ I^1_{1332}\epsilon_{13}\alpha^1_{32} + I^1_{1313}\epsilon_{13}\alpha^1_{13} + I^1_{1331}\epsilon_{13}\alpha^1_{31} + I^1_{1312}\epsilon_{13}\alpha^1_{12}$$

$$+ I^1_{1321}\epsilon_{13}\alpha^1_{21} + I^1_{1211}\epsilon_{12}\alpha^1_{11} + I^1_{1222}\epsilon_{12}\alpha^1_{22} + I^1_{1233}\epsilon_{12}\alpha^1_{33}$$

$$+ I^1_{1223}\epsilon_{12}\alpha^1_{23} + I^1_{1232}\epsilon_{12}\alpha^1_{32} + I^1_{1213}\epsilon_{12}\alpha^1_{13} + I^1_{1231}\epsilon_{12}\alpha^1_{31}$$

$$+ I^1_{1212}\epsilon_{12}\alpha^1_{12} + I^1_{1221}\epsilon_{12}\alpha^1_{21}$$. (3b)

We now wish to impose orthotropic symmetry. In order to do this, first rotate $180°$ about the x_3 axis [28]. The direction cosines for this transformation are

$$[a_{ik'}] = \begin{bmatrix} -1 & 0 & 0 \\ 0 & -1 & 0 \\ 0 & 0 & 1 \end{bmatrix}$$. (4b)

Therefore, since ε_{ij} is a second order tensor,

$$\varepsilon_{k'l'} = \varepsilon_{ij} a_{ik'} a_{jl'}$$. (5b)

It follows that

$$[\varepsilon_{k'l'}] = \begin{bmatrix} \varepsilon_{11} & \varepsilon_{12} & -\varepsilon_{13} \\ \varepsilon_{12} & \varepsilon_{22} & -\varepsilon_{23} \\ -\varepsilon_{13} & -\varepsilon_{23} & \varepsilon_{33} \end{bmatrix}$$. (6b)

Furthermore,

$$[\alpha_{k'l'}^1] = \begin{bmatrix} \alpha_{11}^1 & \alpha_{12}^1 & -\alpha_{13}^1 \\ \alpha_{21}^1 & \alpha_{22}^1 & -\alpha_{23}^1 \\ -\alpha_{31}^1 & -\alpha_{32}^1 & \alpha_{33}^1 \end{bmatrix}$$. (7b)

Since u_1^c must be independent of coordinate system

$$u_1^c = I_{p'q'r's'}^1 \varepsilon_{p'q'} \alpha_{r's'}^1$$. (8b)

Substituting (6b) and (7b) into (8b) and comparing this result to (3b) will result in

$$I_{1123}^1 = I_{1132}^1 = I_{1113}^1 = I_{1131}^1 = I_{2223}^1 = I_{2232}^1 = 0$$

$$I_{2213}^1 = I_{2231}^1 = I_{3323}^1 = I_{3332}^1 = I_{3313}^1 = I_{3331}^1 = 0$$

$$I_{2311}^1 = I_{2322}^1 = I_{2333}^1 = I_{2312}^1 = I_{2321}^1 = I_{1311}^1 = 0$$

$$I_{1322}^1 = I_{1333}^1 = I_{1312}^1 = I_{1321}^1 = I_{1223}^1 = I_{1232}^1 = 0$$

$$I_{1213}^1 = I_{1231}^1 = 0$$. (9b)

Rotating 180° about the x_2 axis gives

$$[a_{ik'}] = \begin{bmatrix} -1 & 0 & 0 \\ 0 & 1 & 0 \\ 0 & 0 & -1 \end{bmatrix} \qquad . \ (10b)$$

Therefore,

$$[\varepsilon_{k'1'}] = \begin{bmatrix} \varepsilon_{11} & -\varepsilon_{12} & \varepsilon_{13} \\ -\varepsilon_{12} & \varepsilon_{22} & -\varepsilon_{23} \\ \varepsilon_{13} & -\varepsilon_{23} & \varepsilon_{33} \end{bmatrix} \qquad . \ (11b)$$

Furthermore,

$$[\alpha_{k'1'}^1] = \begin{bmatrix} \alpha_{11}^1 & -\alpha_{12}^1 & \alpha_{13}^1 \\ -\alpha_{21}^1 & \alpha_{22}^1 & -\alpha_{23}^1 \\ \alpha_{31}^1 & -\alpha_{32}^1 & \alpha_{33}^1 \end{bmatrix} \qquad . \ (12b)$$

Substituting (11b) and (12b) into (8b) and comparing to (3b) results in

$$I_{1112}^1 = I_{1121}^1 = I_{2212}^1 = I_{2221}^1 = I_{3312}^1 = I_{3321}^1 = 0$$

$$I_{2313}^1 = I_{2331}^1 = I_{1323}^1 = I_{1332}^1 = I_{1211}^1 = I_{1222}^1 = I_{1233}^1 = 0 \qquad . \ (13b)$$

Rotating 180° about the x_1 axis yields no additional constraints. Therefore, imposition of orthotropic symmetry on I_{ijkl}^1 reduces the number of constants to 15. These are

$$\begin{array}{lll} I_{11}^1 \equiv I_{1111}^1 & I_{12}^1 \equiv I_{1122}^1 & I_{21}^1 \equiv I_{2211}^1 \\[4pt] I_{22}^1 \equiv I_{2222}^1 & I_{13}^1 \equiv I_{1133}^1 & I_{31}^1 \equiv I_{3311}^1 \\[4pt] I_{33}^1 \equiv I_{3333}^1 & I_{23}^1 \equiv I_{2233}^1 & I_{32}^1 \equiv I_{3322}^1 \\[4pt] I_{44}^1 \equiv I_{2323}^1 & I_{45}^1 \equiv I_{2332}^1 & I_{56}^1 \equiv I_{1313}^1 \\[4pt] I_{57}^1 \equiv I_{1331}^1 & I_{68}^1 \equiv I_{1212}^1 & I_{69}^1 \equiv I_{2121}^1 \end{array} \qquad . \ (14b)$$

Therefore, the orthotropic damage modulus matrix is given by

$$
[I^1] = \begin{bmatrix}
I^1_{11} & I^1_{12} & I^1_{13} & 0 & 0 & 0 & 0 & 0 & 0 \\
I^1_{21} & I^1_{22} & I^1_{23} & 0 & 0 & 0 & 0 & 0 & 0 \\
I^1_{31} & I^1_{32} & I^1_{33} & 0 & 0 & 0 & 0 & 0 & 0 \\
0 & 0 & 0 & I^1_{44} & I^1_{45} & 0 & 0 & 0 & 0 \\
0 & 0 & 0 & 0 & 0 & I^1_{56} & I^1_{57} & 0 & 0 \\
0 & 0 & 0 & 0 & 0 & 0 & 0 & I^1_{68} & I^1_{69}
\end{bmatrix}
\qquad . \ (15b)
$$

For the case where

$$
[\alpha^1] = [\,0 \quad \alpha^1_2 \quad 0 \quad 0 \quad \alpha^1_5 \quad 0 \quad 0 \quad \alpha^1_8 \quad 0\,] \qquad . \ (16b)
$$

equation (15b) reduces to

$$
[I^1] = \begin{bmatrix}
0 & I^1_{12} & 0 & 0 & 0 & 0 & 0 & 0 & 0 \\
0 & I^1_{22} & 0 & 0 & 0 & 0 & 0 & 0 & 0 \\
0 & I^1_{23} & 0 & 0 & 0 & 0 & 0 & 0 & 0 \\
0 & 0 & 0 & 0 & I^1_{45} & 0 & 0 & 0 & 0 \\
0 & 0 & 0 & 0 & 0 & 0 & 0 & 0 & 0 \\
0 & 0 & 0 & 0 & 0 & 0 & 0 & I^1_{68} & 0
\end{bmatrix}
\qquad . \ (17b)
$$

APPENDIX C: DETERMINATION OF THE I MATRIX

At a material point in V_L the stress-strain relation in the absence of temperature change is

$$\sigma_{ij} = C_{ijkl}\epsilon_{kl} \qquad . \quad (1c)$$

Integrating over the local volume (excluding cracks) gives

$$\sigma'_{Lij} = \frac{1}{V_L}\int_{V_L-V_C}\sigma_{ij}dV = \frac{1}{V_L}\int_{V_L-V_C}C_{ijkl}\epsilon_{kl}dV \qquad . \quad (2c)$$

where σ'_{Lij} is the average stress outside the damage zones. In this section this value of the stress tensor is assumed to be identical to the average stress σ_{Lij}, which includes the average of the stress in the damage zones. Assuming that C_{ijkl} is spatially homogeneous in V_L, the above may be written

$$\sigma'_{Lij} = \frac{C_{ijkl}}{V_L}\int_{V_L-V_C}\epsilon_{kl}dV = \frac{C_{ijkl}}{V_L}\int_{V_L-V_C}\frac{1}{2}(u_{k,l}+u_{l,k})dV \qquad . \quad (3c)$$

Using the divergence theorem on the last term gives

$$\sigma'_{Lij} = C_{ijkl}\left[\frac{1}{V_L}\int_{S_1}\frac{1}{2}(u_kn_l+u_ln_k)dS + \frac{1}{V_L}\int_{S_2}\frac{1}{2}(u_kn_l+u_ln_k)dS\right] \qquad . \quad (4c)$$

Or, equivalently,

$$\sigma'_{Lij} = C_{ijkl}(\epsilon_{Lkl}-\frac{1}{2}\alpha_{kl}-\frac{1}{2}\alpha_{lk}) \qquad . \quad (5c)$$

However, the Taylor series expansion has already given (for isothermal conditions)

$$\sigma'_{Lij} = C_{ijkl}\epsilon_{kl}+I_{ijkl}\alpha_{kl} \qquad . \quad (6c)$$

Therefore, equating like terms in equations (5c) and (6c) gives

$$I_{ijkl} = -C_{ijkl} \qquad\qquad k=l$$

$$I_{ijkl} = -\frac{1}{2}(C_{ijkl}+C_{ijlk}) \qquad\qquad k \neq l \qquad\qquad\qquad . \quad (7c)$$

APPENDIX D: LAMINATE EQUATIONS

The values of generalized plane strain are given by

$$
\begin{Bmatrix} \epsilon_x \\ \epsilon_y \\ \epsilon_z \\ \epsilon_{xy} \end{Bmatrix} = \begin{Bmatrix} \epsilon_x^o \\ \epsilon_y^o \\ \epsilon_z^o \\ \epsilon_{xy}^o \end{Bmatrix} + z \begin{Bmatrix} \kappa_x \\ \kappa_y \\ 0 \\ \kappa_{xy} \end{Bmatrix} \qquad , \quad (1d)
$$

where the superscript o denotes the midsurface strains and the κ matrix denotes the midsurface curvatures. Under the condition of generalized plane strain there is no warping allowed out-of-plane, which implies that $\kappa_z=0$.

It is now assumed that no moments or curvatures are imposed and that all laminates studied are symmetric through the thickness (including damage). Therefore, in order to determine the resultant forces, it is necessary only to integrate the given stress state over the laminate thickness to obtain

$$
\begin{Bmatrix} N_x \\ N_y \\ N_z \\ N_{xy} \end{Bmatrix} = \int_{-t/2}^{t/2} \begin{Bmatrix} \sigma_x \\ \sigma_y \\ \sigma_z \\ \sigma_{xy} \end{Bmatrix} dz \qquad , \quad (2d)
$$

where t is the total thickness of the laminate.

Substituting equations (8a) and (1d) into (2d) for the case where there are no rotations results in

$$
\{N\} = \int_{-t/2}^{t/2} ([\bar{C}]\{\epsilon^o\} + [\bar{I}^1]\{\bar{\alpha}^1\}) dz \qquad , \quad (3d)
$$

where {N} denotes the force resultants, overbars denote that these quantities are transformed to global coordinates, and {ϵ^o} represents the mid-surface strains. Note that since transverse cracks are assumed to go completely through the thickness of the cracked plies the stiffness and damage are assumed to be spacially constant through the thickness of a single ply. Therefore, equation (3d) can be written as

$$\{N\} = \sum_{k=1}^{n} ([\bar{C}]_k (z_k - z_{k-1})\{\varepsilon^0\} + [\bar{I}^1]_k (z_k - z_{k-1})\{\bar{\alpha}^1\}_k) \qquad . \quad (4d)$$

where k specifies the ply and $z_k - z_{k-1}$ is the thickness of each ply. One can define

$$A_{ij} \equiv \sum_{k=1}^{n} (\bar{C}_{ij})_k \ (z_k - z_{k-1}) \qquad . \quad (5d)$$

and

$$\{D\} \equiv \begin{Bmatrix} D_1^1 \\ D_2^1 \\ D_3^1 \\ D_4^1 \end{Bmatrix} = \sum_{k=1}^{n} ([\bar{I}^1]_k (z_k - z_{k-1})\{\bar{\alpha}^1\}_k) \qquad . \quad (6d)$$

where A_{ij} represents the laminate averaged stiffness matrix and $\{D\}$ is the laminate averaged damage term. Thus, the laminate averaged constitutive equations become

$$\{N\} = [A]\{\varepsilon^0\} + \{D\} \qquad . \quad (7d)$$

Experimental testing is often conducted on uniaxial testing machines in which the applied force resultants are input and the strains are experimentally determined output. Therefore, at times, it is more convenient to express the strains in terms of the applied force resultants as follows:

$$\{\varepsilon^0\} = [A]^{-1}(\{N\} - \{D\}) \qquad . \quad (8d)$$

Note also that moments will be produced even in the absence of strain if the damage state is not symmetric through the thickness. However, for the case considered herein, it will be assumed that all damage states are symmetric, and moments are therefore not considered.

APPENDIX E: TRANSFORMATION EQUATIONS FOR THE DAMAGE TENSOR AND THE DAMAGE MODULUS TENSOR

Consider a coordinate rotation θ in the laminate plane (x_1-x_2 plane) measured clockwise from the ply coordinate system to the laminate coordinate system. For this case the direction cosines are

$$[a_{ik'}] = \begin{bmatrix} \cos\theta & -\sin\theta & 0 \\ \sin\theta & \cos\theta & 0 \\ 0 & 0 & 1 \end{bmatrix} \qquad . \ (1e)$$

Recall that since α_{ij}^1 is a second order tensor

$$\bar{\alpha}_{k'1'}^1 = \alpha_{ij}^1 a_{ik'} a_{j1'} \qquad . \ (2e)$$

Substituting (1e) into (2e) for α_{ij}^1 given by equation (16b) gives

$$\{\bar{\alpha}^1\} = \begin{Bmatrix} \alpha_{12}^1\cos\theta\sin\theta + \alpha_{22}^1\sin^2\theta \\ -\alpha_{12}^1\sin\theta\cos\theta + \alpha_{22}^1\cos^2\theta \\ 0 \\ 0 \\ \alpha_{32}^1\cos\theta \\ 0 \\ \alpha_{32}^1\sin\theta \\ \alpha_{12}^1\cos^2\theta + \alpha_{22}^1\sin\theta\cos\theta \\ -\alpha_{12}^1\sin^2\theta + \alpha_{22}^1\sin\theta\cos\theta \end{Bmatrix} \qquad . \ (3e)$$

Furthermore, $\bar{I}_{p'q'r's'}^1$ is given by

$$\bar{I}_{p'q'r's'}^1 = I_{ijkl}^1 a_{ip'} a_{jq'} a_{kr'} a_{1s'} \qquad . \ (4e)$$

Substituting the nonzero components from equation (17b) into (4e) gives

$$\overline{I}^1_{p'q'r's'} = I^1_{12}a_{1p'}a_{1q'}a_{2r'}a_{2s'} + I^1_{22}a_{2p'}a_{2q'}a_{2r'}a_{2s'}$$
$$+ I^1_{32}a_{2p'}a_{2q'}a_{3r'}a_{3s'} + I^1_{68}a_{2p'}a_{1q'}a_{1r'}a_{2s'} \quad . \quad (5e)$$

APPENDIX F: DIMENSIONAL ANALYSIS OF STRAIN
ENERGY RELEASE RATES

This appendix develops an approximate dimensional analysis of the strain energy release rate of a cross-ply laminate containing matrix cracks in the 90° plies. The analysis does not attempt to fully address the complexity of the cracking process. For example, the nonlinear material effects, crack-tip blunting at the 0/90 interfaces, and the relative thickness of the 0° constraint layers are not included in the simplified analysis. In spite of these limitations, the analysis does adequately account for the influence on the strain energy release rate due to the spacing of pre-existing matrix cracks in the 90° layers and the thickness of the 90° layers. The experimental results displayed in nondimensional form in Fig. F2 suggest that these are the two important dimensional parameters for cross-ply laminates and all other effects are secondary.

Consider the cracked 90° layer shown in Fig. F1. The total strain energy in the region surrounding the crack that includes the strain energy available to be released during crack extension is given by

$$U = U_A + U_B \qquad . \quad (1f)$$

where U_A is the strain energy ahead of the advancing crack, and U_B is the strain energy behind the advancing crack.

In terms of strain energy density, U_o, equation (1f) becomes

$$U = (U_o)_A [t(w-a)\ell_E] + (U_o)_B[ta\ell_E] \qquad . \quad (2f)$$

where ℓ_E is the effective length of the material from which strain energy will be released by the advancing crack. It should be noted that we are not suggesting that strain energy is only released from a volume of material that is a rectangular parallelepiped. This concept of an effective length is used only as a convenience , as will become evident in the following development. The effective length is a function of both the crack spacing, S, and the thickness of the 90° layer. Therefore, ℓ_E can be expressed as

$$\ell_E = ct \qquad . \quad (3f)$$

where c is a nondimensional function of the crack spacing and the 90° layer thickness. In addition, the strain energy density ahead of the crack and behind the crack can be expressed as functions of the strain energy density in the 90° layer in the absence of cracks multiplied by some dimensionless constant that depends on the existing matrix crack spacing and the thickness of the 90° layer. Written symbolically, then

$$(U_o)_A = U_o \, f_A \tag{4f}$$

and

$$(U_o)_B = U_o \, f_B \tag{5f}$$

where U_o is the strain energy density in the 90° layer in the absence of cracks, and f_A and f_B are functions of the crack spacing, S, and thickness, t. Substituting (3f), (4f) and (5f) into (2f) yields

$$U = U_o f_A [ct^2(w-a)] + U_o f_B [ct^2 a]$$
$$= U_o ct^2 [f_A W + a(f_B - f_A)] \tag{6f}$$

Strain energy release rate at each crack tip is defined as follows

$$G = -\frac{1}{2t} \, \frac{\partial U}{\partial a} \tag{7f}$$

Substituting (6f) into (7f) thus gives

$$G = \frac{1}{2} U_o ct (f_A - f_B) \tag{8f}$$

Notice that c, f_A and f_B are all functions of the layer thickness and existing matrix crack spacing. Therefore, define a new function f such that

$$f(S,t) = c(f_A - f_B) \tag{9f}$$

Since the function f(S,t) is a dimensionless function, it must be a function of S/t. Therefore,

$$c(f_A - f_B) = f(S/t) \tag{10f}$$

Substituting (10f) into (8f) yields the following expression for the available strain energy release rate for matrix cracks

$$G = \frac{1}{2}t[U_o f(S/t)]$$

. (11f)

Therefore, the available strain energy release rate due to matrix cracks in a 90° layer is linearly proportional to the thickness of the 90° layer. The quantity in the brackets in equation (11f) is related to the properties of the composite material system and the laminate stacking sequence. This quantity can be determined from experimental data.

If it is assumed that cracking occurs when the available strain energy release rate is equal to the critical strain energy release rate which is constant for all matrix cracking, then

$$G = G_{cR}$$

. (12f)

Furthermore, for a linear elastic material with rigid fibers, the strain energy density is given by

$$U_o = \frac{1}{2}E_{22} \, \varepsilon_{22}^2$$

. (13f)

Substituting (11f) and (13f) into (12f) and solving for strain results in the following expression for the strain in the 90° layer at which matrix crack extension occurs:

$$\varepsilon_{22} = \left[\frac{G_{cR}}{tE_{22}f(S/t)}\right]^{1/2}$$

. (14f)

Rearranging gives

$$\frac{4G_{cR}}{tE_{22} \, \varepsilon_{22}^2} = f(S/t)$$

. (15f)

Finally, the thickness of the 90° layer is given by

$$t = nt_1$$

. (16f)

where t_1 is the thickness of one ply and n is the number of consecutive 90° plies. Substituting equation (16f) into (15f) results in

$$\frac{4G_{cR}}{t_1 E_{22}}\left[\frac{1}{n\epsilon_{22}^2}\right] = f(S/t) \qquad . \quad (17f)$$

If the influence function, $f(S/t)$, is constant for all laminate stacking sequences, then the left hand side of equation (15f) will be a function of matrix crack surface area only.

The terms in parentheses on the left and right hand sides of equation (17f) are laminate specific while all other terms are constants. The function $f(S/t)$ is constant for all laminates then a plot of $n\epsilon_{22}^2$ versus t/S should be the same for all laminates. The experimental data is plotted in Fig. F2 and as can be seen the data for all laminates follow the same trend curve. Therefore, it can be seen that the available strain energy release rate is a function of the 90° layer thickness and the matrix crack surface area. All other laminate parameters such as the number of consecutive 0° plies results in second order effects on the energy release rate.
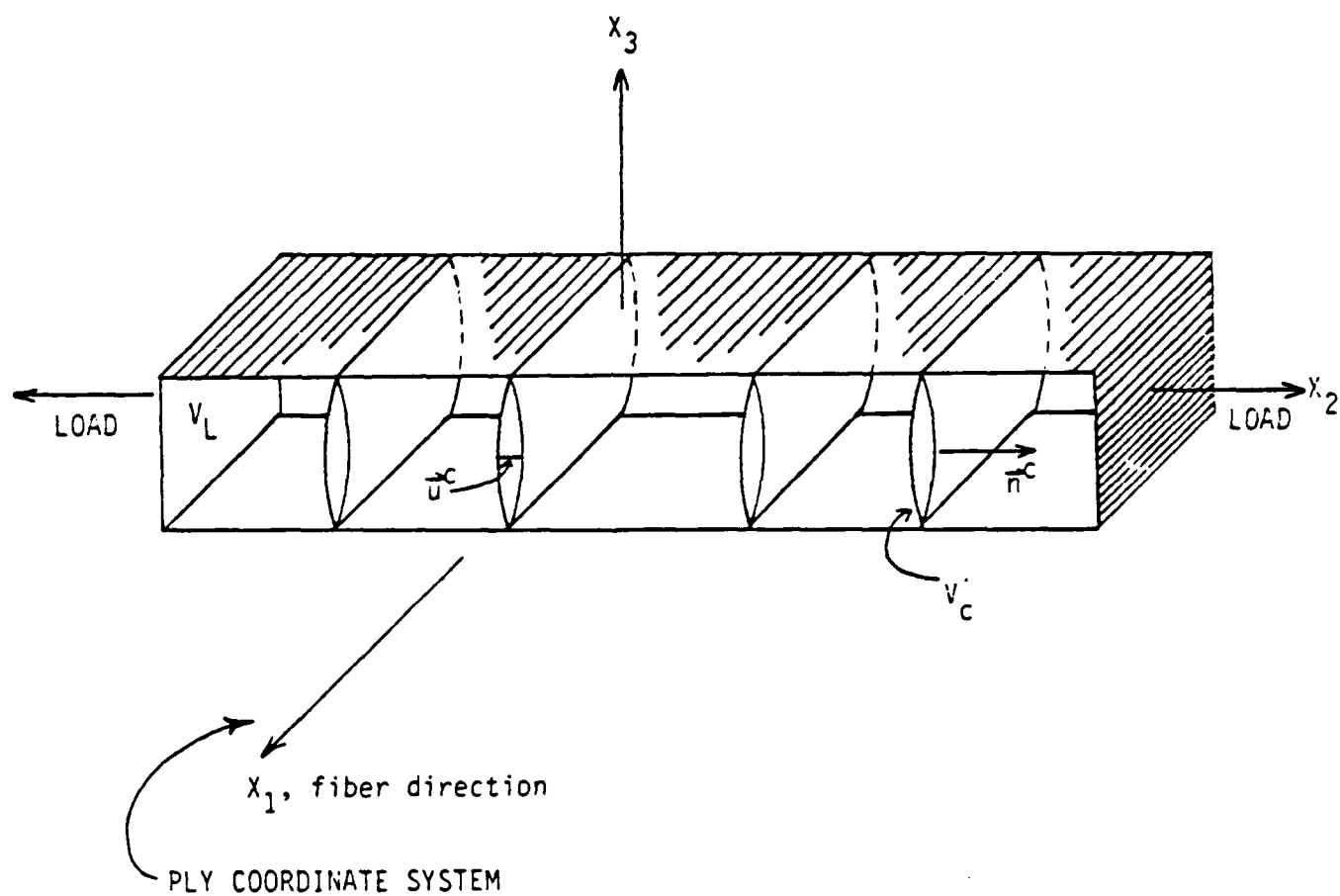
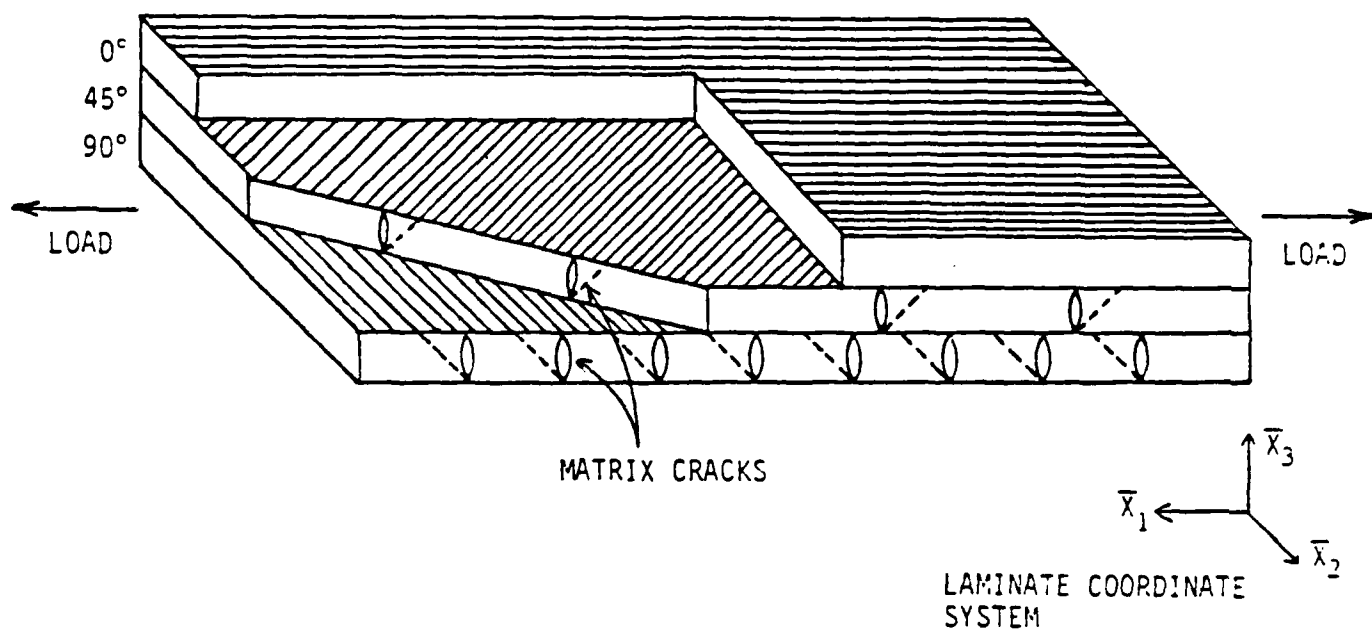Fig. 1   Transverse Matrix Cracking in a Single Ply

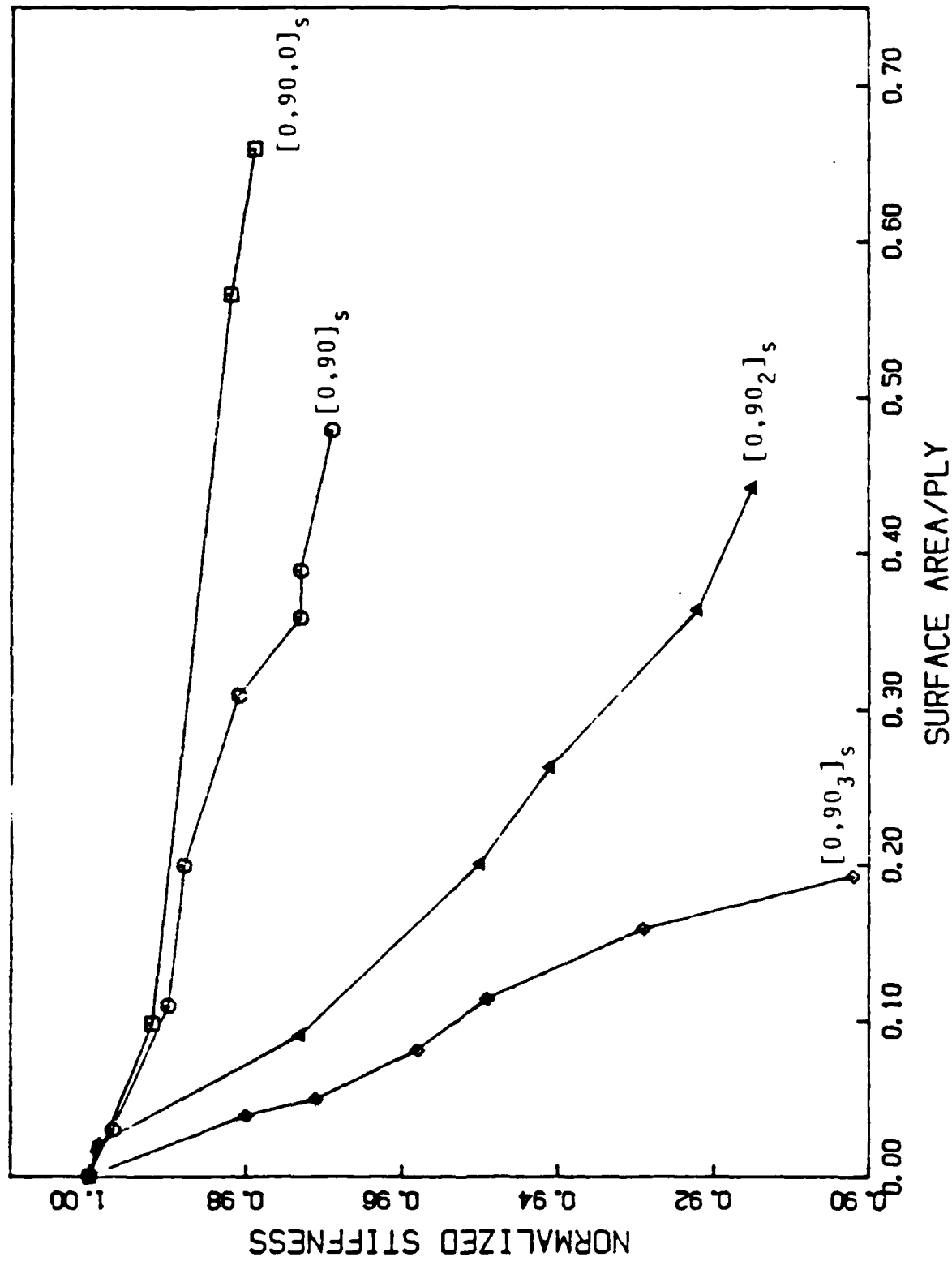Fig. 2   Matrix Cracking in a Laminated Continuous Fiber Composite

Fig. 3   Experimental Results for Stiffness Loss vs. Crack Area for
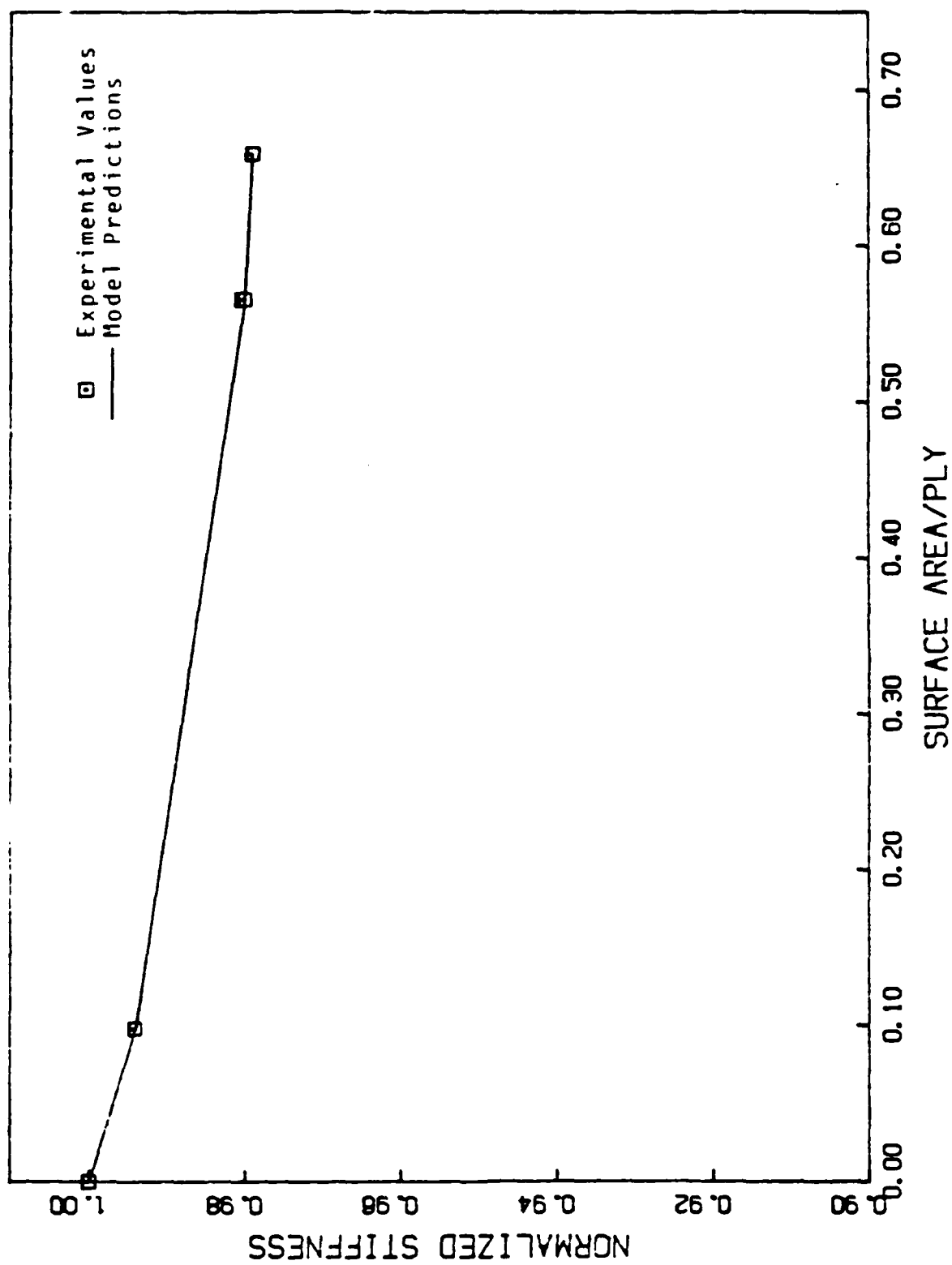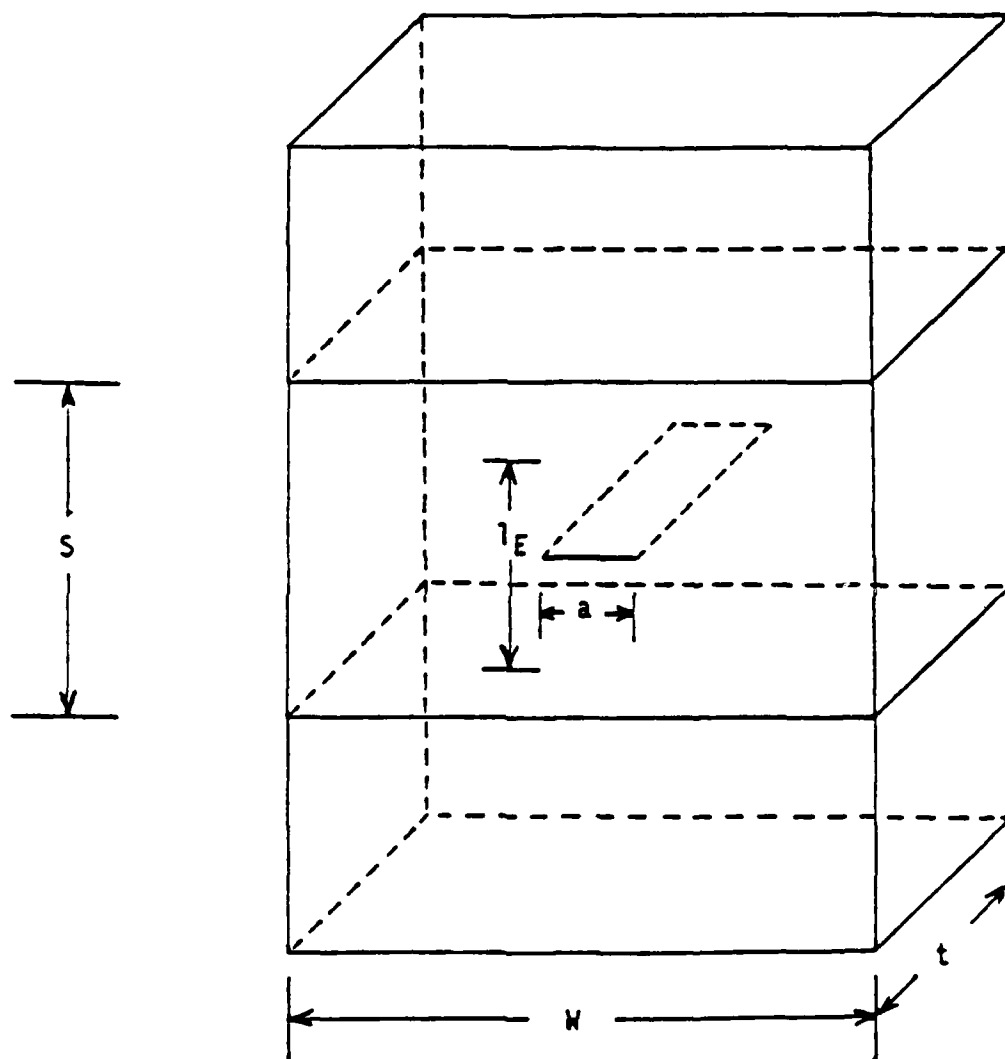Several Crossply Laminates

Fig. 4 Model vs. Experiment for $[0,90,0]_s$ Laminate

$l_E \equiv$ effective length of material in which strain energy
is released during crack extension

S = spacing between two adjacent fully developed matrix
cracks

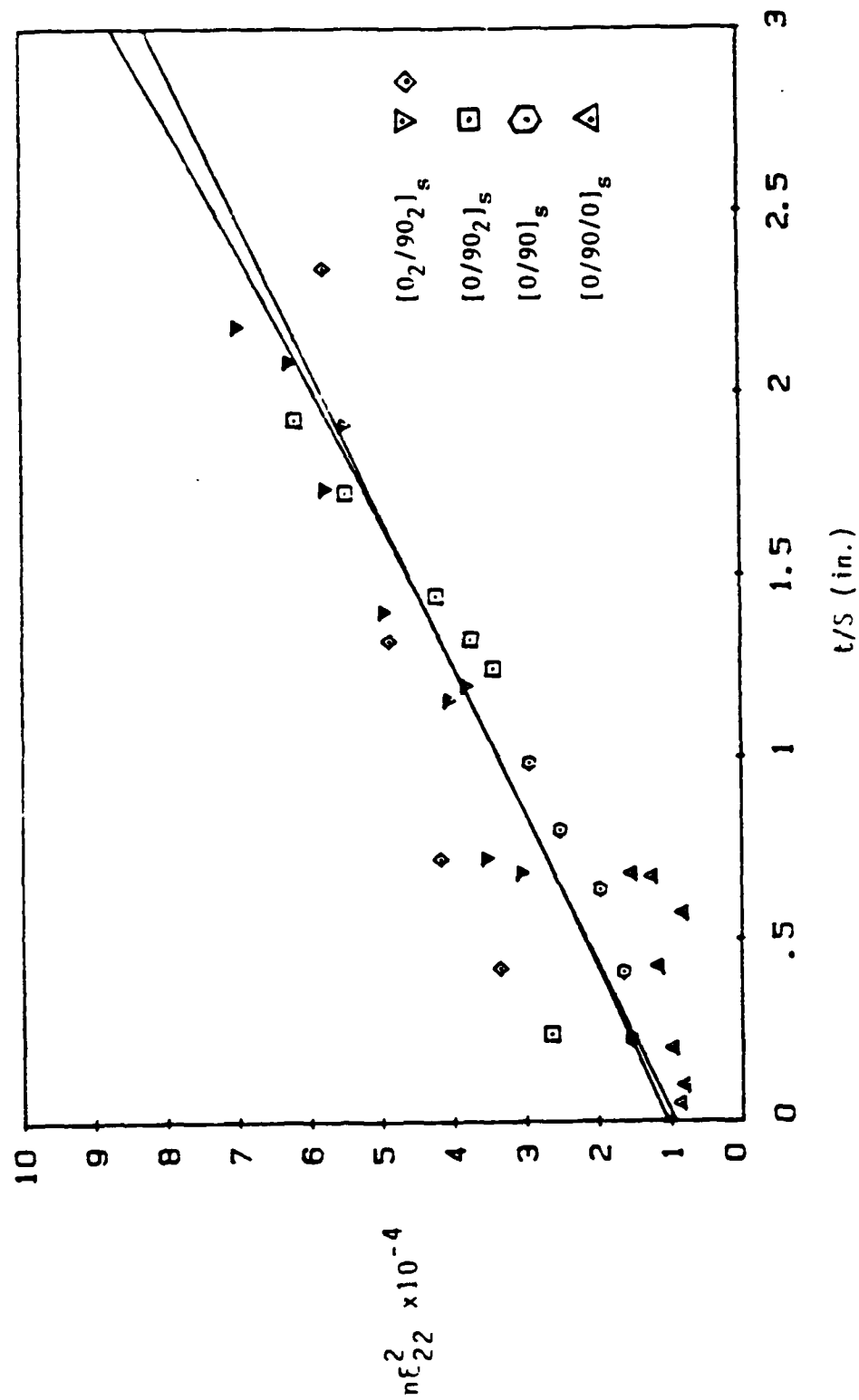Fig. F1 Crack Geometry in the 90° Layer

Fig. F2 Experimental strain energy release rate results for a variety of cross-ply laminates. (The solid lines are a straight line and quadratic least squares curve fit).

Appendix 7.3

A DAMAGE DEPENDENT CONSTITUTIVE MODEL FOR LAMINATED COMPOSITES

by

David H. Allen
Associate Professor
Aerospace Engineering Department
Texas A&M University
College Station, Texas 77843

Scott E. Groves
Research Scientist
Lawrence Livermore National Laboratories
Livermore, California 94550

and

Charles E. Harris
Assistant Professor
Aerospace Engineering Department
Texas A&M University
College Station, Texas 77843

ABSTRACT

Experimental evidence has shown that significant stiffness loss occurs in graphite/epoxy laminates when matrix cracking and interply delaminations exist. Therefore, a cumulative damage model for predicting stiffness loss in graphite/epoxy laminates is proposed herein by applying a thermomechanical constitutive theory for elastic composites with distributed damage. The model proceeds from a continuum mechanics and thermodynamics approach wherein the distributed damage is characterized by a set of second order tensor valued internal state variables. The internal state variables represent locally averaged measures of matrix cracking and interply delaminations. The model formulation provides a set of damage dependent laminated plate equations. These are developed by modifying the classical Kirchhoff plate theory. The effect of the matrix cracking enters the formulation through alteration in the individual lamina constitution. The effect of interply delamination enters the formulation through modifications of the Kirchhoff displacements. The corresponding internal state variables are defined utilizing the kinematics of the interply delaminated region and the divergence theorem. These internal state variables depend on the components of the displacements created by the delamination.

KEY WORDS

laminated composites, damage, graphite/epoxy, continuum mechanics, plate theory, internal state variables, matrix cracking, delamination

1

INTRODUCTION

Damage accumulation in composite laminates has become an extremely important design consideration in modern aerospace structures. Consequently, the composite designer must be aware of the effect of damage on the structural response. Previous research in damage mechanics has experimentally identified the various types of damage and their initiation mechanisms. This has been supported by extensive analytical investigations describing the stress and deformation fields in the damaged region. These methods include finite element analysis, finite differencing, shear lag, fracture mechanics, nonlinear viscoelasticity, and general boundary value problem solutions for special crack geometries.

In spite of the considerable research that has occurred, a comprehensive understanding and formulation of the mechanics of damage in composite materials is not yet complete. Only recently has significant attention been given to the development of cumulative damage models capable of predicting the material response due to damage. These models proceed from three conceptually different bases: 1) fracture mechanics in conjunction with microcracking [1-7], 2); empiricism [8-12]; and 3) phenomenological internal state variable theories which are based on thermodynamics [13-20].

As shown in Fig. 1., experimental evidence indicates that axial stiffness of graphite/epoxy crossply laminates is significantly affected by matrix cracking and interply delamination. The stiffness values are normalized and compared to the matrix crack density prior to saturation and then to the observable surface area of delaminations after saturation. The surface area of cracking for each damage mode was determined from edge replicas and X-ray radiographs which were obtained periodically throughout the load history. The

2

X-ray radiograph corresponding to matrix crack saturation in the 90° plies of a $[0_2,90_2)_s$ laminate is shown in Fig. 2 and the radiograph corresponding to approximately 35% delamination, as measured by an optical planimeter, at the 0°-90° interface is shown in Fig. 3. Further discussion of the experimental observation of the effect of damage mechanisms such as matrix cracking and interply delamination on stiffness in crossply laminates is presented in references 21 through 23.

On the basis of these experimental results, a cumulative damage model for predicting stiffness loss in composite laminates in the presence of matrix cracks and interply delaminations is proposed herein . The constitutive model represents an extension of the internal state variable approach formulated by Allen, et al. [19,20]. The theoretical development utilizes the concepts of continuum damage mechanics wherein the effects of the internal microcracking are reflected through alterations of the local constitutive relations. This procedure is pragmatic when compared to other alternatives such as treating each internal crack boundary as a surface in a mulitiply connected domain, thus producing an analytically untenable boundary value problem. In order for the model to be accurate, statistical homogeneity of the damage is required on a local volume scale which is large compared to the laminate microstructure but small compared to the boundary value problem of interest. Previous applications of the model [20,24] have considered matrix cracking only. It is assumed that this damage is statistically homogeneous in the local volume of the cracked plies. Therefore, the effect of matrix cracking is directly reflected through alterations of the individual lamina constitutive properties. In the current paper, interply delaminations will be included in the previously proposed theory. Since interply delaminations are not statistically homogeneous in the out-of-plane coordinate direction, a

3

kinematic constraint equation is utilized to modify the previous theory.

The stiffness of multilayered laminates can be obtained by averaging the individual lamina constitutive properties. For undamaged laminates this may be accomplished by imposing the Kirchhoff hypothesis for plates [25] and integrating the local ply constitutive equations over the laminate thickness. Higher order plate theories such as those developed by Mindlin [26], Reissner [27], and Reddy [28] which account for transverse shear deformations could be utilized as well. A modified form of the Kirchhoff hypothesis is assumed to suffice herein.

MODEL DEVELOPMENT

The Kirchhoff hypothesis must be altered to reflect the kinematic changes due to damage in the local volume element, V_L, as shown in Fig. 4. The effect of interply delamination is to produce a jump discontinuity in the displacement field. By contrast, the kinematic effects of matrix cracking have already been locally averaged into ply constitutive properties [20]. Thus, the effect of interply delamination enters the laminate formulation through alteration in the through-thickness kinematics and the effect of matrix cracking enters the laminate formulation through alteration in the individual lamina constitutive properties.

The deformation geometry and through-thickness variation of displacements for region V_L are shown in Fig. 5. Here u_k^D is the jump discontinuity due to interply delamination. Because of the delamination, the normals to the midplane are no longer constrained to remain normal after deformation. Line A-A' represents the actual before and after kinematics due to delamination. On the other hand, line C-C' represents the average effect of the

4

delaminations in V_L. The rotation, β, in each ply will also be altered by the delamination as shown in Fig. 5. This implies that β may also be subject to a jump discontinuity at the damaged ply interface. The x component of the displacement field shown in Fig. 5 is therefore assumed to be given by

$$u(x,y,z) = u^0(x,y) - z [\beta^0 + H(z-z_i) \beta_i^D] + H(z-z_i) u_i^D \qquad (1)$$

where u^0 is the midplane displacement, β^0 is the undamaged ply rotation, β_i^D is the ply jump rotation in the x-z plane due to delamination, u_i^D is the ply jump extension, and $H(z-z_i)$ is the Heavyside step function. For notational simplicity the Heavyside step function will be written as $H(z_i) \equiv H(z-z_i)$. The subscript i denotes the ith interface location of the interply delamination and the repeated i subscripts imply a summation over the number of damaged ply interfaces. It is apparent from Fig. 5 that u^0, β^0, β_i^D, and u_i^D depend only on the x and y coordinates.

Similarly, the displacement in the y coordinate direction is assumed to be given by

$$v(x,y,z) = v^0(x,y) - z (\psi^0 + H(z_i) \psi_i^D) + H(z_i) v_i^D \qquad (2)$$

where v^0 is the midplane displacement, ψ^0 is the undamaged ply rotation, ψ_i^D is the ply jump rotation in the y-z plane due to delamination, and v_i^D is the ply jump extension in the y coordinate direction.

The through-thickness displacement is assumed to be given by

$$w(x,y,z) = w^0(x,y) + H(z_i) w_i^D \qquad (3)$$

The displacement equations are averaged over the local area, A_L, shown in Fig. 4, in order to produce locally averaged displacements to be utilized in the laminate formulation. Thus,

$$u_L(x,y,z) = \frac{1}{A_L} \int_{A_L} [u^0 - z(\beta^0 + H(z_i)(\beta_i^D)) + H(z_i) u_i^D] dx dy \tag{4}$$

$$v_L(x,y,z) = \frac{1}{A_L} \int_{A_L} [v^0 - z(\psi^0 + H(z_i)(\psi_i^D)) + H(z_i) v_i^D] dx dy \tag{5}$$

and

$$w_L(x,y,z) = \frac{1}{A_L} \int_{A_L} [w^0 + H(z_i) w_i^D] dx dy \tag{6}$$

By averaging the displacements, the delamination jump discontinuities are also averaged over A_L.

The laminate strains are given by

$$\epsilon_{L_x} = \frac{\partial u_L}{\partial x} \tag{7}$$

$$\epsilon_{L_y} = \frac{\partial v_L}{\partial y} \tag{8}$$

$$\epsilon_{L_z} = \frac{\partial w_L}{\partial z} \tag{9}$$

$$\gamma_{L_{yz}} = \frac{\partial v_L}{\partial z} + \frac{\partial w_L}{\partial y} \tag{10}$$

$$\gamma_{L_{xz}} = \frac{\partial u_L}{\partial z} + \frac{\partial w_L}{\partial x} \tag{11}$$

6

$$\gamma_{L_{xy}} = \frac{\partial u_L}{\partial y} + \frac{\partial v_L}{\partial x} \tag{12}$$

Thus, due to the interply delamination all six components of the strain must be included in the laminate formulation.

The laminate constitution is obtained by integrating the stress in each lamina over the laminate thickness. The local lamina constitution is assumed to be anisotropic since the jump displacements resulting from delamination produce local anisotropic responses. That is, the out-of-plane shear strains, $\gamma_{L_{xz}}$ and $\gamma_{L_{yz}}$, resulting from delamination will contribute to the force resultants. The local lamina constitution is given by [20]

$$\left\{ \begin{array}{c} \sigma_{L_x} \\ \sigma_{L_y} \\ \sigma_{L_{xy}} \end{array} \right\} = \left[\begin{array}{cccccc} Q_{11} & Q_{12} & Q_{13} & Q_{14} & Q_{15} & Q_{16} \\ Q_{12} & Q_{22} & Q_{23} & Q_{24} & Q_{25} & Q_{26} \\ Q_{16} & Q_{26} & Q_{36} & Q_{46} & Q_{56} & Q_{66} \end{array} \right] \left\{ \begin{array}{c} \epsilon_{L_x} - \alpha^M_{xx} \\ \epsilon_{L_y} - \alpha^M_{yy} \\ \epsilon_{L_z} - \alpha^M_{zz} \\ \gamma_{L_{yz}} - 0 \\ \gamma_{L_{xz}} - 0 \\ \gamma_{L_{xy}} - \alpha^M_{xy} \end{array} \right\} \tag{13}$$

where $[Q]$ is the transformed anisotropic stiffness matrix for the lamina and α^M_{xx}, α^M_{yy}, α^M_{zz}, and α^M_{xy} represent the strain-like internal state variables for matrix cracking in terms of laminate coordinates, defined in references 19 and 20.

The resultant midplane forces and moments per unit width of region V_L in the laminate are given by

$$\left\{ \begin{array}{c} N_x \\ N_y \\ N_{xy} \end{array} \right\} \equiv \int_{-t/2}^{t/2} \left\{ \begin{array}{c} \sigma_x \\ \sigma_y \\ \sigma_{xy} \end{array} \right\} dz \tag{14}$$

and

$$\left\{ \begin{array}{c} M_x \\ M_y \\ M_{xy} \end{array} \right\} \equiv \int_{-t/2}^{t/2} \left\{ \begin{array}{c} \sigma_x \\ \sigma_y \\ \sigma_{xy} \end{array} \right\} z \, dz \tag{15}$$

where t is the laminate thickness.

In order to obtain the resultant laminate forces, first substitute equation (13) into (14) to obtain

$$\{N\} = \int_{-t/2}^{t/2} [Q] \, \{\{\epsilon_L\} - \{\alpha^M\}\} \, dz \tag{16}$$

The locally averaged strains are substituted into equation (16) to give

$$\{N\} = \int_{-t/2}^{t/2} [Q] \left[\frac{1}{A_L} \int_{A_L} \left\{ \begin{array}{c} \frac{\partial u}{\partial x} \\ \frac{\partial v}{\partial y} \\ \frac{\partial w}{\partial z} \\ \frac{\partial v}{\partial z} + \frac{\partial w}{\partial y} \\ \frac{\partial u}{\partial z} + \frac{\partial w}{\partial x} \\ \frac{\partial u}{\partial y} + \frac{\partial v}{\partial x} \end{array} \right\} dxdy \quad - \quad \{\alpha^M\} \right] dz \tag{17}$$

where u, v, and w represent the modified Kirchhoff displacements.

The divergence theorem is now utilized in order to simplify the volume

8

integrals in equation (17). The main objective of applying the divergence theorem is to obtain an expression for an internal state variable for interply delamination which is similar in form to the ISV for matrix cracking. The ISV for interply delamination should reflect the kinematics of the cracking process shown in Fig. 6. Applying the divergence theorem to the resultant forces yields

$$
\{N\} = \frac{1}{A_L} \int_S [Q] \left\{ \begin{array}{c} u\, n_x \\ v\, n_y \\ w\, n_z \\ v\, n_z + w\, n_y \\ u\, n_z + w\, n_x \\ u\, n_y + v\, n_x \end{array} \right\} dS - \sum_{k=1}^{n} [Q]_k (z_k - z_{k-1}) \{\alpha^M\}_k
$$

(18)

where n_x, n_y, and n_z represent the components of the unit outer normal on surface S. Note that the integration over S includes both the external boundary of V_L, S_1, and the internal crack boundaries, S_2, as shown in Fig. 6. The last term in equation (18) is obtained by noting that [Q] and $\{\alpha^m\}$ are piecewise constant in each ply, denoted by the subscript k, which ranges from one to the number of plies.

The next step is to substitute in the actual modified Kirchhoff displacements given by equations (1), (2), and (3) into equation (18). It is noted that for terms involving gradients in z, only those terms that are dependent on z need be retained. Thus, equation (18) becomes

9

$$\{N\} = \frac{1}{A_L} \int_S [Q] \left\{ \begin{array}{l} [u^0 - z(\beta^0 + H(z_i)\ \beta_i^D) + H(z_i)\ u_i^D]\ n_x \\[6pt] [v^0 - z(\psi^0 + H(z_i)\ \psi_i^D) + H(z_i)\ v_i^D]\ n_y \\[6pt] [\ H(z_i)\ w_i^D]\ n_z \\[6pt] [-z(\psi^0 + H(z_i)\ \psi_i^D) + H(z_i)\ v_i^D]\ n_z\ + \\[6pt] [w^0 + H(z_i)w_i^D]\ n_y \\[6pt] [-z(\beta^0 + H(z_i)\ \beta_i^D) + H(z_i)\ u_i^D]\ n_z\ + \\[6pt] [w^0 + H(z_i)\ w_i^D]\ n_x \\[6pt] [u^0 - z(\beta^0 + H(z_i)\ \beta_i^D) + H(z_i)\ u_i^D]\ n_y\ + \\[6pt] [v^0 - z(\psi^0 + H(z_i)\ \psi_i^D) + H(z_i)\ v_i^D]\ n_x \end{array} \right\} dS$$

$$- \sum_{k=1}^{n} [Q]_k (z_k - z_{k-1})\ \{\alpha^M\}_k \tag{19}$$

The next step is to integrate equation (19) over S_1 and S_2. This result will be simplified by separating the extensional and rotational terms over S_1 into two different separate terms. On the delamination surface, S_2, n_z is assumed to be the only nonzero component of the unit outer normal because the integration is performed with respect to undeformed coordinates.

The surface S_1 represents the external boundary of an equivalent local volume which contains no cracks. Therefore, it is assumed that no cracks intersect S_1. It follows that the terms containing the superscript D are all zero on S_1. Therefore, integrating the undamaged displacement terms in equation (19) on S_1 gives

10

$$\{N_1\} \equiv \frac{1}{A_L} \int_{S_1} [Q] \begin{Bmatrix} u_L^0 n_x \\ v_L^0 n_y \\ 0 \\ w_L^0 n_y \\ w_L^0 n_x \\ u_L^0 n_y + v_L^0 n_x \end{Bmatrix} dS \equiv \sum_{k=1}^{n} [Q]_k (z_k - z_{k-1}) \begin{Bmatrix} \varepsilon_{Lx}^0 \\ \varepsilon_{Ly}^0 \\ 0 \\ \gamma_{Lyz}^0 \\ \gamma_{Lxz}^0 \\ \gamma_{Lxy}^0 \end{Bmatrix} \quad (20)$$

In a similar manner, the rotational displacements acting on S_1 result in the average mid-plane rotations which when integrated over S_1 yield the average curvatures of the laminate. Thus, the undamaged rotations in equation (19) are defined as

$$\{N_2\} \equiv -\frac{1}{A_L} \int_{S_1} [Q] \begin{Bmatrix} \beta^0 n_x \\ \psi^0 n_y \\ 0 \\ \psi^0 n_z \\ \beta^0 n_z \\ \beta^0 n_y + \psi^0 n_x \end{Bmatrix} z dS \equiv \frac{-1}{2} \sum_{k=1}^{n} [Q]_k (z_k^2 - z_{k-1}^2) \begin{Bmatrix} \kappa_{Lx} \\ \kappa_{Ly} \\ 0 \\ \kappa_{Lyz} \\ \kappa_{Lxz} \\ \kappa_{Lxy} \end{Bmatrix} (21)$$

where $\{\kappa_L\}$ denotes the average midplane curvatures.

Now consider the integration of equations (19) over the delamination surface S_2. Because the integration is performed in undeformed coordinates $n_x = n_y = 0$, $n_z = \pm 1$, and the integral simplifies to

11

$$\frac{1}{A_L} \int_{S_2} [Q] \begin{Bmatrix} 0 \\ 0 \\ H(z_i)\, w_i^D n_z \\ H(z_i)[v_i^D - z(\psi_i^D)]n_z \\ H(z_i)[u_i^D - z(\beta_i^D)]n_z \\ 0 \end{Bmatrix} dS =$$

$$\sum_{i=1}^{d} \frac{1}{A_L} \int_{S_{2i}} [Q]_i \begin{Bmatrix} 0 \\ 0 \\ w_i^D n_z \\ [v_i^D - z(\psi_i^D)]n_z \\ [u_i^D - z(\beta_i^D)]n_z \\ 0 \end{Bmatrix} dS \qquad (22)$$

where d is the number of delaminated interplies and S_{2i} is the surface area of all delaminations in V_L in the ith ply interface.

Now again consider Fig. 6. The integration for a typical delamination given in equation (22) must be carried out over both top and bottom surfaces of the crack faces. Since the matrix [Q] is in most applications constant but with different values on each crack face the displacement terms in equation (22) may be written in the following form

12

$$\{N_3\} \equiv \sum_{i=1}^{d} \frac{1}{A_L} \left([Q]_i^T \int_{S_{2i}^T} \begin{Bmatrix} 0 \\ 0 \\ w_i^D \\ v_i^D \\ u_i^D \\ 0 \end{Bmatrix} n_z dS + [Q]_i^B \int_{S_{2i}^B} \begin{Bmatrix} 0 \\ 0 \\ w_i^D \\ v_i^D \\ u_i^D \\ 0 \end{Bmatrix} n_z dS \right) \tag{23}$$

where superscripts T apply to the top crack face and superscripts B apply to the bottom crack face.

Now suppose furthermore that the average displacements at each ply interface, represented by the two integral terms in equation (23), are symmetric about the ply interface. It follows that

$$\{N_3\} = \sum_{i=1}^{d} [\bar{Q}]_i t_i \begin{Bmatrix} 0 \\ 0 \\ \alpha_{1i}^D \\ \alpha_{2i}^D \\ \alpha_{3i}^D \\ 0 \end{Bmatrix} \tag{24}$$

where

$$[\bar{Q}_1]_i \equiv \frac{[Q]_i^T + [Q]_i^B}{2} \tag{25}$$

and the following components of the delamination ISV are now defined

13

$$\alpha_{1i}^{D} \equiv \frac{2}{V_{Li}} \int_{S_{2i}} w_i^{D} n_z dS \tag{26a}$$

$$\alpha_{2i}^{D} \equiv \frac{2}{V_{Li}} \int_{S_{2i}} v_i^{D} n_z dS \tag{26b}$$

$$\alpha_{3i}^{D} \equiv \frac{2}{V_{Li}} \int_{S_{2i}} u_i^{D} n_z dS \tag{26c}$$

and

$$V_{Li} \equiv t_i A_L \tag{27}$$

where t_i is defined to be the thickness of the two plies above and below the delamination, as shown in Fig. 6. In addition, it is assumed that $S_{2i}^{T} = S_{2i}^{B}$. It is noteworthy that the definitions of the internal state variables (ISV's) given by equations (30) are similar to those given for matrix cracking [19,20]. In the current paper α_{1i}^{D}, α_{2i}^{D}, and α_{3i}^{D} represent average crack opening displacements in the ith deplied interface in the z, y, and x coordinate directions. It can be seen that for these three components of the ISV for delamination the local volume V_L is represented by the ply on either side of the delamination.

Now consider the rotation terms in equation (22)

$$\{N_4\} \equiv \sum_{i=1}^{d} \frac{1}{A_L} \int_{S_{2i}} [Q]_i \left\{ \begin{array}{c} 0 \\ 0 \\ 0 \\ -z\psi_i^D \\ -z\beta_i^D \\ 0 \end{array} \right\} n_z dS$$

$$= \sum_{i=1}^{d} \frac{1}{A_L} (z_i [Q]_i^T \int_{S_{2i}^T} \left\{ \begin{array}{c} 0 \\ 0 \\ 0 \\ -\psi_i^D \\ -\beta_i^D \\ 0 \end{array} \right\} n_z dS + z_i [Q]_i^B \int_{S_{2i}^B} \left\{ \begin{array}{c} 0 \\ 0 \\ 0 \\ -\psi_i^D \\ -\beta_i^D \\ 0 \end{array} \right\} n_z dS) \tag{28}$$

The above may be written

$$\{N_4\} = \sum_{i=1}^{d} (z_i [Q]_i^T \left\{ \begin{array}{c} 0 \\ 0 \\ 0 \\ -\overline{\psi}_i^{DT} \\ -\overline{\beta}_i^{DT} \\ 0 \end{array} \right\} + z_i [Q]_i^B \left\{ \begin{array}{c} 0 \\ 0 \\ 0 \\ -\overline{\psi}_i^{DB} \\ -\overline{\beta}_i^{DB} \\ 0 \end{array} \right\}) \tag{29}$$

where

$$\overline{\psi}_i^{DT} \equiv \frac{1}{A_L} \int_{S_{2i}^T} \psi_i^D n_z dS \tag{30a}$$

$$\overline{\beta}_i^{DT} \equiv \frac{1}{A_L} \int_{S_{2i}^T} \beta_i^D n_z dS \tag{30b}$$

15

$$\overline{\psi}_i^{DB} \equiv \frac{1}{A_L} \int_{S_{2i}^B} \psi_i^D \, n_z dS \qquad\qquad (30c)$$

$$\overline{\beta}_i^{DB} \equiv \frac{1}{A_L} \int_{S_{2i}^B} \beta_i^D n_z dS \qquad\qquad (30d)$$

are the average rotations on the top and bottom crack surfaces in the delaminated ply. It is now assumed that the average rotation is independent of z between delaminations. Thus, since $n_z^T = - n_z^B = 1$,

$$\overline{\alpha}_{4(i+1)}^D \equiv \overline{\psi}_i^{DB} = -\overline{\psi}_{i+1}^{DT} \qquad\qquad i=1,\ldots,d-1$$

$$\alpha_{5(i+1)}^D \equiv \overline{\beta}_i^{DB} = -\overline{\beta}_{i+1}^{DT} \qquad\qquad i=1,\ldots,d-1 \qquad\qquad (31)$$

Suppose we also define

$$\alpha_{41}^D \equiv -\overline{\psi}_1^{DT} \, , \, \overline{\beta}_{51}^D \equiv -\overline{\beta}_1^{DT}$$

$$\alpha_{4(d+1)}^D \equiv \overline{\psi}_d^{DB} \, , \quad \alpha_{5(d+1)}^D \equiv \overline{\beta}_d^{DB} \qquad\qquad (32)$$

as shown in Fig. 7. Equation (29) may then be written as follows:

16

$$\{N_4\} = z_1 \, [Q]_1^T \left\{ \begin{matrix} 0 \\ 0 \\ 0 \\ \alpha_{41}^D \\ \alpha_{51}^D \\ 0 \end{matrix} \right\} + \sum_{i=2}^{d} \left(- z_{i-1}[Q]_{i-1}^B + z_i \, [Q]_i^T\right) \left\{ \begin{matrix} 0 \\ 0 \\ 0 \\ \alpha_{41}^D \\ \alpha_{51}^D \\ 0 \end{matrix} \right\}$$

$$- z_d \, [Q]_d^B \left\{ \begin{matrix} 0 \\ 0 \\ 0 \\ \alpha_{4(d+1)}^D \\ \alpha_{5(d+1)}^D \\ 0 \end{matrix} \right\} \tag{33}$$

Now let

$$[\bar{Q}_2]_i \equiv \frac{-z_{i-1}[Q]_{i-1}^B + z_i \, [Q]_i^T}{(z_i - z_{i-1})} \tag{34}$$

Then, equation (37) may be written

$$\{N_4\} = \sum_{i=1}^{d+1} (z_i - z_{i-1}) \, [\bar{Q}_2]_i \left\{ \begin{matrix} 0 \\ 0 \\ 0 \\ \alpha_{41}^D \\ \alpha_{51}^D \\ 0 \end{matrix} \right\} \tag{35}$$

where, by definition

17

$$z_0 \equiv 0, \quad [Q]_0^B \equiv [0], \quad z_{d+1} \equiv 0, \quad [Q]_{d+1}^T \equiv [0] \tag{36}$$

Equations (20), (21), (24), and (35) may now be substituted into equation (19) to give

$$\{N\} = \sum_{k=1}^{n} [Q]_k \, (z_k - z_{k-1}) \, \{\epsilon_L^0\} - \frac{1}{2} \sum_{k=1}^{n} [Q]_k \, (z_k^2 - z_{k-1}^2) \, \{\kappa_L\}$$

$$+ \sum_{i=1}^{d} [\bar{Q}_1]_i \; t_i \begin{Bmatrix} 0 \\ 0 \\ \alpha_{1i}^D \\ \alpha_{2i}^D \\ \alpha_{3i}^D \\ 0 \end{Bmatrix} + \sum_{i=1}^{d+1} (z_i - z_{i-1}) \, [\bar{Q}_2]_i \begin{Bmatrix} 0 \\ 0 \\ 0 \\ \alpha_{4i}^D \\ \alpha_{5i}^D \\ 0 \end{Bmatrix}$$

$$- \sum_{k=1}^{n} [Q]_k \, (z_k - z_{k-1}) \, \{\alpha^M\}_k \tag{37}$$

The moment resultants are obtained in a similar manner to the force resultants. Applying the divergence theorem to the moment resultants given in equation (15), z must be transferred inside the displacement gradients. Thus, equation (15) is written as

18

$$\{M\} = \int_{-t/2}^{t/2} [Q] \frac{1}{A_L} \int_{A_L} \left\{ \begin{array}{c} \frac{\partial}{\partial x}(zu) \\[4pt] \frac{\partial}{\partial y}(zv) \\[4pt] \frac{\partial}{\partial z}(zw) - w \\[4pt] \frac{\partial}{\partial z}(zv) - v + \frac{\partial}{\partial y}(zw) \\[4pt] \frac{\partial}{\partial z}(zu) - u + \frac{\partial}{\partial x}(zw) \\[4pt] \frac{\partial}{\partial y}(zu) + \frac{\partial}{\partial x}(zv) \end{array} \right\} dxdy - \{\alpha^M\}z \,dz \qquad (38)$$

where equation (13) has been utilized to obtain the above result.

Note that the terms involving gradients in z yield extra terms for which the divergence theorem does not apply. Applying the divergence theorem to equation (38) gives

$$\{M\} = \frac{1}{A_L} \int_S [Q] \left\{ \begin{array}{c} z\,u\,n_x \\ z\,v\,n_y \\ z\,w\,n_z \\ z\,v\,n_z + z\,w\,n_y \\ z\,u\,n_z + z\,w\,n_x \\ z\,u\,n_y + z\,v\,n_x \end{array} \right\} dS - \frac{1}{A_L} \int_{V_L} [Q] \left\{ \begin{array}{c} 0 \\ 0 \\ w \\ v \\ u \\ 0 \end{array} \right\} dxdydz$$

$$- \frac{1}{2} \sum_{k=1}^{n} [Q]_k (z_k^2 - z_{k-1}^2) \,\{\alpha^M\}_k \qquad (39)$$

It is now assumed that the applied moments are independent of rigid body motions. Therefore, the second term in equation (39) may be neglected.

The modified Kirchhoff displacements are substituted into equation (39) to give

19

$$\{M\} = \frac{1}{A_L} \int_S [Q] \left\{ \begin{array}{l} [u^0 - z(\beta^0 + H(z_i)\ \beta_i^D) + H(z_i)\ u_i^D]\ n_x \\[4pt] [v^0 - z(\psi^0 + H(z_i)\ \psi_i^D) + H(z_i)\ v_i^D]\ n_y \\[4pt] [\ H(z_i)\ w_i^D]\ n_z \\[4pt] [-z(\psi^0 + H(z_i)\ \psi_i^D) + H(z_i)\ v_i^D]\ n_z + \\[4pt] [w^0 + H(z_i)w_i^D]\ n_y \\[4pt] [-z(\beta^0 + H(z_i)\ \beta_i^D) + H(z_i)\ u_i^D]\ n_z + \\[4pt] [w^0 + H(z_i)\ w_i^D]\ n_x \\[4pt] [u^0 - z(\beta^0 + H(z_i)\ \beta_i^D) + H(z_i)\ u_i^D]\ n_y + \\[4pt] [v^0 - z(\psi^0 + H(z_i)\ \psi_i^D) + H(z_i)\ v_i^D]\ n_x \end{array} \right\} z\ dS$$

$$- \sum_{k=1}^{n} [Q]_k (z_k^2 - z_{k-1}^2)\ \{\alpha^M\}_k \tag{40}$$

The next step is to integrate the first term in equation (40) over S_1 and S_2. Again, this result will be simplified by separating the extensional and rotational terms over S_1 into two different terms. Thus, equation (40) becomes

20

$$\{M\} = \frac{1}{A_L} \int_{S_1} [Q] \begin{Bmatrix} [u^0 + H_1 u_1^D] \, n_x \\ [v^0 + H_1 v_1^D] \, n_y \\ H_1 w_1^D \, n_z \\ H_1 v_1^D \, n_z + [w^0 + H_1 w_1^D] \, n_y \\ H_1 u_1^D \, n_z + [w^0 + H_1 w_1^D] \, n_x \\ [u^0 + H_1 u_1^D] \, n_y + [v^0 + H_1 v_1^D] \, n_x \end{Bmatrix} z \, dS$$

$$- \frac{1}{A_L} \int_{S_1} [Q] \begin{Bmatrix} [\beta^0 + H_1(\beta_1^D)] \, n_x \\ [\psi^0 + H_1(\psi_1^D)] \, n_y \\ 0 \\ [\psi^0 + H_1(\psi_1^D)] \, n_z \\ [\beta^0 + H_1(\beta_1^D)] \, n_z \\ [\beta^0 + H_1(\beta_1^D)] \, n_y + \\ [\psi^0 + H_1(\psi_1^D)] \, n_x \end{Bmatrix} z^2 \, dS$$

$$+ \frac{1}{A_L} \int_{S_2} [Q] \begin{Bmatrix} 0 \\ 0 \\ H_1 w_1^D n_z \\ H_1 [v_1^D - z(\psi_1^D)] \, n_z \\ H_1 [u_1^D - z(\beta_1^D)] \, n_z \\ 0 \end{Bmatrix} z \, dS$$

$$- \frac{1}{2} \sum_{k=1}^{n} [Q]_k (z_k^2 - z_{k-1}^2) \, \{\alpha^M\}_k \tag{41}$$

Integrating the undamaged displacement terms in equation (41) on S_1 gives

21

$$\{M_1\} \equiv \frac{1}{A_L} \int_{S_1} [Q] \begin{Bmatrix} u_\ell n_x \\ v_\ell n_y \\ 0 \\ w_\ell n_y \\ w_\ell n_x \\ u_\ell n_y + v_\ell n_x \end{Bmatrix} z\,dS \equiv \frac{1}{2} \sum_{k=1}^n [Q]_k (z_k^2 - z_{k-1}^2) \begin{Bmatrix} \varepsilon_{\ell x} \\ \varepsilon_{\ell y} \\ 0 \\ \gamma_{\ell yz} \\ \gamma_{\ell xz} \\ \gamma_{\ell xy} \end{Bmatrix} \quad (42)$$

Similarly,

$$\{M_2\} \equiv -\frac{1}{A_L} \int_{S_1} [Q] \begin{Bmatrix} \beta^o n_x \\ \psi^o n_y \\ 0 \\ \psi^o n_z \\ \beta^o n_z \\ \beta^o n_y + \psi^o n_x \end{Bmatrix} z^2\,dS \equiv -\frac{1}{3} \sum_{k=1}^n [Q]_k (z_k^3 - z_{k-1}^3) \begin{Bmatrix} \kappa_{Lx} \\ \kappa_{Ly} \\ 0 \\ \kappa_{Lyz} \\ \kappa_{Lxz} \\ \kappa_{Lxy} \end{Bmatrix} \quad (43)$$

Now consider the term in equation (41) which is integrated over S_2. Because the integration is performed in undeformed coordinates $n_x = n_y = 0$, $n_z = \pm 1$, and this term reduces to

22

$$\frac{1}{A_L} \int_{S_2} [Q] \begin{Bmatrix} 0 \\ 0 \\ H(z_i) \, w_i^D n_z \\ H(z_i)[v_i^D - z(\psi_i^D)]n_z \\ H(z_i)[u_i^D - z(\beta_i^D)]n_z \\ 0 \end{Bmatrix} z \, dS \quad = $$

$$\sum_{i=1}^{d} \frac{1}{A_L} \int_{S_{2i}} [Q]_i \begin{Bmatrix} 0 \\ 0 \\ w_i^D n_z \\ [v_i^D - z(\psi_i^D)]n_z \\ [u_i^D - z(\beta_i^D)]n_z \\ 0 \end{Bmatrix} z \, dS \tag{44}$$

where d is the number of delaminated interplies and S_{2i} is the surface area of all delaminations in V_L in the ith ply interface.

Integrating the displacement equation (44) over the top and bottom delamination surfaces gives

$$\{M_3\} \equiv \sum_{i=1}^{d} \frac{1}{A_L} \left(z_i [Q]_i^T \int_{S_{2i}^T} \begin{Bmatrix} 0 \\ 0 \\ w_i^D \\ v_i^D \\ u_i^D \\ 0 \end{Bmatrix} n_z \, dS + z_i [Q]_i^B \int_{S_{2i}^B} \begin{Bmatrix} 0 \\ 0 \\ w_i^D \\ v_i^D \\ u_i^D \\ 0 \end{Bmatrix} n_z \, dS \right) \tag{45}$$

23

where superscripts T apply to the top crack face and superscripts B apply to the bottom crack face.

Now suppose furthermore that the average displacements at each ply interface, represented by the two integral terms in equation (45), are symmetric about the ply interface. It follows that

$$\{M_3\} = \sum_{i=1}^{d} [\overline{Q}_3]_i t_i^2 \begin{Bmatrix} 0 \\ 0 \\ \alpha_{1i}^D \\ \alpha_{2i}^D \\ \alpha_{3i}^D \\ 0 \end{Bmatrix} \tag{46}$$

where

$$[\overline{Q}_3]_i \equiv \frac{z_i([Q]_i^T + [Q]_i^B)}{2t_i} \tag{47}$$

Now consider the rotation terms in equation (44):

$$\{M_4\} \equiv \sum_{i=1}^{d} \frac{1}{A_L} \int_{S_{2i}} [Q]_i \left\{ \begin{array}{c} 0 \\ 0 \\ 0 \\ -z^2 \psi_i^D \\ -z^2 \beta_i^D \\ 0 \end{array} \right\} n_z dS$$

$$= \sum_{i=1}^{d} \frac{1}{A_L} \left(z_i^2 [Q]_i^T \int_{S_{2i}^T} \left\{ \begin{array}{c} 0 \\ 0 \\ 0 \\ -\psi_i^D \\ -\beta_i^D \\ 0 \end{array} \right\} n_z dS + z_i^2 [Q]_i^B \int_{S_{2i}^B} \left\{ \begin{array}{c} 0 \\ 0 \\ 0 \\ -\psi_i^D \\ -\beta_i^D \\ 0 \end{array} \right\} n_z dS \right) \tag{48}$$

The above may be written

$$\{M_4\} = \sum_{i=1}^{d} \left(z_i^2 [Q]_i^T \left\{ \begin{array}{c} 0 \\ 0 \\ 0 \\ -\overline{\psi}_i^{DT} \\ -\overline{\beta}_i^{DT} \\ 0 \end{array} \right\} + z_i^2 [Q]_i^B \left\{ \begin{array}{c} 0 \\ 0 \\ 0 \\ -\overline{\psi}_i^{DB} \\ -\overline{\beta}_i^{DB} \\ 0 \end{array} \right\} \right) \tag{49}$$

Now let

$$[\overline{Q}_4]_i \equiv \frac{-z_{i-1}^2 [Q]_{i-1}^B + z_i^2 [Q]_i^T}{(z_i^2 - z_{i-1}^2)} \tag{50}$$

Then, equation (49) may be written

25

$$\{M_4\} = \sum_{i=1}^{d+1} (z_i^2 - z_{i-1}^2) \, [\bar{Q}_4]_i \begin{Bmatrix} 0 \\ 0 \\ 0 \\ \alpha_{4i}^D \\ \alpha_{5i}^D \\ 0 \end{Bmatrix} \tag{51}$$

Equations (42), (43), (46), and (51) may now be substituted into equation (41) to give

$$\{M\} = \frac{1}{2} \sum_{k=1}^{n} [Q]_k \, (z_k^2 - z_{k-1}^2) \, \{\varepsilon_L^0\} - \frac{1}{3} \sum_{k=1}^{n} [Q]_k \, (z_k^3 - z_{k-1}^3) \, \{\kappa_L\}$$

$$+ \sum_{i=1}^{d} [\bar{Q}_3]_i \; t_i^2 \begin{Bmatrix} 0 \\ 0 \\ \alpha_{1i}^D \\ \alpha_{2i}^D \\ \alpha_{3i}^D \\ 0 \end{Bmatrix} \quad + \sum_{i=1}^{d+1} [\bar{Q}_4]_i (z_i^2 - z_{i-1}^2) \begin{Bmatrix} 0 \\ 0 \\ 0 \\ \alpha_{4i}^D \\ \alpha_{5i}^D \\ 0 \end{Bmatrix}$$

$$- \frac{1}{2} \sum_{k=1}^{n} [Q]_k \, (z_k^2 - z_{k-1}^2) \, \{\alpha^M\}_k \tag{52}$$

COMPARISON OF MODEL PREDICTIONS TO EXPERIMENTAL RESULTS

The suitability of the above damage-dependent laminate analysis equations must be assessed by comparing displacements predicted by the damage model to experimentally measured values. This is accomplished herein by comparing model predictions to the damage-degraded engineering modulus, E_x, of several laminates determined from tensile coupon tests. A limited number of test results have been obtained for AS-4/3502 graphite/epoxy laminates with a quasi-isotropic and several cross-ply stacking sequences. The combined matrix cracking and delamination damage modes were generated by tension-tension fatigue loading (R=0.1) at 2 Hz and the engineering modulus of the laminate was measured by a 1.0 in. extensometer.

A reasonable indication of the validity and usefulness of the postulated damage-dependent laminate analysis equations may be obtained by comparing results obtained for a somewhat simplified but nonetheless realistic laminate with damage. The special case considered herein is a symmetric, balanced laminate subjected to an in-plane loading N_x and with a single delamination interface site that is symmetric about the laminate midplane. Defining the engineering modulus as follows

$$E_x \equiv \frac{1}{t} \frac{\partial N_x}{\partial \epsilon_x} \tag{53}$$

and using equation (37), the damage-dependent engineering modulus is given by

$$E_x = \frac{1}{n} \sum_{k=1}^{n} (Q_{11})_k - \frac{1}{n} \sum_{k=1}^{n} (Q_{11})_k \left(\frac{\partial \alpha_x^M}{\partial \epsilon_x}\right)_k + \frac{t_1}{t} \left[\frac{(Q_{15})_1^T + (Q_{15})_1^B}{2}\right] \frac{\partial \alpha_3^D}{\partial \epsilon_x} \tag{54}$$

27

where α_x^M and α_3^D are the only contributing ISV's for matrix crack damage and delamination damage, respectively, for the special case of interest here. The procedure for specifying the value of the ISV for a particular damage state is presented in Reference 22 and makes use of the strain energy release rate for crack surface area creation. The expression for the matrix crack ISV specified for a single 90° ply is given by [22]

$$\frac{\partial \alpha_x^M}{\partial \epsilon_x} = \frac{1}{2} n \frac{(p+q)}{q} \frac{E_{xo}}{I_{22}'} \left(\frac{E_{x1}}{E_{xo}} \Big|_S - 1 \right) \tag{55}$$

where n is the number of consecutive 90° plies in the 90° layer, p is the number of 0° plies, q is the number of 90° plies in the laminate and $E_{x1}/E_{xo}|_S$ was determined experimentally for the $[0/90/0]_s$ laminate containing a single 90° layer with matrix crack surface area, S. Using the O'Brien [30] delamination strain energy release rate model as a first approximation the delamination ISV is given by

$$\frac{\partial \alpha_3^D}{\partial \epsilon_x} = -\frac{n}{2} \frac{(E_x - E^*)}{[(\bar{Q}_{15})_1^T + (\bar{Q}_{15})_1^B]} \left(\frac{S_D}{S} \right) \tag{56}$$

where n is the number of plies in the laminate, S_D is the delamination surface area, S is the total interface surface area of the local volume, and E^* is given by

$$E^* = \frac{1}{t} \sum_{i=1}^{d} E_i t_i \tag{57}$$

where E_i is equal to E_x for the sublaminates and t_i is the thickness of the sublaminates formed by the delamination. Therefore, equations (54-57) may be used to predict the damage degraded engineering modulus of any symmetric,

28

balanced laminate with one symmetrically located delamination site.

A comparison of the model prediction of E_x to experimental results is presented in Table 1 for the $[0_2/90_2]_s$ and $[0/\pm45/90]_s$ laminates. The damage degraded modulus has been normalized by the initial undamaged modulus. X-ray radiographs of the damage states are shown in Figs. 3 and 8 for the $[0_2/90_2]_s$ and $[0/\pm45/90]_s$ laminates, respectively. The comparison between the theoretical and experimental results is quite good. While this is a very limited comparison, the results are very encouraging because the stiffness loss in the $[0_2/90_2]_s$ laminate is primarily due to matrix cracking, whereas the stiffness loss in the $[0/\pm45/90]_s$ laminate is primarily due to the delaminations.

SUMMARY AND CONCLUSIONS

This paper has presented a formulation of a cumulative damage model for continuous fiber composites in the presence of matrix cracking and interply delamination. The model represents a set of damage dependent laminate plate equations. The laminate equations were developed utilizing classical Kirchhoff plate theory as well as standard continuum mechanics. The key developments of the theory are enumerated below:

1. The damage is reflected in the laminate equations through the second order tensor-valued internal state variables. These ISV's are dependent on the observed surface area of damage. The emphasis of this research has been to obtain a consistent definition of the ISV for interply delamination.

2. Although the ISV's are defined similarily, they enter the formulation in different ways. The ISV for matrix cracking enters at the ply level through alteration in the lamina constitution because this damage is fully contained within the cracked plies. The ISV for interply delamination enters at the laminate level through alteration in the Kirchhoff displacements. This is due to the fact that the delamination occurs at the interface of dissimilar materials, which results in statistical nonhomogeneity and thus cannot be reflected through changes in the lamina constitution. The separation of the ISV's between lamina and laminate behavior was a major part of the model development.

3. Because the ISV for interply delamination represents the three out-of-plane strain components, an anisotropic material response must be assumed in order to couple the out-of-plane strains with the in-plane laminate forces. Therefore, all six components of the strain are accounted for in the overall constitutive response. This assumption was a key part of the model development which eventually led to the consistent definition of the ISV for interply delamination.

4. By averaging the modified kinematic relations over the local domain of interest and then applying the divergence theorem the actual definition of the ISV was obtained.

5. The local anisotropic properties were defined in terms of the response of the sublaminate, created by the delamination, to the applied "jump" displacements.

30

6. The ISV's have been related to the surface area of damage using linear elastic fracture mechanics. By determining the energy release rate for each damage mode the ISV's are fully defined.

A total of three new changes were introduced to the standard laminate equations: 1) the ISV for matrix cracking, 2) the ISV for interply delamination, and 3) the local anisotropic stiffness.

The ultimate objective of any continuum mechanics model is to design structural components so as to avoid failure. In the sense that laminated composites fail due to a complex sequence of damage events, it is essential to capture the important features of the damage process in order to accurately predict failure. Obviously this will be a complex task in laminated composites, but, as Einstein once put it, a good theory should be as simple as possible but no simpler than that.

The authors have constructed a continuum damage model for laminated continuous fiber composites. This model utilizes second order tensor-valued internal state variables to account for both matrix cracking and delamination at the sub-laminate level in such a way as to produce a stacking sequence independent model. The input properties may be obtained from a single [0,90,0] specimen.

The model has thus far been shown to be accurate in predicting both in-plane and out-of-plane stiffness loss in crossply specimens with both vertical and curved matrix cracks. Efforts are currently underway to compare model stiffness predictions to experiment for quasi-isotropic laminates with both matrix cracks and delaminations. The initial comparison are quite encouraging. Research is also underway to develop stacking sequence independent ISV growth laws for matrix cracking and delaminations.

31

The ultimate goal of this research is to develop a model capable of predicting failure of a component subjected to loads resulting in stress gradients. Toward this end, it is believed by these authors that the essential ingredients are now in place for constructing a failure function which describes fiber fracture as a function of matrix cracking and delamination.

ACKNOWLEDGEMENT

REFERENCES

1. Chou, P.C., Wang, A.S.D., and Miller, H., "Cumulative Damage Model for Advanced Composite Materials," AFWAL-TR-82-4083, Air Force Wright Aeronautical Laboratories, April 1982.

2. Waddoups, M.E., Eisenmann, J.R., and Kaminski, B.E., "Macroscopic Fracture Mechanics of Advanced Composite Materials," J. Co⸳⸳site Materials, Vol. 5, pp. 446-454, 1971.

3. Hahn, H.T., "Fracture Behavior of Composite Laminates," Proc. Int. Conference on Fracture Mechanics and Technology, Sigthoff, Noordhoff, Hong Kong, 1977.

4. Morris, D.H. and Hahn, H.T., "Fracture Resistance Characterization of Graphite/Epoxy Composites," Composite Materials: Testing and Design, ASTM STP 617, Eds, American Society for Testing and Materials, Philadelphia, PA., pp. 5-17, 1977.

5. Yeow, Y.T., Morris, D.H., and Brinson, H.F., "The Fracture Behavior of Graphite/Epoxy Laminates," Experimental Mechanics, Vol. 19, pp. 1-8, 1979.

6. Schapery, R.A., "Models for Damage Growth and Fracture in Nonlinear Viscoelastic Particulate Composites," MM-3168-82-5, Mechanics and Materials Center, Texas A&M University, August 1982.

7. Schapery, R.A. "Continuum Aspects of Crack Growth in Time Dependent Materials," MM-4665-83-2, Mechanics and Materials Center, Texas A&M University, February 1983.

8. Chou, P.C. and Croman, R., "Residual Strength in Fatigue Based on the Strength-Life Equal Rank Assumption," <u>J. Composite Materials</u>, Vol. 12, April 1978, pp. 177-194.

9. Gottesman, T., Hashin, Z., and Brull, M.A., "Effective Elastic Properties of Cracked Materials," N00014-78-C-0544, TR-6, ONR, May 1981.

10. Hashin, Z., "A Reinterpretation of the Palmgreen-Miner Rule for Fatigue Life Prediction," <u>J. Applied Mechanics</u>, Vol. 47, June 1980, pp. 324-329.

11. Laws, N., Dvorak, G.J., and Hejazi, M., "Stiffness Changes in Unidirectional Composites Caused By Cracked Systems," <u>Mechanics of Materials 2</u>, (1983) 123-137, North Holland.

12. Dvorak, G.J., "Analysis of Progressive Matrix Cracking in Composite Laminates," AFOSR-82-0308, Rensselaer Polytechnic Institute, March 1985.

13. Talreja, R., "Fatigue of Composite Materials: Damage Mechanisms and Fatigue-Life Diagrams," <u>Proc. Royal Society of London</u>, A 378, pp. 461-475, 1981, Printed in Great Britain.

14. Talreja, R., "A Continuum Mechanics Characterization of Damage in Composite Materials," <u>Proc. Royal Society of London</u>, Vol. 399A, 1985, pp. 195-216.

15. Coleman, B.D. and Gurtin, M.E., "Thermodynamics With Internal State Variables," <u>J. Chem. Phys.</u>, Vol. 47, No. 2, 1967, pp. 597-613.

16. Krajcinovic, D. and Fonseka, G.U., "The Continuous Damage Theory of Brittle Materials, Part I: General Theory," <u>J. Applied Mechanics</u>, Vol. 48, 1981, pp. 809-815.

17. Fonseka, G.U. and Krajcinovic, D., "The Continuous Damage Theory of Brittle Materials, Part II: Uniaxial and Plane Response Modes," <u>Journal of Applied Mechanics</u>, Vol. 48, 1981, pp. 816-824.

18. Krajcinovic, D., "Constitutive Equations for Damaging Materials," <u>Journal of Applied Mechanics</u>, Transactions of the ASME, 83-APM-12, Houston, 1983.

19. Allen, D.H., Harris, C.E., and Groves, S.E.,"A Thermomechanical Constitutive Theory for Elastic Composites with Distributed Damage - Part I: Theoretical Development," to appear in <u>International Journal of Solids and Structures</u>, 1987 (also reported in Texas A&M University Mechanics and Materials Center, MM-5023-85-17, October, 1985).

20. Allen, D.H., Harris, C.E., and Groves, S.E.,"A Thermomechanical Constitutive Theory for Elastic Composites with Distributed Damage - Part II: Application to Matrix Cracking in Laminated Composites," to appear in <u>International Journal of Solids and Structures</u>, 1987 (also reported in Texas A&M University Mechanics and Materials Center, MM-5023-85-15, October, 1985).

21. Groves, S.E., Harris, C.E., Highsmith, A.L., Allen, D.H., and Norvell, G., "An Experimental and Analytical Treatment of the Mechanics of Damage in Laminated Composites," to appear in Experimental Mechanics, 1987.

22. Norvell, G., "An Investigation of Damage Accumulation in Graphite/Epoxy Laminates," Thesis, Texas A&M University, 1985.

23. Georgiou, I.T.,"Initiation Mechanisms and Fatigue Growth of Internal Delaminations in Graphite/Epoxy Crossply Laminates," Thesis, Texas A&M University, 1986.

24. Allen, D.H., Harris, C.E., Groves, S.E., and Norvell, R.G., "Characterization of Stiffness Loss in Crossply Laminates with Curved Cracks," to appear in Journal of Composite Materials, 1987 (also reported in Texas A&M University Mechanics and Materials Center, MM-5023-86-14, June, 1986).

25. Jones, R.M., Mechanics of Composite Materials, McGraw-Hill, 1975.

26. Mindlin, R.D.,"Influence of Rotary Inertia and Shear on Flexural Motions of Isotropic, Elastic Plates," J. Applied Mechanics, Vol. 18, (Trans. ASME 73) A31, 1951.

27. Reissner, E.,"The Effect of Transverse Shear Deformation on the Bending of Elastic Plates," J. Applied Mechanics, Vol. 12 (Trans ASME 67) A67, 1945.

28. Reddy, J.N.,"A Refined Nonlinear Theory of Plates with Transverse Shear Deformation," Int. J. Solids & Structures, Vol. 20, 1984.

29. Groves, S.E., " A Study of Damage Mechanics in Continuous Fiber Composite Laminates with Matrix Cracking and Interply Delaminations," Dissertation, Texas A & M University, 1986.

30. O'Brien, T.K., "Characterization of Delamination Onset and Growth in a Composite Laminate," Damage in Composite Materials, K.L. Reifsnider, Ed., ASTM STP 775, American Society for Testing and Materials, Philadelphia, pp. 141-167, 1982.

TABLE 1 RESULTS FOR GRAPHITE/EPOXY LAMINATES

LAMINATE STACKING SEQUENCE	$[0_2/90_2]_s$	$[0/\pm 45/90]_s$
NUMBER OF CRACKS PER INCH IN 90° LAYER	54	44
DELAMINATION INTERFACE	0/90	-45/90
PERCENT DELAMINATION	47.3	57.0
$\dfrac{E_x}{E_{x_o}}$ EXPERIMENTAL	0.949	0.888
$\dfrac{E_x}{E_{x_o}}$ MODEL PREDICTION	0.939	0.878

FIGURE CAPTIONS

Fig. 1. Axial stiffness loss in a $[0_2,90_2]_s$ graphite/epoxy laminate with matrix cracking and interply delaminations.

Fig. 2. Matrix crack saturation in a $[0_2,90_2]_s$ laminate.

Fig. 3. Interply delamination in a $[0_2,90_2]_s$ laminate.
300,000 cycles.

Fig. 4. Characteristic local region of damage. a) general laminate, b) exploded view of V_L with damage.

Fig. 5. Deformation geometry for region A_L.

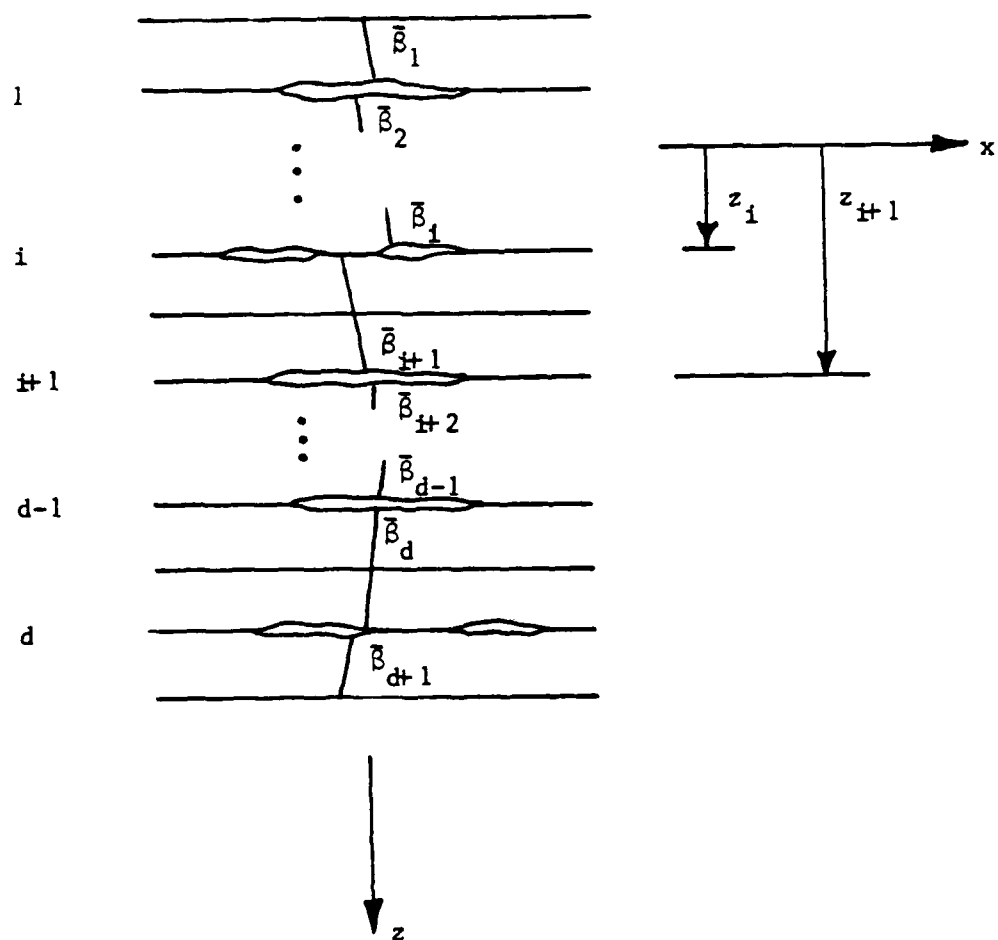Fig. 6. Interply delamination in a laminated continuous fiber composite.

Fig. 7. Schematic of delaminated region in a composite layup.

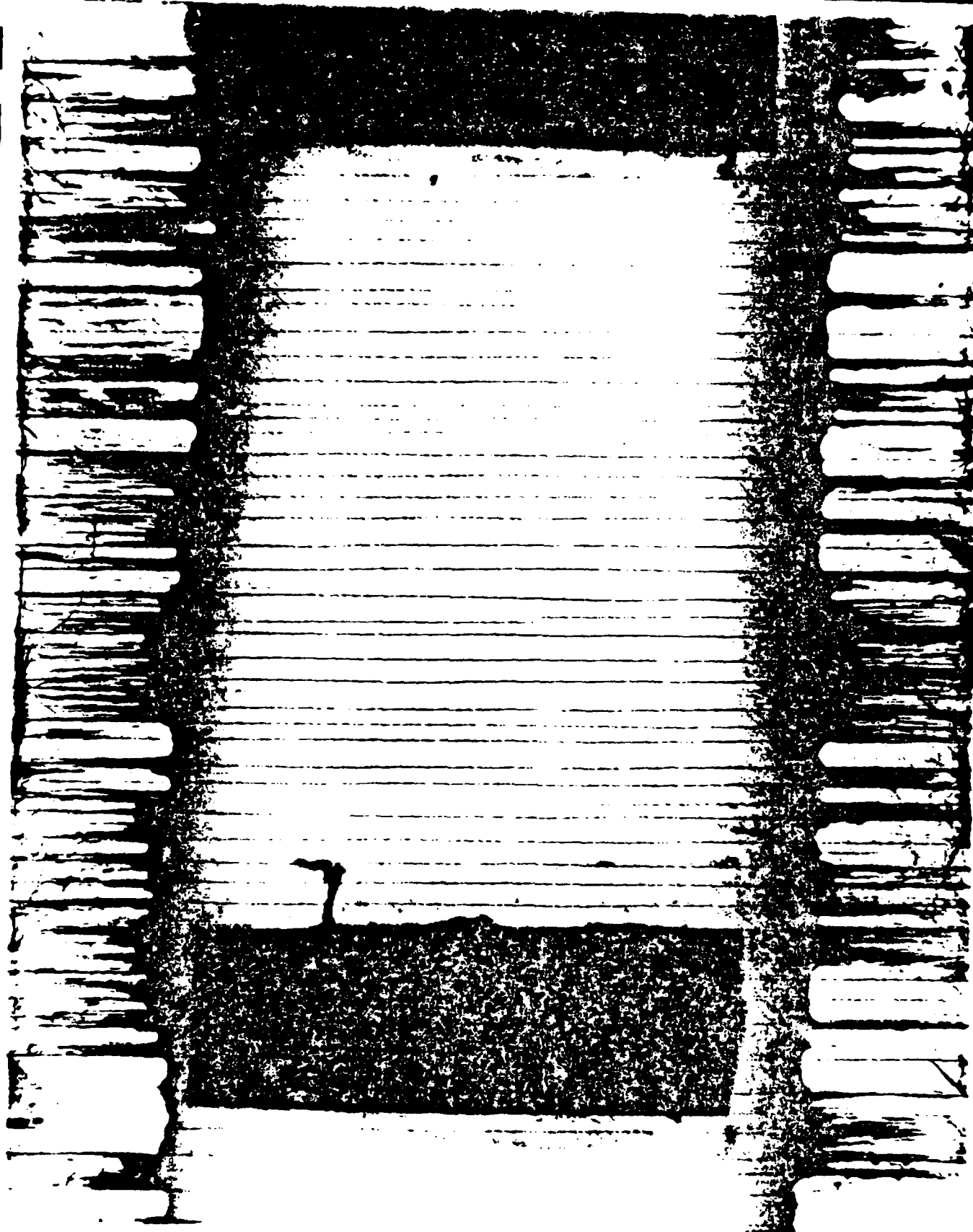Fig. 8. Combined damage mode in $[0/\pm45/90]_s$ due to tension-tension fatigue.
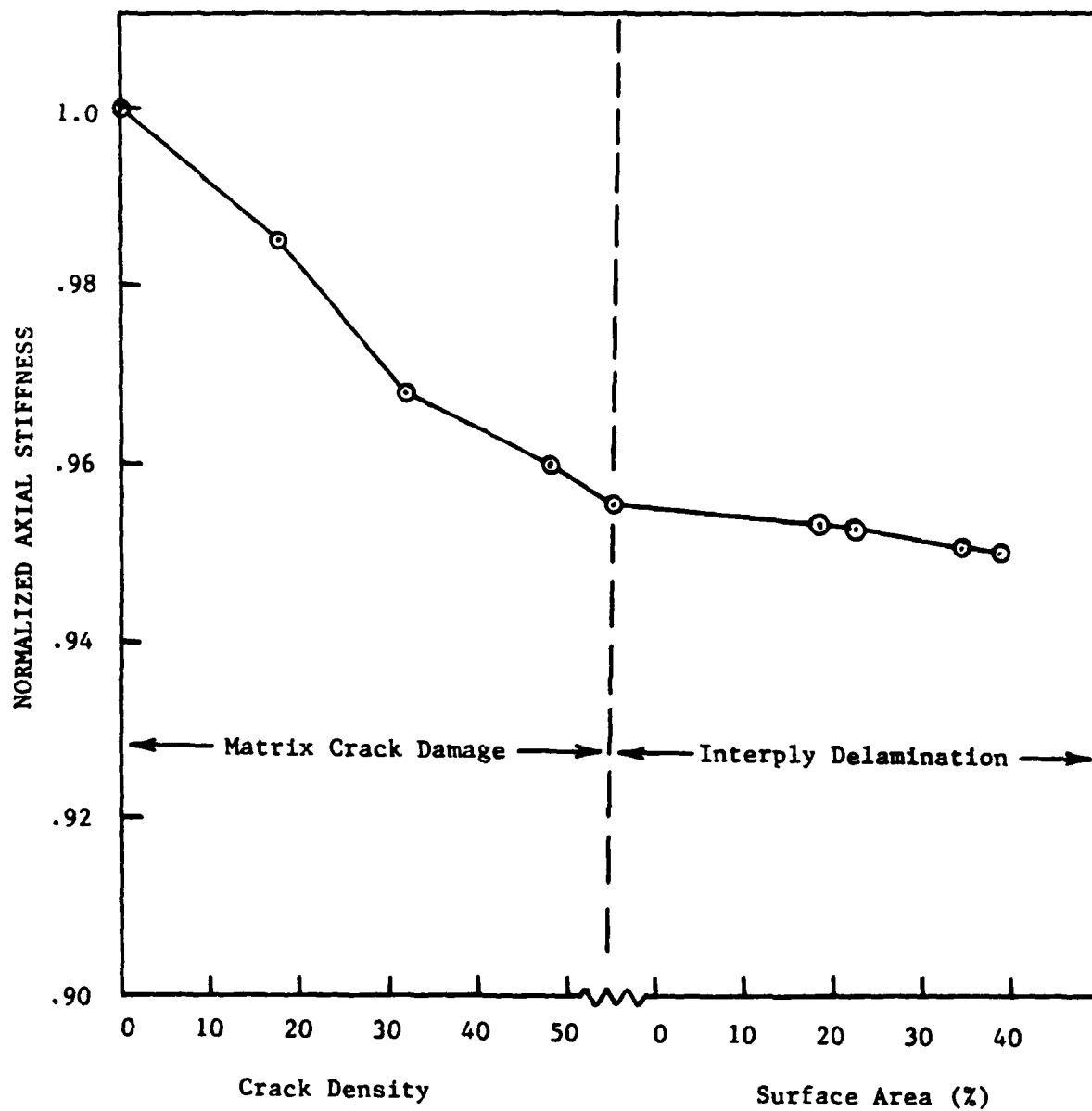
Fig. 1. Axial stiffness loss in a $[0_2,90_2]_s$ graphite/epoxy laminate
with matrix cracking and interply delamination.
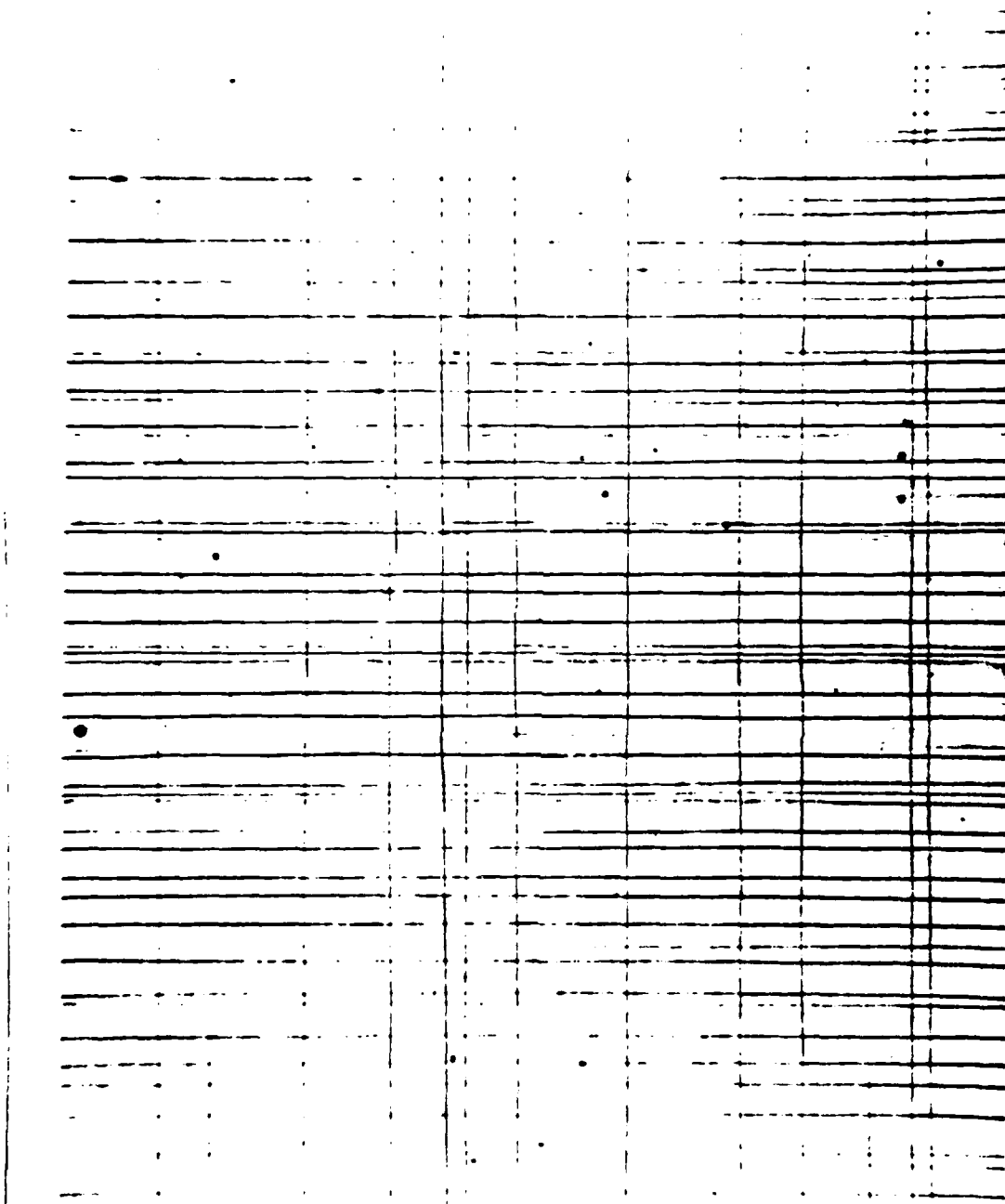
Fig. 2.   Matrix crack saturation in a $[0_2,90_2]_s$ laminate.
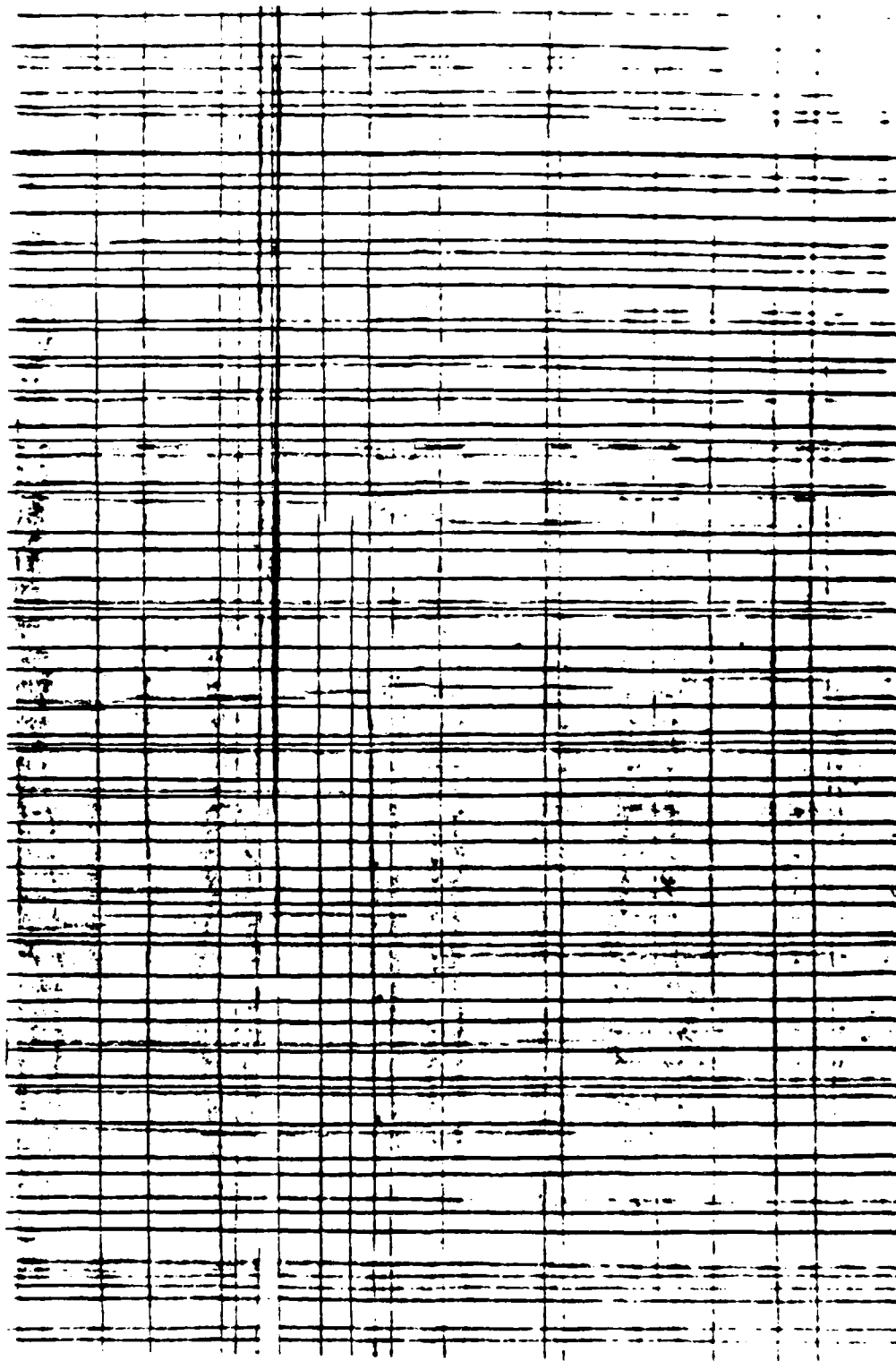
Fig. 3. Interply delamination in a $[0_2,90_2]_s$ laminate. 300,000 cycles.
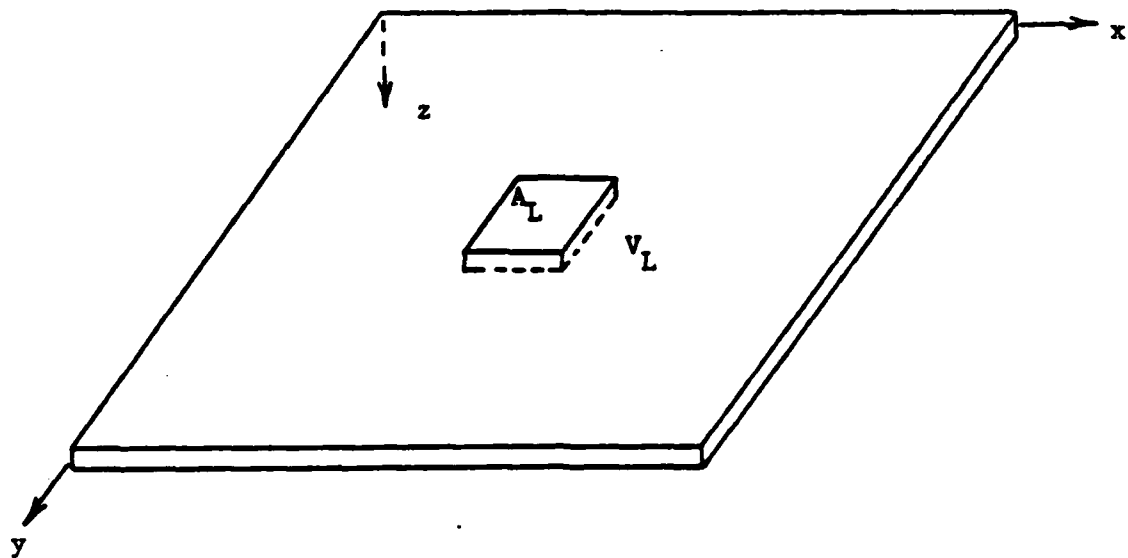
a) general laminate
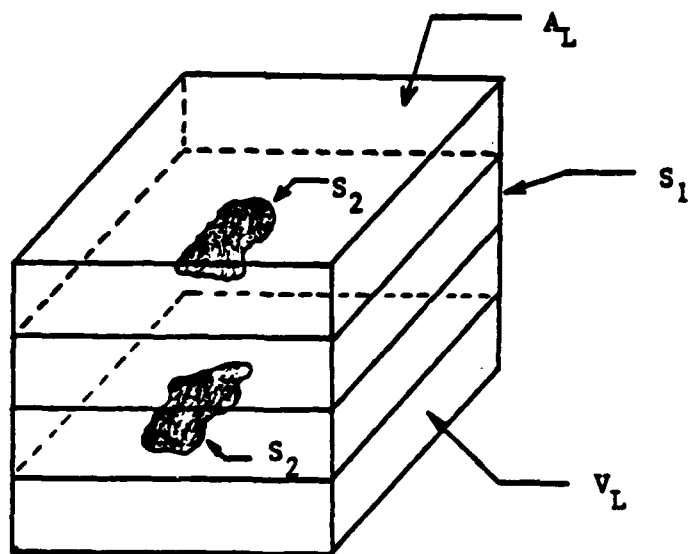
b) exploded view with damage

Fig. 4. Characteristic local region of damage. a) general
laminate, b) exploded view of V_L with damage.
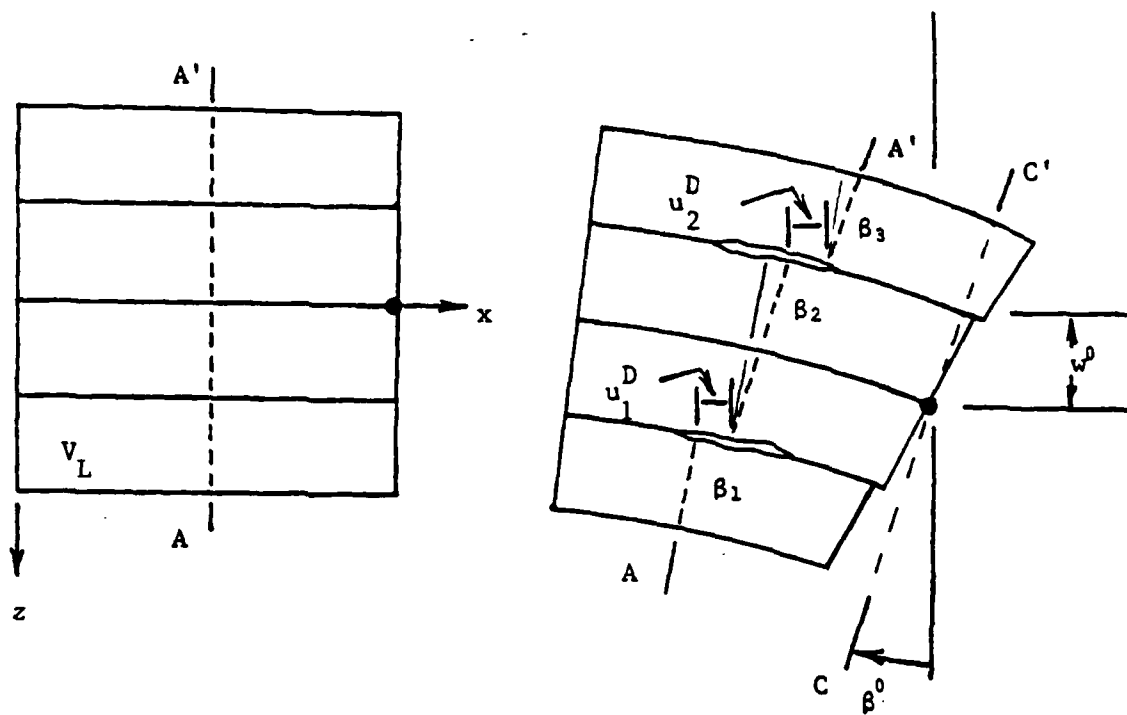
Fig. 5. Deformation geometry for region A_L.
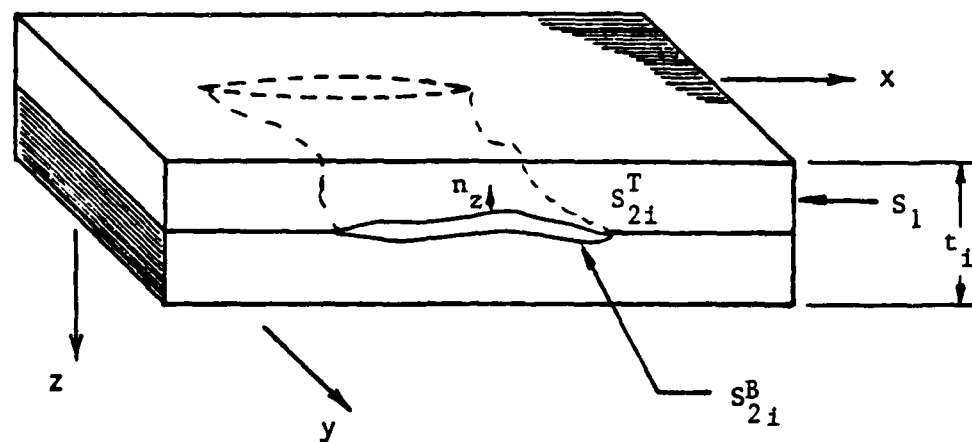
$$\underset{\sim}{u}^D = u^D \, \widehat{e}_x + v^D \, \widehat{e}_y + w^D \, \widehat{e}_z$$

$$\underset{\sim}{n}^D = 0 \, \widehat{e}_x + 0 \, \widehat{e}_y + n_z \, \widehat{e}_z$$

$$S = S_1 + S_2$$

Fig. 6. Interply delamination in a laminated continuous
fiber composite.

Fig. 7. Schematic of Delaminated Region
in a Composite Layup

Fig. 8 Combined Damage Mode in $[0/\pm45/90]_s$ Due to Tension-Tension Fatigue

Appendix 7.4

MODELLING STIFFNESS LOSS IN QUASI-ISOTROPIC
LAMINATES DUE TO MICROSTRUCTURAL DAMAGE

by

D.H. Allen
C.E. Harris
E.W. Nottorf
Aerospace Engineering Department
Texas A&M University
College Station, Texas 77843

and

S.E. Groves
Lawrence Livermore National Labs
Livermore, CA 94550

Abstract

Continuous fiber laminated composites are known to undergo substantial load induced damage in the form of matrix cracking, interior delamination, fiber fracture, etc. These damage modes produce significant losses in component performance measures such as stiffness, residual strength, and life. The authors have previously constructed a general model for predicting the response of laminated composites with damage. The current paper utilizes the model to predict stiffness loss as a function of damage in quasi-isotropic and angle-ply laminates with matrix cracks. It is shown that the model is capable of predicting the stiffness loss for any layup by utilizing the same input data, thus producing a model which is independent of stacking sequence. The favorable comparisons of the model to experimental results reported herein support the validity of the model.

Introduction

The thermomechanical response of laminated continuous fiber composites is quite complex due to stress concentrations resulting from fiber-matrix interaction and the layered orthotropy of the medium. The stress concentrations resulting from this local material inhomogeneity are significant in the sense that they may cause substantial impairment of component performance. However, the development of microcracks can often be utilized advantageously as a toughening mechanism. Just as the small scale material inhomogeneity tends to initiate cracks, it also serves as a crack arrestor. Thus, a field of microcracks develops, and the resulting loss of local structural integrity causes load transferral which is similar to plasticity in pure metals. Therefore, if the effects of microcracks in laminated composites can be accurately modelled, it is possible to utilize a greater portion of component life.

The difficulty in developing a useful model lies in the inherent complexity of microstructural damage in laminated composites. Unlike pure metals, it is not uncommon for laminated continuous fiber composites to develop several different modes of damage such as matrix cracking, interply delamination, fiber fracture, fiber-matrix debond, and fiber crimping. In addition, there is significant interaction between the various modes of damage. For example, interply delamination tends to initiate at the intersection of matrix cracks in adjacent plies, and fiber fracture tends to concentrate near the delamination sites. The cracks are so numerous and diverse that any attempt to model each crack individually is hopelessly complex. However, the scale of the cracks is usually very small compared to the scale of the structural component. Because of this, it is possible to

2

assume that the body remains continuous and the effects of microcracks may be introduced via appropriate spatially variable reductions in the elastic constitutive properties. Such an approach is called continuum damage mechanics (Kachanov, 1958; Kachanov, 1986).

The concept of continuum damage mechanics has been utilized extensively over the past twenty-five years (Bazant, 1986; Krajcinovic, 1984; Krajcinovic, 1986). However, most applications have been for initially isotropic media. Very few attempts have been made to utilize this concept for laminated composite media (Talreja, 1985; Allen, Harris, and Groves, 1987; Weitsman, 1985). The primary difficulty has been the layered orthotropy of these materials. The authors have recently developed a damage model which is applicable to laminated fibrous composites (Allen, Harris, and Groves, 1987; Allen, Harris, Groves, and Norvell, 1987; Allen, Groves, and Harris, 1987). This microstructural damage may be induced by mechanical loads or environment such as elevated temperature. The model has been utilized to predict the response of composite crossply laminates with matrix cracks, and these results compare favorably to experiment (Allen, Harris, and Groves, 1987; Allen, Harris, Groves, and Norvell, 1987), as shown in Fig. 1. The model has also been developed for the case of combined matrix cracking and interply delamination (Allen, Harris, and Groves, 1987; Allen, Groves, and Harris, 1987).

The purpose of the current paper is to demonstrate the use of the model to predict various components of reduced stiffness for quasi-isotropic laminates with matrix cracks in the off-axis plies, as shown in Fig. 2. It will be shown that this can be accomplished by using experimental data from $[0,90,0]_s$ and $[\pm 45]_{2s}$ specimens, thus demonstrating that the model is independent of stacking sequence. The paper will close with a comparison of

3

Voigt notation. Note that since α_{ij}^M is in general asymmetric

$$\alpha_1^M \equiv \alpha_{11}^M \qquad \alpha_4^M \equiv \alpha_{23}^M \qquad \alpha_7^M \equiv \alpha_{31}^M$$

$$\alpha_2^M \equiv \alpha_{22}^M \qquad \alpha_5^M \equiv \alpha_{32}^M \qquad \alpha_8^M \equiv \alpha_{12}^M \qquad (3)$$

$$\alpha_3^M \equiv \alpha_{33}^M \qquad \alpha_6^M \equiv \alpha_{13}^M \qquad \alpha_9^M \equiv \alpha_{21}^M$$

Although matrix cracks are sometimes observed to be curved (Allen, Harris, Groves, and Norvell, 1987), it is assumed in this paper that all matrix cracks are normal to the laminate midplane, as shown in Fig. 2. For this case

$$\vec{n}^C = 0\ \vec{e}_1 + 1\ \vec{e}_2 + 0\ \vec{e}_3 \qquad (4)$$

in ply coordinates. Therefore, the only non-zero components of α_j^M are α_2^M, α_5^M, and α_8^M. Also, due to in-plane symmetry of each ply it is assumed that α_5^M is negligible. Furthermore, it can be shown that $I_{ij}^M \propto -C_{ij}$ (Allen, Harris, and Groves, 1987), so that equation (2) reduces to

$$\sigma_i = C_{ij}\epsilon_j - C_{12}\alpha_2^M - C_{16}\alpha_8^M \qquad (5)$$

Standard laminate equations may be obtained from equations (5) by utilizing the Kirchhoff hypothesis for thin plates. The resulting forces per unit length, {N}, are given by (Allen, Harris, and Groves, 1987; Allen, Groves, and Harris, 1987)

5

$$\{N\} = \sum_{k=1}^{n} [\overline{C}]_k (z_k - z_{k-1}) \{\epsilon_L^0\} + \frac{1}{2} \sum_{k=1}^{n} [\overline{C}]_k (z_k^2 - z_{k-1}^2) \{\kappa_L\}$$

$$- \sum_{k=1}^{n} [\overline{C}]_k (z_k - z_{k-1}) \{\alpha^M\}_k \tag{6}$$

where n is the number of plies, $\{\epsilon_L^0\}$ are the midplane strains, $\{\kappa_L\}$ are the midplane rotations, and overbars denote that quantities are transformed from ply coordinates to laminate coordinates. Similarly, the moments per unit length, $\{M\}$, are given by

$$\{M\} = \frac{1}{2} \sum_{k=1}^{n} [\overline{C}]_k (z_k^2 - z_{k-1}^2) \{\epsilon_L^0\} + \frac{1}{3} \sum_{k=1}^{n} [\overline{C}]_k (z_k^3 - z_{k-1}^3) \{\kappa_L\}$$

$$- \frac{1}{2} \sum_{k=1}^{n} [\overline{C}]_k (z_k^2 - z_{k-1}^2) \{\alpha^M\}_k \tag{7}$$

Furthermore, the damage tensor $\{\alpha^M\}$ is transformed to global coordinates in each ply. Thus, for the case of vertical matrix cracks

$$\overline{\alpha}_1^M = \sin^2\theta \ \alpha_2^M - \sin\theta \cos\theta \ \alpha_8^M$$

$$\overline{\alpha}_2^M = \cos^2\theta \ \alpha_2^M + \sin\theta \cos\theta \ \alpha_8^M$$

$$\overline{\alpha}_8^M = -\sin\theta \cos\theta \ \alpha_2^M + \cos^2\theta \ \alpha_8^M$$

$$\overline{\alpha}_9^M = -\sin\theta \cos\theta \ \alpha_2^M - \sin^2\theta \ \alpha_8^M \tag{8}$$

where θ is the angle relating the ply coordinates, denoted x_j, to the laminate coordinates, denoted $\overline{x}_j$, as shown in Fig. 4. All other components of $\overline{\alpha}_j^M$ are

6

zero due to the previously discussed assumptions.

The components of the reduced stiffness, S'_{ij}, may be obtained by differentiating equation (6) with respect to the midplane strains to obtain

$$S'_{ij} \equiv \frac{1}{h} \frac{\partial N_i}{\partial \epsilon^0_j} = \frac{1}{h} \sum_{k=1}^{n} [(\bar{C}_{ij})_k t_k - (\bar{C}_{11})_k t_k (\frac{\partial \bar{\alpha}^M_1}{\partial \epsilon^0_j})_k$$

$$- (\bar{C}_{12})_k t_k (\frac{\partial \bar{\alpha}^M_2}{\partial \epsilon^0_j})_k - (\bar{C}_{16})_k t_k (\frac{\partial \bar{\alpha}^M_8}{\partial \epsilon^0_j} + \frac{\partial \bar{\alpha}^M_9}{\partial \epsilon^0_j})_k] \qquad (9)$$

where h is the laminate thickness.

It has been previously shown (Allen, Harris, Groves, and Norvell, 1987) that the damage parameters in equation (9) transform according to the following transformation

$$\frac{\partial \bar{\alpha}^M_{\overline{ij}}}{\partial \epsilon^0_{\overline{mn}}} = a_{\overline{ip}} a_{\overline{jq}} a_{\overline{mr}} a_{\overline{ns}} \frac{\partial \alpha^M_{pq}}{\partial \epsilon^0_{rs}} \qquad (10)$$

where $a_{\overline{ip}}$ are the direction cosines relating the ply coordinates to the laminate coordinates, given by

$$[a_{\overline{ip}}] = \begin{bmatrix} \cos\theta & -\sin\theta & 0 \\ \sin\theta & \cos\theta & 0 \\ 0 & 0 & 1 \end{bmatrix} \qquad (11)$$

Therefore, it can be seen from equations (9) and (10) that the damage dependent stiffness can be evaluated if the last term in equation (10) can be determined. Since it was previously assumed that only $\alpha^M_2 = \alpha^M_{22}$ and $\alpha^M_8 = \alpha^M_{12}$ are not negligible for the current application, it is necessary to evaluate $\partial \alpha^M_{22}/\partial \epsilon^0_{rs}$ and $\partial \alpha^M_{12}/\partial \epsilon^0_{rs}$. To do this, first note that for the case of vertical matrix cracks the damage induces orthotropy which is concurrent with
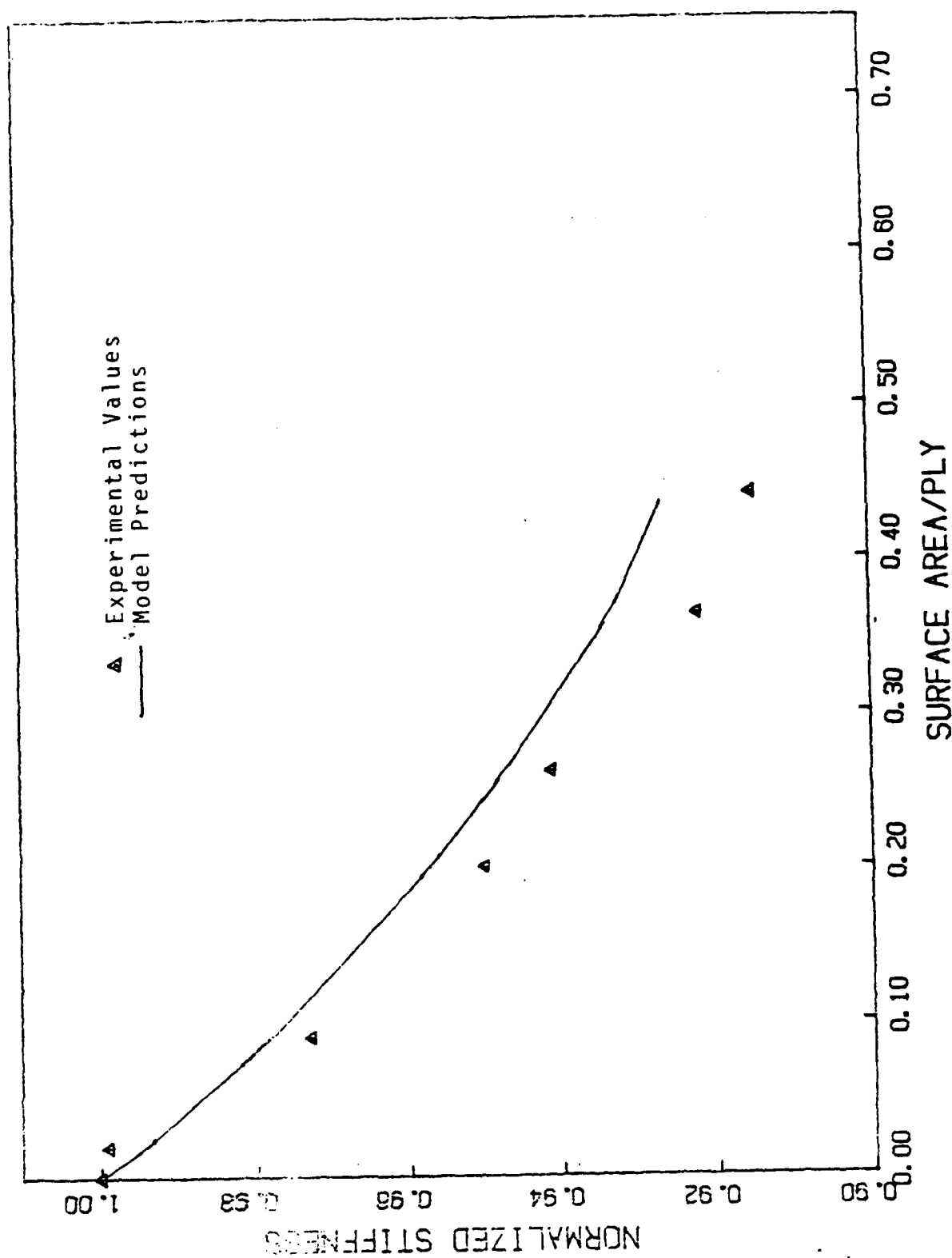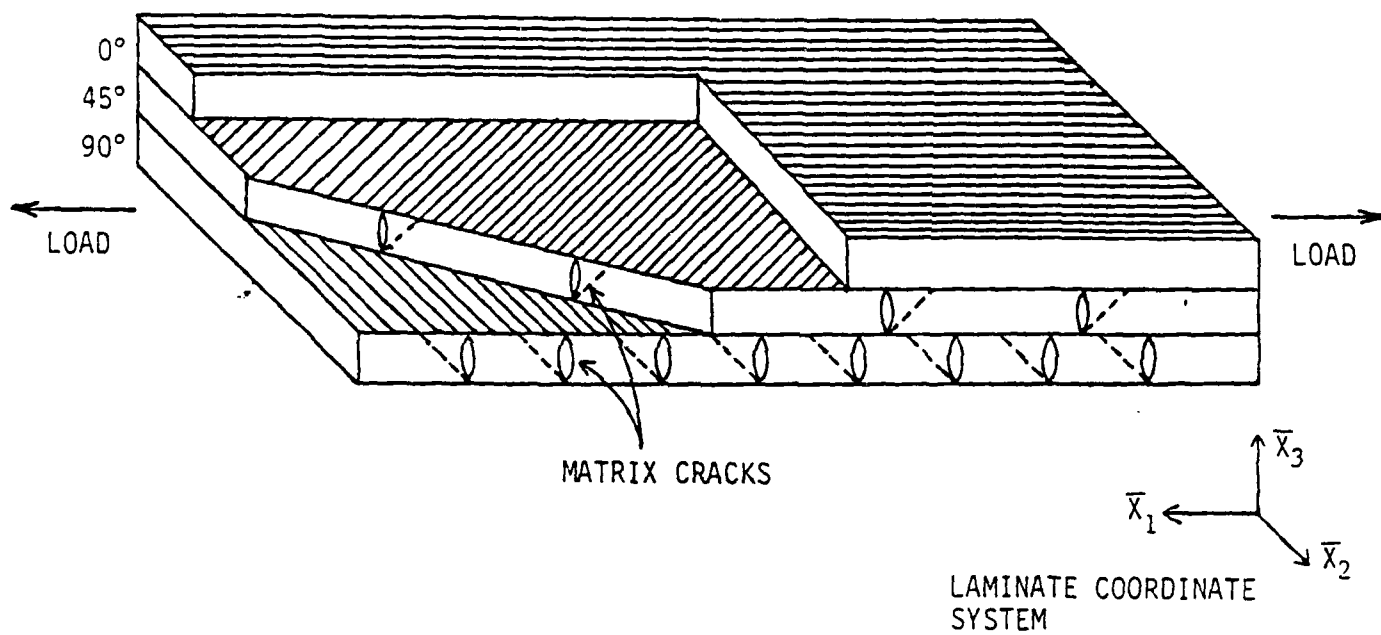
Fig. 1   Model vs. Experiment for $[0,90_2]_s$ Laminate

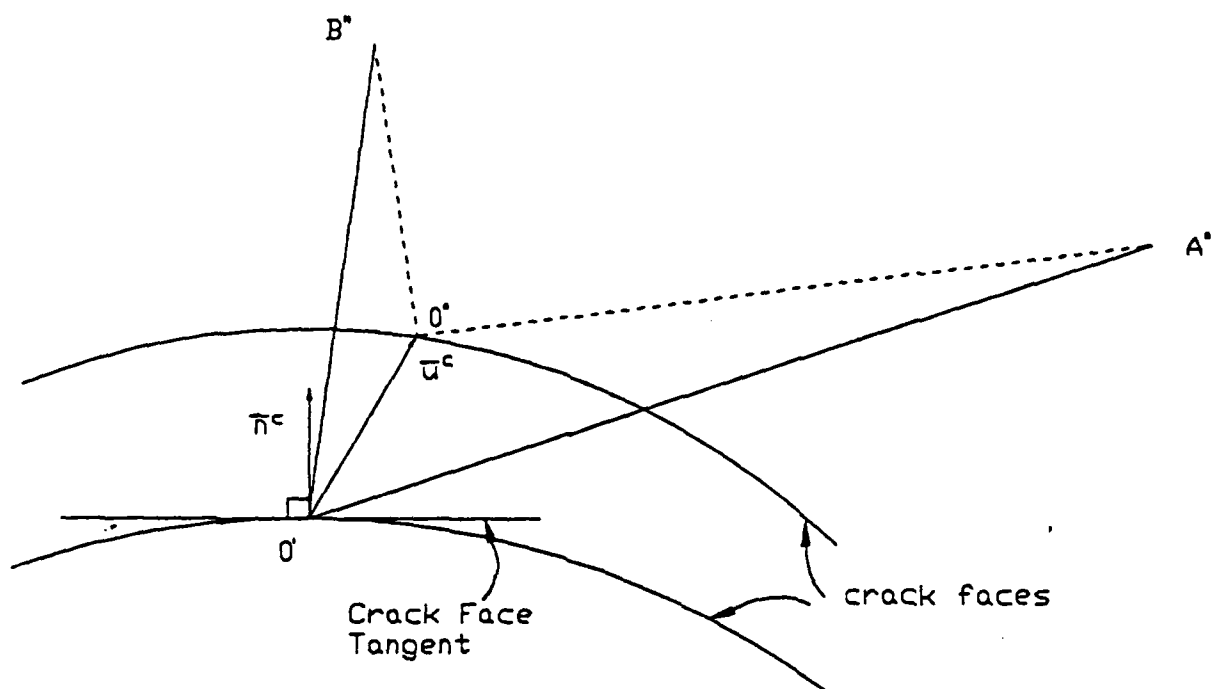Fig. 2   Matrix Cracking in a Laminated Continuous Fiber Composite

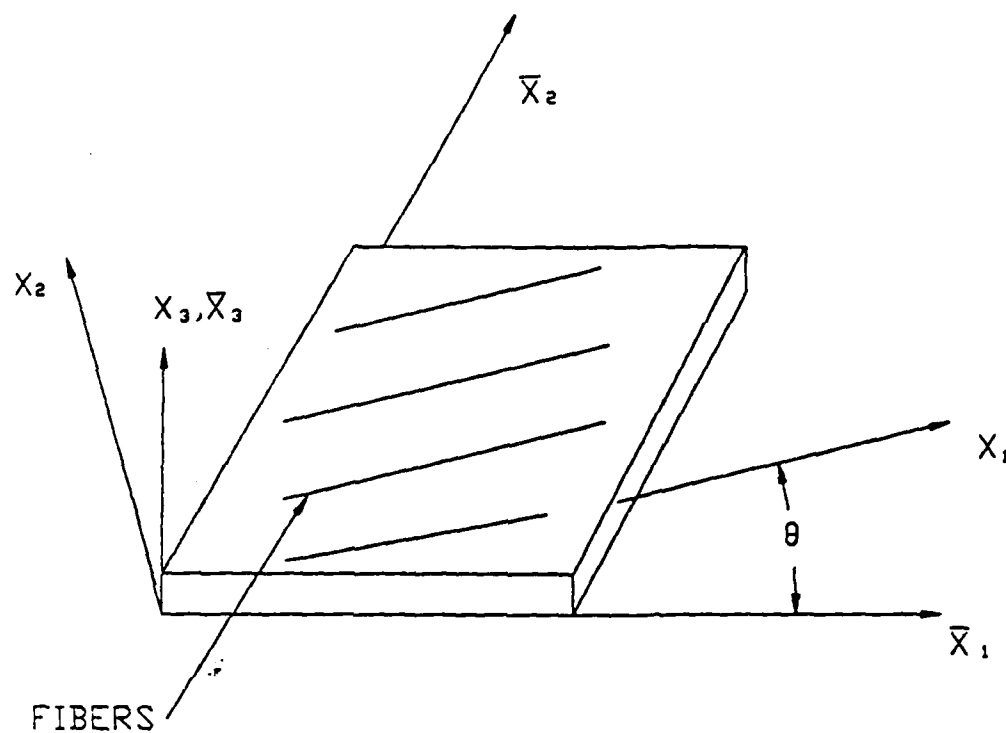Fig. 3 Description of the Internal State at oint O'

X_1, X_2, X_3 —PLY COORDINATES

$\overline{X}_1, \overline{X}_2, \overline{X}_3$ —LAMINATE COORDINATES
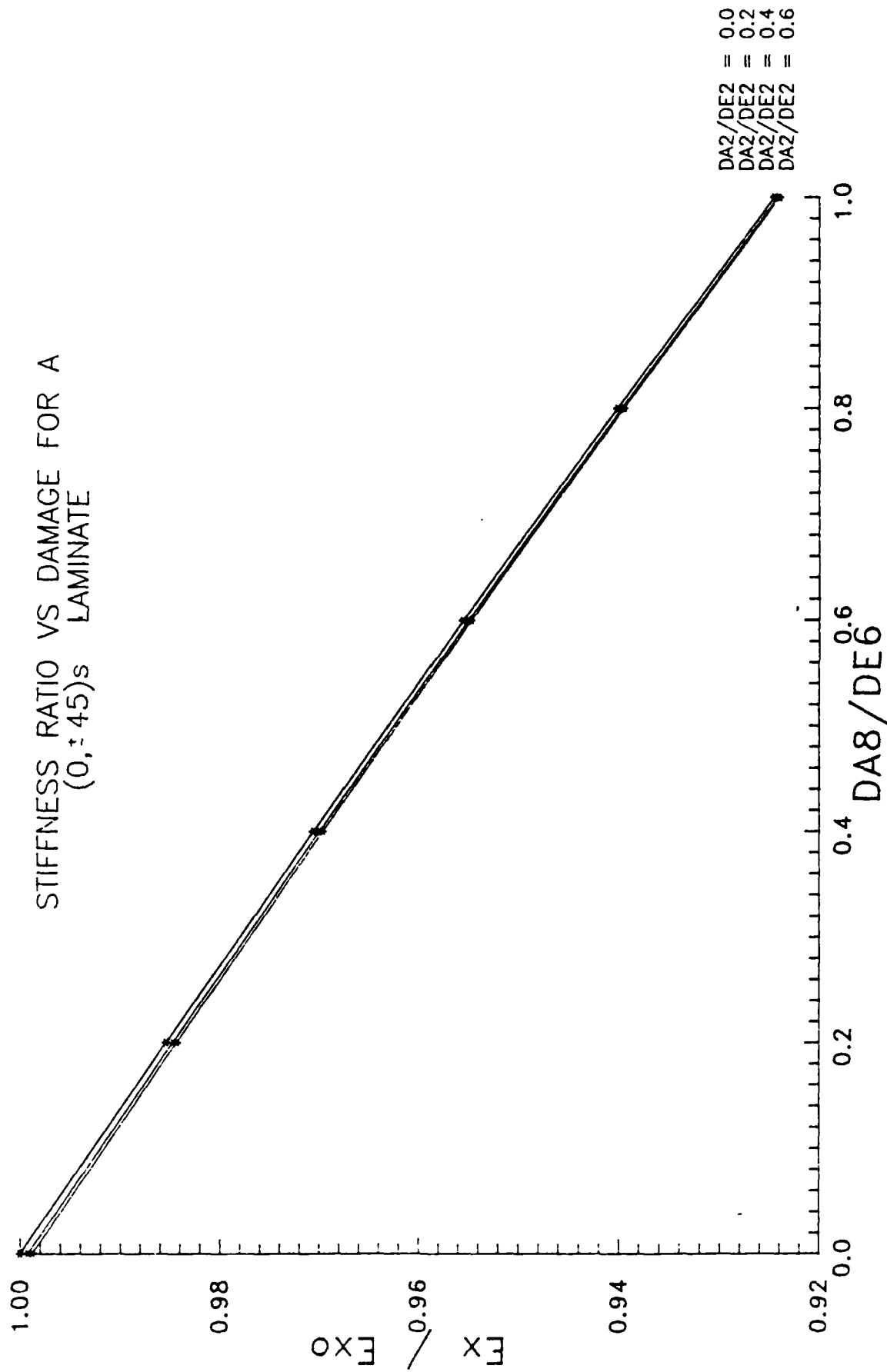
Fig. 4 Description of Coordinate Systems

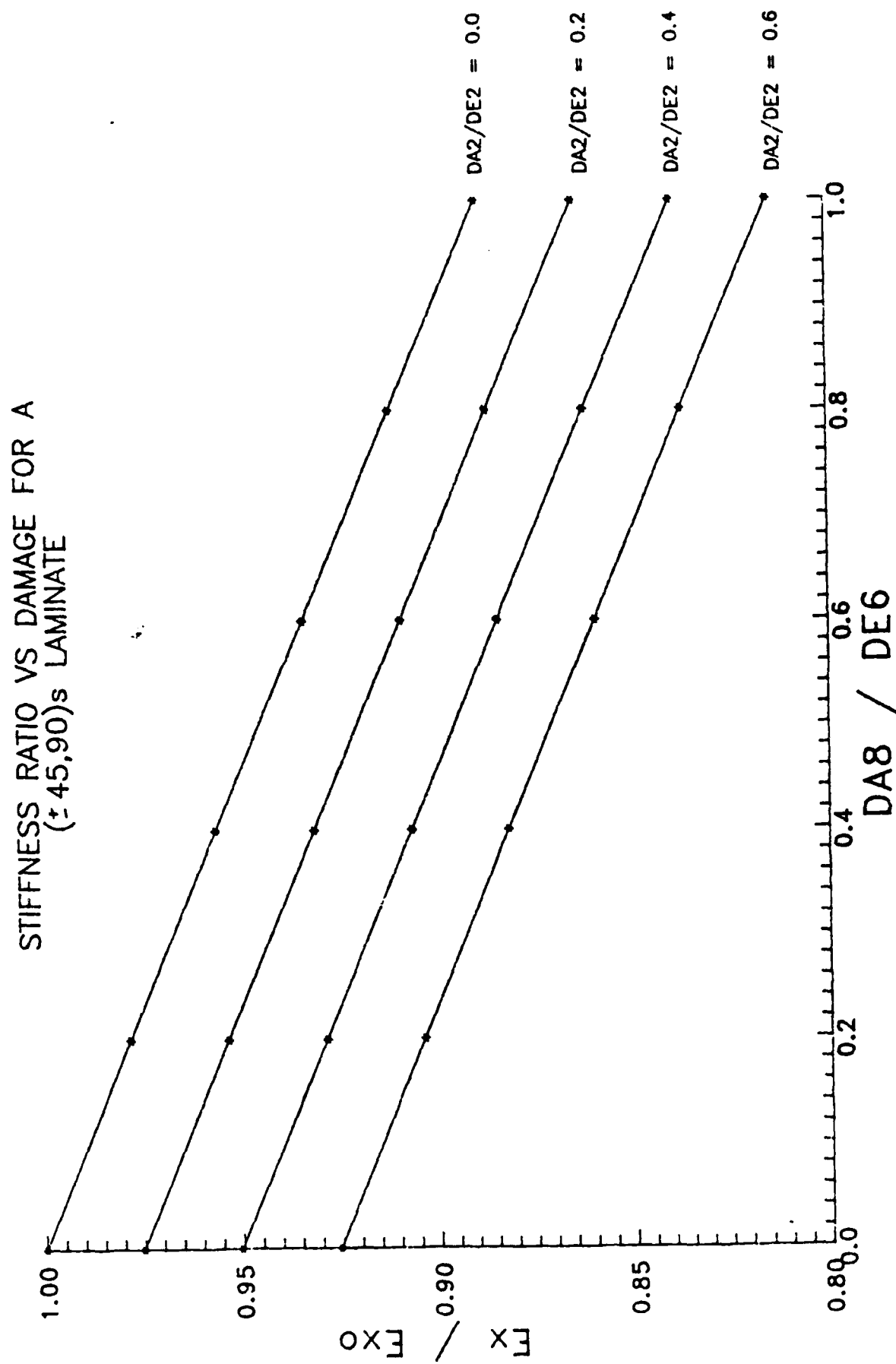Fig. 5 Stiffness Ratio Versus Damage for a $(0, \pm 45)_s$ Laminate

Fig. 6 Stiffness Ratio Versus Damage for a $(\pm 45,90)_s$ Laminate

Appendix 7.5

A CONTINUUM DAMAGE MODEL OF FATIGUE-INDUCED
DAMAGE IN LAMINATED COMPOSITES

by

Charles E. Harris

and

David H. Allen

Aerospace Engineering Department
Texas A&M University
College Station, Texas 77843

Encyclopedia of Composites

SAMPE

1988

INTRODUCTION

Fatigue induced damage in composite materials has been the subject of numerous experimental investigations. The specific damage mechanisms have been identified and the progression of damage is phenomenologically well understood, as evidenced by numerous experimental studies documented in the open literature. For example, the American Society for Testing and Materials has devoted a number of Special Technical Publications (723, 775, 836, 876) exclusively to the topic of damage in composites [1-4]. While these experimental investigations have been supported by analytical research, there are relatively few mathematical models that predict the effect of damage on the structural response of composites. Those that can be identified [5-9] are either limited in scope or still under development.

The writers have formulated a very promising model that predicts the stress-strain behavior of continuous fiber reinforced laminated composites in the presence of microstructural damage. The model is based on the concept of continuum damage mechanics and uses internal state variables to characterize the various damage modes. The associated internal state variable growth laws are mathematical models of the loading history induced development of microstructural damage. The damage model addresses both extension and bending and is developed in the form of modified laminate analysis equations for easy implementation. This model of the stress-strain behavior of laminates with fatigue-induced damage is the subject of this paper.

The continuum damage mechanics approach accounts for the effect of microstructural damage on structural behavior through damage dependent constitutive relationships. Locally averaged constitutive properties are computed from a representative local volume sufficient to represent the damage but small relative to the boundary value problem of interest. Thus, the

1

effects of internal boundaries are reflected in constitutive equations rather than internal boundary conditions. This is in contrast to the fracture mechanics approach wherein each crack is treated as an internal boundary and boundary conditions are specified on the crack faces. This is not a practical approach to composite material systems that develop widespread load-induced microstructural damage. On the other hand, continuum damage mechanics may be used in conjunction with fraction mechanics to represent a macrocrack (via boundary conditions) in a field of microcracks (via degraded material constitution).

Continuum damage mechanics was first applied to metallic alloys in an attempt to address issues in plasticity [10]. Recently the concept has been applied to composite materials, although the first applications were to randomly distributed particulate reinforced composites [11,12]. Several newly developed models address matrix cracks in continuous fiber reinforced laminates [6-8]. Only two attempts [13,14] have been made to extend the concept to include interply delaminations as well as matrix cracks.

This paper is a comprehensive survey of the model development research of the writers. The emphasis is placed on describing the experimental development of damage under fatigue loading and the application of the model to predict the response of the damaged laminate. While the model is completely documented herein, the detailed theoretical developments are given elsewhere [5].

EXPERIMENTAL PROGRAM

There were three objectives of the experimental program. These were to observe and document the progression of damage in laminated composites when subjected to a tension-tension fatigue loading; establish fundamental damage growth law data and strain energy release rate data required to specify the

2

material constants in the model; and to generate experimental results for comparison to the model predictions of the damage-dependent engineering moduli. The material system selected for study was graphite/epoxy, AS-4/3502. A comprehensive data base has been generated for a variety of cross-ply and quasi-isotropic laminates and a limited data base is also available for several angle-ply laminates.

The AS-4/3502 laminate panels were fabricated by a standard pre-preg tape layup and hot press curing procedure. The panels were cured according to the curing cycle recommended by the tape vendor. The following lamina properties were measured: $E_{11} = 21.0 \times 10^6$ psi, $E_{22} = 1.39 \times 10^6$ psi, $G_{12} = 0.694 \times 10^6$ psi and $\nu_{12} = 0.310$, where the subscript 1 refers to the fiber direction and 2 refers to the transverse direction. The fiber volume fraction was measured to be approximately 65% and the average per ply thickness was 0.0052 in.

All fatigue tests were conducted by an MTS 880 computerized testing system. The fatigue tests were run in load control at R = 0.1 and at a frequency of 2 hz. The maximum stress was typically 70-75% of the laminate's ultimate strength of the laminate. In most tests, a 1.0 in. gage length biaxial extensometer was used to simultaneously measure axial and transverse strain. In some instances only the axial strain was measured by a uniaxial extensometer. While the dynamic modulus was monitored continuously, the "static" axial modulus and Poisson's ratio of the laminate were determined at various intervals throughout the test by interrupting the cyclic loading and running standard monotonic tensile tests. At these same intervals, the damage state was documented by x-ray radiography and edge replication. A few selected specimens were destructively examined by sectioning and viewing in the scanning electron microscope to better understand the local damage states.

The tensile test coupons were 1.0 in. wide and 11.0 in. long. Epoxy end

3

tabs were used to minimize the local effects of the wedge-action friction grips. Since 1.0 in. gage length extensometers were used to measure the strain in the 1.0 in. wide specimens, the cross-sectional area of the local volume was taken to be 1.0 in^2. Therefore, the damage evaluations characterized the damage state in the 1.0 in. x 1.0 in. gage length region over which the damage-dependent strain was measured. Whenever the damage state is quantified herein, it will be understood to be for this 1.0 in^2 region.

EXPERIMENTAL CHARACTERIZATION OF FATIGUE DAMAGE

The first mode of damage to develop in the typical cross-ply laminate was matrix cracks in the 90° plies. Extensive matrix cracking typically developed during the first loading cycle. Matrix crack saturation in the 90° plies occurred early in the fatigue life with very little additional crack formation thereafter. The second mode of damage was matrix crack formation in the 0° plies. These so-called axial splits began to develop at about the same time that the matrix cracks saturated in the 90° plies. After a period of matrix crack growth in the 0° plies, delaminations began to form at the intersection of the crossing matrix cracks in adjacent plies. Continued cyclic loading resulted in a growth and coalescence of the delaminations. Fiber fracture also occurred in regions localized near the matrix cracks in adjacent plies. Extensive fiber fracture could not be readily observed nondestructively and no additional damage modes were observed prior to catastrophic failure of the specimen. This progression of damage is illustrated in Fig. 1 by the series of x-ray radiographs of the $[0_2/90_2]_s$ laminate. Figure 2 shows a photographic enlargement of the fully developed damage state in the $[0_2/90_2]_s$ laminate taken at 400,000 cycles with S_{max} at 75% of S_{ULT}. Figures 3 and 4 present similar information for the $[0/90_2]_s$ laminate with the fully developed damage

4

state taken at 1,003,000 cycles with S_{MAX} at 71% of S_{ULT}. Finally, Fig. 5 shows the fully developed damage state in a $[0/90_3]_s$ laminate taken at 200,000 cycles with S_{max} at 73% of S_{ULT}.

The x-ray radiographs of Figs. 2, 4 and 5 show two fundamentally different damage states. Notice that the axial splits in the $[0_2/90_2]_s$ laminate, Figs. 1 and 2, are continuous throughout the photographic field of view. Also, the delaminations tend to grow in an axial direction along the splits. On the other hand, the axial splits in the $[0/90_2]_s$ and $[0/90_3]_s$ laminates, Figs. 3-5, are not continuous and typically terminate in the photographic field of vision. Also, these splits tend to develop across the laminate width prior to exhibiting extensive axial growth. The delamination patterns are somewhat similar and tend to form at adjacent crossing crack locations across the specimen width prior to growing and coalescing axially. This pattern is clearly illustrated in Fig. 5. The differences in these damage growth patterns may be quite important when developing damage growth laws and can be qualitatively explained by the differences in the local stress states of these laminates [15].

The progression of damage in quasi-isotropic laminates also originated with matrix cracks in the 90° plies followed by matrix cracking in the 45° plies. While the matrix cracks in the 90° plies appear to saturate, this was not observed to be the case in the 45° plies. Also, unlike the 90° plies, the matrix cracks in the 45° plies do not typically extend completely across the plies and tend to form in local patterns. This is illustrated in the x-ray radiograph, Fig. 6, of a $[90/\pm45/0]_s$ laminate where many short cracks in the -45° plies lie along the longer cracks in the adjacent +45 plies. It is also obvious from Fig. 6 that extensive edge delaminations developed rather than interior delaminations at matrix crack crossing points. This same type of

5

damage pattern occurred in the $[0/\pm45/90]_s$ laminate as shown in Fig. 7. In both laminates, catastrophic failure precipitated by the massive free edge delaminations occurred prior to the observation of interior delaminations at crossing cracks. This may be an important observation relative to the development of the damage growth laws. However, once the delaminations are present in the local volume there may be no fundamental difference between the effect of free edge induced delaminations and interior delaminations on damage dependent laminate properties.

The axial modulus was observed to decrease with increasing damage in all laminates studied herein. The cross-ply laminates typically exhibited a rapid rate of change in the modulus while the matrix cracks formed in the 90° plies; whereas after saturation the rate of modulus degradation was quite slow while the axial splits and delaminations grew. Just prior to fracture the modulus was observed to change rapidly. This is probably due to extensive coalescence of delaminations and fiber fracture. The quasi-isotropic laminates exhibited a similar pattern, although somewhat more dramatic changes in the modulus occurred with the development of the free edge delaminations. Quantitative values of axial modulus and Poisson's ratio will be given in a later section when the model predictions are compared to the experimental results.

MODEL DEVELOPMENT

The writers have developed a model that predicts the response of laminates with both matrix cracks and interior delaminations such as the damage states described in the previous section. This problem is complicated by two factors. First, because these two damage mechanisms are oriented differently, they require two separate tensor-valued damage parameters. Furthermore, the mechanics of these two damage modes are substantially

6

different. The matrix cracks may be assumed to be statistically homogeneous over each ply in a small local volume element. Therefore, classical local volume averaging may be used to obtain this damage parameter. On the other hand, delaminations are not statistically homogeneous in the z coordinate direction. This requires that a modification be made to statistical averaging techniques. Although statistical homogeneity is assumed in the x and y coordinate directions, a kinematic constraint similar to the Kirchhoff-Love hypothesis is applied in the z direction. The resulting damage parameter is a weighted measure of damage, with delaminations away from the neutral surface causing a greater effect on laminate properties.

The model development proceeds from the assumption that all material inelasticity is contained within small zones surrounding the microcracks. The effect of matrix cracks on ply level constitutive equations is accounted for via the local volume average of the diadic product of the crack opening displacement vector u_i^C and the crack face normal n_j^C

$$\alpha_{ij}^M = \frac{1}{V_L} \int_{S_C} u_i^C n_j^C ds \tag{1}$$

where V_L is the local volume for which cracking can be considered statistically homogeneous, and S_C is the surface area of matrix cracks in V_L. For matrix cracking, V_L is typically one ply in thickness. The ply level stress-strain relations are therefore given by

$$\sigma_{ij} = C_{ijk\ell}(\varepsilon_{k\ell} - \alpha_{k\ell}^M) \tag{2}$$

where $C_{ijk\ell}$ is the elastic (undamaged) modulus tensor.

In order to account for interply delamination the following kinematic

7

assumption is made (See Fig. 8.):

$$u(x,y,z) = u^o(x,y) - z[\beta^o + H(z-z_k)\beta_k^D] + H(z-z_k)u_k^D \tag{3}$$

$$v(x,y,z) = v^o(x,y) - z[\psi^o + H(z-z_k)\psi_k^D] + H(z-z_k)v_k^D \tag{4}$$

and

$$w(x,y,z) = w^o(x,y) - H(z-z_k)w_k^D \tag{5}$$

where u and v are components of the in-plane displacement, w is the out-of-plane displacement, and H is the Heavyside step function. Furthermore, β and ψ represent rotations of the midplane. The quantities with superscripts o are undamaged midsurface values, and quantities with superscripts D are caused by interlaminar cracking. Finally, a repeated index k is assumed to be summed from one to the total number of delaminated ply interfaces.

Employing standard laminate averaging techniques will result in the following laminate equations

$$\{N\} = \sum_{k=1}^{n} [Q]_k (z_k - z_{k-1}) \{\epsilon_L^o\} - \frac{1}{2} \sum_{k=1}^{n} [Q]_k (z_k^2 - z_{k-1}^2) \{\kappa_L\}$$

$$+ \sum_{i=1}^{d} [\overline{Q}_1]_i \ t_i \begin{Bmatrix} 0 \\ 0 \\ \alpha_{1i}^D \\ 0 \\ \alpha_{2i}^D \\ \alpha_{3i}^D \\ 0 \end{Bmatrix} + \sum_{i=1}^{d+1} (z_i - z_{i-1}) [\overline{Q}_2]_i \begin{Bmatrix} 0 \\ 0 \\ 0 \\ \alpha_{4i}^D \\ \alpha_{5i}^D \\ 0 \end{Bmatrix}$$

$$- \sum_{k=1}^{n} [Q]_k (z_k - z_{k-1}) \{\alpha^M\}_k \tag{6}$$

8

$$\{M\} = \frac{1}{2} \sum_{k=1}^{n} [Q]_k \, (z_k^2 - z_{k-1}^2) \, \{\epsilon_L^0\} - \frac{1}{3} \sum_{k=1}^{n} [Q]_k \, (z_k^3 - z_{k-1}^3) \, \{\kappa_L\}$$

$$+ \sum_{i=1}^{d} [\bar{Q}_3]_i \; t_i^2 \begin{Bmatrix} 0 \\ 0 \\ \alpha_{1i}^D \\ \alpha_{2i}^D \\ \alpha_{3i}^D \\ 0 \end{Bmatrix} + \sum_{i=1}^{d+1} [\bar{Q}_4]_i (z_i^2 - z_{i-1}^2) \begin{Bmatrix} 0 \\ 0 \\ 0 \\ \alpha_{4i}^D \\ \alpha_{5i}^D \\ 0 \end{Bmatrix}$$

$$- \frac{1}{2} \sum_{k=1}^{n} [Q]_k \, (z_k^2 - z_{k-1}^2) \, \{\alpha^M\}_k \tag{7}$$

where $\{N\}$ and $\{M\}$ are the resultant forces and moments per unit length respectively, and $\{\alpha^M\}_k$ and $\{\alpha_L^D\}$ represent the damage due to matrix cracking and interply delamination, respectively. Furthermore, n is the number of plies, and d is the number of delaminated ply interfaces, as shown in Fig. 9.

The internal state variable for delamination, $\{\alpha_L^D\}$, is obtained by employing the divergence theorem on a local volume element of the laminate. The resulting procedure gives [13]

$$\alpha_{1i}^D = \frac{2}{V_{Li}} \int_{S_{2i}} w_i^D n_z dS \tag{8a}$$

$$\alpha_{2i}^D = \frac{2}{V_{Li}} \int_{S_{2i}} v_i^D n_z dS \tag{8b}$$

$$\alpha_{3i}^D = \frac{2}{V_{Li}} \int_{S_{2i}} u_i^D n_z dS \tag{8c}$$

$$\alpha_{4i}^D = \frac{1}{A_L} \int_{S_{2i}^B} \psi_i^D n_z dS \tag{8d}$$

9

$$\alpha_{5i}^D = \frac{1}{A_L} \int_{S_{2i}^B} \beta_i^D n_z dS \tag{8e}$$

where the subscript i is associated with the ith delaminated ply interface. Furthermore, V_{Li} is equivalent to $t_i A_L$, where t_i is the thickness of the two plies above and below the delamination, as shown in Fig. 10. By definition, the z component of the unit normal, n_z, is equivalent to unity.

Furthermore, the matrices [Q] with subscripts k are the standard elastic property matrices for the undamaged plies. The matrices [Q̄] with subscripts i apply to the ith delaminated ply interface. They represent average properties of the plies above and below the delamination. These are described in further detail in reference 13.

Determination of E_x and ν_{xy} for the Mixed Damage Mode

Now, suppose that one is interested in modeling stiffness loss as a function of damage state. In order to do this, it is necessary to construct the (stacking sequence independent) material parameters developed in the previous section. The loading direction engineering modulus, E_x, and Poisson's ratio, ν_{xy}, of the laminate are defined as

$$E_x \equiv \frac{1}{t} \frac{\partial N_x}{\partial \epsilon_x} \tag{9}$$

$$\nu_{xy} \equiv \frac{\frac{1}{t} \frac{\partial N_x}{\partial \epsilon_y}}{\frac{1}{t} \frac{\partial N_y}{\partial \epsilon_y}} \tag{10}$$

where t is the laminate thickness.

For the purpose of comparing the model predictions to experimental

10

results, we will confine this development to the case of a symmetric, balanced laminate with delamination sites symmetrically located with respect to the laminate midplane. For this special case, $\{\kappa\}=0$ and the fourth term in equation (6) is zero. Furthermore, $\alpha_{1i}^D=0$ and the third term in equation (6) is the same for both delamination sites. Substituting equation (6) into equations (9) and (10) results in the following expressions for E_x and υ_{xy}

$$E_x = \frac{1}{n} \sum_{k=1}^{n} (Q_{11})_k (1 - \frac{\partial\alpha_x^M}{\partial\epsilon_x})_k + 2(\frac{2}{n})(\overline{Q}_{14}\frac{\partial\alpha_2^D}{\partial\epsilon_x} + \overline{Q}_{15}\frac{\partial\alpha_3^D}{\partial\epsilon_x}) \qquad (11)$$

$$\upsilon_{xy} = \frac{\frac{1}{n} \sum_{k=1}^{n} (Q_{12})_k (1 - \frac{\partial\alpha_x^M}{\partial\epsilon_y})_k + 2(\frac{2}{n})(\overline{Q}_{14}\frac{\partial\alpha_2^D}{\partial\epsilon_y} + \overline{Q}_{15}\frac{\partial\alpha_3^D}{\partial\epsilon_y})}{\frac{1}{n} \sum_{k=1}^{n} (Q_{22})_k (1 - \frac{\partial\alpha_y^M}{\partial\epsilon_y})_k + 2(\frac{2}{n})(\overline{Q}_{24}\frac{\partial\alpha_2^D}{\partial\epsilon_y} + \overline{Q}_{25}\frac{\partial\alpha_3^D}{\partial\epsilon_y})} \qquad (12)$$

where it is assumed that all plies have the same thickness so that

$$z_k - z_{k-1} = t_{ply} \qquad (13a)$$

$$\frac{t_{ply}}{t} = \frac{1}{n} \qquad (13b)$$

$$\frac{t_1}{t} = \frac{2}{n} \qquad (13c)$$

Furthermore,

$$[\overline{Q}]_k = \begin{bmatrix} \overline{Q}_{11} & \overline{Q}_{12} & \overline{Q}_{13} & \overline{Q}_{14} & \overline{Q}_{15} & \overline{Q}_{16} \\ \overline{Q}_{12} & \overline{Q}_{22} & \overline{Q}_{23} & \overline{Q}_{24} & \overline{Q}_{25} & \overline{Q}_{26} \\ \overline{Q}_{16} & \overline{Q}_{26} & \overline{Q}_{36} & \overline{Q}_{46} & \overline{Q}_{56} & \overline{Q}_{66} \end{bmatrix} \qquad (14)$$

11

It has been previously shown [13] that

$$\overline{Q}_{15} = \frac{N_x}{\epsilon_{L_{xz}}} = \frac{\overline{Q}_{11}^T \overline{Q}_{11}^B}{\overline{Q}_{11}^T - \overline{Q}_{11}^B} \tag{15}$$

$$\overline{Q}_{14} = \frac{N_x}{\epsilon_{L_{yz}}} = \frac{\overline{Q}_{12}^T \overline{Q}_{12}^B}{\overline{Q}_{12}^T - \overline{Q}_{12}^B} \tag{16}$$

$$\overline{Q}_{25} = \frac{N_y}{\epsilon_{L_{xz}}} = \frac{\overline{Q}_{21}^T \overline{Q}_{21}^B}{\overline{Q}_{21}^T - \overline{Q}_{21}^B} \tag{17}$$

and

$$\overline{Q}_{24} = \frac{N_y}{\epsilon_{L_{yz}}} = \frac{\overline{Q}_{22}^T \overline{Q}_{22}^B}{\overline{Q}_{22}^T - \overline{Q}_{22}^B} \tag{18}$$

where the superscripts A and B designate the properties of the ply immediately above and below the delamination, respectively.

Determination of Internal State Variables

Implementation of equations (11) and (12) to predict the damage degraded laminate moduli requires the specification of the partial derivatives of the internal state variables with respect to strain for a given damage state. In the absence of growth laws, the damage state must be determined experimentally. Expressions for the internal state variables have been previously developed by the authors [6] by employing energy principles. In the original constitutive theory formulation [5] the local energy loss contribution to the Helmholtz free energy is directly related to the internal

12

state variables as follows:

$$u_L^C = I_{ij}\epsilon_i\alpha_j + \text{H.O.T.'S}$$ (19)

where contracted notation is employed. Furthermore, the local energy loss is also directly related to the fracture mechanics based strain energy release rate for crack creation during load-up

$$u_L^C = \frac{1}{V_L} \int_{S_M} (G_{I_M} + G_{II_M})\, dS + \frac{1}{V_L} \int_{S_D} (G_D)\, dS$$ (20)

where G_{I_M} and G_{II_M} are the mode I and II strain energy release rates for matrix cracking, G_D is the strain energy release rate for internal delaminations, S_M is the matrix crack surface area, and S_D is the delamination surface area. Neglecting the higher order terms and equating equations (19) and (20) provides a direct relationship between the internal state variables and the damage state. Therefore, the internal state variables required by equations (11) and (12) may be specified for a given damage state provided appropriate expressions for the strain energy release rates are known.

In the case of matrix cracking in cross-ply laminates where only the opening mode of fracture is involved the authors have developed the following expression

$$\frac{\partial\alpha_x^M}{\partial\epsilon_x} = \frac{1}{2}\, m\, \frac{(p+q)}{q}\, \frac{E_{x_0}}{E_{22}} \left. \left(\frac{E_{x_1}}{E_{x_0}}\right|_{S_{M_1}} - 1\right)$$ (21)

where m is the number of consecutive 90° plies, p is the number of 0° plies, q is the number of 90° plies, E_{x_0} is the initial undamaged modulus, and E_{x_1} is the damage-degraded modulus corresponding to matrix crack damage state

13

S_{M_1}. The term in the parentheses was determined experimentally from tests on a $[0/90/0]_s$ laminate and is given by

$$\frac{E_{x_1}}{E_{x_0}}\bigg|_S = 0.99969 - 0.061607\ S + 0.04623\ S^2 \tag{22}$$

Finite element studies have shown that the effects of adjacent layer constraint on the energy released by the 90° layers is a second order effect [16]. Therefore, by using the following second order tensor transformation

$$\frac{\partial \bar{\alpha}_{\overline{ij}}^{M}}{\partial \bar{\epsilon}_{\overline{mn}}^{0}} = a_{\overline{ip}}\ a_{\overline{jp}}\ a_{\overline{mr}}\ a_{\overline{ns}}\ \frac{\partial \alpha_{pq}^{M}}{\partial \epsilon_{rs}^{0}} \tag{23}$$

where no bars refer to the crack coordinate system and the over bars refer to the laminate coordinate system, equation (21) is generally applicable to matrix crack damage in any ply of any laminate stacking sequence.

In the case of off-axis plies, other than 90°, the tensor transformation law given by equation (23) also requires the determination of $\partial \alpha_{12}^{M}/\partial \epsilon_{12}$ for matrix crack damage. This damage parameter is related to shear deformation at the ply level which gives rise to the sliding mode of relative crack face displacements. Considering a $[\pm 45]_{2s}$ laminate where each ply is more-or-less in a state of pure shear equations (19) and (20) reduce to [16]

$$\frac{\partial \alpha_{12}}{\partial \epsilon_{12}} = 2\ [1 - \frac{(G_{12})_{EXP}}{(G_{12})_0}]\ \frac{S_M}{S_{EXP}} \tag{24}$$

where $(G_{12})_{EXP}$ is interpreted as the effective shear modulus for the damaged ply and is computed by

$$(G_{12})_{EXP} = \frac{\bar{\sigma}_x}{2(\epsilon_x - \epsilon_y)} \tag{25}$$

14

$(G_{12})_{EXP}/(G_{12})_0 = 0.822$ for S_{EXP} corresponding to 21 cracks per inch in each ply of the $[\pm 45]_{2s}$. Since the plies of the $[\pm 45]_{2s}$ are in pure shear, expression (24) may be used to determine $\partial \alpha_{12}/\partial \epsilon_{12}$ for any ply with matrix crack damage. The fiber (crack) orientation of the cracked ply is accounted for by the coordinate transformation given by equation (23).

The delamination internal state variable was determined from energy principles as well, except O'Brien's [17] strain energy release rate model was used rather than experimental results. Since O'Brien's model assumes that the strain energy release rate is independent of the size of the delamination, the internal state variable is linear in delamination surface area. Therefore,

$$\frac{\partial \alpha_3^D}{\partial \epsilon_x} = - \frac{n}{2} \frac{(E_{x_0} - E^*)}{\overline{Q}_{15}} \left(\frac{S_D}{S}\right) \tag{26}$$

where n is the number of plies in the laminate, S_D is the delamination area and S is the total interfacial area in the local volume. E^* is the modulus of the sublaminates formed by the delamination and is given by

$$E^* = \frac{1}{t} \sum_{i=1}^{d} E_i t_i \tag{27}$$

where d is the number of sublaminates and t is the laminate thickness. By similar reasoning,

$$\frac{\partial \alpha_2^D}{\partial \epsilon_y} = - \frac{n}{2} \frac{(E_{y_0} - E^*)}{\overline{Q}_{24}} \left(\frac{S_D}{S}\right) \tag{28}$$

Finally, as a first approximation for the cross-derivatives in equations (11), and (12), we have

$$\frac{\partial \alpha_x^M}{\partial \epsilon_y} = \frac{S_{12}}{S_{22}} \frac{\partial \alpha_x^M}{\partial \epsilon_x} \tag{29}$$

$$\frac{\partial \alpha_3^D}{\partial \epsilon_y} = \frac{S_{12}}{S_{22}} \frac{\partial \alpha_3^D}{\partial \epsilon_x} \tag{30}$$

$$\frac{\partial \alpha_2^D}{\partial \epsilon_x} = \frac{S_{12}}{S_{11}} \frac{\partial \alpha_3^D}{\partial \epsilon_x} \tag{31}$$

where S_{ij} is defined by the following undamaged laminate stress-strain relationships using the first term of equation (6)

$$S_{11} = \frac{1}{t} \frac{\partial N_x}{\partial \epsilon_x} \tag{32}$$

$$S_{22} = \frac{1}{t} \frac{\partial N_y}{\partial \epsilon_y} \tag{33}$$

$$S_{12} = \frac{1}{t} \frac{\partial N_x}{\partial \epsilon_y} \tag{34}$$

As an example, consider the case of cross-ply laminates where the delamination site is at a 0/90 interface. Equations (11) and (12) reduce to the following simplified forms

$$E_x = E_{x_0}[1 - \frac{1}{nE_{x_0}} \sum_{k=1}^{n} (Q_{11})_k (\frac{\partial \alpha_x^M}{\partial \epsilon_x})_k - \frac{1}{2} (1 - \frac{E^*}{E_{x_0}})(\frac{S_D}{S})] \tag{35}$$

$$\upsilon_{xy} = \upsilon_{xy_0}[1 - 2(\frac{p}{n} \frac{E_{22}}{E_{11} + E_{22}} + \frac{q}{n})(\frac{S_D}{S})] \tag{36}$$

where E_{11}, E_{12} and υ_{12} are the standard lamina properties.

COMPARISON OF MODEL PREDICTIONS TO
EXPERIMENTAL RESULTS

While the damage-dependent laminate analysis model may be used to predict any of the effective engineering moduli of a laminate, experimental results are only available for the axial modulus and Poisson's ratio. Therefore, the general utility of the model will be demonstrated by comparing model predictions to experimental results for E_x and ν_{xy} for the fully developed damage states illustrated in Figs. 2,4,5-7. The delamination interface location was determined experimentally and the delamination area was estimated from the x-ray radiographs using an optical planimeter procedure. In both the model analysis and data reduction, it was assumed that the delamination sites were symmetrically located about the laminate midplane and contained the same delamination surface area.

The bar chart of Fig. 11 compares the model predictions to the experimental values of the engineering modulus, E_x, for combined matrix cracking and delamination. The delamination interface location and percent of delamination area are listed in the figure underneath the laminate stacking sequence. As can be seen, the comparison between model results and the experimental results is quite good. Some limited results for Poisson's ratio are given in Fig. 12 using the same bar chart format. With the exception of the $[0/90_2]_s$ laminate, these results are also quite good. The experimental value for the $[0/90_2]_s$ laminate is quite suspicious since this laminate exhibits a much larger change in Poisson's ratio than the other laminates without a corresponding difference in the delamination surface area. It should be noted that values of Poisson's ratio for the quasi-isotropic laminates are not available.

17

SUMMARY AND CONCLUSIONS

The authors have formulated a constitutive model for laminated composites with both matrix cracks and delamination damage. The model is based on the concept of continuum damage mechanics and uses second-order tensor valued internal state variables to represent each mode of damage. The internal state variables are the local volume averaged measure of the relative crack face displacements. The local volume for matrix crack damage is at the ply level, whereas the local volume for delamination damage is at the laminate level. Therefore, the damage-dependent constitutive model takes the form of laminate analysis equations modified by inclusion of the internal state variables.

This paper demonstrates the applicability of the model to predict the degraded engineering modulus, E_x, and Poisson's ratio, ν_{xy}, of quasi-isotropic and cross-ply laminates of graphite/epoxy. The comparison between model predictions and experimental results is very close. The authors submit that the good agreement reported herein supports the validity of the model formulation and the physical interpretation of the internal state variables.

ACKNOWLEDGEMENTS

REFERENCES

1. Fatigue of Fibrous Composite Materials, ASTM STP 723, American Society for Testing and Materials, 1981.

2. Damage in Composite Materials, ASTM STP 775, K.L. Reifsnider, Ed., American Society for Testing and Materials, 1982.

3. Effects of Defects in Composite Materials, ASTM STP 836, D.J. Wilkins, Ed., American Society for Testing and Materials, 1984.

18

4. Delamination and Debonding of Materials, ASTM STP 876, W.S. Johnson, Ed., American Society for Testing and Materials, 1985.

5. Allen, D.H., Harris, C.E. and Groves, S.E., "A Thermomechanical Constitutive Theory for Elastic Composites with Distributed Damage - Part I: Theoretical Development," International Journal of Solids and Structures, Vol. 23, No. 9, pp. 1301-1318, 1987.

6. Allen, D.H., Harris, C.E., and Groves, S.E., "A Thermomechanical Constitutive Theory for Elastic Composites with Distributed Damage - Part II: Application to Matrix Cracking in Laminated Composites," International Journal of Solids and Structures, Vol. 23, No. 9, pp. 1319-1338, 1987 .

7. Talreja, R., "A Continuum Mechanics Characaterization of Damage in Composite Materials," Proc. R. Soc. London, Vol. 399A, 1985, pp. 195-216.

8. Weitsman, Y., "Environmentally Induced Damge in Composites," Proc. of the 5th Symposium on Continuum Modeling of Discrete Structures, A.J.M. Spencer, Ed., Nottingham, U.K., 1985.

9. Reifsnider, K.L. and Stinchcomb, W.W., "A Critical-Element Model of the Residual Strength and Life of Fatigue-Loaded Composite Coupons," Composite Materials: Fatigue and Fracture, ASTM STP 907, H.T. Hahn, Ed., American Society for Testing and Materials, 1986, pp. 298-313.

10. Kachanov, L.M., "On the Creep Fracture time," IZU. AN SSR, Otd. Tekhn. Nauk, No. 8, pp. 26-31, 1958.

11. Krajcinovic, D., "Continuum Damage Mechanics," Applied Mechanics Reviews, Vol. 37, pp. 1-6, 1984.

12. Krojcinovic, D., "Update to Continuum Damage Mechanics," Applied Mechanics Update 1986, Steele, C.R. and Springer, G.S., Eds., The American Society of Mechanical Engineers, pp. 403-406, 1986.

13. Allen, D.H., Harris, C.E., and Groves, S.E., "Damage Modelling in Laminated Composites," Proceedings of IUTAM/ICM Symposium on Yielding, Damage and Failure of Anisotropic Solids, Grenoble, France, 1987.

14. Talreja, R., "Stiffness Properties of Composite Laminates with Matrix Cracking and Interior Delaminations," Danish Center for Applied Mathematics and Mechanics, The Technical University of Denmark, No. 321, March 1986.

15. Georgiou, I.T., "Initiation Mechanisms and Fatigue Growth of Internal Delaminations in Graphite/Epoxy Cross-Ply Laminates," MS Thesis, Texas A&M University, College Station, Texas 77843, December 1986.

16. Harris, C.E., Allen, D.H., and Nottorf, E.W., "Modelling Stiffness Loss in Quasi-Isotropic Laminates Due to Microstructural Damage," to appear in Journal of Engineering Materials and Technology, American Society of Mechanical Engineers, 1988.
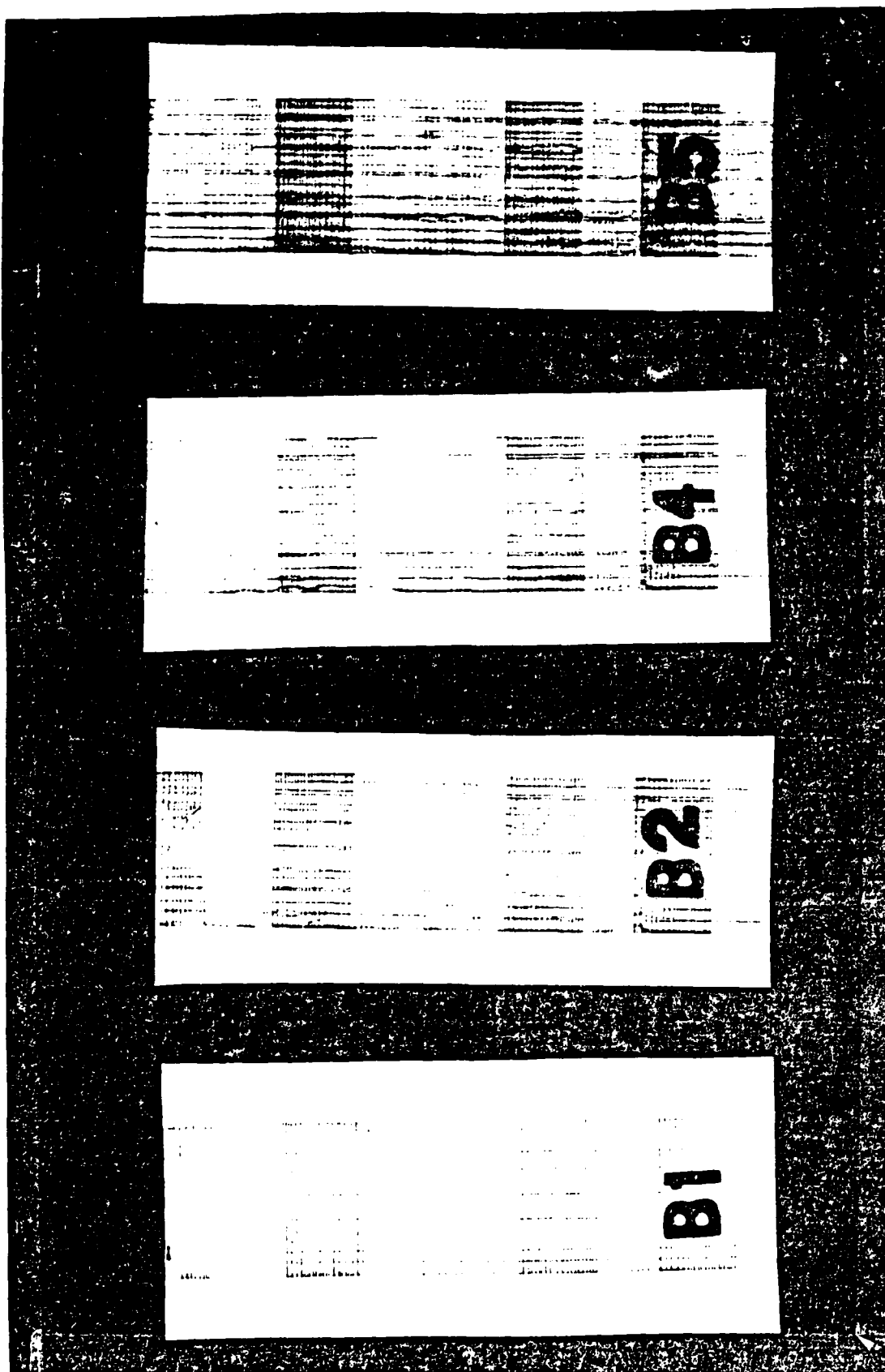
LIST OF FIGURE CAPTIONS

Fig. 1 Progression of Damage in a $[0_2/90_2]_s$ Laminate

Fig. 2 Enlarged X-ray Radiograph of Damage in a $[0_2/90_2]_s$ Laminate at 400,000 Cycles with S_{max} = 75% of S_{ULT}

Fig. 3 Progression of Damage in a $[0/90_2]_s$ Laminate

Fig. 4 Enlarged X-ray Radiograph of Damage in a $[0/90_2]_s$ Laminate at 1,003,000 Cycles with S_{max} = 71% of S_{ULT}

Fig. 5 Enlarged X-ray Radiograph of Damage in a $[0/90_3]_s$ Laminate at 200,000 Cycles with S_{max} = 73% of S_{ULT}

Fig. 6 Enlarged X-ray Radiograph of Damage in a $[90/\pm45/0]_s$ Laminate at 50,000 Cycles with S_{max} = 73% of S_{ULT}

Fig. 7 Enlarged X-ray Radiograph of Damage in a $[0/\pm45/90]_s$ Laminate at 17,000 Cycles with S_{max} = 76% of S_{ULT}

Fig. 8 Deformation Geometry for Region A_L

Fig. 9 Schematic of Delaminated Region in a Composite Layup

Fig. 10 Interply Delamination in a Laminated Continuous Fiber Composite

Fig. 11 Comparison of Experimental Results and Model Predictions of the Laminate Engineering Modulus, E_x, Degraded by Both Matrix Cracking and Delamination Damage

Fig. 12 Comparison of Experimental Results and Model Predictions of the Laminate Engineering Poisson's Ratio, ν_{xy}, Degraded by Both Matrix Cracking and Delamination Damage

19

17. O'Brien, T.K., "Characterization of Delamination Onset and Growth in a Composite Laminate," _Damage in Composite Materials, ASTM STP 775_, K.L. Reifsnider, Ed., American Society for Testing and Materials, pp. 141-167, 1982.

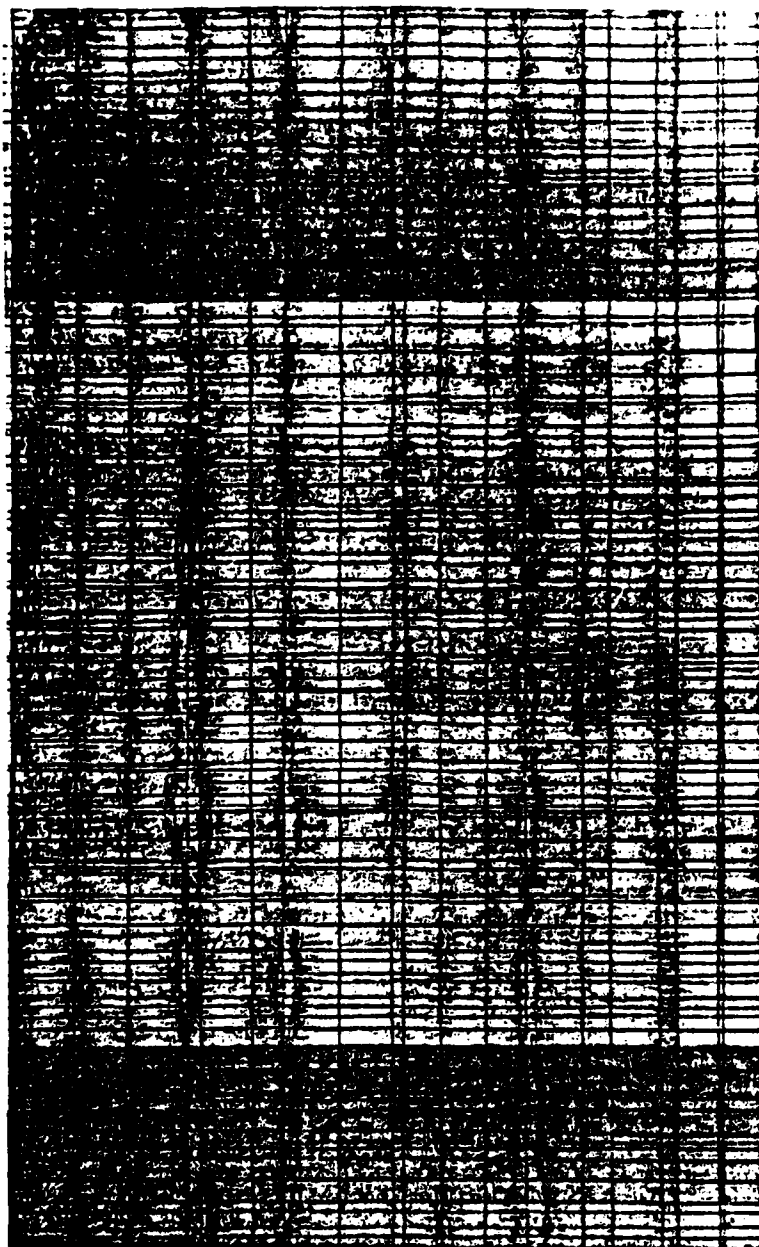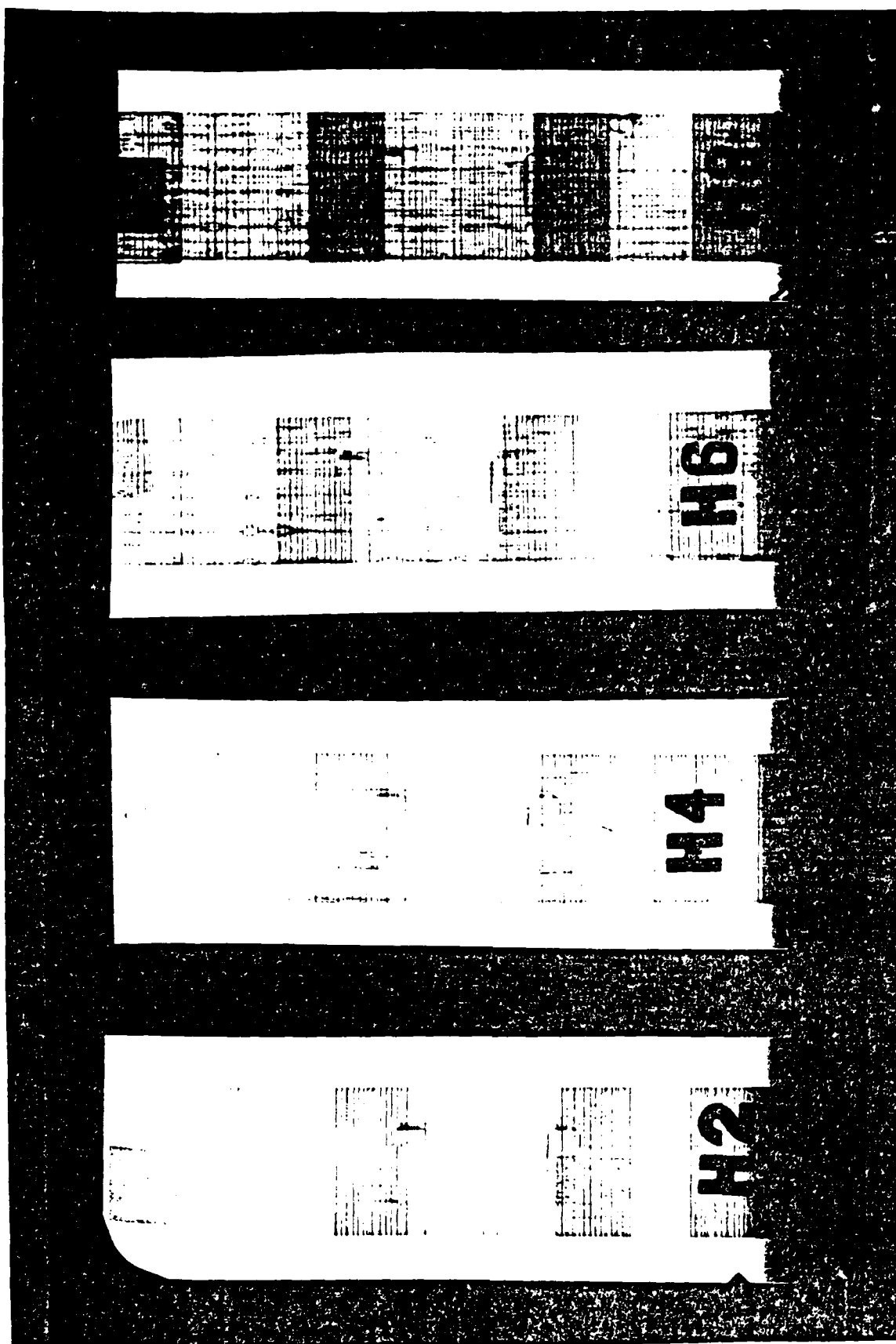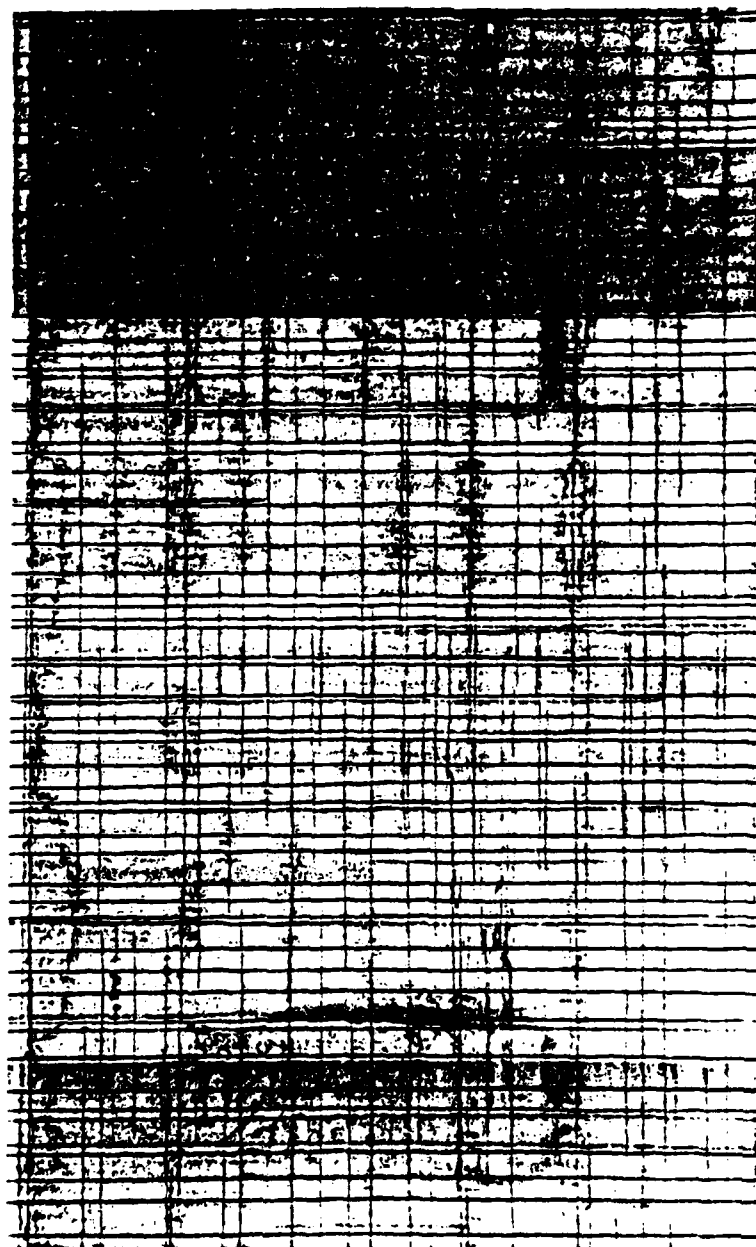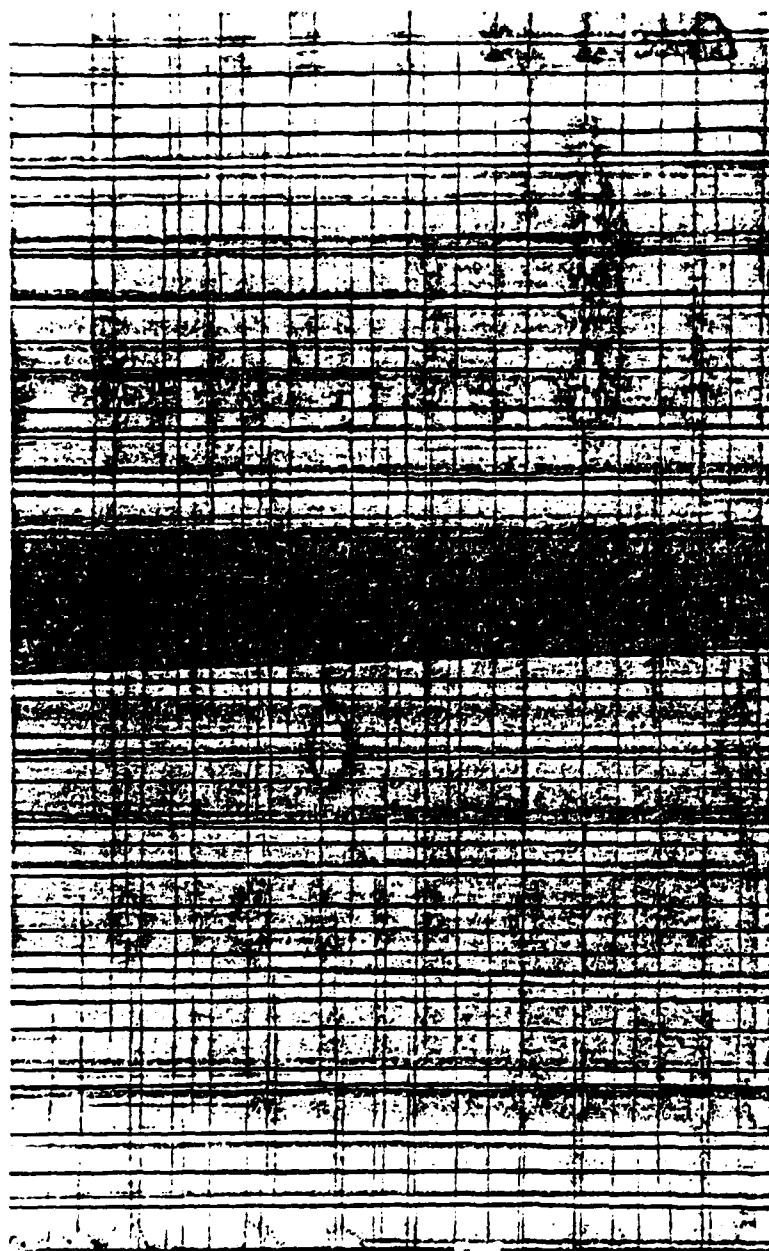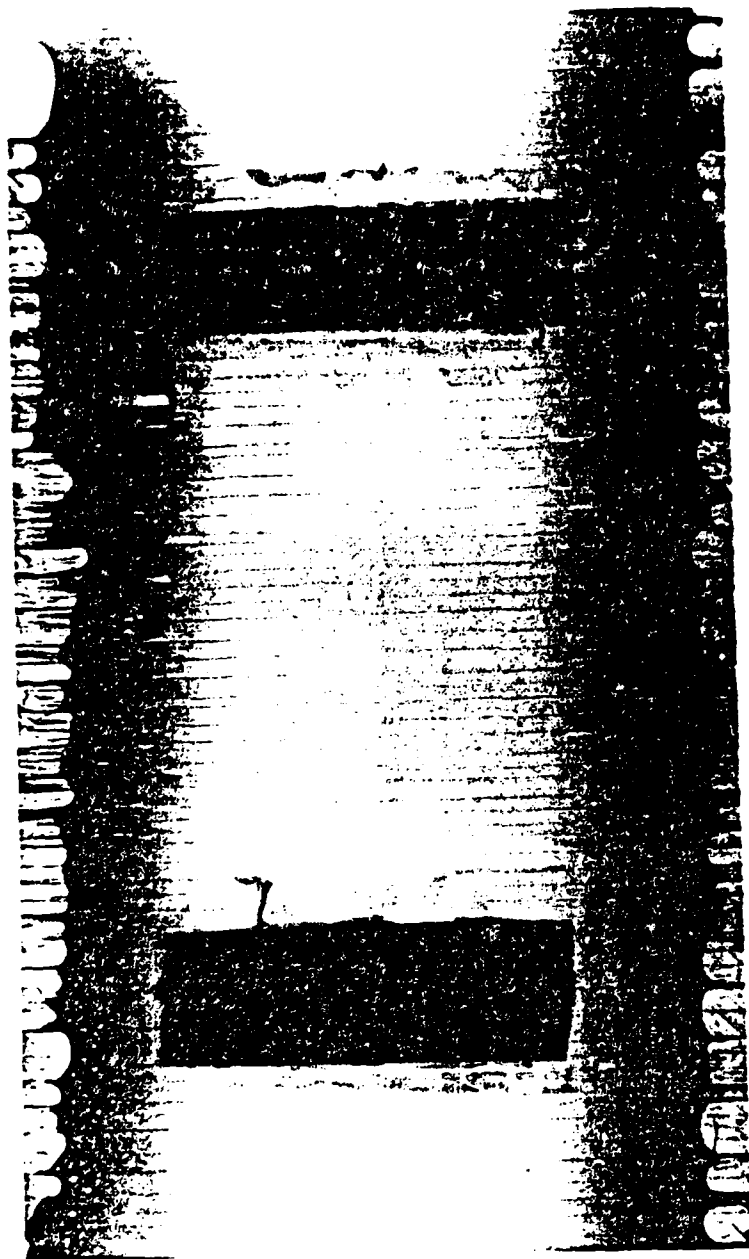Fig. 1 Progression of Damage in a $[0_2/90_2]_s$ Laminate

Fig. 2 Enlarged X-ray Radiograph of Damage in a $[0_2/90_2]_s$ Laminate at 400,000 Cycles with S_{max} = 75% of S_{ULT}

Fig. 3 Progression of Damage in a $[0/90_2]_s$ Laminate

Fig. 4 Enlarged X-ray Radiograph of Damage in a $[0/90_2]_s$ Laminate at 1,003,000 Cycles with S_{max} = 71% of S_{ULT}

Fig. 5 Enlarged X-ray Radiograph of Damage in a $[0/90_3]_s$ Laminate at 200,000
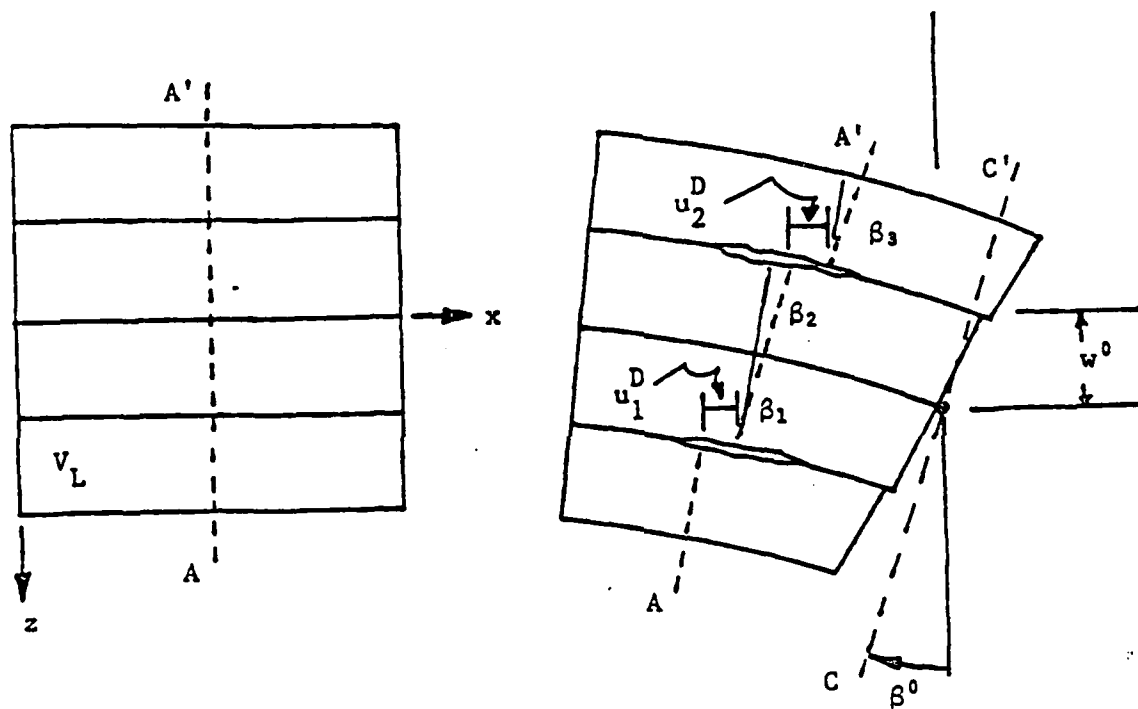Cycles with S_{max} = 73% of S_{ULT}

Fig. 6 Enlarged X-ray Radiograph of Damage in a $[90/\pm45/0]_s$ Laminate at 50,000 Cycles with S_{max} = 73% of S_{ULT}

Fig. 7 Enlarged X-ray Radiograph of Damage in a $[0/\pm45/90]_s$ Laminate at 17,000 Cycles with S_{max} = 76% of S_{ULT}
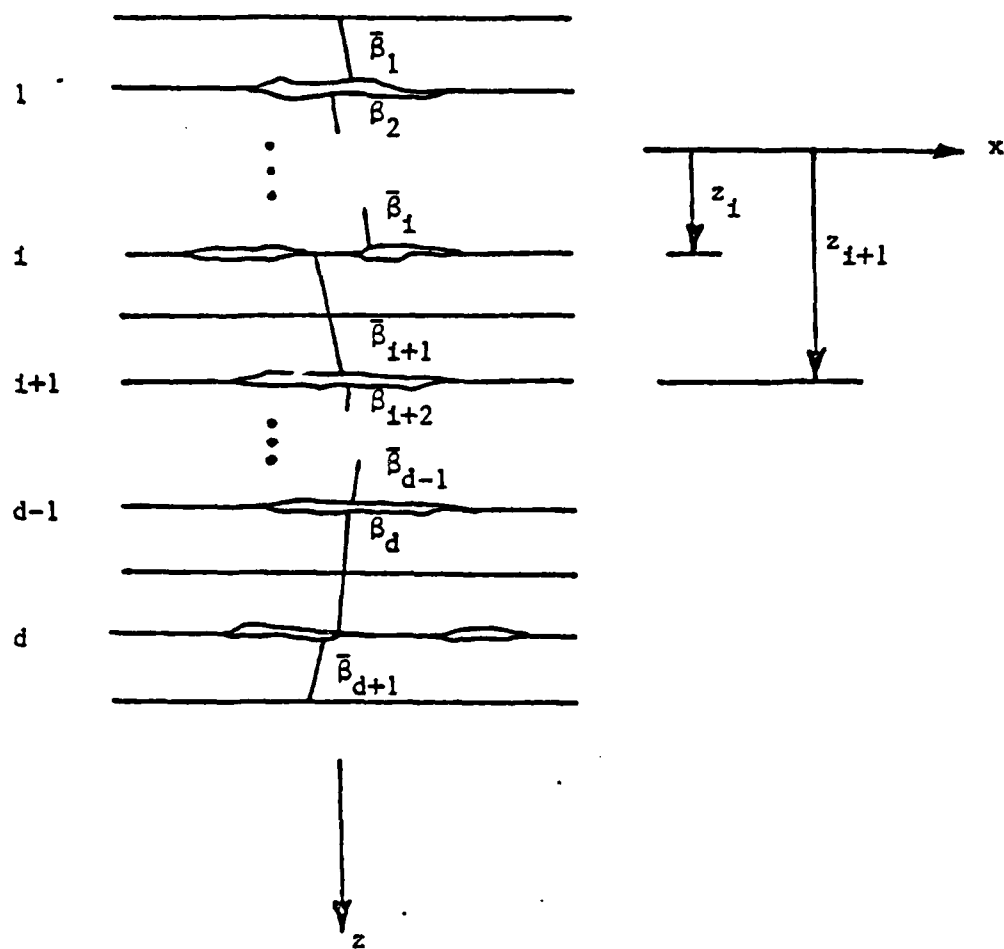
Fig. 8 Deformation Geometry for Region A_L

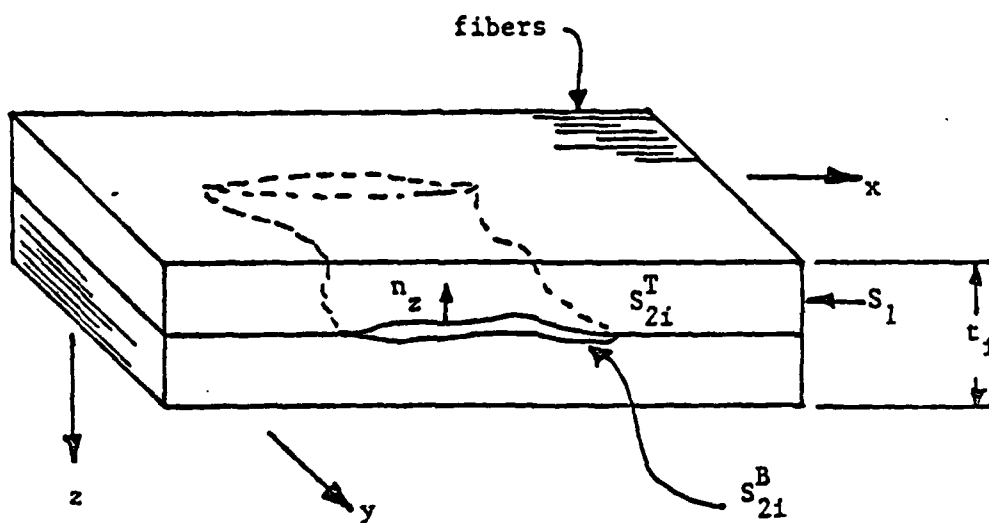Fig. 9   Schematic of Delaminated Region in a Composite Layup

Fig. 10 Interply Delamination in a Laminated Continuous Fiber Composite
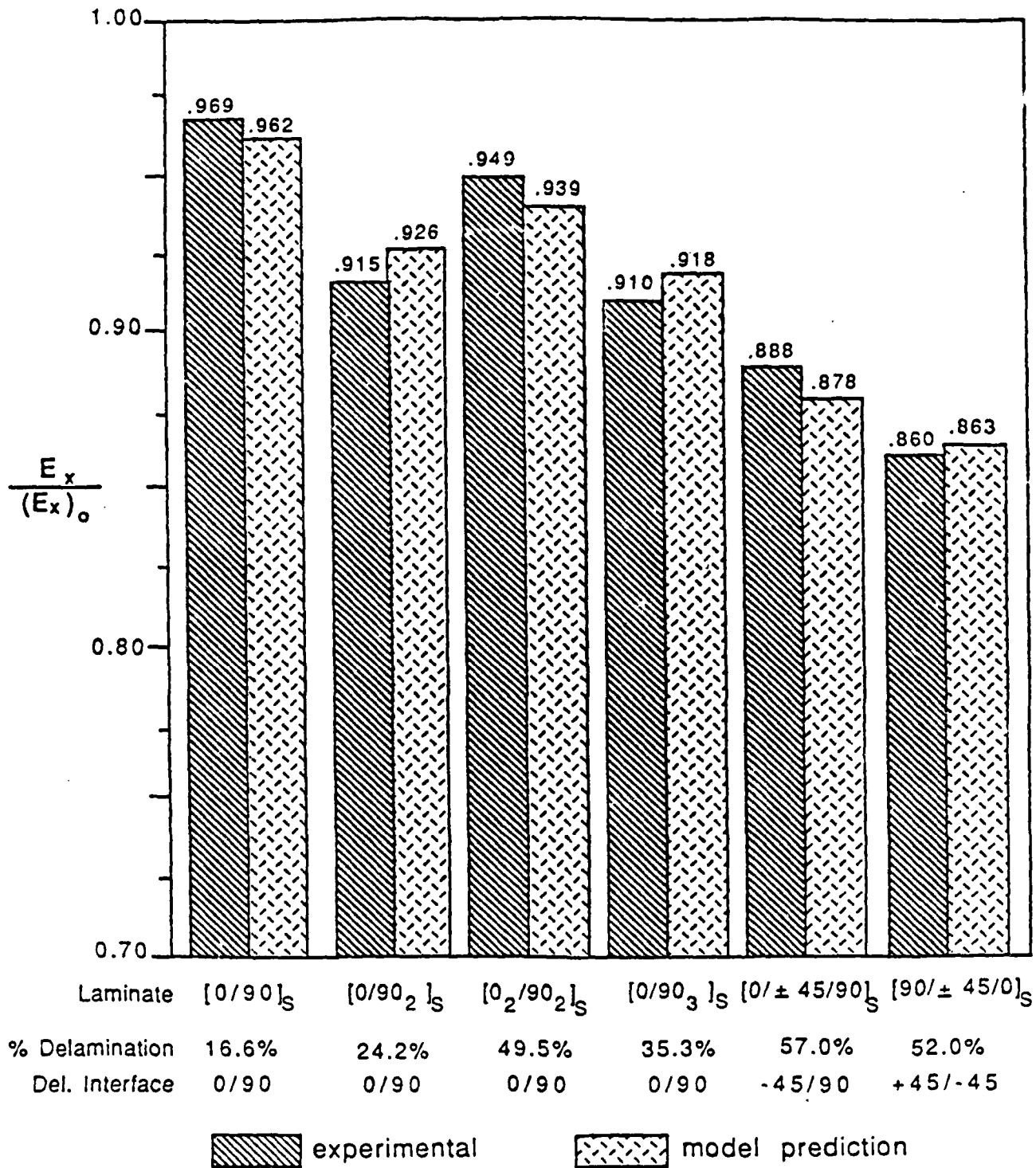
Damage-Dependent Laminate E_x

$$\frac{E_x}{(E_x)_o}$$

Bar values (experimental / model prediction):
.969 / .962
.915 / .926
.949 / .939
.910 / .918
.888 / .878
.860 / .863

Laminate	$[0/90]_S$	$[0/90_2]_S$	$[0_2/90_2]_S$	$[0/90_3]_S$	$[0/\pm 45/90]_S$	$[90/\pm 45/0]_S$
% Delamination	16.6%	24.2%	49.5%	35.3%	57.0%	52.0%
Del. Interface	0/90	0/90	0/90	0/90	-45/90	+45/-45

experimental   model prediction

Fig. 11 Comparison of Experimental Results and Model Predictions of the Laminate Engineering Modulus, E_x, Degraded by Both Matrix Cracking and Delamination Damage
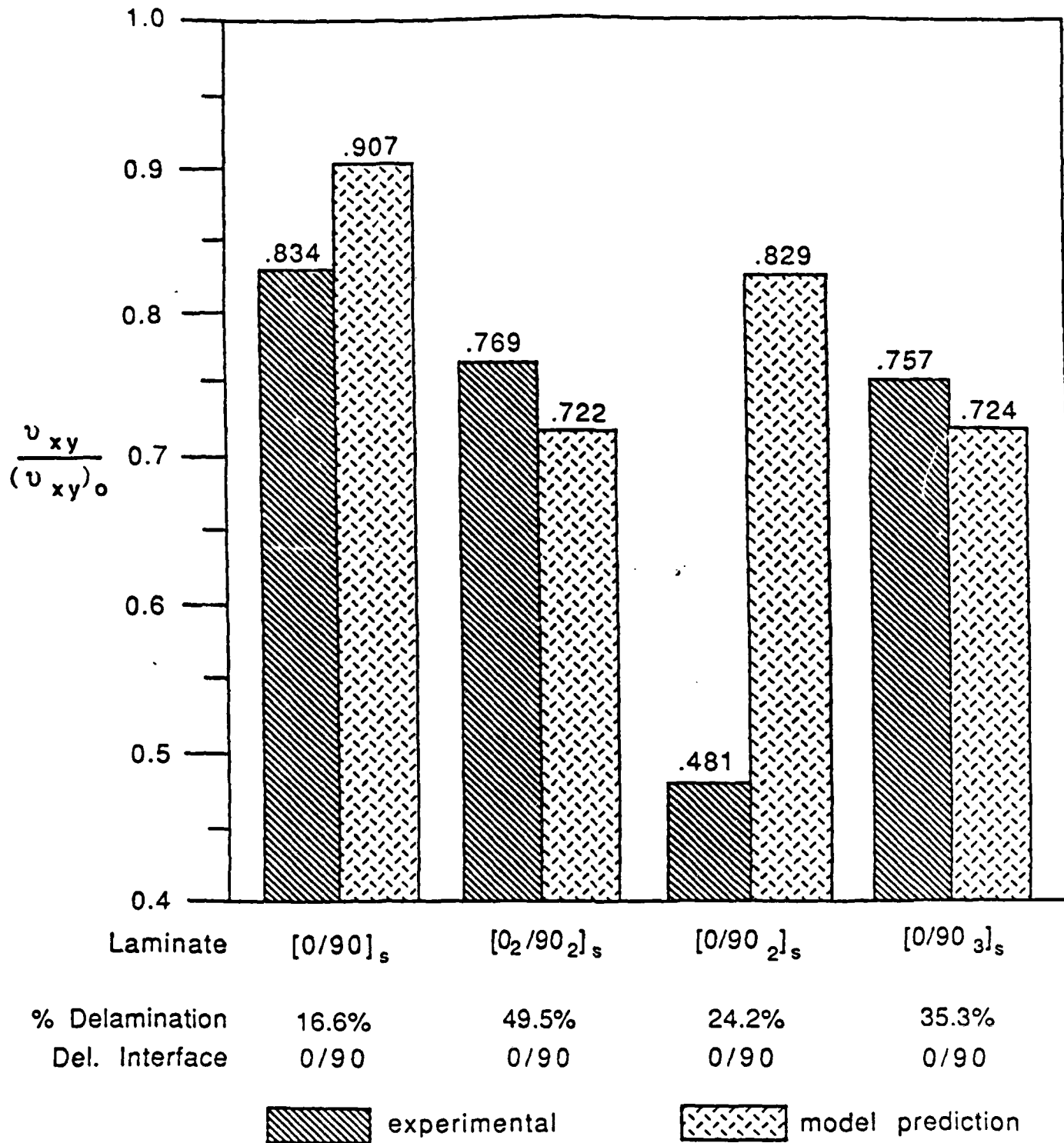
Fig. 12 Comparison of Experimental Results and Model Predictions of the Laminate Engineering Poisson's Ratio, v_{xy}, Degraded by Both Matrix Cracking and Delamination Damage

Appendix 7.6

Damage Modelling In Laminated Composites

by

D.H. Allen
C.E. Harris

Aerospace Engineering Department
Texas A&M University
College Station, Texas 77843

and

S.E. Groves
Lawrence Livermore National Labs
Livermore, CA 94550

Proceedings IUTAM/ICM Symposium on Yielding,
Damage and Failure of Anisotropic Solids

Grenoble, France

1987

Damage Modelling In Laminated Composites

by

D.H. Allen
C.E. Harris

Aerospace Engineering Department
Texas A&M University
College Station, Texas 77843

and

S.E. Groves
Lawrence Livermore National Labs
Livermore, CA 94550

Abstract - In this paper a damage model is presented for laminated continuous fiber composites. Because of the layered anisotropy of the medium of interest, at least two distinct orthotropic damage modes are observed in laminated composites: matrix cracks and interply delaminations. Due to statistical inhomogeneity in the coordinate dimension normal to the plane of the laminate, second order tensor internal state variables are constructed which represent a weighted average of both matrix cracks and delaminations.

It is shown herein that linear elastic fracture mechanics may be utilized to construct the parameters necessary to characterize the material properties in the stress-strain-damage constitutive equations. The resulting model is then independent of the stacking sequence and ply orientation in the laminate. Recently obtained comparisons of model predictions to experimental results reported herein support the validity of the model.

1

1. Introduction

The first application of continuum damage mechanics is attributed to L.M. Kachanov [8]. In this method it is recognized that the exact analysis of a multiply connected domain with numerous microcracks is hopelessly complex. Therefore, the effects of these microcracks on macrophysical response are reflected via one or more internal state variables [14] called damage parameters. The initial use of damage mechanics appears to have been a logical one. It was observed that in metals classical plasticity theory breaks down when significant grain boundary sliding and/or microcavitation occur because the initial elastic properties are not observed on unloading [15].

In the last twenty years there has been an incredible expansion of research in damage mechanics, as evidenced by two recent review articles [5,11,12] and the publication of the first textbook devoted entirely to damage mechanics [9]. However, as pointed out in reference 12, although substantial research has been performed on metals, concrete, and geologic media, very little research has been detailed on laminated composite media. In fact, to these authors' knowledge, only three concerted efforts have reached the open literature at the time of this writing. These are due to Talreja [16-20], Allen, et al. [1-4], and Weitsman [21]. In fact, the first two authors of this paper became acquainted with Dr. Talreja in the summer of 1983, while the latter was on sabbatical at the Virginia Polytechnic Institute and State University. At that time Dr. Talreja was completing his first paper on the subject, while the current model was just beginning to be formulated. Due to discussions at that time, the current model owes some credit to the work of Dr. Talreja. Doubtless there are numerous other applications of damage

2

mechanics to laminated composites on the threshold of making their way into the literature. However, we are unaware of them at the time of this writing.

The principal difficulty in laminated composites, unlike metals and concrete, is that the layered orthotropy of the medium produces multiple damage modes, each possessed of some degree of anisotropy. Therefore, whereas it is often sufficient to deal with a single isotropic (scalar valued) damage tensor in initially isotropic and homogeneous media, this simplicity cannot be utilized in laminated composites. Furthermore, each of the damage mechanisms is interrelated and extremely difficult to distinguish experimentally. Finally, the damage may not be considered to be statistically homogeneous through the laminate thickness. Nevertheless, the application of continuum damage mechanics to laminated composites appears to be a fruitful quest because the most obvious alternative would be to attempt to solve a highly anisotropic multiply connected boundary value problem.

An example of a composite laminate with two distinct modes of damage is shown in Fig. 1 [7]. In this example, there are matrix cracks in the crossplies and delaminations at the ply interfaces. Note that the cracks are oriented and statistically nonhomogeneous in the out-of-plane coordinate direction. Experimental observation [6] indicates that the matrix cracks are load induced, whereas the delaminations are driven by stress concentrations at the matrix crack tips. Therefore, significant interaction of the damage modes is observed. Although not shown in the figure, there are often additional damage modes observed prior to component failure, including fiber-matrix debonding, fiber fracture and fiber crimping and/or buckling in compression. An excellent review of the genesis of these events is described in further detail in reference 19.

3

The ultimate objective of any continuum mechanics model is to design away from failure. In the sense that laminated composites fail due to a complex sequence of damage events, it is essential to capture the important features of the damage process in order to accurately predict failure. Obviously this will be a complex task in laminated composites, but, as Einstein once put it, a good theory should be as simple as possible but no simpler than that.

2. Model Development

The authors have been developing a model for predicting the constitutive behavior of laminated continuous fiber composites [1-4]. This model utilizes the concept of continuum damage mechanics, in the sense that the effects of microcracks are reflected via internal state variables (ISV's) in the constitutive equations, rather than treating each microcrack as a separate internal boundary. Furthermore, the model is phenomenological because only the average macroscale effect of microcracking is modelled rather than the effect of each individual crack. Because cracking is not statistically homogeneous in the coordinate direction normal to the laminate, statistical weighting is necessary in this direction, and this is accomplished via kinematic constraints. Therefore, the constitutive equations are laminate equations, rather than standard stress-strain equations.

A continuum damage model must contain four essential ingredients in order to be complete: 1) stress-strain-damage equations; 2) damage growth laws for the damage ISV's; 3) a failure function describing local failure in terms of the damage ISV's and observable state variables; and 4) an algorithm for solving boundary value problems in which the state is nonhomogeneous. If steps one through three can be accomplished accurately, then step four is

4

relatively straightforward, involving a procedure not unlike extending an elastic algorithm to include plasticity. Steps two and three tend to be the most complex, especially for laminated composites. Although there has been some research on these two components of the model, the authors would consider this work exploratory at this time. The subject of the current paper is step one. The fundamental difficulty in this procedure is to develop a model which is independent of ply orientation and stacking sequence. Of course, the ultimate goal of this research is step three, to predict failure as a function of the current damage state.

Research is currently underway to extend the model to predict the response of laminates with both matrix cracks and interior delaminations [3], as shown in Fig. 1. This problem is complicated by two factors. First, because these two damage mechanisms are oriented differently, they require two separate tensor-valued damage parameters. Furthermore, the mechanics of these two damage modes are substantially different. The matrix cracks may be assumed to be statistically homogeneous over each ply in a small local volume element. Therefore, classical local volume averaging may be used to obtain this damage parameter. On the other hand, delaminations are not statistically homogeneous in the z coordinate direction. This requires that a modification be made to statistical averaging techniques. Although statistical homogeneity is assumed in the x and y coordinate directions, a kinematic constraint similar to the Kirchhoff-Love hypothesis is applied in the z direction. The resulting damage parameter is a weighted measure of damage, with delaminations away from the neutral surface causing a greater effect on laminate properties.

The model development proceeds from the assumption that all material inelasticity is contained within small zones surrounding the microcracks. The effect of matrix cracks on ply level constitutive equations is accounted for

5

via the local volume average of the diadic product of the crack opening displacement vector u_i^C and the crack face normal n_j^C [11]:

$$\alpha_{ij}^M = \frac{1}{V_L} \int_{S_C} u_i^C n_j^C ds \tag{1}$$

where V_L is the local volume for which cracking can be considered statistically homogeneous, and S_C is the surface area of cracks in V_L. For matrix cracking V_L is typically one ply in thickness. The ply level stress-strain relations are therefore given by

$$\sigma_{ij} = C_{ijk\ell}(\varepsilon_{k\ell} - \alpha_{k\ell}^M) \tag{2}$$

In order to account for interply delamination the following kinematic assumption is made (See Fig. 2.):

$$u(x,y,z) = u^O(x,y) - z[\beta^O + H(z-z_k)\beta_k^D] + H(z-z_k)u_k^D \tag{3}$$

$$v(x,y,z) = v^O(x,y) - z[\psi^O + H(z-z_k)\psi_k^D] + H(z-z_k)v_k^D \tag{4}$$

and

$$w(x,y,z) = w^O(x,y) - H(z-z_k)w_k^D \tag{5}$$

where u and v are components of the in-plane displacement and w is the out-of-plane displacement and H is the Heavyside step function. Furthermore, β and ψ represent rotations of the midplane. The quantities with superscripts o are undamaged midsurface values, and quantities with superscripts D are caused by interlaminar cracking.

6

Employing standard laminate averaging techniques will result in the following laminate equations [3]

$$\{N\} = \sum_{k=1}^{n} [Q]_k \ (z_k - z_{k-1}) \ \{\epsilon_L^0\} - \frac{1}{2} \sum_{k=1}^{n} [Q]_k \ (z_k^2 - z_{k-1}^2) \ \{\kappa_L\}$$

$$+ \sum_{i=1}^{d} [\bar{Q}_1]_i \ t_i \begin{Bmatrix} 0 \\ 0 \\ \alpha_{1i}^D \\ \alpha_{2i}^D \\ \alpha_{3i}^D \\ 0 \end{Bmatrix} + \sum_{i=1}^{d+1} (z_i - z_{i-1}) \ [\bar{Q}_2]_i \begin{Bmatrix} 0 \\ 0 \\ 0 \\ \alpha_{4i}^D \\ \alpha_{5i}^D \\ 0 \end{Bmatrix}$$

$$- \sum_{k=1}^{n} [Q]_k \ (z_k - z_{k-1}) \ \{\alpha^M\}_k \tag{6}$$

$$\{M\} = \frac{1}{2} \sum_{k=1}^{n} [Q]_k \ (z_k^2 - z_{k-1}^2) \ \{\epsilon_L^0\} - \frac{1}{3} \sum_{k=1}^{n} [Q]_k \ (z_k^3 - z_{k-1}^3) \ \{\kappa_L\}$$

$$+ \sum_{i=1}^{d} [\bar{Q}_3]_i \ t_i^2 \begin{Bmatrix} 0 \\ 0 \\ \alpha_{1i}^D \\ \alpha_{2i}^D \\ \alpha_{3i}^D \\ 0 \end{Bmatrix} + \sum_{i=1}^{d+1} [\bar{Q}_4]_i (z_i^2 - z_{i-1}^2) \begin{Bmatrix} 0 \\ 0 \\ 0 \\ \alpha_{4i}^D \\ \alpha_{5i}^D \\ 0 \end{Bmatrix}$$

$$- \frac{1}{2} \sum_{k=1}^{n} [Q]_k \ (z_k^2 - z_{k-1}^2) \ \{\alpha^M\}_k \tag{7}$$

7

where $\{N\}$ and $\{M\}$ are the resultant forces and moments per unit length respectively, and $\{\alpha^M\}_k$ and $\{\alpha_L^D\}$ represent the damage due to matrix cracking and interply delamination, respectively. Furthermore, n is the number of plies, and d is the number of delaminated ply interfaces, as shown in Fig. 3.

The internal state variable for delamination, $\{\alpha_L^D\}$, is obtained by employing the divergence theorem on a local volume element of the laminate. The resulting procedure gives [3]

$$\alpha_{1i}^D = \frac{2}{V_{Li}} \int_{S_{2i}} w_i^D n_z dS \tag{8a}$$

$$\alpha_{2i}^D = \frac{2}{V_{Li}} \int_{S_{2i}} v_i^D n_z dS \tag{8b}$$

$$\alpha_{3i}^D = \frac{2}{V_{Li}} \int_{S_{2i}} u_i^D n_z dS \tag{8c}$$

$$\alpha_{4i}^D = \frac{1}{A_L} \int_{S_{2i}^B} \psi_i^D n_z dS \tag{8d}$$

$$\alpha_{5i}^D = \frac{1}{A_L} \int_{S_{2i}^B} \beta_i^D n_z dS \tag{8e}$$

where the subscript i is associated with the ith delaminated ply interface. Furthermore, V_{Li} is equivalent to $t_i A_L$, where t_i is the thickness of the two plies above and below the delamination, as shown in Fig. 4.

Furthermore, the matrices [Q] with subscripts k are the standard elastic property matrices for the undamaged plies. The matrices $[\overline{Q}]$ with subscripts i apply to the ith delaminated ply interface. They represent average properties of the plies above and below the delamination. These are described in further detail in reference 3.

3. Determination of E_x for the Mixed Damage Mode:

Now, suppose that one is interested in modeling stiffness loss as a function of damage state. In order to do this it is necessary to construct the (stacking sequence independent) material parameters developed in the previous section. To do this, consider a symmetric balanced laminate so that $\{\kappa_L\} = \{0\}$ and define the loading direction engineering modulus of the laminate to be

$$E_x \equiv \frac{1}{t} \frac{\partial N_x}{\partial \epsilon_x} \tag{9}$$

Differentiating equation (6) yields

$$E_x = \frac{1}{n} \sum_{k=1}^{n} (Q_{11})_k - \frac{1}{n} \sum_{k=1}^{n} (Q_{11})_k \left(\frac{\partial \alpha_x^M}{\partial \epsilon_x}\right)_k + \frac{1}{t} \sum_{i=1}^{d} \left[\frac{(Q_{15})_i^T + (Q_{15})_i^B}{2}\right] t_i \frac{\partial \alpha_{3i}^D}{\partial \epsilon_x}$$

$$+ \frac{1}{t} \sum_{i=1}^{d+1} \left[- z_{i-1}(Q_{15})_{i-1}^B + z_i (Q_{15})_i^T \right] \frac{\partial \alpha_{5(i+1)}^D}{\partial \epsilon_x} \tag{10}$$

where

$$[Q]_k = \begin{matrix} Q_{11} & Q_{12} & Q_{13} & Q_{14} & Q_{15} & Q_{16} \\ Q_{12} & Q_{22} & Q_{23} & Q_{24} & Q_{25} & Q_{26} \\ Q_{16} & Q_{26} & Q_{36} & Q_{46} & Q_{56} & Q_{66} \end{matrix} \tag{11}$$

and the superscripts T and B represent the plies above and below the delamination, respectively.

For the case where delamination sites are symmetrically located about the laminate midplane and with equal damage, the last term in equation (10) is zero.

Thus,

$$E_x = \frac{1}{n} \sum_{k=1}^{n} (Q_{11})_k (1 - \frac{\partial \alpha_x^M}{\partial \epsilon_x})_k + \frac{1}{t} \sum_{i=1}^{d} [\frac{(Q_{15})_i^T + (Q_{15})_i^B}{2}] \, t_i \, \frac{\partial \alpha_{3i}^D}{\partial \epsilon_x} \qquad (12)$$

Now consider a single delamination site (d=1)

$$E_x = \frac{1}{n} \sum_{k=1}^{n} (Q_{11})_k (1 - \frac{\partial \alpha_x^M}{\partial \epsilon_x})_k + \frac{t_1}{t} \frac{(Q_{15})_1^T + (Q_{15})_1^B}{2} \, \frac{\partial \alpha_3^D}{\partial \epsilon_x} \qquad (13)$$

where $t_1 = 2t_{ply}$ and $t = nt_{ply}$ for all plies having thickness t_{ply}. Finally, it can be shown that

$$\frac{(Q_{15})_1^T + (Q_{15})_1^B}{2} = \frac{(Q_{11}')_1^T + (Q_{11}')_1^B}{2} \qquad (14)$$

where

$$Q_{11}' = Q_{11}\cos^4\theta + 2 (Q_{12} + 2Q_{66}) \sin^2\theta \cos^2\theta + Q_{22}\sin^4\theta \qquad (15)$$

Therefore, E_x reduces to

$$E_x = \frac{1}{n} \sum_{k=1}^{n} (Q_{11})_k (1 - \frac{\partial \alpha_x^M}{\partial \epsilon_x})_k + \frac{1}{n} [(Q_{11}')_1^T + (Q_{11}')_1^B] \, \frac{\partial \alpha_3^D}{\partial \epsilon_x} \qquad (16)$$

If we now consider the energy loss associated with one symmetric delamination site and ignore any energy loss associated with crack interactions, the energy loss in the local volume is given by

$$u_L^C = I_{16}^D \, \epsilon_{L1} \, \alpha_{L6}^D + H.O.T. \qquad (17)$$

10

Neglecting the higher order terms as was done in the original constitutive model formulation [1,2], the local energy loss may be expressed in laminate form as

$$u_L^C = I_{16}^D \epsilon_x \, \alpha_3^D \qquad (18)$$

where

$$I_{16}^D = \frac{1}{n} \, [(\bar{Q}_{15})_1^T + (\bar{Q}_{15})_1^B] \qquad (19)$$

By restricting the energy loss to that associated with crack creation during loadup, we may use fracture mechanics concepts to express the local energy loss as follows

$$u_L^C = - \frac{1}{V_L} \int_{S_D} G_D dS \qquad (20)$$

where V_L is given by tS, t is the laminate thickness, S is the total area of the interface, S_D is the delaminated area ($S_D < S$), and G_D is the delamination strain energy release rate. Equating these two expressions for u_L^C yields the following general expression for the delamination ISV

$$\alpha_3^D = - \frac{1}{I_{16}^D \, t \, S \, \epsilon_x} \int_{S_D} G_D dS \qquad (21)$$

We now need an expression for the strain energy release rate of delamination. As a first approximation we will use O'Brien's strain energy release rate model [13] which was developed for free edge delaminations. This model has the advantage of accounting for both the laminate stacking sequence and the delamination site(s) without requiring laminate specific experimental data. The strain energy release rate is given by

$$G_D = \frac{\epsilon_x^2 t}{2} (E_{LAM} - E^*) \qquad (22)$$

11

where E_{LAM} is equivalent to E_x, t is the laminate thickness, d is the number of sublaminates formed by delamination(s), E_i equals E_x for the ith sublaminate, t_i is the thickness of the ith sublaminate, and

$$E^* = \frac{1}{t} \sum_{i=1}^{d} E_i t_i \tag{23}$$

Since G_D is assumed to be constant in S in the previous expression, α_3^D reduces to

$$\alpha_3^D = - \frac{1}{I_{16}^D t \, \epsilon_x} \left[\frac{\epsilon_x^2 t}{2} (E_x - E^*) \right] \frac{S_D}{S} \tag{24}$$

Substituting for I_{16}^D and rearranging gives

$$\alpha_3^D = - \frac{n}{2} \epsilon_x \frac{(E_x - E^*)}{[(\overline{Q}_{15})_1^T + (\overline{Q}_{15})_1^B]} \left(\frac{S_D}{S} \right) \tag{25}$$

or

$$\frac{\partial \alpha_3^D}{\partial \epsilon_x} = - \frac{n}{2} \frac{(E_x - E^*)}{[(\overline{Q}_{15})_1^T + (\overline{Q}_{15})_1^B]} \left(\frac{S_D}{S} \right) \tag{26}$$

Now substituting expression (26) into (16) yields

$$E_x = \frac{1}{n} \sum_{k=1}^{n} (Q_{11})_k (1 - \frac{\partial \alpha_x^M}{\partial \epsilon_x})_k - \frac{1}{2} (E_x - E^*)(\frac{S_D}{S}) \tag{27}$$

By dividing by the initial undamaged modulus, E_{xo}, we obtain the following expression for combined matrix cracking and delaminations:

12

$$\frac{E_x}{E_{xo}} = 1 - \frac{1}{nE_{xo}} \sum_{k=1}^{n} (Q_{11})_k \left(\frac{\partial \alpha_x^M}{\partial \epsilon_x}\right)_k - \frac{1}{2}\left(1 - \frac{E^*}{E_{xo}}\right)\left(\frac{S_D}{S}\right) \tag{28}$$

This expression is valid for the following case: 1) A symmetric, balanced laminate; 2) two delamination sites located symmetric with respect to the laminate midplane with equal damage at each interface; 3) the strain energy release rate is not a function of the delamination surface area; 4) there are no energy losses associated with crack interaction; and 5) the ISV's are linear in strain (ϵ_x) on unloading and subsequent reloading prior to new damage formation.

An expression for the ISV for matrix cracking was previously developed in reference 2. For matrix crack damage in a single 90° ply,

$$\frac{\partial \alpha_x^M}{\partial \epsilon_x} = \frac{1}{2} n \frac{(p+q)}{q} \frac{E_{xo}}{I_{22}'} \left(\frac{E_{x1}}{E_{xo}}\bigg|_{S_{M_1}} - 1\right) \tag{29}$$

where n is the number of consecutive 90° plies in the 90° layer, p is the number of 0° plies, q is the number of 90° plies in the laminate, E_{x1}/E_{xo} was determined experimentally for the $[0,90,0]_s$ laminate containing a single 90° layer, and S_{M_1} is the matrix crack surface area at time t_1.

Equations (26) and (29) provide quantitative values of the ISV for delaminations and matrix cracks, respectively, and require only the value of the current damage state, S_D and S_{M_1}. Equation (28) may then be used to predict the damage-dependent loading-direction modulus of the laminate at the current damage state. The mathematical expressions explicitly account for the effects of laminate stacking sequence, relative matrix crack damage in each ply, and the delamination interface site. Aside from the standard laminate analysis material constants, the damage model only requires the experimental

13

determination of the current damage state. (Research is currently underway to establish ISV damage growth laws which will predict the values of the ISV's directly from the loading history of the material.)

4. Comparison of Model Predictions to Experimental Results

The suitability of the above damage-dependent laminate analysis equations must be assessed by comparing displacements predicted by the damage model to experimentally measured values. This is accomplished herein by comparing model predictions to the damage-degraded engineering modulus, E_x, of several laminates determined from tensile coupon tests. A limited number of test results have been obtained for AS4/3502 graphite/epoxy laminates with a quasi-isotropic and several cross-ply stacking sequences. The combined matrix cracking and delamination damage modes were generated by tension-tension fatigue loading (R=0.1) at 2 Hz and the engineering modulus of the laminate was measured by a 1.0 in. extensometer.

A comparison of the model prediction of E_x to experimental results is presented in Table 1 for $[0_2/90_2]_s$, $[0/90_3]_s$ cross-ply laminates, and for $[0/\pm45/90]_s$ and $[90/\pm45/0]_s$ quasi-isotropic laminates. The damage degraded modulus has been normalized by the initial undamaged modulus. X-ray radiographs of the combined-mode damage state are shown in Figs. 5 through 8 for the laminates listed in Table 1. The comparison between the theoretical and experimental results is quite good. While this is a very limited comparison, the results are very encouraging because the stiffness loss in the cross-ply laminates is primarily due to matrix cracking, whereas the stiffness loss in the quasi-isotropic laminates is primarily due to the

14

delaminations.

5. Summary and Conclusions

The authors have constructed a continuum damage model for laminated continuous fiber composites. This model utilizes second order tensor-valued internal state variables to account for both matrix cracking and delamination at the sub-laminate level in such a way as to produce a stacking sequence independent model. The input properties may be obtained from a single [0,90,0] specimen.

The model has thus far been shown to be accurate in predicting both in-plane and out-of-plane stiffness loss in crossply specimens with both vertical and curved matrix cracks. Efforts are currently underway to compare model stiffness predictions to experiment for quasi-isotropic laminates with both matrix cracks and delaminations. The initial comparisons are quite encouraging. Research is also underway to develop stacking sequence independent ISV growth laws for matrix cracking and delaminations.

The ultimate goal of this research is to develop a model capable of predicting failure of a component subjected to loads resulting in stress gradients. Toward this end, it is believed by these authors that the essential ingredients are now in place for constructing a failure function which describes fiber fracture as a function of matrix cracking and delamination.

6. Acknowledgement

7. References

1 Allen, D.H., Groves, S.E., and Harris, C.E., "A Thermomechanical Constitutive Theory for Elastic Composites with Distributed Damage - Part I: Theoretical Development," Texas A&M University Mechanics and Materials Center, MM 5023-85-17, October, 1985.

2 Allen, D.H., Harris, C.E., and Groves, S.E., "A Thermomechanical Constitutive Theory for Elastic Composites with Distributed Damage - Part II: Application to Matrix Cracking in Laminated Composites," Texas A&M University Mechanics and Materials Center, MM 5023-85-15, October, 1985.

3 Allen, D.H., Groves, S.E., and Harris, C.E., "A Cumulative Damage Model for Continuous Fiber Composite Laminates with Matrix Cracking and Interply Delaminations," to appear in Composite Materials Testing and Design, 8th Symposium, ASTM STP, American Society for Testing and Materials, Philadelphia, 1987.

4 Allen, D.H., Harris, C.E., Groves, S.E., and Norvell, R.G., "Characteristics of Stiffness Loss in Crossply Laminates with Curved Matrix Cracks," to appear in Journal of Composite Materials, 1987.

5 Bazant, Z.P., "Mechanics of Distributed Cracking," Applied Mechanics Reviews, Vol. 39, pp. 675-705, 1986.

6 Georgiou, I.T., "Initiation Mechanisms and Fatigue Growth of Internal Delaminations in Graphite/Epoxy Cross-Ply Laminates," Texas A&M University Thesis, December, 1986.

7 Jamison, R.D., Schulte, K., Reifsnider, K.L., and Stinchcomb, W.W., "Characterization and Analysis of Damage Mechanisms in Tension-Tension Fatigue of Graphite/Epoxy Laminates," Effects of Defects in Composite Materials, ASTM STP 836, American Society for Testing and Materials, 1984, pp. 21-55.

8 Kachanov, L.M., "On the Creep Fracture Time," Izv. AN SSR, Otd. Tekhn. Nauk; No. 8, pp. 26-31, 1958 (in Russian).

9 Kachanov, L.M., Introduction to Continuum Damage Mechanics, Martinus Nijhoff, Dordrecht, 1986.

10 Kachanov, M.L., "Continuum Model of Medium with Cracks," Mekhanika Tverdogo Tela, Izv. AN SSSR, Vol. 7, pp. 54-59, 1972.

11 Krajcinovic, D., "Continuum Damage Mechanics," Applied Mechanics Reviews, Vol. 37, pp. 1-6, 1984.

12 Krajcinovic, D., "Update to Continuum Damage Mechanics," Applied Mechanics Update 1986, Steele, C.R., and Springer, G.S., Eds., The American Society of Mechanical Engineers, pp. 403-406, 1986.
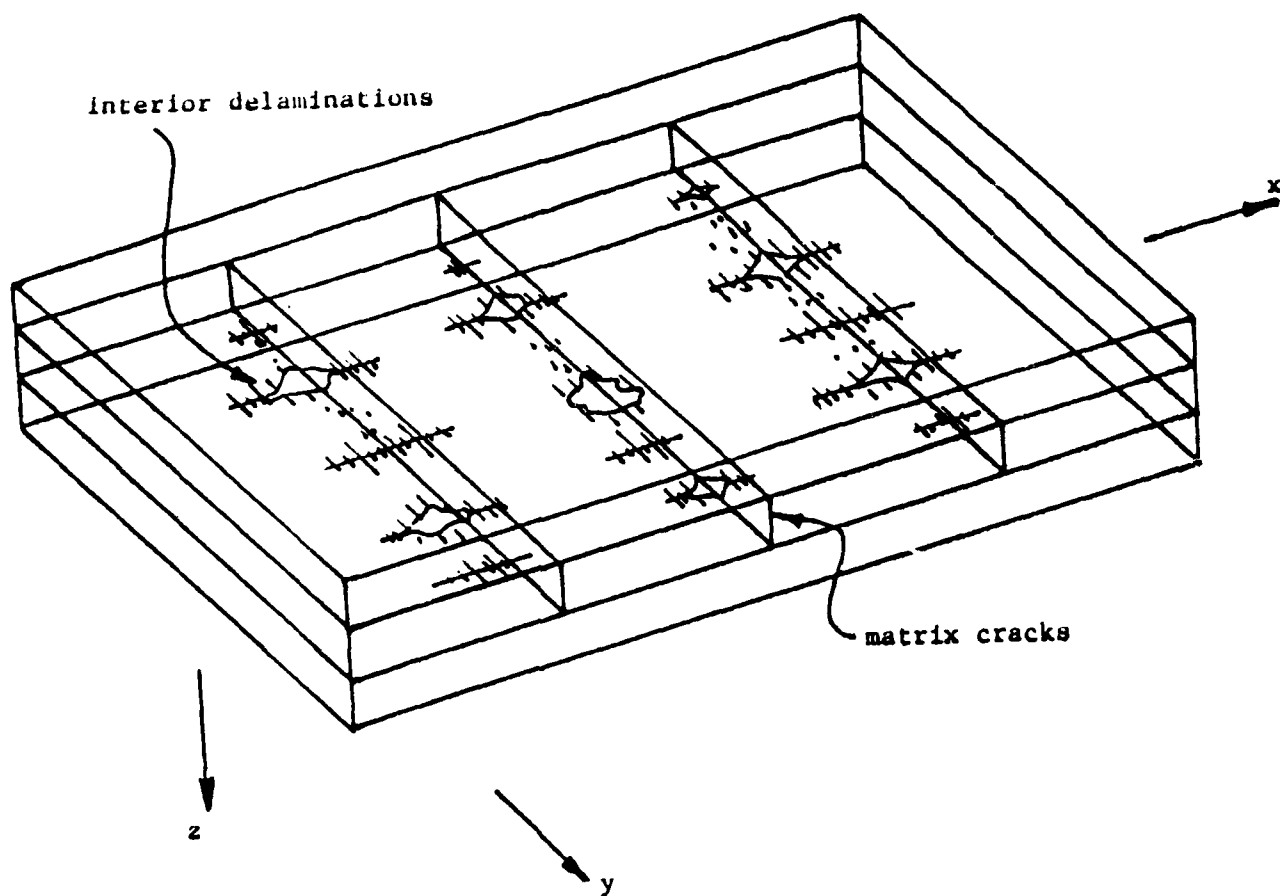
16

13 O'Brien, T.K., "Characterization of Delamination Onset and Growth in a Composite Laminate," Damage in Composite Materials, K.L. Reifsnider, Ed., ASTM STP 775, American Society for Testing and Materials, Philadelphia, pp. 141-167, 1982.

14 Onsager, L.,"Reciprocal Relations in Irreversible Process I.," Physics Review, Vo. 37, pp. 405-426, 1931.

15 Rabotnov, Y.N., Creep Problems in Structural Members, North-Holland, Amsterdam, 1969.

16 Talreja, R., "A Continuum Mechanics Characterization of Damage in Composite Materials," Proc. R. Soc. London, Vol. 399A, 1985, pp. 195-216.

17 Talreja, R., "Residual Stiffness Properties of Cracked Composite Laminates," Advances in Fracture Research, Proc. Sixth Int. Conf. de Fracture, New Delhi, India, Vol. 4, pp. 3013-3019, 1985.

18 Talreja, R., "Transverse Cracking and Stiffness Reduction in Composite Laminates," Journal of Composite Materials, Vol. 21, pp. 355-375, 1985.

19 Talreja, R., Fatigue of Composite Materials, Technical University of Denmark, Lyngby, Denmark, 1985.

20 Talreja, R., "Stiffness Properties of Composite Laminates with Matrix Cracking and Interior Delamination," Danish Center for Applied Mathematics and Mechanics, The Technical University of Denmark, No. 321, March, 1986.

21 Weitsman, Y., "Environmentally Induced Damage in Composites," Proceedings of the 5th Symposium on Continuum Modeling of Discrete Structures, A.J.M. Spencer, Ed., Nottingham, U.K., 1985.
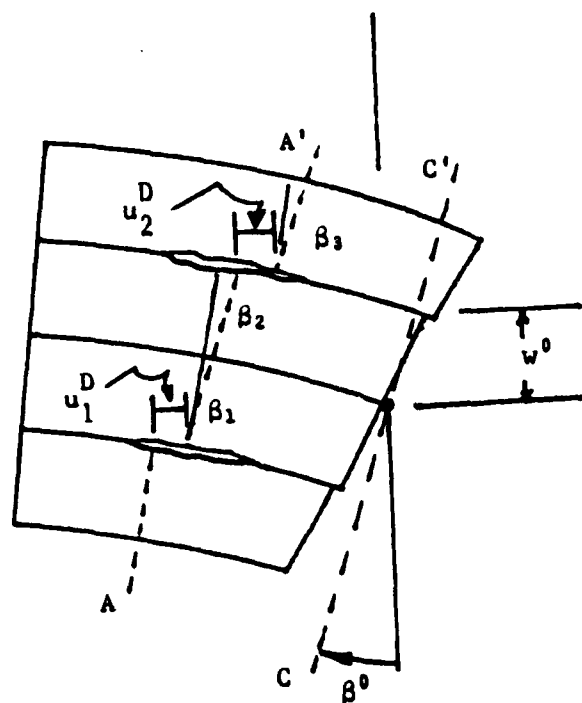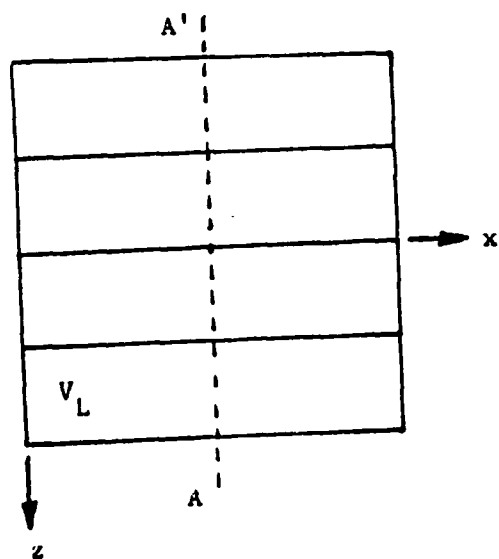
Table 2 Comparison of Model Predictions to Experimental Results
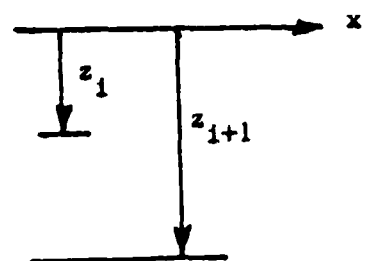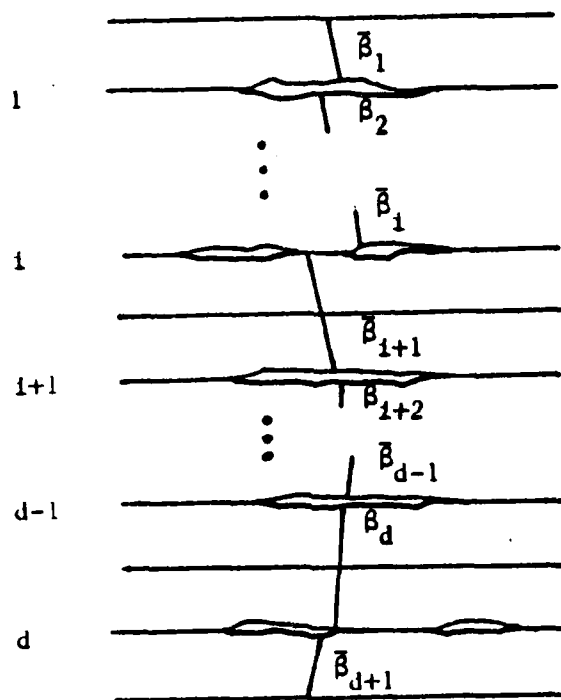with Matrix Cracks and Delaminations

LAMINATE STACKING SEQUENCE	$[0_2/90_2]_s$	$[0/90_3]_s$	$[0/\pm45/90]_s$	$[90/\pm45/0]_s$
NUMBER OF CRACKS PER INCH IN 90° LAYER	54	38	44	18
DELAMINATION INTERFACE	0/90	0/90	-45/90	+45/-45
PERCENT DELAMINATION	47.3	17.2	57.0	52.0
$\dfrac{E_x}{E_{x_o}}$ EXPERIMENTAL	0.949	0.910	0.888	0.860
$\dfrac{E_x}{E_{x_o}}$ MODEL PREDICTION	0.939	0.918	0.878	0.863

LIST OF FIGURE CAPTIONS

interior delaminations

matrix cracks

x

z

y

fibers

n_z

S_{21}^T

S_1

t_1

S_{21}^B

x

z

y

$[a_2/90_2]_3$
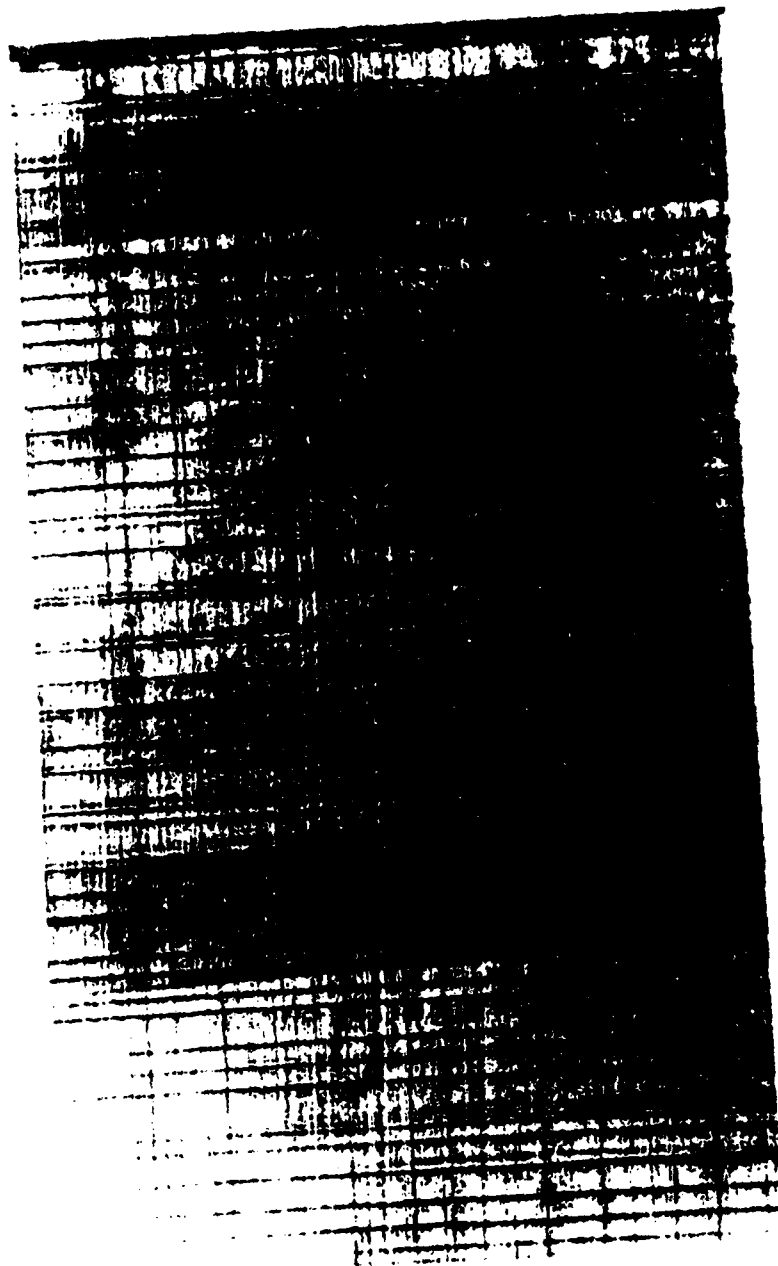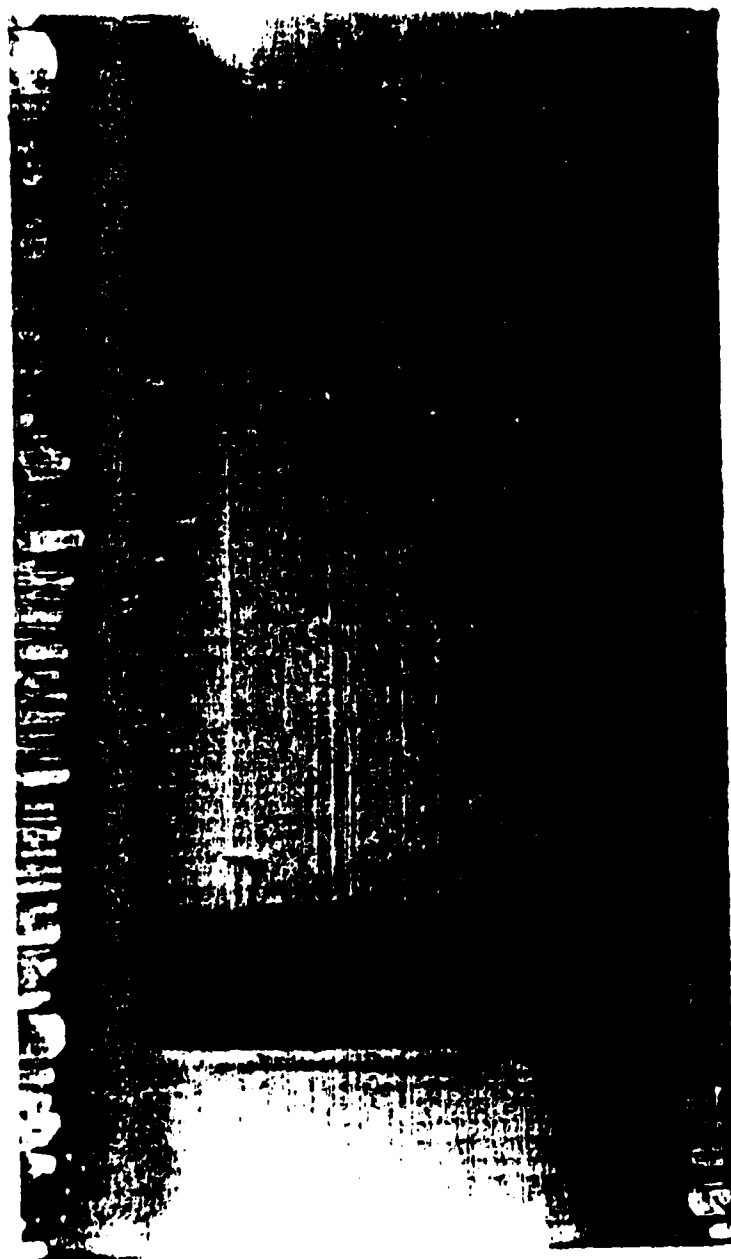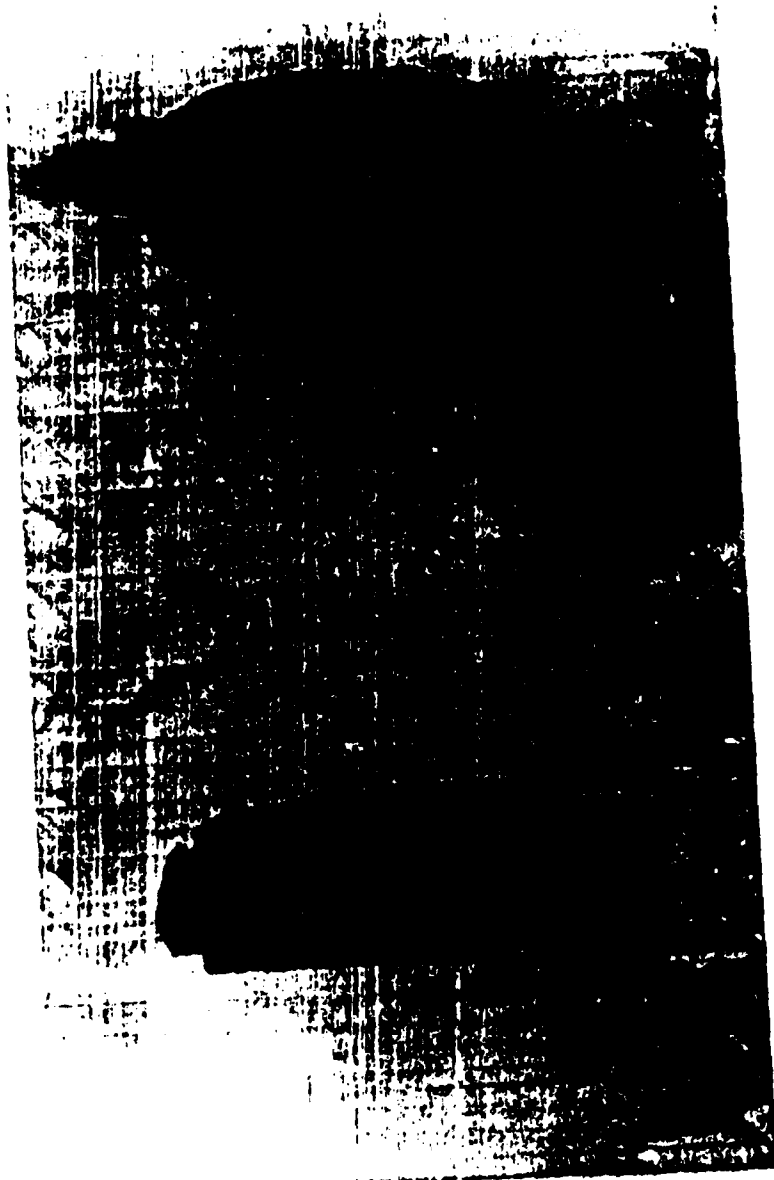
[.0/90.]ₛ

$[0/\pm 45/0]_s$

Appendix 7.7

DAMAGE-INDUCED CHANGES IN THE POISSON'S RATIO OF
CROSS-PLY LAMINATES: AN APPLICATION OF A CONTINUUM
DAMAGE MECHANICS MODEL FOR LAMINATED COMPOSITES

by

C.E. Harris
D.H. Allen
E.W. Nottorf

Aerospace Engineering Department
Texas A&M University
College Station, Texas   77843

Damage-Induced Changes in the Poisson's Ratio of Cross-Ply Laminates
An Application of a Continuum Damage Mechanics Model for Laminated Composites

by

Charles E. Harris
David H. Allen
Eric W. Nottorf

Aerospace Engineering Department
Texas A&M University
College Station, Texas 77843

ABSTRACT

A damage-dependent constitutive model for laminated composites has been developed for the combined damage modes of matrix cracks and delaminations. The model is based on the concept of continuum damage mechanics and uses second-order tensor valued internal state variables to represent each mode of damage. The internal state variables are defined as the local volume average of the relative crack face displacements. Since the local volume for delaminations is specified at the laminate level, the constitutive model takes the form of laminate analysis equations modified by the internal state variables. Model implementation is demonstrated for E_x and ν_{xy} of quasi-isotropic and cross-ply laminates. The model predictions are in close agreement to experimental results obtained for graphite/epoxy laminates.

INTRODUCTION

It is a well established fact that composite material systems develop extensive patterns of microstructural damage as a result of mechanical or environmental load history. Many composite structures are damage tolerant because they retain load-carrying capacity and structural integrity after the development of microstructural damage. The physical properties of the material system are altered by the damage and, furthermore, the development of the damage is a precursor to structural failure. Using the concept of continuum damage mechanics, the authors have developed a constitutive model for fiber-reinforced laminated composites which includes the influence of microstructural damage on the stress-strain behavior of a composite structure. The influence of the combined damage modes of matrix cracking and delamination on the laminate engineering modulus, E_x, and Poisson's ratio, ν_{xy}, is the subject of this paper.

The first application of continuum mechanics is attributed to L.M. Kachanov [1]. In this method it is recognized that the exact analysis of a multiply connected domain with numerous microcracks is hopelessly complex. Therefore, the effects of these microcracks on macrophysical response are reflected via one or more internal state variables [2] called damage parameters. The initial use of damage mechanics appears to have been a logical one. It was observed that in metals classical plasticity theory breaks down when significant grain boundary sliding and/or macrocavitation occur because the initial elastic properties are not observed on unloading [3]. In the last twenty years there has been an incredible expansion of research in damage mechanics, as evidenced by two recent review articles [4,5,6] and the publication of the first textbook devoted entirely to damage mechanics [7]. Although substantial research has been performed on metals, concrete, and geologic media, as pointed out in reference 12, very little research has been detailed on laminated composite media. In fact, to these authors' knowledge, only three concerted efforts have reached the open literature at the time of this writing. These are due to Talreja [8-12], Allen, et al. [13-16], and Weitsman [17].

The authors have developed a model for predicting the constitutive behavior of laminated continuous fiber composites [13-16]. This model utilizes the concept of continuum damage mechanics. The effects of microcracks are reflected via internal state variables (ISV's) in the constitutive equations, rather than treating each microcrack as a separate internal boundary. Furthermore, the model is phenomenological because only the average macroscale effect of microcracking is modelled rather than the effect of each individual crack. Because cracking is not statistically homogeneous in the coordinate direction normal to the laminate, statistical weighting is necessary in this direction, and this is accomplished via kinematic constraints.

1

Therefore, the constitutive equations are laminate equations, rather than standard stress-strain equations.

The objective of this research effort is to extend the model to predict the response of laminates with both matrix cracks and interior delaminations [15], as shown in Fig. 1. This problem is complicated by two factors. First, because these two damage mechanisms are oriented differently, they require two separate tensor-valued damage parameters. Furthermore, the mechanics of these two damage modes are substantially different. The matrix cracks may be assumed to be statistically homogeneous over each ply in a small local volume element. Therefore, classical local volume averaging may be used to obtain this damage parameter. On the other hand, delaminations are not statistically homogeneous in the z coordinate direction. This requires that a modification be made to statistical averaging techniques. Although statistical homogeneity is assumed in the x and y directions, a kinematic constraint similar to the Kirchhoff-Love hypothesis is applied in the z direction. The resulting damage parameter is a weighted measure of damage, with delaminations away from the neutral surface causing a greater effect on laminate properties.
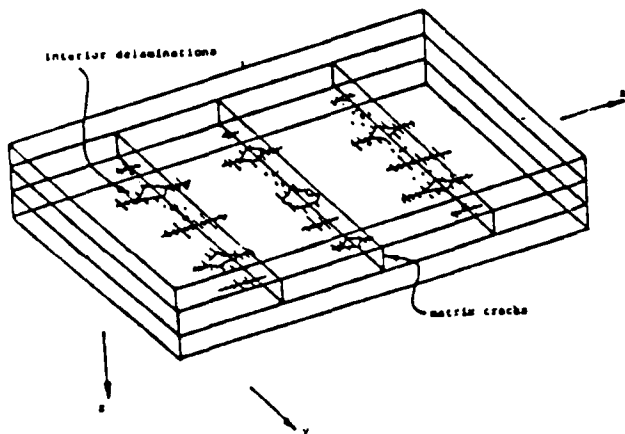
MODEL DEVELOPMENT

The model development proceeds from the assumption that all material inelasticity is contained within small zones surrounding the microcracks. The effect of matrix cracks on ply level constitutive equations is accounted for via the local volume average of the diadic product of the crack opening displacement vector u_i^C and the crack face normal n_j^C :

$$\alpha_{ij}^M = \frac{1}{V_L} \int_{S_C} u_i^C n_j^C \, ds \qquad (1)$$

where V_L is the local volume for which cracking can be considered statistically homogeneous, and S_C is the surface area of cracks in V_L. For matrix cracking, V_L is typically one ply in thickness. The ply level stress-strain relations are therefore given by

$$\sigma_{ij} = C_{ijk\ell}(\epsilon_{k\ell} - \alpha_{k\ell}^M) \qquad (2)$$

In order to account for interply delamination the following kinematic assumption is made (See Fig. 2):

$$u(x,y,z) = u^0(x,y) - z[\beta^0 + H(z-z_k)\alpha_k^D]$$
$$+ H(z-z_k)u_k^D \qquad (3)$$

$$v(x,y,z) = v^0(x,y) - z[\psi^0 + H(z-z_k)\psi_k^D]$$
$$+ H(z-z_k)v_k^D \qquad (4)$$

and

$$w(x,y,z) = w^0(x,y) - H(z-z_k)w_k^D \qquad (5)$$

where u and v are components of the in-plane displacement and w is the out-of-plane displacement and H is the Heavyside step function. Furthermore, β and ψ represent rotations of the midplane. The quantities with superscripts o are undamaged midsurface values, and quantities with superscripts D are caused by interlaminar cracking.

Employing standard laminate averaging techniques will result in the following laminate equations [15]

$$\{N\} = \sum_{k=1}^{n} [Q]_k (z_k - z_{k-1}) \{\epsilon_L^0\}$$

$$- \frac{1}{2} \sum_{k=1}^{n} [Q]_k (z_k^2 - z_{k-1}^2) \{\kappa_L\}$$

$$+ \sum_{i=1}^{d} [\bar{Q}_1]_i \, t_i \begin{Bmatrix} 0 \\ 0 \\ \alpha_{11}^D \\ 0 \\ \alpha_{21}^D \\ 0 \\ \alpha_{31}^D \\ 0 \end{Bmatrix}$$

$$+ \sum_{i=1}^{d+1} (z_i - z_{i-1}) [\bar{Q}_2]_i \begin{Bmatrix} 0 \\ 0 \\ 0 \\ 0 \\ u_{4i}^D \\ u_{5i}^D \\ 0 \end{Bmatrix}$$

$$- \sum_{k=1}^{n} [Q]_k (z_k - z_{k-1}) \{\alpha^M\}_k \qquad (6)$$

Fig. 2 Deformation Geometry for Region A_L

$$\{N\} = \frac{1}{2} \sum_{k=1}^{n} |Q|_k \ (z_k^2 - z_{k-1}^2) \ \{\epsilon_L^0\}$$

$$- \frac{1}{3} \sum_{k=1}^{n} |Q|_k (z_k^3 - z_{k-1}^3) \ \{\kappa_L\}$$

$$+ \sum_{i=1}^{d} |\bar{Q}_3|_i \ t_i^2 \begin{Bmatrix} 0 \\ 0 \\ 0 \\ a_{11}^D \\ a_{21}^D \\ a_{3i}^D \\ 0 \end{Bmatrix}$$

$$+ \sum_{i=1}^{d+1} |\bar{Q}_4|_i (z_i^2 - z_{i-1}^2) \begin{Bmatrix} 0 \\ 0 \\ 0 \\ a_{41}^D \\ a_{51}^D \\ 0 \end{Bmatrix}$$

$$- \frac{1}{2} \sum_{k=1}^{n} |Q|_k \ (z_k^2 - z_{k-1}^2) \ \{a^M\}_k \qquad (7)$$

where $\{N\}$ and $\{M\}$ are the resultant forces and moments per unit length, respectively, and $\{a^M\}_k$ and $\{a_L^D\}$ represent the damage due to matrix cracking and interply delamination, respectively. Furthermore, n is the number of plies, and d is the number of delaminated ply interfaces, as shown in Fig. 3.

The internal state variable for delamination, $\{a_L^D\}$, is obtained by employing the divergence theorem on a local volume element of the laminate. The resulting procedure gives [15]

$$a_{11}^D = \frac{2}{V_{Li}} \int_{S_{2i}} w_i^D n_2 dS \qquad (8a)$$

$$a_{21}^D = \frac{2}{V_{Li}} \int_{S_{2i}} v_i^D n_2 dS \qquad (8b)$$

$$a_{3i}^D = \frac{2}{V_{Li}} \int_{S_{2i}} u_i^D n_2 dS \qquad (8c)$$

$$a_{41}^D = \frac{1}{A_L} \int_{S_{2i}^B} v_i^D n_2 dS \qquad (8d)$$

$$a_{5i}^D = \frac{1}{A_L} \int_{S_{2i}^B} \beta_i^D n_2 dS \qquad (8e)$$

where the subscript i is associated with the ith delaminated ply interface. Furthermore, V_{Li} is equivalent to t_iA_L, where t_i is the thickness of the two plies above and below the delamination, as shown in Fig. 4.
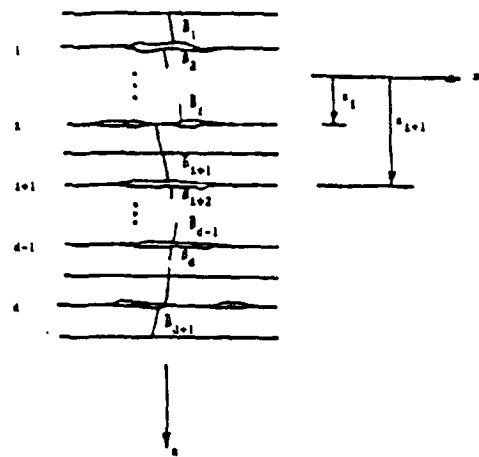

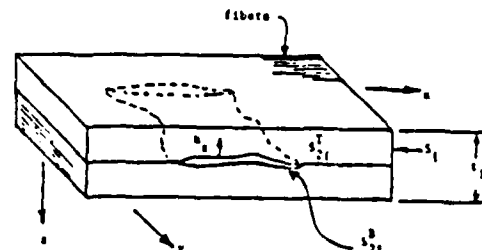Fig. 3 Schematic of Delaminated Region in a Composite Layup

Fig. 4 Interply Delamination in a Laminated Continuous Fiber Composite

3

Furthermore, the matrices $|Q|$ with subscripts k are the standard elastic property matrices for the undamaged plies. The matrices $|\bar{Q}|$ with subscripts i apply to the ith delaminated ply interface. They represent average properties of the plies above and below the delamination. These are described in further detail in reference 18.

DETERMINATION OF E_x and ν_{xy} FOR THE MIXED DAMAGE MODEL

Suppose that one is interested in modeling stiffness loss as a function of damage state. In order to do this, it is necessary to construct the (stacking sequence independent) material parameters developed in the previous section. The loading direction engineering modulus, E_x, and Poisson's ratio, ν_{xy}, of the laminate are defined as

$$E_x = \frac{1}{t} \frac{\partial N_x}{\partial c_x} \qquad (9)$$

$$\nu_{xy} = \frac{\frac{1}{t} \frac{\partial N_x}{\partial c_y}}{\frac{1}{t} \frac{\partial N_y}{\partial c_y}} \qquad (10)$$

where t is the laminate thickness.

For the purpose of comparing the model predictions to experimental results, we will confine this development to the case of a symmetric, balanced laminate with delamination sites located symmetrically with respect to the laminate midplane. For this special case, $(\kappa)=0$ and the fourth term in equation (6) is zero. Furthermore, $a_{11}^0 = 0$ and the third term in equation (6) is the same for both delamination sites. Substituting equation (6) into equations (9) and (10) results in the following expressions for E_x and ν_{xy}

$$E_x = \frac{1}{n} \sum_{k=1}^{n} (Q_{11})_k (1 - \frac{\partial u_x^M}{\partial c_x})_k$$
$$+ 2(\frac{2}{n}) (\bar{Q}_{14} \frac{\partial u_2^0}{\partial c_x} + \bar{Q}_{15} \frac{\partial a_3^0}{\partial c_x}) \qquad (11)$$

$$\nu_{xy} = \frac{\frac{1}{n} \sum_{k=1}^{n} (Q_{12})_k (1 - \frac{\partial u_x^M}{\partial c_y})_k + 2(\frac{2}{n})(\bar{Q}_{14} \frac{\partial a_2^0}{\partial c_y} + \bar{Q}_{15} \frac{\partial a_3^0}{\partial c_y})}{\frac{1}{n} \sum_{k=1}^{n} (Q_{22})_k (1 - \frac{\partial u_y^M}{\partial c_y})_k + 2(\frac{2}{n})(\bar{Q}_{24} \frac{\partial a_2^0}{\partial c_y} + \bar{Q}_{25} \frac{\partial u_3^0}{\partial c_y})} \qquad (12)$$

where it is assumed that all plies have the same thickness so that

$$z_k - z_{k-1} = t_{ply} \qquad (13a)$$

$$\frac{t_{ply}}{t} = \frac{1}{n} \qquad (13b)$$

$$\frac{t_1}{t} = \frac{2}{n} \qquad (13c)$$

furthermore, damage introduces local anisotropy so that

$$|Q|_k = \begin{vmatrix} Q_{11} & Q_{12} & Q_{13} & Q_{14} & Q_{15} & Q_{16} \\ Q_{12} & Q_{22} & Q_{23} & Q_{24} & Q_{25} & Q_{26} \\ Q_{16} & Q_{26} & Q_{36} & Q_{46} & Q_{56} & Q_{66} \end{vmatrix} \qquad (14)$$

It has been previously shown $|18|$ that

$$\bar{Q}_{14} = \frac{1}{2}(\bar{Q}_{12}^A + \bar{Q}_{12}^B) \qquad (15)$$

$$\bar{Q}_{15} = \frac{1}{2}(\bar{Q}_{11}^A + \bar{Q}_{11}^B) \qquad (16)$$

$$\bar{Q}_{24} = \frac{1}{2}(\bar{Q}_{22}^A + \bar{Q}_{22}^B) \qquad (17)$$

$$\bar{Q}_{25} = \frac{1}{2}(\bar{Q}_{12}^A + \bar{Q}_{12}^B) \qquad (18)$$

where the superscripts A and B designate the properties of the ply immediately above and below the delamination, respectively.

DETERMINATION OF INTERNAL STATE VARIABLES

Implementation of equations (11) and (12) to predict the damage degraded laminate moduli requires the specification of the partial derivatives of the internal state variables with respect to strain for a given damage state. In the absence of growth laws, the damage state must be determined experimentally. Expressions for the internal state variables have been previously developed by the authors [14,15] by employing energy principles. In the original constitutive theory formulation [13] the local energy loss contribution to the Helmholtz free energy is directly related to the internal state variables. Furthermore, the local energy loss is also directly related to the fracture mechanics based strain energy release rate for crack creation during load-up. Therefore, expressions for the internal state variables have been developed from expressions for the strain energy release rate for each damage mode. In the case of matrix cracking in cross-ply laminates,

$$\frac{\partial u_x^M}{\partial c_x} = \frac{1}{2} m \frac{(p+q)}{q} \frac{E_{x_0}}{E_{22}} (\frac{E_{x_1}}{E_{x_0}} \Big|_{S_{M_1}} - 1) \qquad (19)$$

where m is the number of consecutive 90° plies, p is the number of 0° plies, q is the number of 90° plies, E_{x_0} is the initial undamaged modulus, and E_{x_1} is the damage-degraded modulus corresponding to matrix crack damage state S_{M_1}. The term in the parenthesis was determined experimentally from tests on a $[0/90/0]_s$ laminate and is given by

$$\frac{E_{x_1}}{E_{x_0}} \Big|_S = 0.99969 - 0.061607 \, S + 0.04623 \, S^2 \qquad (20)$$

4

Finite element studies have shown that the effects of adjacent layer constraint on the energy released by the 90° layers is a second order effect [19]. Therefore, by using the following second order tensor transformation [19] law

$$\frac{\partial \omega^M_{ij}}{\partial \epsilon^0_{mn}} = a_{ip} \, a_{jp} \, a_{mr} \, a_{ns} \, \frac{\partial \omega^M_{pq}}{\partial \epsilon^0_{rs}} \qquad (21)$$

where the unbarred quantities are in the crack coordinate system and the barred quantities are in the laminate coordinate system, equation (19) is generally applicable to matrix crack damage in any ply of any laminate stacking sequence.

The delamination internal state variable was determined from energy principles as well, except O'Brien's [20] strain energy release rate model was used rather than experimental results. Since O'Brien's model assumes that the strain energy release is independent of the size of the delamination, the internal state variable is linear in delamination surface area. Therefore,

$$\frac{\partial \omega^D_3}{\partial \epsilon_x} = -\frac{n}{2} \frac{(E_{x_0} - E^*)}{\bar{Q}_{15}} \left(\frac{S_0}{S}\right) \qquad (22)$$

where n is the number of plies in the laminate, S_0 is the delamination area and S is the total interfacial area in the local volume. E^* is the modulus of the sublaminates formed by the delamination and is given by

$$E^* = \frac{1}{t} \sum_{i=1}^{d} E_i t_i \qquad (23)$$

where d is the number of sublaminates and t is the laminate thickness. By similar reasoning,

$$\frac{\partial \omega^D_2}{\partial \epsilon_y} = -\frac{n}{2} \frac{(E_{y_0} - E^*)}{\bar{Q}_{24}} \left(\frac{S_0}{S}\right) \qquad (24)$$

Finally, as a first approximation for the cross-derivatives in equations (11), we assume that

$$\frac{\partial \omega^M_x}{\partial \epsilon_y} = \frac{S_{12}}{S_{22}} \frac{\partial \omega^M_x}{\partial \epsilon_x} \qquad (25)$$

$$\frac{\partial \omega^D_3}{\partial \epsilon_y} = \frac{S_{12}}{S_{22}} \frac{\partial \omega^D_3}{\partial \epsilon_x} \qquad (26)$$

$$\frac{\partial \omega^D_2}{\partial \epsilon_x} = \frac{S_{12}}{S_{11}} \frac{\partial \omega^D_3}{\partial \epsilon_x} \qquad (27)$$

where S_{ij} is defined by the following undamaged laminate stress-strain relationships using the first term of equation (6)

$$S_{11} = \frac{1}{t} \frac{\partial N_x}{\partial \epsilon_x} \qquad (28)$$

$$S_{22} = \frac{1}{t} \frac{\partial N_y}{\partial \epsilon_y} \qquad (29)$$

$$S_{12} = \frac{1}{t} \frac{\partial N_x}{\partial \epsilon_y} \qquad (30)$$

Consider the case of cross-ply laminates where the delamination site is at a 0/90 interface. Equations (11) and (12) reduce to the following simplified forms

$$E_x = E_{x_0} \left[1 - \frac{1}{nE_{x_0}} \sum_{k=1}^{n} (Q_{11})_k \left(\frac{\partial \omega^M_x}{\partial \epsilon_x}\right)_k \right.$$
$$\left. - \frac{1}{2} \left(1 - \frac{E^*}{E_{x_0}}\right) \left(\frac{S_0}{S}\right) \right] \qquad (31)$$

$$\nu_{xy} = \nu_{xy_0} \left[1 - 2\left(\frac{p}{n} \frac{E_{22}}{E_{11} + E_{22}} \right. \right.$$
$$\left. \left. + \frac{q}{n}\right) \left(\frac{S_0}{S}\right) \right] \qquad (32)$$

where E_{11}, E_{12} and ν_{12} are the standard lamina properties.

EXPERIMENTAL PROGRAM

A limited experimental program has been conducted to verify the accuracy of the constitutive model formulation. Experimental tests have been conducted on tensile specimens from a number of quasi-isotropic and cross-ply laminates. The material system is AS4/3502 graphite/epoxy with $E_{11}=21.0\times10^6$psi (144.8 GPa), $E_{22}=1.39\times10^6$psi (9.58 GPa), $\nu_{12}=0.310$ and $G_{12}=0.694\times10^6$psi (4.79 GPa). The fiber volume fraction is approximately 65% and the per ply thickness is 0.0055 in. (0.132 mm). The loading-direction modulus and Poisson's ratio were measured by a biaxial extensometer with a 1 in. gage length. Damage was developed under tension-tension fatigue at 2Hz and R=0.1. The progression of damage was documented by periodic examinations by x-ray radiography and edge replication. Modulus measurements were taken at each examination.

COMPARISON OF EXPERIMENTAL RESULTS TO MODEL PREDICTIONS

The comparison of model predictions to experimental results for E_x and ν_{xy} are displayed in graphical form in the bar charts of Figs. 5 and 6, respectively. Matrix cracks in the 90° layers are at the saturation damage state for all laminates. The delamination interface location and percent of delamination is listed under the laminate stacking sequences in the bar charts. It
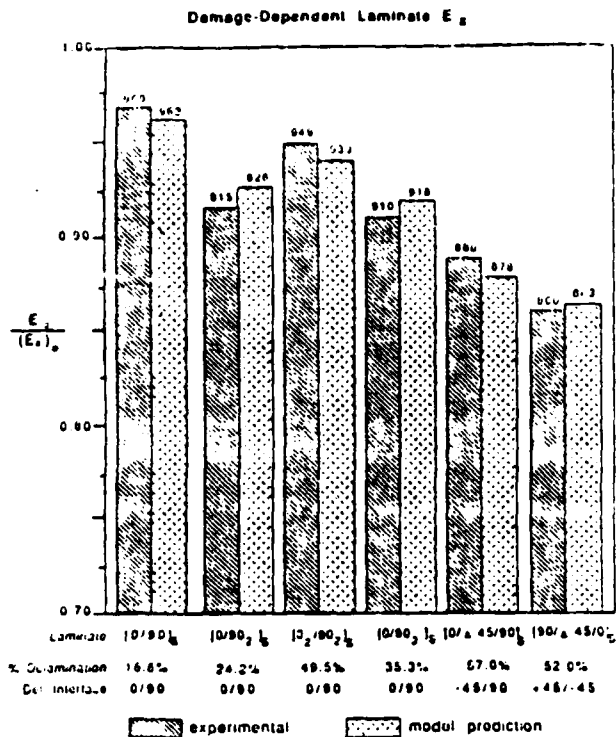
Damage-Dependent Laminate E_x

Fig 5 Comparison of Experimental Results and Model Predictions of the Laminate Engineering Modulus, E_x Degraded by Both Matrix Cracking and Delamination Damage
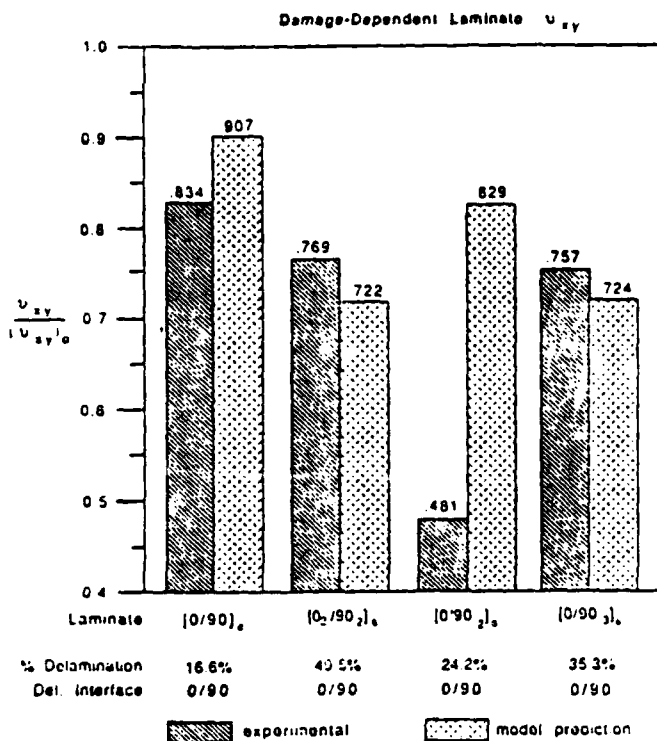

Damage-Dependent Laminate ν_{xy}

Fig 6 Comparison of Experimental Results and Model Predictions of the Laminate Engineering Poisson's Ratio, ν_{xy}, Degraded by Both Matrix Cracking and Delamination Damage

should be noted that the Poisson's ratio values for the two quasi-isotropic laminates are not given because they were not measured experimentally. The comparison between the experimental results and model results is quite close for E_x. However, there are some discrepancies in the comparison of ν_{xy} values. The authors attribute these discrepancies to the difficulty in measuring Poisson's ratio. Because Poisson's ratio is quite small for cross-ply laminates, the measurement is more sensitive to experimental error.

SUMMARY AND CONCLUSIONS

The authors have formulated a constitutive model for laminated composites with both matrix cracks and delamination damage. The model is based on the concept of continuum damage mechanics and uses second-order tensor valued internal state variables to represent each mode of damage. The internal state variables are the local volume averaged measure of the relative crack face displacements. The local volume for matrix crack damage is at the ply level, whereas the local volume for delamination damage is at the laminate level. Therefore, the damage-dependent constitutive model takes the form of laminate analysis equations modified by inclusion of the internal state variables.

This paper demonstrates the applicability of the model to predict the degraded engineering modulus, E_x, and Poisson's ratio, ν_{xy}, of quasi-isotropic and cross-ply laminates of graphite/epoxy. The comparison between model predictions and experimental results is very close. The authors believe that the good agreement reported herein demonstrates the validity of the model formulation and the physical interpretation of the internal state variables.

REFERENCES

1. Kachanov, L.M., "On the Creep Fracture Time," Izv. AN SSR, Otd. Tekhn. Nauk; No. 8, pp. 26-31, 1958 (in Russian).

2. Onsager, L., "Reciprocal Relations in Irreversible Process I.," Physics Review, Vol. 37, pp. 405-426, 1931.

3. Rabotnov, Y.N., Creep Problems in Structural Members, North-Holland, Amsterdam, 1969.

4. Bazant, Z.P., "Mechanics of Distributed Cracking," Applied Mechanics Reviews, Vol. 39, pp. 675-705, 1986.

5. Krajcinovic, D., "Continuum Damage Mechanics," Applied Mechanics Reviews, Vol. 37, pp. 1-6, 1984.

6. Krajcinovic, D., "Update to Continuum Damage Mechanics," Applied Mechanics Update 1986, Steele, C.R., and Springer, G.S., Eds., The American Society of Mechanical Engineers, pp. 403-406, 1986.

7. Kachanov, L.M., Introduction to Continuum Damage Mechanics, Martinus Nijhoff, Dordrecht, 1986.

8. Talreja, R., "A Continuum Mechanics Characterization of Damage in Composite Materials," Proc. R. Soc. London, Vol. 399A, 1985, pp. 195-216.

9. Talreja, R., "Residual Stiffness Properties of Cracked Composite Laminates," Advances in Fracture Research, Proc. Sixth Int. Conf. de Fracture, New Delhi, India, Vol. 4, pp. 3013-3019, 1985.

10. Talreja, R., "Transverse Cracking and Stiffness Reduction in Composite Laminates," Journal of Composite Materials, Vol. 21, pp. 355-375, 1985.

11. Talreja, R., Fatigue of Composite Materials, Technical University of Denmark, Lyngby, Denmark, 1985.

12. Talreja, R., "Stiffness Properties of Composite Laminates with Matrix Cracking and Interior Delamination," Danish Center for Applied Mathematics and Mechanics, The Technical University of Denmark, No. 321, March, 1986.

13. Allen, D.H., Harris, C.E., and Groves, S.E., "A Thermomechanical Constitutive Theory for Elastic Composites with Distributed Damage - Part I: Theoretical Development," to appear in International Journal of Solids and Structures, 1987.

14. Allen, D.H., Harris, C.E., and Groves, S.E., "A Thermomechanical Constitutive Theory for Elastic Composites with Distributed Damage - Part II: Application to Matrix Cracking in Laminated Composites," to appear in International Journal of Solids and Structures, 1987.

15. Allen, D.H., Groves, S.E., and Harris, C.E., "A Cumulative Damage Model for Continuous Fiber Composite Laminates with Matrix Cracking and Interply Delaminations," to appear in Composite Materials Testing and Design, 8th Symposium, ASTM STP, American Society for Testing and Materials, Philadelphia, 1987.

16. Allen, D.H., Grove, S.E., Harris, C.E., and Norvell, R.G., "Characteristics of Stiffness Loss in Crossply Laminates with Curved Matrix Cracks," to appear in Journal of Composite Materials, 1987.

17. Weitsman, Y., "Environmentally Induced Damage in Composites," Proceedings of the 5th Symposium on Continuum Modeling in Discrete Structures, A.J.M. Spencer, Ed., Nottingham, U.K., 1985.

18. Groves, S.E., "A Study of Damage Mechanics in Continuous Fiber Composite Laminates with Matrix Cracking and Internal Delaminations," Ph.D. Thesis, Texas A&M University, College Station, TX 77843, December 1986.

19. Harris, C.E., Allen, D.H., and Nottorf, E.W., "Modelling Stiffness Loss in Quasi-Isotropic Laminates Due to Microstructural Damage," to appear in Journal of Engineering Materials and Technology, American Society of Mechanical Engineers, January, 1988.

20. O'Brien, T.K., "Characterization of Delamination Onset and Growth in a Composite Laminate," Damage in Composite Materials, K.L. Reifsnider, Ed., ASTM STP 775, American Society for Testing and Materials, Philadelphia, pp. 141-167, 1982.

Appendix 7.8

EFFECT OF MICROSTRUCTURAL DAMAGE ON
PLY STRESSES IN LAMINATED COMPOSITES

by

D.H. Allen
E.W. Nottorf
Aerospace Engineering Department
Texas A&M University
College Station, Texas 77843

and

C.E. Harris
NASA Langley Research Center
Hampton, VA 23665

ABSTRACT

A continuum damage mechanics framework is utilized herein to develop laminate equations for layered orthotropic composites undergoing microstructural damage. The theory is capable of modelling the effects of both matrix cracks and interply delaminations on both the internal forces and moments resulting at the laminate level. The two damage modes are accounted for via second order tensor valued internal state variables which account for the locally averaged kinematics of microcracking in each damage model.

It is shown herein that the model may be utilized to determine the effects of microcracking on ply level stresses, and this is demonstrated for several example cases. Finally, it is shown that the accurate prediction of ply stresses serves as a precursor to the development of evolution laws governing the growth of damage.

1

INTRODUCTION

Laminated composites with non-metallic matrix material are known to undergo a substantial amount of microstructural damage, including matrix cracking, interply delamination, and fiber-matrix debonding. Over the past decade, numerous papers have documented the effects of this type of damage [1,2]. This damage can be very forgiving in the sense that the cracks cause localized and spatially variable component stiffness reduction which in turn induces load redistribution so that structural performance is not substantially impaired. In many materials the resulting stiffness loss is almost inconsequential, usually less than ten percent for the axial component, so that it is often assumed to be negligible when performing elastic stress analyses. In addition, it is often not practical to calculate ply stresses in the presence of damage since the damage may void the kinematic assumptions (such as Kirchhoff-Love) and thus necessitate the development of highly complex algorithms in order to calculate stresses in the damaged areas of the component. Unstable crack growth in highly damaged areas can eventually have a catastrophic effect resulting in component failure, usually due to fracture. Thus, although elastic properties are not substantially degraded, small losses in these properties ultimately cannot be ignored.

It is generally hypothesized that the growth of damage is driven by local stresses, which are in turn affected by the damage process. Therefore, although damage may not profoundly affect stiffness, it cannot be ignored in the prediction of failure. The question which remains open at this time is how much detail must be included in an attempt to model the effects of damage on failure. Must each crack be followed from inception to ultimate arrest, or can the effects of each crack be simplified in the model? Obviously, a model which follows every crack will be highly complex, since typical structural

components can undergo tens of thousands of microcracks prior to failure. The current research effort attempts to simplify this problem by applying continuum damage mechanics to the analysis of laminated composites. In this approach, first proposed by L.M. Kachanov in 1958 [3], it is hypothesized that the effect of microcracks may be locally averaged on a scale which is small compared to the scale of the structural component. Although the procedure has been extensively utilized in the literature, it has not been applied to laminated orthotropic media until recently. At the time of this writing, the authors are aware of three efforts in the open literature: Talreja [4-8], Weitsman [9], and the model discussed herein [10-15]. The current model may well be the only one which has been utilized to model ply level stresses, so that damage evolution laws and failure can be modelled.

The authors have previously developed a damage model which is applicable to laminated composites [10]. This microstructural damage may be induced by mechanical loads or environment such as elevated temperature. The model has been utilized to predict the stiffness loss in composite crossply laminates with matrix cracks, and these results compare favorably to experiment [11,12]. The model has also been developed for the case of combined matrix cracking and interply delamination [13]. The model has been recently compared to experimental results for axial stiffness [14] and in-plane Poisson's ratio [15] in the presence of both damage modes.

In the current paper, the model is used to predict the effects of both matrix cracks and delaminations on ply level stresses. It is shown that the stress distribution is substantially altered by the damage state. Furthermore, the predicted stresses are significantly affected by stacking sequence. The outcome of the research is to show how the development of damage causes stress redistribution which drives the development of new damage modes.

3

MODEL DEVELOPMENT

The detailed development of the damage model has been previously documented in a series of publications [10-15]. Therefore, in the current paper these developments will be reviewed only in enough detail to demonstrate the procedure for calculating ply stresses in damaged laminates.

It is assumed that the effects of matrix cracking are reflected in the ply level stress-strain relations [11]:

$$
\begin{Bmatrix} \sigma_{L_x} \\ \sigma_{L_y} \\ \sigma_{L_z} \\ \sigma_{L_{yz}} \\ \sigma_{L_{xz}} \\ \sigma_{L_{xy}} \end{Bmatrix} =
\begin{bmatrix}
Q_{11} & Q_{12} & Q_{13} & Q_{14} & Q_{15} & Q_{16} \\
Q_{12} & Q_{22} & Q_{23} & Q_{24} & Q_{25} & Q_{26} \\
Q_{13} & Q_{23} & Q_{33} & Q_{34} & Q_{35} & Q_{36} \\
Q_{14} & Q_{24} & Q_{34} & Q_{44} & Q_{45} & Q_{46} \\
Q_{15} & Q_{25} & Q_{35} & Q_{45} & Q_{55} & Q_{56} \\
Q_{16} & Q_{26} & Q_{36} & Q_{46} & Q_{56} & Q_{66}
\end{bmatrix}
\begin{Bmatrix} \epsilon_{L_x} - \alpha^M_{xx} \\ \epsilon_{L_y} - \alpha^M_{yy} \\ \epsilon_{L_z} - \alpha^M_{zz} \\ \gamma_{L_{yz}} - 0 \\ \gamma_{L_{xz}} - 0 \\ \gamma_{L_{xy}} - \alpha^M_{xy} \end{Bmatrix}
\tag{1}
$$

where σ_{Lij} are the components of the locally averaged stress tensor, ϵ_{Lij} are the components of the locally averaged strain tensor, and Q_{ij} are the components of the elastic (undamaged) modulus tensor in ply coordinates. Furthermore, α^M_{ij} are the components of a second order damage tensor, defined by [10]

$$
\alpha^M_{ij} = \frac{1}{V_L} \int_{S_C} u^C_i n^C_j ds
\tag{2}
$$

where V_L is an arbitrarily chosen local volume element of ply thickness which is sufficiently large that α^M_{ij} does not depend on the size of V_L, u^C_i are crack opening displacements in V_L, n^C_j are the components of a unit normal to the crack faces, and S_C is the surface area of matrix cracks in V_L. For vertical matrix cracks ($n_z = 0$), α^M_{xz} and α^M_{yz} are identically zero [11].

4

The laminate equations are constructed by assuming that the Kirchhoff-Love hypothesis may be modified to include the effects of jump displacements u_i^D, v_i^D, and w_i^D, as well as jump rotations β_i^D and ψ_i^D for the ith delaminated ply interface, as shown in Fig. 1. Thus,

$$u(x,y,z) = u^0(x,y) \quad - \quad z \left[\beta^0 + H(z-z_i) \, \beta_i^D \right] \quad + \quad H(z-z_i) \, u_i^D \tag{3}$$

$$v(x,y,z) = v^0(x,y) \quad - \quad z \left[\psi^0 + H(z-z_i) \, \psi_i^D \right] \quad + \quad H(z-z_i) \, v_i^D \tag{4}$$

and

$$w(x,y,z) \quad = \quad w^0(x,y) \quad + \quad H(z-z_i) \, w_i^D \tag{5}$$

where the superscripts "o" imply undamaged midsurface quantities, and $H(z-z_i)$ is the Heavyside step function. Also, a repeated index i in a product is intended to imply summation.

The displacement equations are averaged over the local area, A_L, shown in Fig. 2, in order to produce locally averaged displacements to be utilized in the laminate formulation. Thus,

$$u_L(x,y,z) = \frac{1}{A_L} \int_{A_L} [u^0 - z(\beta^0 + H(z-z_i)(\beta_i^D)) + H(z-z_i) \, u_i^D] dxdy \tag{6}$$

$$v_L(x,y,z) = \frac{1}{A_L} \int_{A_L} [v^0 - z(\dot{\psi}^0 + H(z-z_i)(\psi_i^D)) + H(z-z_i) \, v_i^D] dxdy \tag{7}$$

and

5

$$w_L(x,y,z) = \frac{1}{A_L} \int_{A_L} [w^0 + H(z-z_i) \, w_i^D] dxdy \qquad (8)$$

By averaging the displacements, the delamination jump discontinuities are also averaged over A_L.

The laminate strains are given by

$$\varepsilon_{L_x} = \frac{\partial u_L}{\partial x} \qquad (9)$$

$$\varepsilon_{L_y} = \frac{\partial v_L}{\partial y} \qquad (10)$$

$$\varepsilon_{L_z} = \frac{\partial w_L}{\partial z} \qquad (11)$$

$$\gamma_{L_{yz}} = \frac{\partial v_L}{\partial z} + \frac{\partial w_L}{\partial y} \qquad (12)$$

$$\gamma_{L_{xz}} = \frac{\partial u_L}{\partial z} + \frac{\partial w_L}{\partial x} \qquad (13)$$

$$\gamma_{L_{xy}} = \frac{\partial u_L}{\partial y} + \frac{\partial v_L}{\partial x} \qquad (14)$$

Thus, due to the interply delamination all six components of the strain must be included in the laminate formulation.

The laminate constitution is obtained by integrating the stress in each lamina over the laminate thickness. The local lamina constitution is assumed to be anisotropic since the jump displacements resulting from delamination produce local anisotropic responses. That is, the out-of-plane shear strains, $\gamma_{L_{xz}}$ and $\gamma_{L_{yz}}$ resulting from delamination will contribute to the force resultants.

6

The resultant midplane forces and moments per unit width of region V_L in the laminate are given by

$$\begin{Bmatrix} N_x \\ N_y \\ N_{xy} \end{Bmatrix} \equiv \int_{-t/2}^{t/2} \begin{Bmatrix} \sigma_{L_x} \\ \sigma_{L_y} \\ \sigma_{L_{xy}} \end{Bmatrix} dz \tag{15}$$

and

$$\begin{Bmatrix} M_x \\ M_y \\ M_{xy} \end{Bmatrix} \equiv \int_{-t/2}^{t/2} \begin{Bmatrix} \sigma_{L_x} \\ \sigma_{L_y} \\ \sigma_{L_{xy}} \end{Bmatrix} z \, dz \tag{16}$$

where t is the laminate thickness.

The resultant laminate equations may be obtained by substituting equations (6) through (8) into equations (9) through (13), and this result into equations (1). This result is then substituted into equations (15) and (16), and the divergence theorem is employed to obtain the following laminate equations [13]:

$$\{N\} = \sum_{k=1}^{n} [Q]_k (z_k - z_{k-1}) \{\varepsilon_L^0\} - \frac{1}{2} \sum_{k=1}^{n} [Q]_k (z_k^2 - z_{k-1}^2) \{\kappa_L\}$$

$$+ \sum_{i=1}^{d} [\bar{Q}_1]_i \, t_i \begin{Bmatrix} 0 \\ 0 \\ \alpha_{1i}^D \\ \alpha_{2i}^D \\ \alpha_{3i}^D \\ 0 \end{Bmatrix} + \sum_{i=1}^{d+1} (z_i - z_{i-1}) [\bar{Q}_2]_i \begin{Bmatrix} 0 \\ 0 \\ 0 \\ \alpha_{4i}^D \\ \alpha_{5i}^D \\ 0 \end{Bmatrix}$$

$$- \sum_{k=1}^{n} [Q]_k (z_k - z_{k-1}) \{\alpha^M\}_k \tag{17}$$

7

where z_k is the coordinate of the kth ply interface, $\{\varepsilon_L^O\}$ represents the locally averaged midsurface strains, $\{\kappa_L\}$ represents the locally averaged midsurface rotations, and $[Q]_k$ is the elastic modulus matrix for the kth ply in laminate coordinates. The last term in the above equation, containing $\{\alpha^M\}_k$, represents the effect of matrix cracking in the kth ply on the in-plane forces $\{N\}$. The remaining two terms contain quantities α_{ji}^D, representing components of the internal state variable for the ith delamination, and these terms are summed from one to d, the total number of delaminated ply interfaces. The components α_{1i}^D, α_{2i}^D, and α_{3i}^D are defined by

$$\alpha_{1i}^D \equiv \frac{1}{V_{Li}} \int_{S_{2i}} w_i^D n_z dS \tag{18a}$$

$$\alpha_{2i}^D \equiv \frac{1}{V_{Li}} \int_{S_{2i}} v_i^D n_z dS \tag{18b}$$

$$\alpha_{3i}^D \equiv \frac{1}{V_{Li}} \int_{S_{2i}} u_i^D n_z dS \tag{18c}$$

$$\alpha_{4i}^D \equiv \frac{1}{A_L} \int_{S_{2i}^B} \psi_i^D n_z dS = - \frac{1}{A_L} \int_{S_{2i-1}^T} \psi_{i-1}^D n_z dS \tag{18d}$$

$$\alpha_{5i}^D \equiv \frac{1}{A_L} \int_{S_{2i}^B} \beta_i^D n_z dS = - \frac{1}{A_L} \int_{S_{2i-1}^T} \beta_{i-1}^D n_z dS \tag{18e}$$

where u_i^D, v_i^D, and w_i^D are the components of the crack opening displacements in the local volume V_{Li}, which extends one ply thickness above and below the delaminated ith ply, as shown in Fig. 3. Furthermore, n_z is z-component of unit normal to the delaminations, which is usually of magnitude one. The sign

$$\overline{Q}_{1_{24}} = \frac{N_y}{\varepsilon_{L_{yz}}} = \frac{Q_{22}^T \, S_{22}^T \, t^T + Q_{22}^B \, S_{22}^B \, t^B}{S_{22}^T \, t^T + S_{22}^B \, t^B} \tag{24}$$

Note that the Q_{ij}^T and Q_{ij}^B are in laminate coordinates.

By a similar procedure, the resultant moments are found to be

$$\{M\} = \frac{1}{2} \sum_{k=1}^{n} [Q]_k \, (z_k^2 - z_{k-1}^2) \, \{\varepsilon_L^0\} - \frac{1}{3} \sum_{k=1}^{n} [Q]_k \, (z_k^3 - z_{k-1}^3) \, \{\kappa_L\}$$

$$+ \sum_{i=1}^{d} [\overline{Q}_3]_i \, t_i^2 \begin{Bmatrix} 0 \\ 0 \\ \alpha_{1i}^D \\ \alpha_{2i}^D \\ \alpha_{3i}^D \\ 0 \end{Bmatrix} + \sum_{i=1}^{d+1} [\overline{Q}_4]_i (z_i^2 - z_{i-1}^2) \begin{Bmatrix} 0 \\ 0 \\ 0 \\ \alpha_{4i}^D \\ \alpha_{5i}^D \\ 0 \end{Bmatrix}$$

$$- \frac{1}{2} \sum_{k=1}^{n} [Q]_k \, (z_k^2 - z_{k-1}^2) \, \{\alpha^M\}_k \tag{25}$$

where

$$[\overline{Q}_3]_i \equiv \frac{z_i}{t_i} \, \frac{[Q]_i^T \, [S]_i^T \, t^T}{[S]_i^T \, t^T + [S]_i^B \, t^B} + \frac{[Q]_i^B \, [S]_i^B \, t^B}{[S]_i^T \, t^T + [S]_i^B \, t^B} \tag{26}$$

and

$$[\overline{Q}_4]_i \equiv \frac{-z_{i-1}^2 \, [Q]_{i-1}^B + z_i^2 \, [Q]_i^T}{(z_i^2 - z_{i-1}^2)} \tag{27}$$

As in the case of the force resultant terms, the rotation terms must be supplemented with terms coupling the bending moments with the shearing deformations.

10

It is apparent that for a given set of midsurface strains $\{\varepsilon^0\}$ and $\{\kappa_L\}$, as well as a given damage state, equations (17) and (25) can be used to obtain the force resultants $\{N\}$ and moment resultants $\{M\}$. Since the midsurface terms are considered to be input, it remains only to obtain the current damage state for a given laminate. In principal this should be accomplished via a set of internal state variable evolution laws of the form

$$\dot{\alpha}_{ij}^M = \dot{\alpha}_{ij}^M(\varepsilon_{k\ell}, T, \alpha_{k\ell}^M, \alpha_{k\ell}^D) \tag{28}$$

and

$$\dot{\alpha}_{ij}^D = \dot{\alpha}_{ij}^D(\varepsilon_{k\ell}, T, \alpha_{k\ell}^M, \alpha_{k\ell}^D) \tag{29}$$

where the quantities of interest are for the plies above and below the delamination. However, evolution laws of this type are still in the developmental stage for laminated composites. Therefore, as an interim measure, the authors have developed a procedure for evaluating the damage state which will be discussed later in this paper. Thus, the current internal state can be obtained independently of the laminate stacking sequence.

EVALUATION OF PLY STRESSES

In order to evaluate the stress state in each ply, it is first necessary to substitute displacement equations (6) through (8) into the locally averaged strain definitions (9) through (14). Utilizing the divergence theorem on this result will then give the following equations for the strains in each ply.

$$\varepsilon_{L_x} = \varepsilon_{L_x}^0 - z \left[\kappa_{L_x} + H(z-z_i) \, \alpha_{5i}^D \right] + H(z-z_i) \, \alpha_{3i}^D \tag{30}$$

11

$$\varepsilon_{L_y} = \varepsilon_{L_y}^0 - z \left[\kappa_{L_y} + H(z-z_i) \, \alpha_{4i}^D \right] + H(z-z_i) \, \alpha_{2i}^D \tag{31}$$

$$\varepsilon_{L_z} = \varepsilon_{L_z}^0 + H(z-z_i) \, \alpha_{1i}^D \tag{32}$$

$$\varepsilon_{L_{yz}} = \varepsilon_{L_{yz}}^0 - z \left[\kappa_{L_{yz}} + H(z-z_i) \, \alpha_{4i}^D \right] \tag{33}$$

$$\varepsilon_{L_{xz}} = \varepsilon_{L_{xz}}^0 - z \left[\kappa_{L_{xz}} + H(z-z_i) \, \alpha_{5i}^D \right] \tag{34}$$

$$\varepsilon_{L_{xy}} = \varepsilon_{L_{xy}}^0 - z \kappa_{L_{xy}} \tag{35}$$

The above equations may be utilized to obtain the ply strains, and these results may be substituted into equations (1) to obtain the stresses in each ply. The ply stresses, strains, and damage parameters may then be utilized to develop evolution laws of the form described by equations (28) and (29).

Since the ply stresses determined by this procedure represent locally averaged values, they must be considered to be far-field stresses, so that equations (28) and (29) may more properly be written:

$$\dot{\alpha}_{ij}^M = \dot{\alpha}_{ij}^M \left(\varepsilon_{k\ell}, \, T, \, \alpha_{k\ell}^M, \, \alpha_{k\ell}^D, \, K_I, \, K_{II}, \, K_{III} \right) \tag{36}$$

and

$$\dot{\alpha}_{ij}^D = \dot{\alpha}_{ij}^D \left(\varepsilon_{k\ell}, \, T, \, \alpha_{k\ell}^M, \, \alpha_{k\ell}^D, \, K_I, \, K_{II}, \, K_{III} \right) \tag{37}$$

where K_I, K_{II}, and K_{III} are the stress intensity factors, which relate the far-field stresses to the crack tip stresses for a given crack geometry.

12

However, it is assumed that the geometry of both matrix cracking and delaminations is sufficiently independent of stacking sequence that the stress intensity factors may be treated as "material properties" and thus possess the same stress intensity factor dependence for all stacking sequences. Thus, they are encompassed implicitly in the material constants required to characterize damage evolution laws (28) and (29).

DAMAGE VARIABLE CALCULATION

As previously mentioned, the damage variables can be obtained from evolution laws (28 and 29). Since the formulation of the growth laws is currently in progress, the variables are presently calculated for a specific damage state in the laminate. In laminated continuous fiber composites, the two types of damage variables of interest are for matrix cracks and delaminations. The damage variables can be calculated by using equations (2) and (18). In order to demonstrate the model, the displacement of the crack and the delamination interfaces is assumed to vary sinusoidally with zero displacement at the edges (see Figure 4). When integrating equation (2) with a sinusoidal displacement distribution, the following expression for α_2^M results:

$$\alpha_2^M = \frac{2}{\pi} u_0^M N_C \tag{38}$$

where:

N_C is the number of cracks per inch in the ply.

u_0^M is the maximum displacement of the interface.

13

When dealing with the off-axis plies, a simple geometrical relation is assumed between α_2^M and α_8^M yielding:

$$\alpha_8^M = \frac{2 \sin\theta \cos\theta \, u_0^M \, N_c}{\pi} \tag{39}$$

In this study, the "far-field" ply stresses are calculated for only one fixed input strain (ϵ_{xo}). Since there is a fixed strain input only in the x-direction (all other strains are zero), it is assumed that all of the delamination damage variables except those associated with displacement in the x-direction (α_3^D) have a negligible effect on the laminate stresses. The calculation of the damage variable is approximated by of creating an equivalent effective circular shaped delamination which simulates the separate delaminations found between the actual laminate plies in question (Figure 5). As with the matrix crack damage variable, a sinusoidal delamination interface displacement distribution is assumed. The average surface area of the equivalent delamination is equal to the total delamination area between the laminate plies in question. Using equation (18c) and assuming a sinusoidal interface deformation shape results in:

$$\alpha_3^D = 143.91 \, u_0^D \, r^2 \tag{40}$$

where

u_0^D is the maximum interface displacement in the x direction.

r is the radius of the equivalent delamination size.

14

MODEL RESULTS

A computer code has been constructed to determine the effect of damage on the "far field" ply stresses in composite laminates. Results presented are for a given laminate strain $\epsilon_{xo} = .01$ (all other strains assumed to be zero). Damage variables were calculated for matrix cracks in a saturated damage state using equations (38) and (39) assuming $u_0^M = .0001"$. The off-axis and 90° plies use the matrix crack damage terms of α_8^M and α_2^M, respectively. No damage is assumed in the 0° plies. Since the laminate is subjected only to ϵ_{xo}, α_3^D is assumed to be the only delamination damage component. This term is calculated for an equivalent delamination area by the use of equation (40) with $u_0^D = .00001"$.

The results obtained from the model are shown in Table 1 and Figures 6-11. As evidenced from the results, the damage significantly affects the far-field ply stresses. Damage variables were calculated by using equations (38-40) to simulate damage existing in several previously tested laminates. Matrix cracks had a significant effect on ply stresses in the 90° plies in cross-ply laminates. The largest number of matrix cracks was evident in the 90° plies of the $[0_2/90_2]_s$ laminate resulting in a thirty-four percent far-field ply stress reduction. The two quasi-isotropic laminates developed different damage resulting in dissimilar far-field ply stresses. The $[90/\pm45/0]_s$ laminate exhibited little matrix cracking and corresponding reduction of ply stress in both 90° and ±45° plies. The $[0/\pm45/90]_s$ laminate exhibited a similar stress reduction in the ±45° plies, but showed a substantial stress reduction (fifteen percent verses one percent) in the 90° plies when compared to the $[90/\pm45/0]_s$ laminate. It should be noticed that only the stresses in plies between delaminations were affected by the delamination. This is a result of symmetric delamination damage about the

midplane of the laminate. For this damage state, the resulting a_3^D terms are equal in magnitude, yet opposite in sign. By observing equation (30), it is apparent that for fixed strain and a symmetric damage state, the laminate strains are affected only in the region between the delaminations. The matrix cracks are shown to alter the constitutive nature of the plies, and delamination effects are incorporated into the laminate through the laminate equations. This alteration in ply stresses will significantly affect the growth of new damage in the composite.

SUMMARY AND CONCLUSIONS

The authors have presented a continuum damage model that includes damage terms resulting from both matrix cracking and delamination. This model has the capability of predicting the mechanical constitution of a laminated composite with damage. The model incorporates the effect of damage by tensor valued internal state variables. The internal state variables physically represent the local volume averaged relative crack face displacements. The effect of matrix cracks is in the local ply constitutive behavior. Delamination effects, however, are reflected through the laminate equations.

Results of this work illustrate that the stress state in the laminate is substantially influenced by damage. In the $[0_2/90_2]_s$ laminate, matrix cracks and delaminations reduce the stress in the 90° plies by almost sixty percent. For cross-ply laminates, the damage induced ply stress reduction varies from about forty to sixty percent of undamaged stress in the 90° plies. Stress reduction in angle-ply laminates is less dramatic (depending on location and size of the delamination). This alteration in stress state is critical in determining both the magnitude and location of damage development.

16

ACKNOWLEDGEMENT

REFERENCES

1. Jamison, R.D., Schulte, K., Reifsnider, K.L., and Stinchcomb, W.W., "Characterization and Analysis of Damage Mechanisms in Tension-Tension Fatigue of Graphite/Epoxy Laminates," Effects of Defects in Composite Materials, ASTM STP 836, American Society for Testing and Materials, 1984, pp. 21-55.

2. Georgiou, I.T., "Initiation Mechanisms and Fatigue Growth of Internal Delaminations in Graphite/Epoxy Cross-Ply Laminates," Texas A&M University Thesis, December, 1986.

3. Kachanov, L.M., "On the Creep Fracture Time," Izv. AN SSR, Otd. Tekhn. Nauk; No. 8, pp. 26-31, 1958 (in Russian).

4. Talreja, R., "A Continuum Mechanics Characterization of Damage in Composite Materials," Proc. R. Soc. London, Vol. 399A, 1985, pp. 195-216.

5. Talreja, R., "Residual Stiffness Properties of Cracked Composite Laminates," Advances in Fracture Research, Proc. Sixth Int. Conf. de Fracture, New Delhi, India, Vol. 4, pp. 3013-3019, 1985.

6. Talreja, R., "Transverse Cracking and Stiffness Reduction in Composite Laminates," Journal of Composite Materials, Vol. 21, pp. 355-375, 1985.

7. Talreja, R., Fatigue of Composite Materials, Technical University of Denmark, Lyngby, Denmark, 1985.

8. Talreja, R., "Stiffness Properties of Composite Laminates with Matrix Cracking and Interior Delamination," Danish Center for Applied Mathematics and Mechanics, The Technical University of Denmark, No. 321, March, 1986.

9. Weitsman, Y., "Environmentally Induced Damage in Composites," Proceedings of the 5th Symposium on Continuum Modeling of Discrete Structures, A.J.M. Spencer, Ed., Nottingham, U.K., 1985.

10. Allen, D.H., Harris, C.E., and Groves, S.E., "A Thermomechanical Constitutive Theory for Elastic Composites with Distributed Damage - Part I: Theoretical Development," International Journal of Solids and Structures, Vol. 23, No. 9, pp. 1301-1318, 1987.

11. Allen, D.H., Harris, C.E., and Groves, S.E., "A Thermomechanical Constitutive Theory for Elastic Composites with Distributed Damage - Part II: Application to Matrix Cracking in Laminated Composites," International Journal of Solids and Structures, Vol. 23, No. 9, pp. 1319-1338, 1987.

12. Allen, D.H., Harris, C.E., Groves, S.E., and Norvell, R.G., "Characteristics of Stiffness Loss in Crossply Laminates with Curved Matrix Cracks," to appear in Journal of Composite Materials, Vol. 22, No. 1, pp. 71-80, January, 1988.

13. Allen, D.H., Groves, S.G. and Harris, C.E., "A Cumulative Damage Model for Continuous Fiber Composite Laminates with Matrix Cracking and Interply Delaminations," to appear in Composite Materials: Testing and Design (8th Conference), ASTM STP, American Society for Testing and Materials, Philadelphia, 1988.

14. Allen, D.H., Harris, C.E., and Groves, S.E., "Damage Modelling in Laminated Composites," Proceedings IUTAM/ICM Symposium on Yielding, Damage and Failure of Anisotropic Solids, Grenoble, France, 1987.

15. Harris, C.E., Allen, D.H., and Nottorf, E.W., "Damaged Induced Changes in the Poisson's Ratio of Cross-Ply Laminates: An Application of a Continuum Damage Mechanics Model for Laminated Composites," Damage Mechanics in Composites, A.S.D. Wang and G.K. Haritos, Eds., American Society of Mechanical Engineers, AD-Vol. 12, pp. 17-24, 1987.

Table 1. PLY STRESSES RESULTING FROM MATRIX CRACKING AND DELAMINATION

LAMINATE	PLY	INITIAL PLY STRESS σ (ksi)	STRESS W/MATRIX CRACKS σ (ksi)	STRESS W/MATRIX CRACKS & DELAM. σ (ksi)	DELAMINATION LOCATION AND MAGNITUDE a_3^D	MATRIX DAMAGE VARIABLES	
						a_2^M	a_8^M
$[0/90]_s$	0	211.4	211.4	211.4	0/90	0	0
	90	14.0	9.6	8.5	16.6% .00076	.00318	0
$[0/90_2]_s$	0	211.4	211.4	211.4	0/90	0	0
	90	14.0	9.5	7.9	24.2%	.00326	0
	90	14.0	9.5	7.9	.001109	.00326	0
$[0_2/90_2]_s$	0	211.4	211.4	211.4		0	0
	0	211.4	211.4	211.4	0/90	0	0
	90	14.0	9.2	6.0	49.5%	.00344	0
	90	14.0	9.2	6.0	.002267	.00344	0
$[0/90_3]_s$	0	211.4	211.4	211.4		0	0
	90	14.0	10.6	8.3	0/90	.00247	0
	90	14.0	10.6	8.3	35.3%	.00247	0
	90	14.0	10.6	8.3	.001617	.00247	0
$[0/\pm45/90]_s$	0	211.4	211.4	211.4		0	0
	45	64.4	64.0	64.0	-45/90	0	.00067
	-45	64.4	64.0	64.0	57%	0	-.00067
	90	14.0	11.8	8.2	.002611	.00157	0
$[90/\pm45/0]_s$	90	14.0	13.9	13.9		.00060	0
	+45	64.4	64.0	64.0	+45/-45	0	.00067
	-45	64.4	64.0	48.7	52%	0	-.00067
	0	211.4	211.4	161.0	.002382	0	0

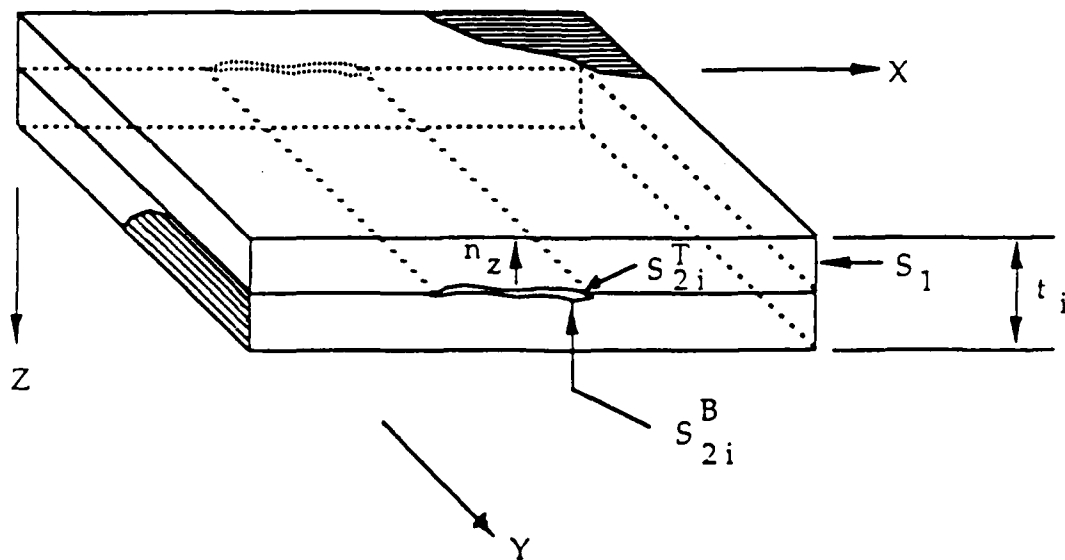Figure 1. Deformation Geometry for Region A_L.
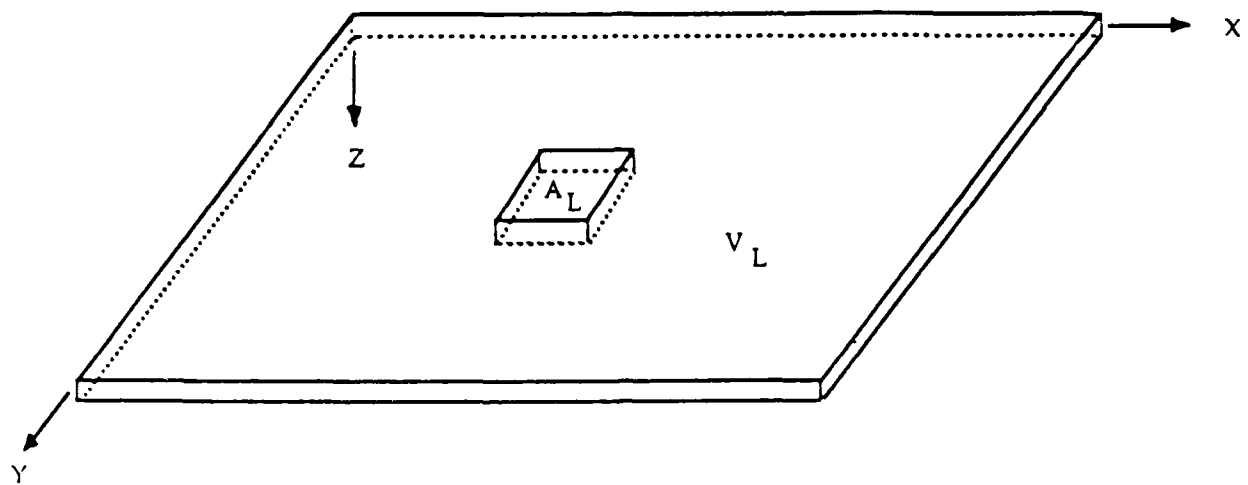
A) General Laminate
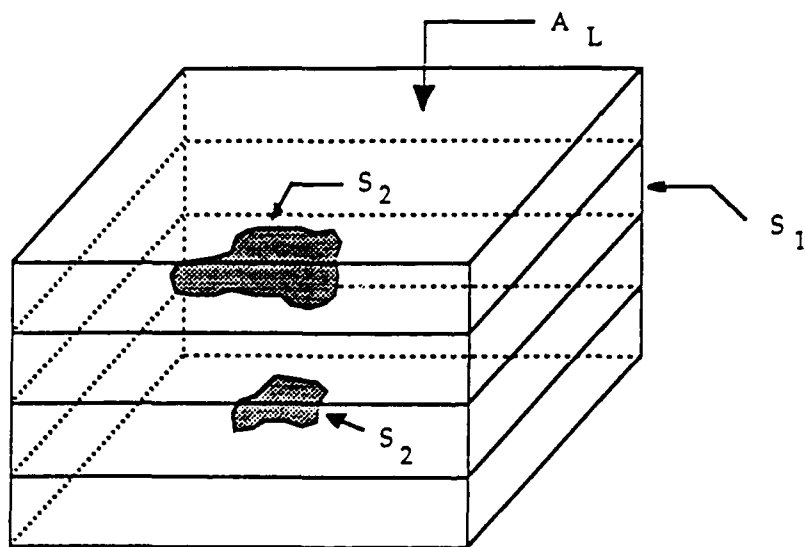
B) Exploded View with Damage

Figure 2. Characteristic Local Region of Damage.

$$\vec{u} = u^D \hat{e}_x + v^D \hat{e}_y + w^D \hat{e}_z$$

$$\vec{n} = 0\ \hat{e}_x + 0\ \hat{e}_y + n\ \hat{e}_z$$

$$S = S_1 + S_{,2}$$

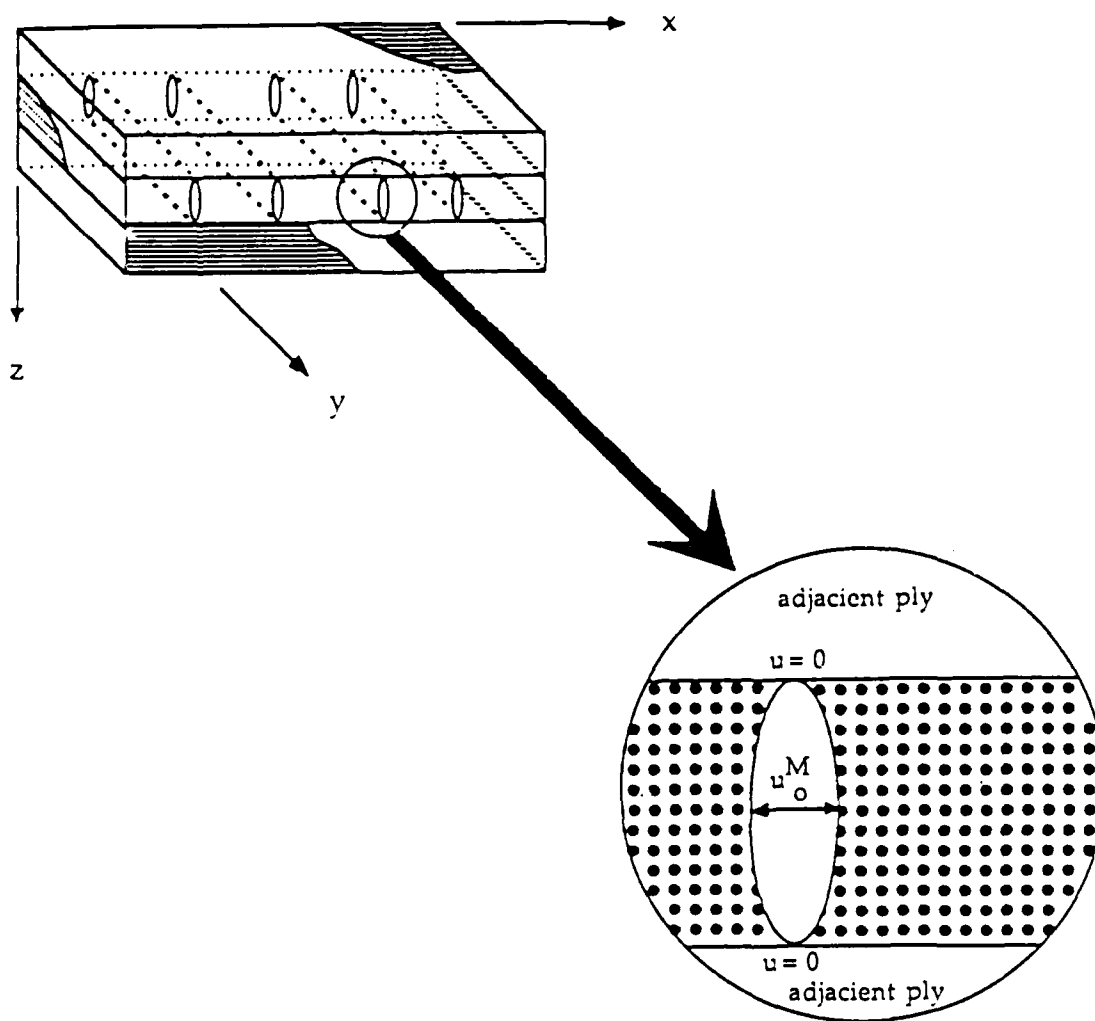Figure 3. Interply Delamination in a Laminated Continuous Fiber
Composite.

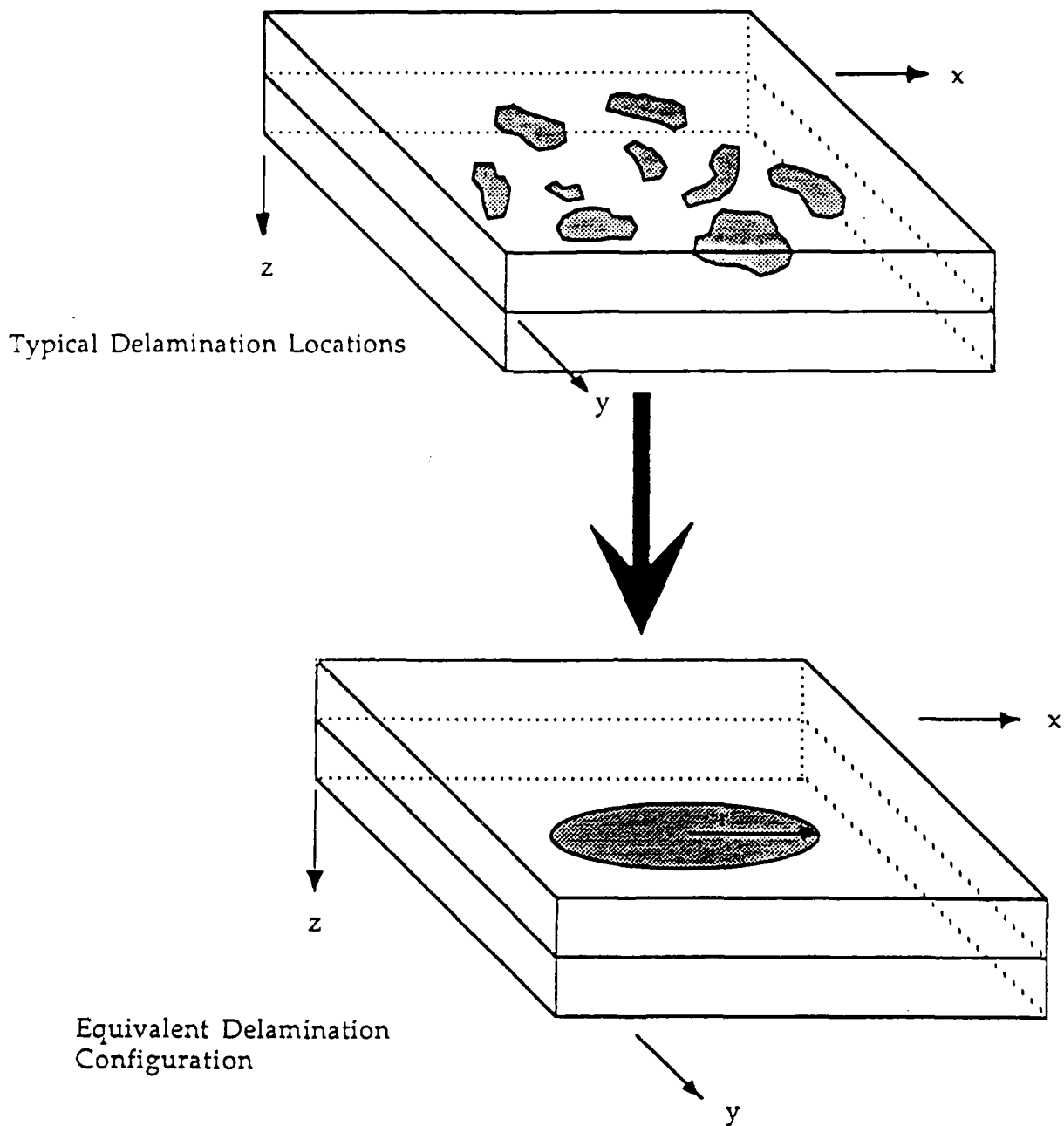Figure 4.   Typical Matrix Crack Geometry in a Composite Laminate

Figure 5. Delamination Sites in Local Volume Reduced into a Single
Equivalent Delamination Site
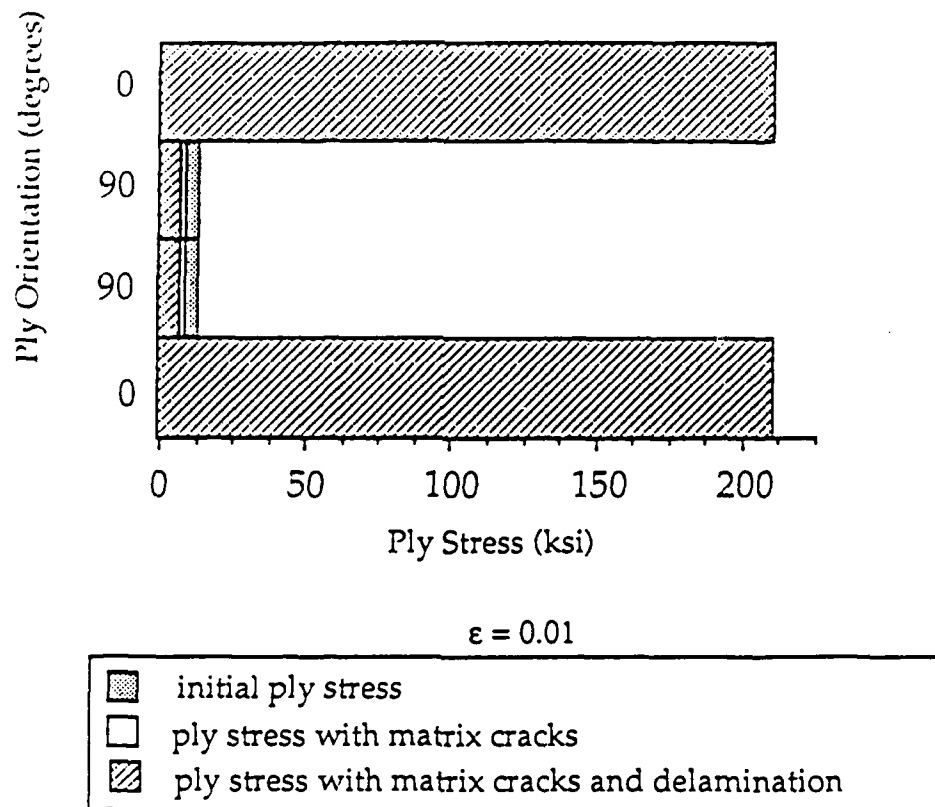
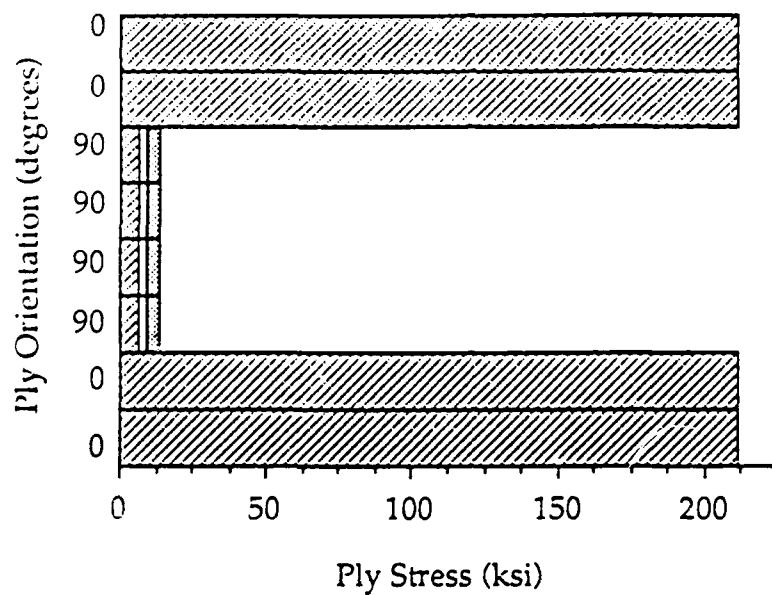Figure 6. Far Field Ply Stresses in a [0/90]s Laminate

ε = 0.01

▨	initial ply stress
☐	ply stress with matrix cracks
▧	ply stress with matrix cracks and delamination
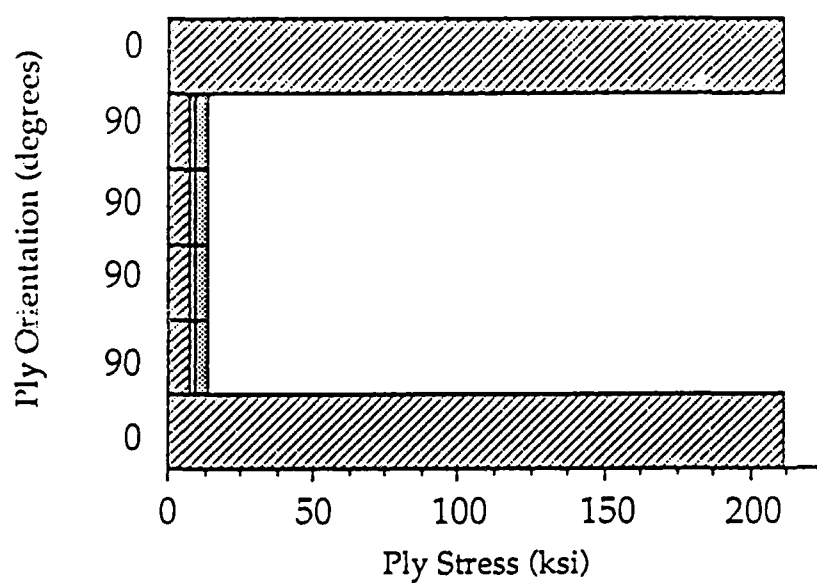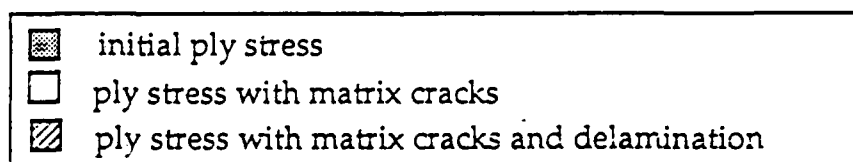
Figure 7.   Far Field Stresses in a $[0/90_2]s$ Laminate

$\varepsilon = 0.01$

initial ply stress
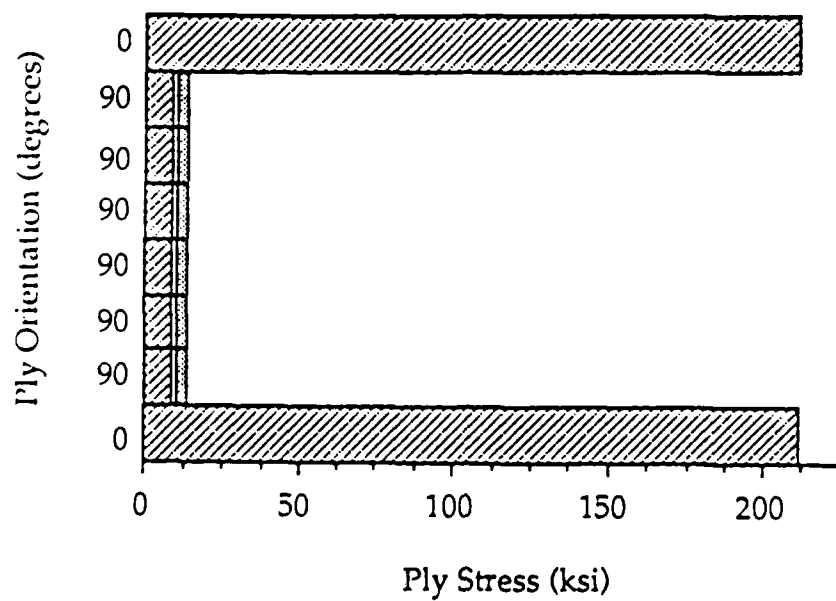ply stress with matrix cracks
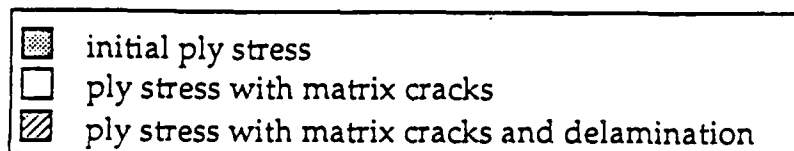ply stress with matrix cracks and delamination
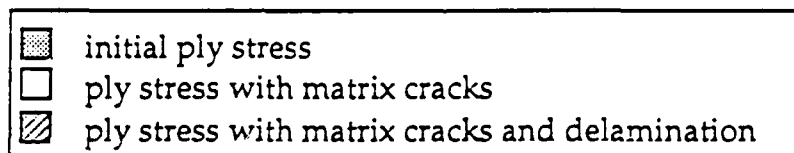
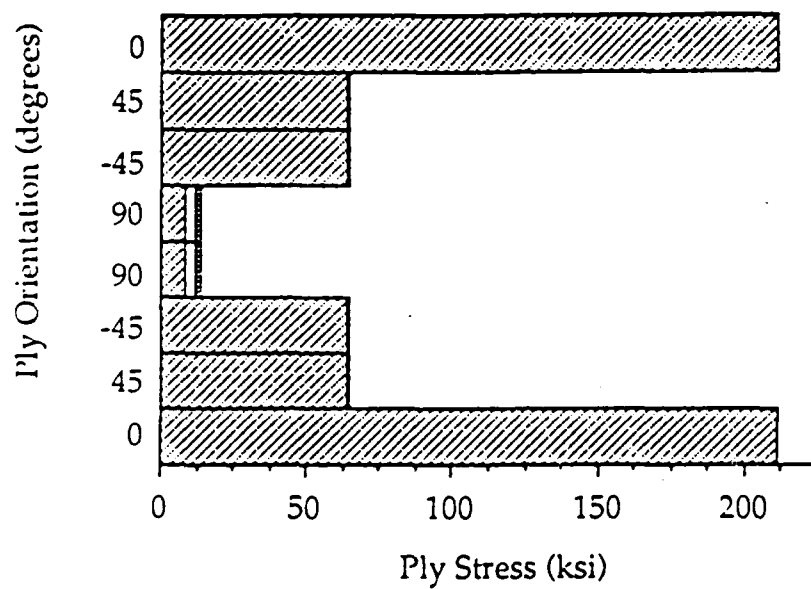Figure 8. Far Field Stresses in a $[0_2/90_2]s$ Laminate

$\varepsilon = 0.01$

Figure 9. Far Field Ply Stresses in a $[0/90_3]s$ Laminate

ε = 0.01

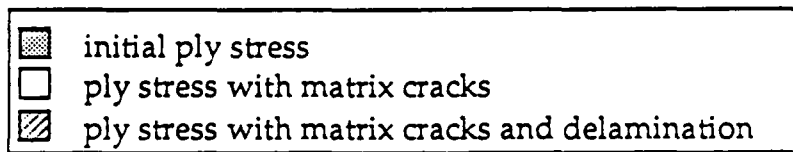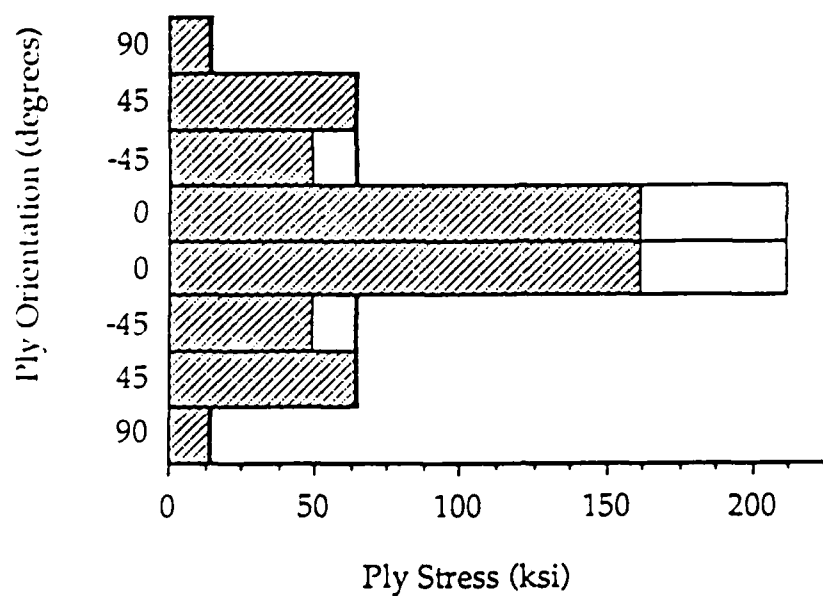|	
▦	initial ply stress
☐	ply stress with matrix cracks
▨	ply stress with matrix cracks and delamination

Figure 10. Far Field Ply Stresses in a [0/±45/90]s Laminate

$\varepsilon = 0.01$

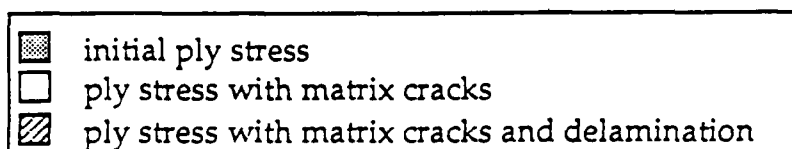|	
▦	initial ply stress
☐	ply stress with matrix cracks
▨	ply stress with matrix cracks and delamination

Figure 11. Far Field Ply Stresses in a [90/±45/0]s Laminate

Appendix 7.9

A CUMULATIVE DAMAGE MODEL OF MATRIX CRACKING AND
DELAMINATIONS IN CONTINUOUS FIBER LAMINATED COMPOSITES

by

D.H. Allen
C.E. Harris

Aerospace Engineering Department
Texas A&M University
College Station, Texas 77843

A CUMULATIVE DAMAGE MODEL OF MATRIX CRACKING AND DELAMINATIONS IN CONTINUOUS FIBER LAMINATED COMPOSITES

by

David H. Allen
Charles E. Harris

Aerospace Engineering Department
Texas A&M University
College Station, Texas 77843

ABSTRACT. A model is presented herein for predicting the effects of microstructural damage on the constitutive behavior of laminated continuous fiber composites. The model is developed using the approach of continuum damage mechanics. Second order tensor valued internal state variables are constructed which reflect the locally averaged effects of both matrix cracks and interply delaminations. Because both of these damage modes exhibit statistical inhomogeneity in the coordinate dimensions normal to the plane of the laminate, the model includes a weighted effect of the distance from the midplane. Linear elastic fracture mechanics is utilized to construct the parameters necessary to characterize the damage dependent material properties. The resulting model is then shown to be independent of the stacking sequence and ply orientation in the laminate. Comparisons of the model predictions to experimental results reported herein for several stacking sequences tend to support the validity of the model.

INTRODUCTION

The method of continuum damage mechanics assumes that the exact analysis of a multiply connected domain with numerous microcracks is hopelessly complex. Alternatively, the effects of these microcracks on the macrophysical response are reflected via one or more internal state variables [1] called damage parameters. The initial use of damage mechanics appears to have been due to the observation that in metals classical plasticity theory breaks down when significant grain boundary sliding and/or microcavitation occur because the initial elastic properties are not observed on unloading [2].

In the last twenty years there has been an incredible expansion of research in damage mechanics, as evidenced by two recent review articles [3,4,5] and the publication of the first textbook devoted entirely to damage mechanics [6]. However, as pointed out in reference 5, although substantial research has been performed on metals, concrete, and geologic media, very little research has been detailed on laminated composite media. In fact, to these authors'

1

knowledge, only three concerted efforts have reached the open literature at the time of this writing. These are due to Talreja [7-11], Allen, et al. [12-15], and Weitsman [16]. Although there may be other applications of damage mechanics to laminated composites on the threshold of making their way into the literature, we are unaware of them at this time.

Unlike metals and concrete, laminated composites are complicated by the fact that the layered orthotropy of the medium produces several distinctly different and anisotropic damage modes. Therefore, whereas it is often sufficient to deal with a single isotropic (scalar valued) damage tensor in initially isotropic and homogeneous media, this simplicity cannot be utilized in laminated composites. Furthermore, each of the damage mechanisms is interrelated and extremely difficult to distinguish experimentally. Finally, the damage may not be considered to be statistically homogeneous through the laminate thickness. Therefore, the application of continuum damage mechanics to laminated composites is much more complicated then many previous applications.

An example of a composite laminate with two distinct modes of damage is shown in Fig. 1 [17]. In this schematic there are matrix cracks in the crossplies and delaminations at the ply interfaces. Note that the cracks are oriented and statistically nonhomogeneous in the out-of-plane coordinate direction. Experimental observation [18] indicates that the matrix cracks are load induced, whereas the delaminations are driven by stress concentrations at the matrix crack tips. Therefore, significant interaction of the damage modes is observed. Although not shown in the figure, there are often additional damage modes observed prior to component failure, including fiber-matrix debonding, fiber fracture and fiber crimping and/or buckling in compression. An excellent review of the genesis of these events is described in further detail in reference 10.

The ultimate objective of any continuum mechanics model is to design away from failure. In the sense that laminated composites fail due to a complex sequence of damage events, it is essential to capture the important features of the damage process in order to accurately predict failure. In other words, the failure function should accurately reflect the history of damage via the damage parameters. Although this will be a complex task in laminated composites, the current paper discusses an ongoing effort to do just that.

A continuum damage model must contain four essential ingredients: 1) stress-strain-damage equations; 2) damage growth laws for the damage ISV's; 3) a failure function describing local failure in terms of the damage ISV's and observable state variables; and 4) an algorithm for solving boundary value problems in which the state is nonhomogeneous. If steps one through three can be accomplished accurately, then step four is relatively straightforward, involving a procedure not unlike extending an elastic algorithm to include plasticity. Steps two and three tend to be the most complex,

2

especially for laminated composites. Although there has been some research on these two components of the model, the authors would consider this work exploratory at this time. The subject of the current paper is step one. The fundamental difficulty in this procedure is to develop a model which is independent of ply orientation and stacking sequence. Of course, the ultimate goal of this research is step three, to predict failure as a function of the current damage state.

MODEL DEVELOPMENT

The authors have been developing a model for predicting the constitutive behavior of laminated continuous fiber composites [12-15]. This model utilizes the concept of continuum damage mechanics, in the sense that the effects of microcracks are reflected via internal state variables (ISV's) in the constitutive equations, rather than treating each microcrack as a separate internal boundary. Because only the average macroscale effect of microcracking is modelled rather than the effect of each individual crack, the model is phenomenological in nature. Since cracking is not statistically homogeneous in the coordinate direction normal to the laminate, statistical weighting is necessary in this direction, and this is accomplished via kinematic constraints imposed on the laminate equations.

The model has recently been extended to predict the response of laminates with both matrix cracks and interior delaminations [14], as shown in Fig. 1. This problem is complicated by two factors. First, because these two damage mechanisms are oriented differently, they require two separate tensor-valued damage parameters. Furthermore, the mechanics of these two damage modes are substantially different. The matrix cracks may be assumed to be statistically homogeneous over each ply in a small local volume element. Therefore, classical local volume averaging may be used to obtain this damage parameter. On the other hand, delaminations are not statistically homogeneous in the z coordinate direction. This requires that a modification be made to statistical averaging techniques. Although statistical homogeneity is assumed in the x and y coordinate directions, a kinematic constraint similar to the Kirchhoff-Love hypothesis is applied in the z direction. The resulting damage parameter is a weighted measure of damage, with delaminations away from the neutral surface causing a greater effect on laminate properties.

The model development proceeds from the assumption that all material inelasticity is contained within small zones surrounding the microcracks. The effect of matrix cracks on ply level constitutive equations is accounted for via the local volume average of the diadic product of the crack opening displacement vector u_i^c and the crack face normal n_j^c.

3

$$\alpha^M_{ij} = \frac{1}{V_L} \int_{S_C} u^C_i n^C_j ds \qquad (1)$$

where V_L is the local volume for which cracking can be considered statistically homogeneous, and S_c is the surface area of cracks in V_L. For matrix cracking V_L is typically one ply in thickness. The ply level stress-strain relations are therefore given by

$$\sigma_{ij} = C_{ijk\ell}(\epsilon_{k\ell} - \alpha^M_{k\ell}) \qquad (2)$$

In order to account for interply delamination the following kinematic assumption is made (See Fig. 2.):

$$u(x,y,z) = u^o(x,y) - z[\beta^o + H(z-z_k)\beta^D_k] + H(z-z_k)u^D_k \qquad (3)$$

$$v(x,y,z) = v^o(x,y) - z[\psi^o + H(z-z_k)\psi^D_k] + H(z-z_k)v^D_k \qquad (4)$$

and

$$w(x,y,z) = w^o(x,y) - H(z-z_k)w^D_k \qquad (5)$$

where u and v are components of the in-plane displacement and w is the out-of-plane displacement and H is the Heavyside step function. Furthermore, β and ψ represent rotations of the midplane. The quantities with superscripts o are undamaged midsurface values, and quantities with superscripts D are caused by interlaminar cracking.

Employing standard laminate averaging techniques will result in the following laminate equations [14]

4

$$\{N\} = \sum_{k=1}^{n} [Q]_k (z_k - z_{k-1}) \{\epsilon_L^0\} - \frac{1}{2} \sum_{k=1}^{n} [Q]_k (z_k^2 - z_{k-1}^2) \{\kappa_L\}$$

$$+ \sum_{i=1}^{d} [\bar{Q}_1]_i \; t_i \begin{Bmatrix} 0 \\ 0 \\ \alpha_{1i}^D \\ \alpha_{2i}^D \\ \alpha_{3i}^D \\ 0 \end{Bmatrix} + \sum_{i=1}^{d+1} (z_i - z_{i-1}) [\bar{Q}_2]_i \begin{Bmatrix} 0 \\ 0 \\ 0 \\ \alpha_{4i}^D \\ \alpha_{5i}^D \\ 0 \end{Bmatrix}$$

$$- \sum_{k=1}^{n} [Q]_k (z_k - z_{k-1}) \{\alpha^M\}_k \qquad (6)$$

$$\{M\} = \frac{1}{2} \sum_{k=1}^{n} [Q]_k (z_k^2 - z_{k-1}^2) \{\epsilon_L^0\} - \frac{1}{3} \sum_{k=1}^{n} [Q]_k (z_k^3 - z_{k-1}^3) \{\kappa_L\}$$

$$+ \sum_{i=1}^{d} [\bar{Q}_3]_i \; t_i^2 \begin{Bmatrix} 0 \\ 0 \\ \alpha_{1i}^D \\ \alpha_{2i}^D \\ \alpha_{3i}^D \\ 0 \end{Bmatrix} + \sum_{i=1}^{d+1} [\bar{Q}_4]_i (z_i^2 - z_{i-1}^2) \begin{Bmatrix} 0 \\ 0 \\ 0 \\ \alpha_{4i}^D \\ \alpha_{5i}^D \\ 0 \end{Bmatrix}$$

$$- \frac{1}{2} \sum_{k=1}^{n} [Q]_k (z_k^2 - z_{k-1}^2) \{\alpha^M\}_k \qquad (7)$$

where $\{N\}$ and $\{M\}$ are the resultant forces and moments per unit length respectively, and $\{\alpha^M\}_k$ and $\{\alpha_L^D\}$ represent the damage due to matrix cracking and interply delamination, respectively. Furthermore, n is the number of plies, and d is the number of delaminated ply interfaces, as shown in Fig. 3.

The internal state variable for delamination, $\{\alpha_L^D\}$, is obtained by employing the divergence theorem on a local volume element of the laminate. The resulting procedure gives [14]

5

$$a_{1i}^{D} = \frac{2}{V_{Li}} \int_{S_{2i}} w_i^{D} n_z dS \tag{8a}$$

$$a_{2i}^{D} = \frac{2}{V_{Li}} \int_{S_{2i}} v_i^{D} n_z dS \tag{8b}$$

$$a_{3i}^{D} = \frac{2}{V_{Li}} \int_{S_{2i}} u_i^{D} n_z dS \tag{8c}$$

$$a_{4i}^{D} = \frac{1}{A_L} \int_{S_{2i}^{B}} \psi_i^{D} n_z dS \tag{8d}$$

$$a_{5i}^{D} = \frac{1}{A_L} \int_{S_{2i}^{B}} \beta_i^{D} n_z dS \tag{8e}$$

where the subscript i is associated with the ith delaminated ply interface. Furthermore, V_{Li} is equivalent to $t_i A_L$, where t_i is the thickness of the two plies above and below the delamination, as shown in Fig. 4.

Furthermore, the matrices [Q] with subscripts k are the standard elastic property matrices for the undamaged plies. The matrices [$\bar{Q}$] with subscripts i apply to the ith delaminated ply interface. They represent average properties of the plies above and below the delamination. These are described in further detail in reference 14.

Determination of E_x and ν_{xy} for the Mixed Damage Mode

Now, suppose that one is interested in modeling stiffness loss as a function of damage state. In order to do this it is necessary to construct the (stacking sequence independent) material parameters developed in the previous section. The loading direction engineering modulus, E_x, and Poisson's ratio, ν_{xy}, of the laminate are defined as

$$E_x \equiv \frac{1}{t} \frac{\partial N_x}{\partial \epsilon_x} \tag{9}$$

$$\nu_{xy} \equiv \frac{\frac{1}{t} \frac{\partial N_x}{\partial \epsilon_y}}{\frac{1}{t} \frac{\partial N_y}{\partial \epsilon_y}} \tag{10}$$

6

For the purpose of comparing the model predictions to experimental results, we will confine this development to the case of a symmetric, balanced laminate with a delamination site symmetrically located with respect to the laminate midplane. For this special case, $\{K\} = 0$ and the fourth term in equation (6) is zero. Furthermore, $\alpha_{1i} = 0$ and the third term in equation 6 is the same for both delamination sites. Substituting equation (6) into equations (9) and (10) results in the following expressions for E_x and ν_{xy}

$$E_x = \frac{1}{n} \sum_{k=1}^{n} (Q_{11})_k (1 - \frac{\partial \alpha_x^M}{\partial \epsilon_x})_k + 2 (\frac{2}{n}) (\overline{Q}_{14} \frac{\partial \alpha_2^D}{\partial \epsilon_x} + \overline{Q}_{15} \frac{\partial \alpha_3^D}{\partial \epsilon_x}) \quad (11)$$

$$\nu_{xy} = \frac{\frac{1}{n} \sum_{k=1}^{n} (Q_{12})_k (1 - \frac{\partial \alpha_x^M}{\partial \epsilon_y})_k + 2 (\frac{2}{n}) (\overline{Q}_{14} \frac{\partial \alpha_2^D}{\partial \epsilon_y} + \overline{Q}_{15} \frac{\partial \alpha_3^D}{\partial \epsilon_y})}{\frac{1}{n} \sum_{k=1}^{n} (Q_{22})_k (1 - \frac{\partial \alpha_y^M}{\partial \epsilon_y})_k + 2 (\frac{2}{n}) (\overline{Q}_{24} \frac{\partial \alpha_2^D}{\partial \epsilon_y} + \overline{Q}_{25} \frac{\partial \alpha_3^D}{\partial \epsilon_y})} \quad (12)$$

where it is assumed that all plies have the same thickness so that

$$z_k - z_{k-1} = t_{ply} \quad (13a)$$

$$\frac{t_{ply}}{t} = \frac{1}{n} \quad (13b)$$

$$\frac{t_1}{t} = \frac{2}{n} \quad (13c)$$

Furthermore, damage introduces local anisotropy so that

$$[Q]_k = \begin{bmatrix} Q_{11} & Q_{12} & Q_{13} & Q_{14} & Q_{15} & Q_{16} \\ Q_{12} & Q_{22} & Q_{23} & Q_{24} & Q_{25} & Q_{26} \\ Q_{16} & Q_{26} & Q_{36} & Q_{46} & Q_{56} & Q_{66} \end{bmatrix} \quad (14)$$

7

It has been previously shown [19] that

$$\overline{Q}_{14} = \frac{1}{2} (\overline{Q}_{12}^{A} + \overline{Q}_{12}^{B}) \tag{15}$$

$$\overline{Q}_{15} = \frac{1}{2} (\overline{Q}_{11}^{A} + \overline{Q}_{11}^{B}) \tag{16}$$

$$\overline{Q}_{24} = \frac{1}{2} (\overline{Q}_{22}^{A} + \overline{Q}_{22}^{B}) \tag{17}$$

$$\overline{Q}_{25} = \frac{1}{2} (\overline{Q}_{12}^{A} + \overline{Q}_{12}^{B}) \tag{18}$$

where the superscripts A and B designate the property of the ply immediately above and below the delamination, respectively.

Determination of Internal State Variables

Implementation of equations (11) and (12) to predict the damage degraded laminate moduli requires the specification of the partial derivatives of the internal state variables for a given damage state. In the absense of growth laws, the damage state must be determined experimentally. Expressions for the internal state variables have been previously developed by the authors [13,14] by employing energy principles. In the original constitutive theory formulation [12] the local energy loss contribution to the Helmholtz free energy is directly related to the internal state variables. Furthermore, the local energy loss is also directly related to the fracture mechanics based strain energy release rate for crack creation during load-up. Therefore, expressions for the internal state variables have been developed from expressions for the strain energy release rate for each damage mode. In the case of matrix cracking in cross-ply laminates,

$$\frac{\partial \alpha_x^M}{\partial \epsilon_x} = \frac{1}{2} m \frac{(p+q)}{q} \frac{E_{x_0}}{E_{22}} \left(\frac{E_{x_1}}{E_{x_0}} \Bigg|_{S_{M_1}} - 1 \right) \tag{19}$$

8

where m is the number of consecutive 90° plies, p is the number of 0° plies, q is the number of 90° plies, E_{x_o} is the initial undamaged modulus, and E_{x_1} is the damage-degraded modulus corresponding to matrix crack damage state S_{M_1}. The term in the parentheses was determined experimentally from tests on a $[0/90/0]_s$ laminate and is given by

$$\frac{E_{x_1}}{E_{x_o}}\bigg|_S = 0.99969 - 0.061607\ S + 0.04623\ S^2 \qquad (20)$$

Finite element studies have shown that the effects of adjacent layer constraint on the energy released by the 90° layers is a second order effect [20]. Therefore, by using the following second order tensor transformation

$$\frac{\partial \bar{\alpha}^M_{ij}}{\partial \bar{\epsilon}^0_{mn}} = a_{\bar{i}p}\ a_{\bar{j}p}\ a_{\bar{m}r}\ a_{\bar{n}s}\ \frac{\partial \alpha^M_{pq}}{\partial \epsilon^0_{rs}} \qquad (21)$$

where no bars refer to the crack coordinate system and the over bars refer to the laminate coordinate system, equation (19) is generally applicable to matrix crack damage in any ply of any laminate stacking sequence.

In the case of off axis plies, other than 90°, the tensor transformation law given by equation (21) also requires the determination of $\partial \alpha^M_{12}/\partial \epsilon_{12}$ for matrix crack damage. This damage parameter is related to shear deformation at the ply level which gives rise to the sliding mode of relative crack face displacements.

Considering only that part of the energy loss, u^C_L, due to shear behavior we have [12]

$$u^C_L = I_{68}\epsilon_6\alpha_8 + H.O.T.'s \qquad (22)$$

where $I_{68}= -G_{12}$, the tensorial shear strain $\epsilon_6=\epsilon_{12}$, and $\alpha_8=\alpha_{12}$ in contracted notation. Using fracture mechanics concepts the local energy loss may also be expressed in terms of the mode II strain energy release rate due to matrix cracking, G_{II_M}, as

$$u^C_L = \frac{1}{V_L} \int_{S_M} G_{II_M} dS \qquad (23)$$

9

where S_M is the matrix crack surface area in the local volume element, and V_L is the local volume for a single ply.

Equating expressions (22) and (23) and neglecting higher order terms yields

$$\alpha_8 = \frac{1}{G_{12}V_L\epsilon_6} \int_{S_M} G_{II_M} dS \tag{24}$$

We now require an expression for G_{II_M} as a function of S_M. The strain energy release rate may be defined as

$$G_{II_M} = -\frac{\partial U}{\partial S} \tag{25}$$

where U = strain energy of the local volume due to shear behavior. For a linear elastic material,

$$U = \frac{1}{2} \epsilon_{12}\sigma_{12}V_L \tag{26}$$

$$= 2G_{12}\epsilon_6^2 V_L$$

where it is recalled that ϵ_6 is the tensorial shear strain. For cracking in the fixed grip case where the "effective" material stiffness is changing while the strain is held constant, substituting equation (26) into equation (25) results in

$$G_{II_M} = -2V_L\epsilon_6^2 \frac{\partial G_{12}}{\partial S} \tag{27}$$

where $\partial G_{12}/\partial S$ is interpreted as the change in the "effective" shear modulus due to matrix crack development. Substituting (27) into (24) yields

$$\alpha_8 = -\frac{2\epsilon_6}{(G_{12})_0} \int_{S_M} \left(\frac{\partial G_{12}}{\partial S}\right) dS \tag{28}$$

where G_{12} in equation (24) is written as $(G_{12})_0$ to distinguish the initial undamaged modulus, $(G_{12})_0$, from the degraded modulus, G_{12}. To evaluate equation (28) and specify the damage parameter, $\partial\alpha_8/\partial\epsilon_6$, we

10

must have an expression for G_{12} as a function of S. Since $\partial G_{12}/\partial S$ is interpreted as the rate of change of the effective shear modulus, this can be determined experimentally from the $[\pm 45]_{2s}$ where the plies are in a state of pure shear. For this laminate

$$G_{12} = \frac{\overline{\sigma}_x}{2(\epsilon_x - \epsilon_y)} \qquad (29)$$

where $\overline{\sigma}_x$ is an applied uniaxial tensile stress, ϵ_x is the strain in the loading direction, and ϵ_y is the strain in the transverse direction. By using a 1.0 in. biaxial extensometer, equation (29) gives G_{12} as a function of matrix crack damage in the 1.0 in. x 1.0 in. local volume as measured in the simple uniaxial test. Determining G_{12} in this manner, $\partial G_{12}/\partial S$ in equation (28) may be directly integrated and the damage parameter becomes

$$\frac{\partial \alpha_8}{\partial \epsilon_6} = - \frac{2}{(G_{12})_0} \int_{S_M} \frac{dG_{12}}{dS} \, dS \qquad (30)$$

The results of monotonic tensile tests on $[\pm 45]_{2s}$ laminates of AS4/3502 graphite-epoxy revealed an approximately linear relationship between G_{12} and S. Furthermore, the number of matrix cracks in each ply was essentially the same. Assuming a linear relationship between G_{12} and S, equation (30) becomes

$$\frac{\partial \alpha_8}{\partial \epsilon_6} \bigg|_{S_M} = 2 \left[1 - \frac{(G_{12})_{EXP}}{(G_{12})_0} \right] \frac{S_M}{S_{EXP}} \qquad (31)$$

where $(G_{12})_{EXP}/(G_{12})_0 = 0.822$ for S_{EXP} corresponding to 21 cracks per inch in each ply of the $[\pm 45]_{2s}$. Since the plies of the $[\pm 45]_{2s}$ are in pure shear, expression (31) may be used to determine $\partial \alpha_8/\partial \epsilon_6$ for any ply with matrix crack damage. The fiber (crack) orientation of the cracked ply is accounted for by the coordinate transformation given by equation (21).

The delamination internal state variable was determined from energy principles as well, except O'Brien's [21] strain energy release rate model was used rather than experimental results. Since O'Brien's model assumes that the strain energy release rate is independent of

11

the size of the delamination, the internal state variable is linear in delamination surface area. Therefore,

$$\frac{\partial \alpha_3^D}{\partial \epsilon_x} = -\frac{n}{2} \frac{(E_{x_o} - E^*)}{\overline{Q}_{15}} \left(\frac{S_D}{S}\right) \tag{32}$$

where n is the number of plies in the laminate, S_D is the delamination area and S is the total interfacial area in the local volume. E^* is the modulus of the sublaminates formed by the delamination and is given by

$$E^* = \frac{1}{t} \sum_{i=1}^{d} E_i t_i \tag{33}$$

where d is the number of sublaminates and t is the laminate thickness. By similar reasoning,

$$\frac{\partial \alpha_2^D}{\partial \epsilon_y} = -\frac{n}{2} \frac{(E_{y_o} - E^*)}{\overline{Q}_{24}} \left(\frac{S_D}{S}\right) \tag{34}$$

Finally, as a first approximation for the cross-derivatives in equations (11) and (12), we have

$$\frac{\partial \alpha_x^M}{\partial \epsilon_y} = \frac{S_{12}}{S_{22}} \frac{\partial \alpha_x^M}{\partial \epsilon_x} \tag{35}$$

$$\frac{\partial \alpha_3^D}{\partial \epsilon_y} = \frac{S_{12}}{S_{22}} \frac{\partial \alpha_3^D}{\partial \epsilon_x} \tag{36}$$

$$\frac{\partial \alpha_2^D}{\partial \epsilon_x} = \frac{S_{12}}{S_{11}} \frac{\partial \alpha_3^D}{\partial \epsilon_x} \tag{37}$$

where S_{ij} is defined by the following undamaged laminate stress-strain relationships using the first term of equation (6)

$$S_{11} = \frac{1}{t} \frac{\partial N_x}{\partial \epsilon_x} \tag{38}$$

12

$$S_{22} = \frac{1}{t} \frac{\partial N_y}{\partial \epsilon_y} \tag{39}$$

$$S_{12} = \frac{1}{t} \frac{\partial N_x}{\partial \epsilon_y} \tag{40}$$

As an example, consider the case of cross-ply laminates where the delamination site is at a 0/90 interface. Equations (11) and (12) reduce to the following simplified forms

$$E_x = E_{x_o} [1 - \frac{1}{n E_{x_o}} \sum_{k=1}^{n} (Q_{11})_k (\frac{\partial \alpha_x^M}{\partial \epsilon_x})_k - \frac{1}{2} (1 - \frac{E^*}{E_{x_o}}) (\frac{S_D}{S})] \tag{41}$$

$$\nu_{xy} = \nu_{xy_o} [1 - 2 (\frac{p}{n} \frac{E_{22}}{E_{11} + E_{22}} + \frac{q}{n}) (\frac{S_D}{S})] \tag{42}$$

where E_{11}, E_{22} and ν_{12} are the standard lamina properties. It should be noted that for cross-ply laminates $\partial \alpha_x^M / \partial \epsilon_x$ is the only nonzero internal state variable for matrix cracking. ($\partial \alpha_x^M / \partial \epsilon_x$ is a ply property given by equation (19).)

Experimental Program

A limited experimental program has been conducted to verify the accuracy of the constitutive model formulation. Experimental tests have been conducted on tensile specimens from a number of quasi-isotropic and cross-ply laminates. The material system is AS4/3502 graphite/epoxy with $E_{11} = 21.0 \times 10^6$ psi (144.8 GPa), $E_{22} = 1.39 \times 10^6$ psi (9.58 GPa), $\nu_{12} = 0.310$ and $G_{12} = 0.694 \times 10^6$ psi (4.79 GPa). The fiber volume fraction is approximately 65% and the per ply thickness is 0.0055 in. (0.132 mm). The loading-direction modulus and Poisson's ratio were measured by a biaxial extensometer with a 2 in. gage length. Damage was developed under tension-tension fatigue at 2Hz and R=0.1. The progression of damage was documented by periodic examinations by x-ray radiography and edge replication. Modulus measurements were taken at each examination.

Comparison of Experimental Results to Model Predictions

The comparison of model predictions to experimental results for

13

E_x and ν_{xy} is displayed in graphical form in the bar charts of Figs. 5 and 6, respectively. Matrix cracks in the 90° layers are at the saturation damage state for all laminates. The delamination interface location and percent of delamination is listed under the laminate stacking sequences in the bar charts. An x-ray radiograph of the typical damage state in a $[0/90_3]_s$ and $[90/\pm45/0]_s$ laminate is shown in Figs. 7 and 8, respectively. It should be noted that Poisson's ratio values for the two quasi-isotropic laminates are not given because they were not measured experimentally. The comparison between the experimental results and model results is quite close for E_x. However, there are some discrepancies in the comparison of ν_{xy} values. The authors attribute these discrepancies to the difficulty in measuring Poisson's ratio. Because Poisson's ratio is quite small for cross-ply laminates, the measurement is more sensitive to experimental error.

SUMMARY AND CONCLUSIONS

The authors have formulated a constitutive model for laminated composites with both matrix cracks and delamination damage. The model is based on the concept of continuum damage mechanics and uses second-order tensor valued internal state variables to represent each mode of damage. The internal state variables are the local volume averaged measure of the relative crack face displacements. The local volume for matrix crack damage is at the ply level, whereas the local volume for delamination damage is at the laminate level. Therefore, the damage-dependent constitutive model takes the form of laminate analysis equations modified by inclusion of the internal state variables.

This paper demonstrates the applicability of the model to predict the degraded engineering modulus, E_x, and Poisson's ratio, ν_{xy}, of quasi-isotropic and cross-ply laminates of graphite/epoxy. The comparison between model predictions and experimental results is very close. The authors believe that the good agreement reported herein demonstrates the validity of the model formulation and the physical interpretation of the internal state variables.

ACKNOWLEDGEMENT

14

REFERENCES

1. Onsager, L., 'Reciprocal Relations in Irreversible Process I.,'
    Physics Review, Vol. 37, pp. 405-426, 1931.

2. Rabotnov, Y.N., Creep Problems in Structural Members, North-
    Holland, Amsterdam, 1969.

3. Bazant, Z.P., 'Mechanics of Distributed Cracking,' Applied
    Mechanics Reviews, Vol. 39, pp. 675-705, 1986.

4. Krajcinovic, D., 'Continuum Damage Mechanics,' Applied Mechanics
    Reviews, Vol. 37, pp. 1-6, 1984.

5. Krajcinovic, D., 'Update to Continuum Damage Mechanics,' Applied
    Mechanics Update 1986, Steele, C.R., and Springer, G.S., Eds.,
    The American Society of Mechanical Engineers, pp. 403-406, 1986.

6. Kachanov, L.M., Introduction to Continuum Damage Mechanics,
    Martinus Nijhoff, Dordrecht, 1986.

7. Talreja, R., 'A Continuum Mechanics Characterization of Damage in
    Composite Material Proc. R. Soc. London, Vol. 399A, 1985, pp.
    195-216.

8. Talreja, R., 'Residual Stiffness Properties of Cracked Composite
    Laminates,' Advances in Fracture Research, Proc. Sixth Int. Conf.
    de Fracture, New Delhi, India, Vol. 4, pp. 3013-3019, 1985.

9. Talreja, R., 'Transverse Cracking and Stiffness Reduction in
    Composite Laminates,' Journal of Composite Materials, Vol. 21,
    pp. 355-375, 1985.

10. Talreja, R., Fatigue of Composite Materials, Technical University
    of Denmark, Lyngby, Denmark, 1985.

11. Talreja, R., 'Stiffness Properties of Composite Laminates with
    Matrix Cracking and Interior Delamination,' Danish Center for
    Applied Mathematics and Mechanics, The Technical University of
    Denmark, No. 321, March, 1986.

12. Allen, D.H., Harris, C.E., and Groves, S.E., 'A Thermomechanical
    Constitutive Theory for Elastic Composites with Distributed
    Damage - Part I: Theoretical Development,' to appear in
    International Journal of Solids and Structures, 1987.

15

13. Allen, D.H., Harris, C.E., and Groves, S.E., 'A Thermomechanical Constitutive Theory for Elastic Composites with Distributed Damage - Part II: Application to Matrix Cracking in Laminated Composites,' to appear in <u>International Journal of Solids and Structures</u>, 1987.

14. Allen, D.H., Groves, S.E., and Harris, C.E., 'A Cumulative Damage Model for Continuous Fiber Composite Laminates with Matrix Cracking and Interply Delaminations,' to appear in <u>Composite Materials Testing and Design, 8th Symposium, ASTM STP</u>, American Society for Testing and Materials, Philadelphia, 1987.

15. Allen, D.H., Harris, C.E., Groves, S.E., and Norvell, R.G., 'Characteristics of Stiffness Loss in Crossply Laminates with Curved Matrix Cracks,' to appear in <u>Journal of Composite Materials</u>, 1987.

16. Weitsman, Y., 'Environmentally Induced Damage in Composites,' <u>Proceedings of the 5th Symposium on Continuum Modeling of Discrete Structures</u>, A.J.M. Spencer, Ed., Nottingham, U.K., 1985.

17. Jamison, R.D., Schulte, K., Reifsnider, K.L., and Stinchcomb, W.W., 'Characterization and Analysis of Damage Mechanisms in Tension-Tension Fatigue of Graphite/Epoxy Laminates,' <u>Effects of Defects in Composite Materials</u>, ASTM STP 836, American Society for Testing and Materials, 1984, pp. 21-55.

18. Georgiou, I.T., 'Initiation Mechanisms and Fatigue Growth of Internal Delaminations in Graphite/Epoxy Cross-Ply Laminates,' Texas A&M University Thesis, December, 1986.

19. Groves, S.E., 'A Study of Damage Mechanics in Continuous Fiber Composite Laminates with Matrix Cracking and Internal Delaminations,' Ph.D Thesis, Texas A&M University, College Station, Tx, December 1986.

20. Harris, C.E., Allen, D.H., and Nottorf, E.W., 'Modelling Stiffness Loss in Quasi-Isotropic Laminates Due to Microstructural Damage,' to appear in <u>Journal of Engineering Materials and Technology</u>, American Society of Mechanical Engineers, Jan. 1988.

21. O'Brien, T.K., 'Characterization of Delamination Onset and Growth in a Composite Laminate,' <u>Damage in Composite Materials</u>, K.L. Reifsnider, Ed., ASTM STP 775, American Society for Testing and Materials, Philadelphia, pp. 141-167, 1982.
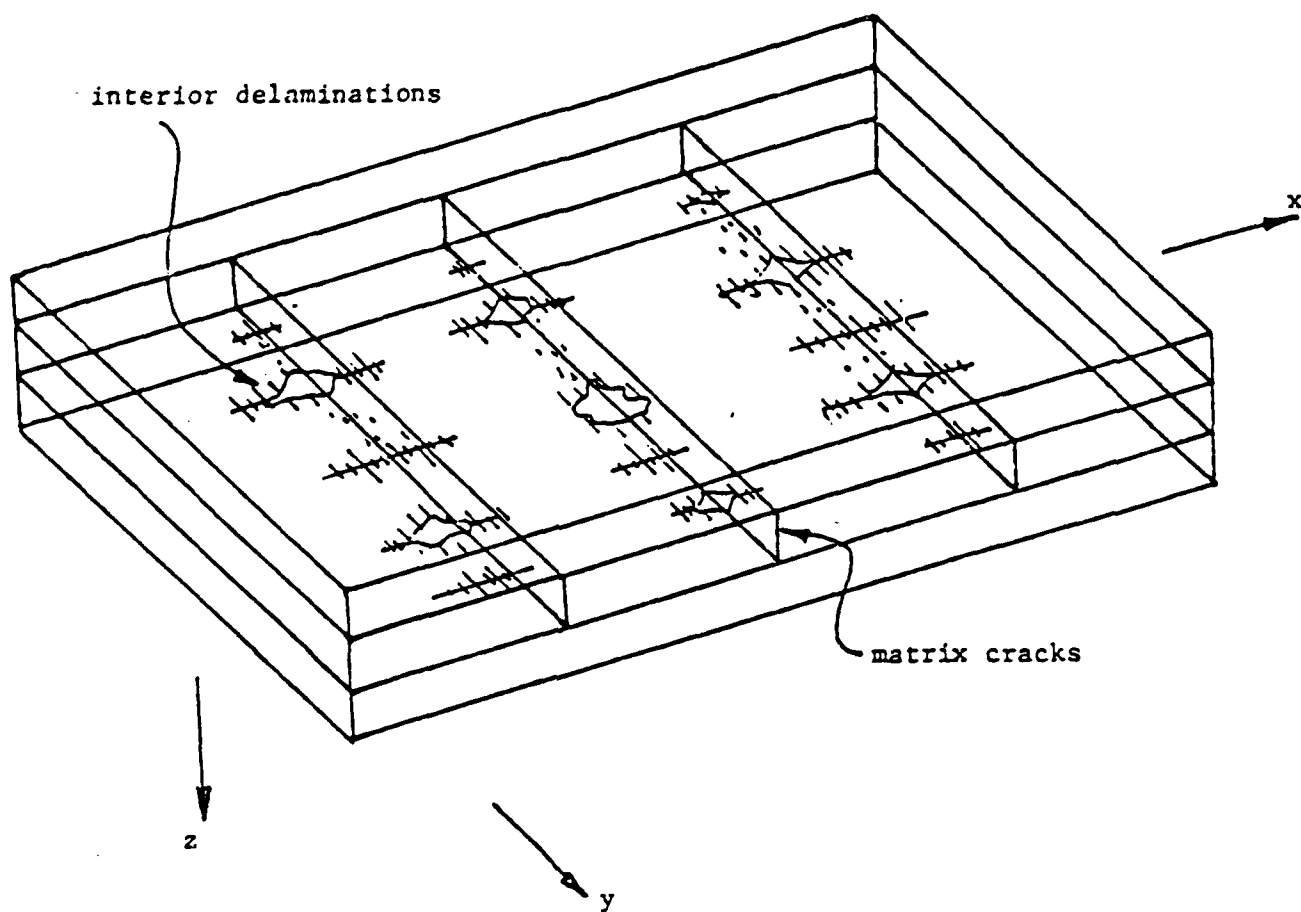
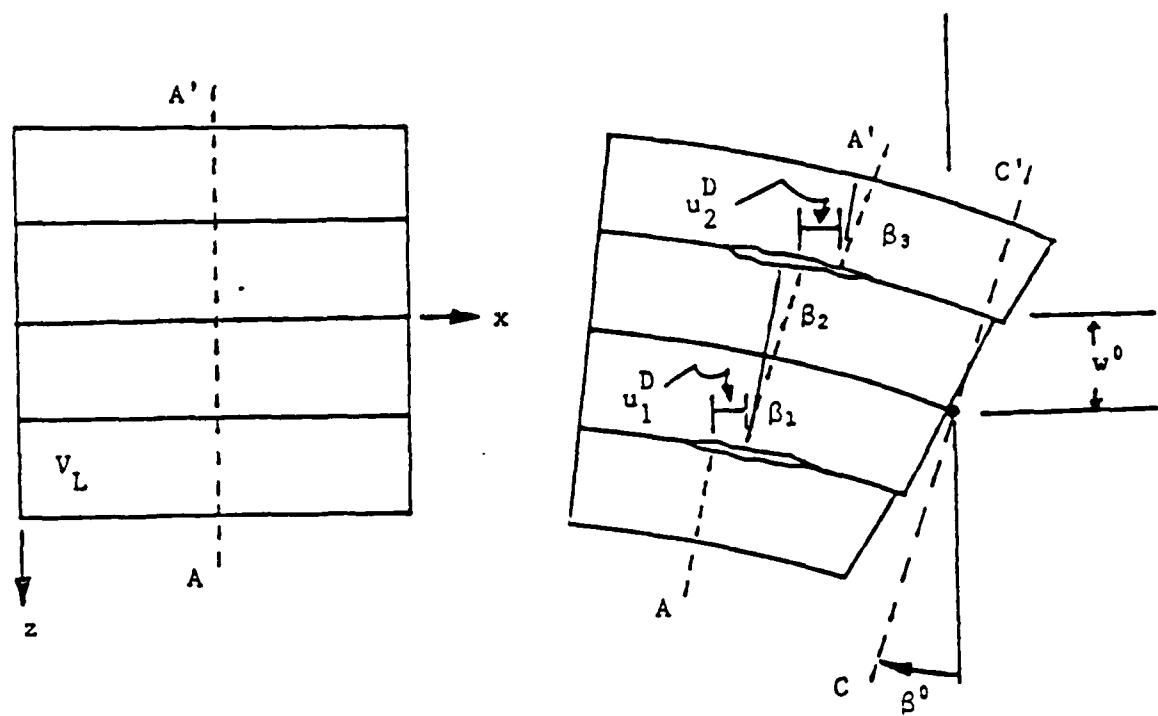Fig. 1 Crossply Laminate Showing Combined Matrix Cracking and Interior Delaminations
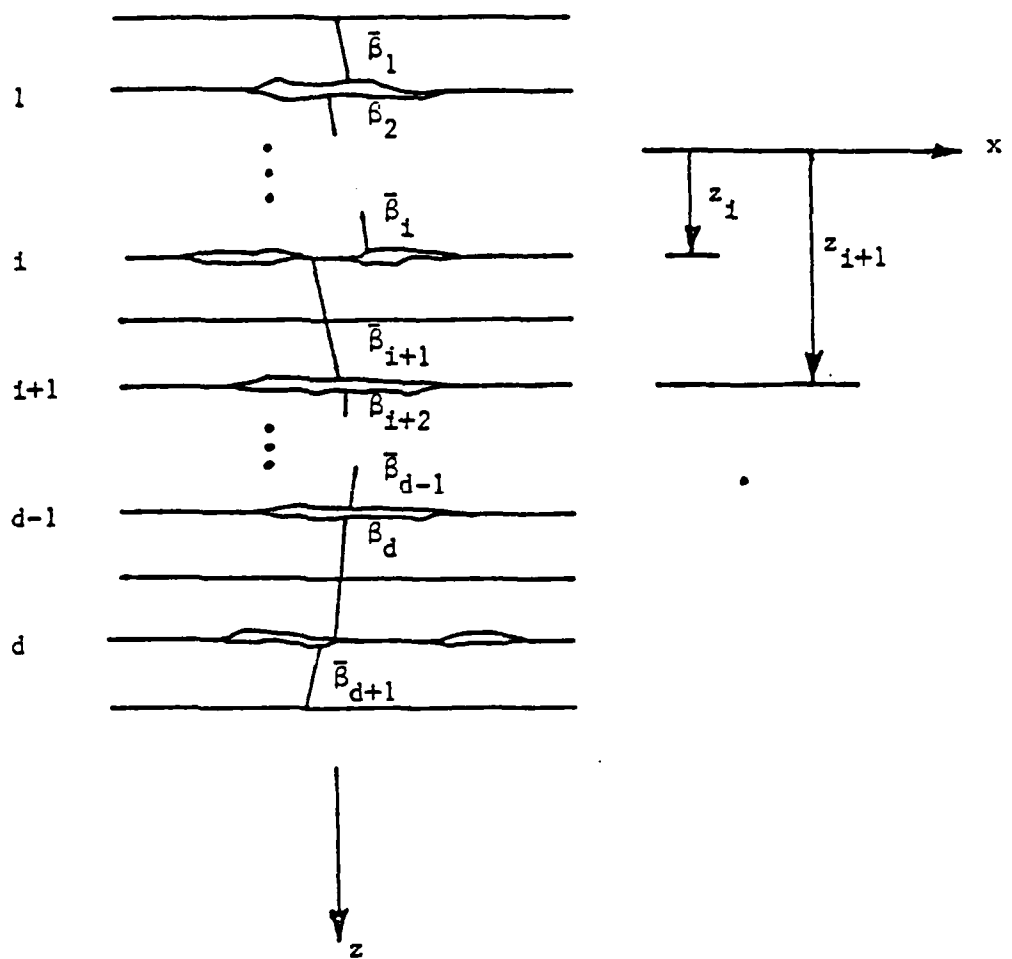
Fig. 2   Deformation Geometry for Region A_L

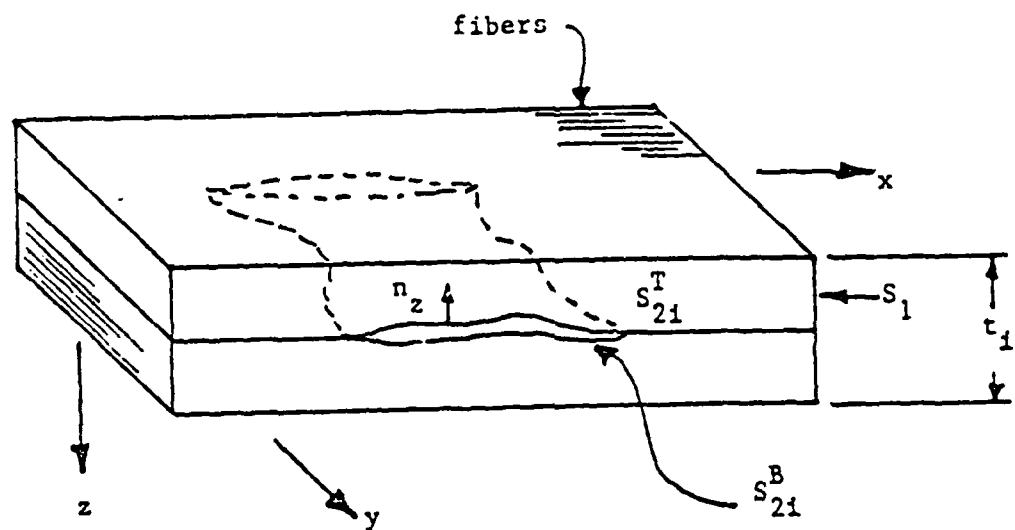Fig. 3 Schematic of Delaminated Region in a Composite Layup

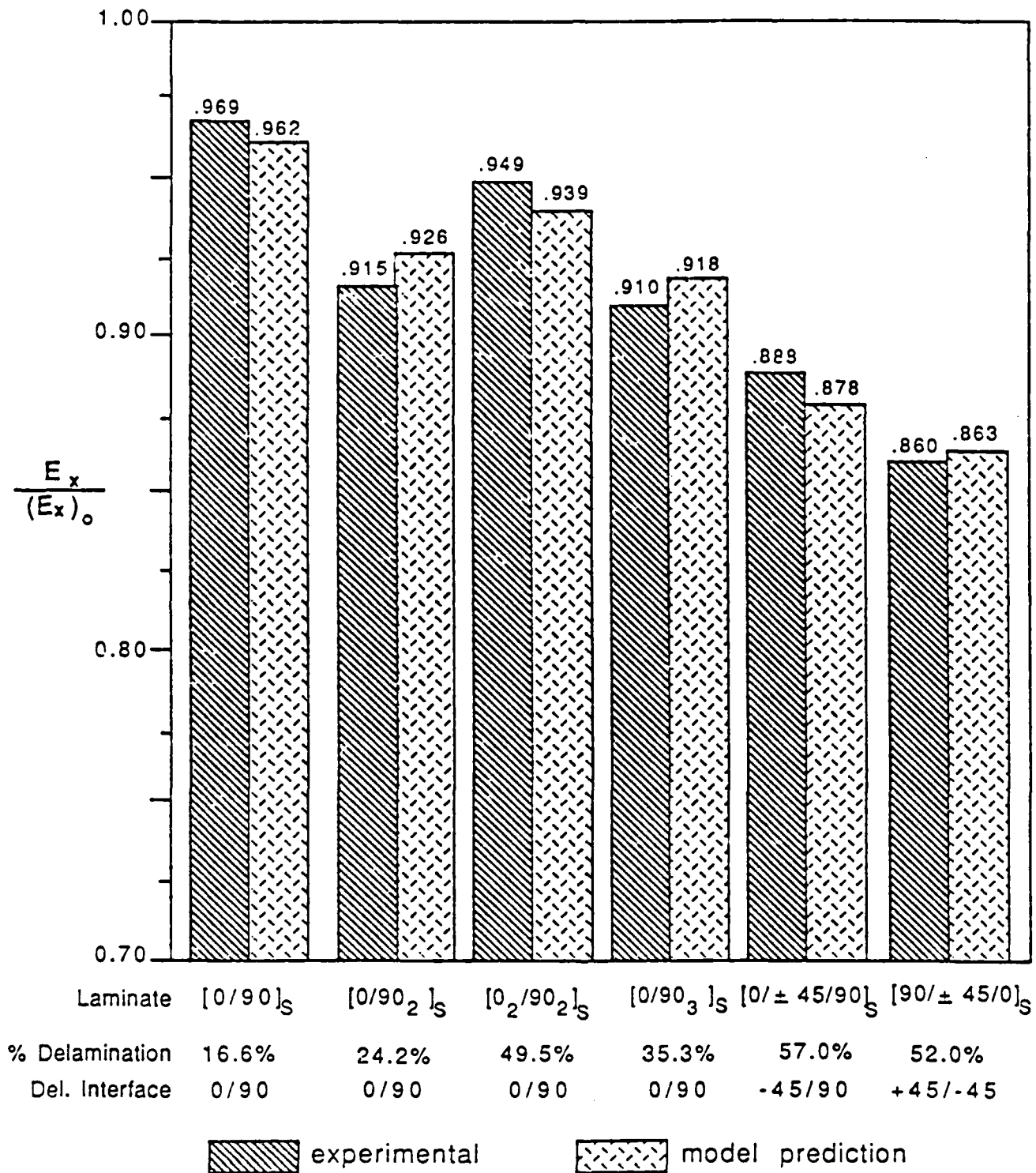Fig. 4 Interply Delamination in a Laminated Continuous Fiber Composite

Fig. 5 Comparison of Experimental Results and Model Predictions of the Laminate Engineering Modulus, E_x Degraded by Both Matrix Cracking and Delamination Damage.
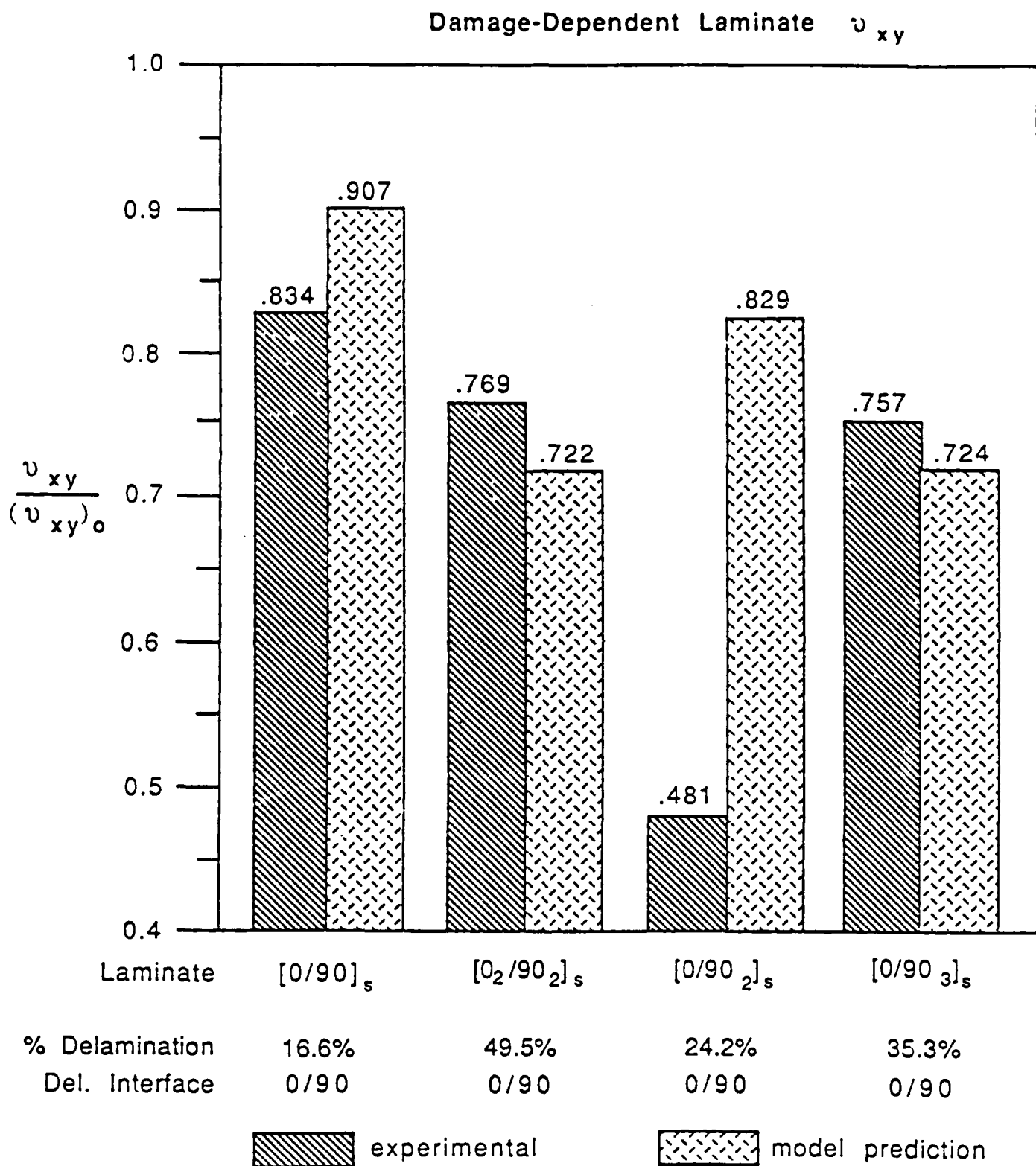
Fig. 6 Comparison of Experimental Results and Model Predictions of the Laminate Engineering Poisson's Ratio, υ_{xy} , Degraded by Both Matrix Cracking and Delamination Damage.
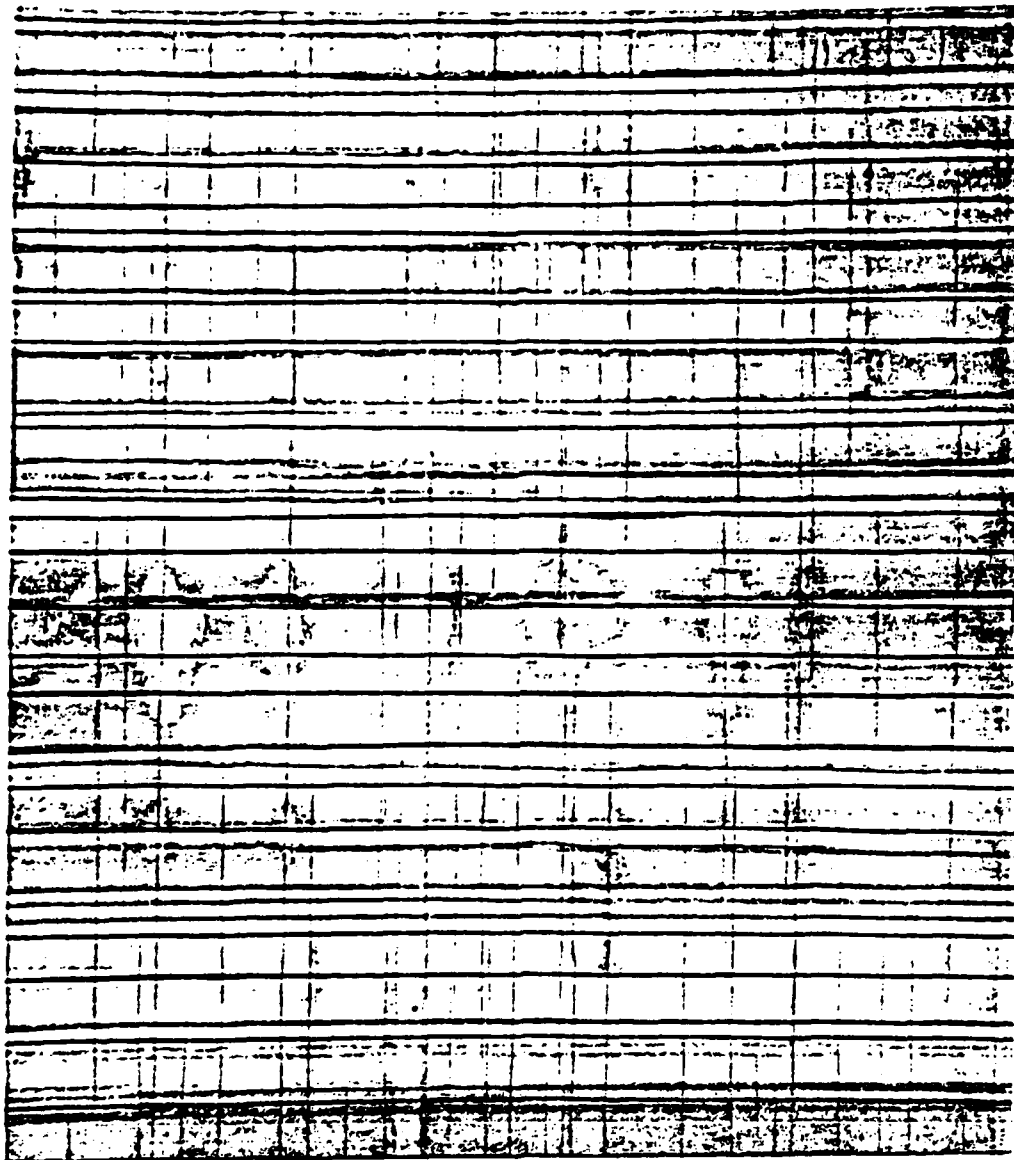
Fig. 7   Typical Fatigue-Induced Damage State in a
          $[0/90_3]_s$ Graphite/Epoxy Laminate; R=0.1;
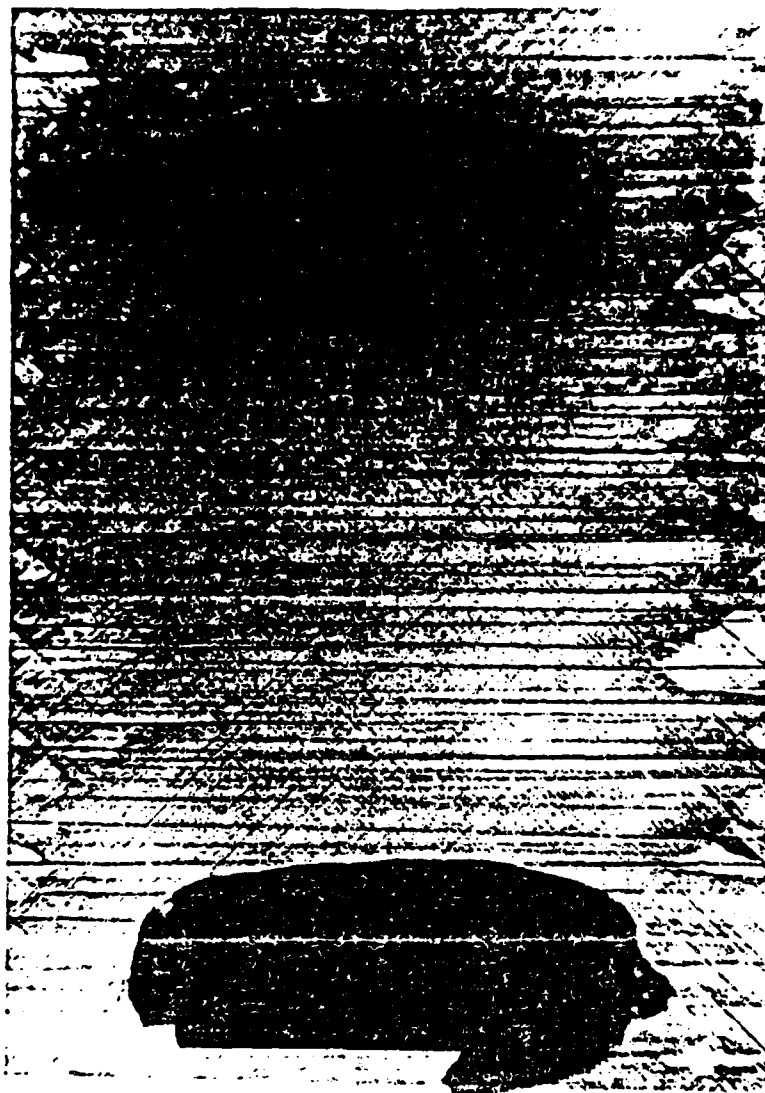   f=2 hz; 200,000 cycles at S_{max}=73% of S_{ult}

Fig. 8   Typical Fatigue-Induced Damage State is a
         $[90/\pm45/0]_s$ Graphite/Epoxy Laminate; R=0.1;
         f=2 hz; 50,000 cycles at S_{max}=73% of S_{ult}.

Appendix 7.10

INTERNAL STATE VARIABLE APPROACH FOR PREDICTING

STIFFNESS REDUCTIONS IN FIBROUS LAMINATED COMPOSITES

WITH MATRIX CRACKS

by

Jong-Won Lee[*],
D. H. Allen[**]

Aerospace Engineering Department
Texas A&M University
College Station, TX. 77843
(409) 845-1669

and
C. E. Harris[***]

June, 1988

   [*] Research Assistant
  [**] Professor
[***] Head, Fatigue and Fracture Branch, NASA Langley Research Center

ABSTRACT

A mathematical model utilizing the Internal State Variable(ISV) concept is proposed for predicting the upper bound of the reduced axial stiffnesses in cross-ply laminates with matrix cracks. The axial crack opening displacement at the matrix crack surface is explicitly expressed in terms of the observable axial strain and the undamaged material properties.

Crack parameters representing the effect of matrix cracks on the observable axial Young's modulus are predicted for Glass/Epoxy and Graphite/Epoxy material systems. The results of the present study show that the matrix crack opening displacement is significantly influenced by the ratio of crack length to the distance between two adjacent cracks resulting in stiffness reduction in a cross-ply laminate with matrix cracks.

Comparisons of the present model with experimental data and other models in the literature shows a good agreement, thus confirming direct applicability of the model to multi-layered cross-ply laminates.

INTRODUCTION

Considerable research has been focused on the mathematical modelling of stiffness reduction in fiber-reinforced laminated composite materials due to matrix cracks. Crack density, or the number of matrix cracks per unit length of each layer, has been frequently utilized as an independent variable to express the effect of matrix cracks on the observable stiffnesses of a laminate. Also, the crack density in each layer has been known to increase monotonically under cyclic loading or monotonically increasing tensile loading.

A number of experimental studies[1-3] have shown that each cracked layer, for example, the 90 degree layer in a $[0/90_n]_s$ laminate subjected to a tensile loading, can carry significant tensile loading. A fundamental question has arisen from the discrepancy between these experimental observations and the classical ply discount method, in which each cracked layer is assume to shed its entire load carrying capacity in the direction normal to the crack surfaces. A typical example of this discrepancy is shown in Fig. 1., which shows that the effective Young's modulus of a $[0/90_n]_s$ laminated specimen in the axial direction approaches asymptotically to the solution from the classical ply discount method as cracks become saturated. This discrepancy is caused by the fact that the classical ply discount method neglects all out-of-plane stress components while each cracked layer, actually a sub-structural component for a laminate, experiences a fairly high level of out-of-plane stress components which are not negligible compared with in-plane stress components.

Among existing theoretical models, Hashin's model[6] based on the complementary strain energy method may be considered as the most effective one for predicting the out-of-plane stresses and therefore, the lower bound of the effective stiffness as a function of crack density. However, there does not exist a relatively simple strain energy method based model for predicting the upper bound of the effective stiffness. Therefore, the present study proposes an explicit solution to the stiffness reduction as a function of crack density in a cross-ply laminate with arbitrary stacking sequence by introducing an Internal State Variable (ISV) based on the strain energy method.

Since matrix cracks in laminated composites can be observed at the specimen edges even with the unaided eye, the readers may be confused by the terminology "INTERNAL," in other words, "HIDDEN FROM OBSERVERS." The internal geometry and therefore the contribution of each crack to the global response of a specimen with many cracks, however, can be neither observed nor measured experimentally within reasonable accuracy. By utilizing the concept of a local volume element representing statistically homogeneous damage state, constitutive equations can be easily reconstructed to relate observable state variables and an internal state variable which is introduced by assuming a statistically homogeneous damage state. In the present study, the average value of matrix crack opening displacement multiplied by the unit normal to the crack surface is defined to be an internal state variable. At a _fixed damage state_ in which the number of matrix cracks per unit length is known, the internal state variable for representing the crack opening displacement will be explicitly expressed in terms of the kinematics of

internal cracks.

Following a brief literature survey, the theoretical development is presented along with a parameter sensitivity study of $[0_q/90_r]_s$ type laminate configurations. The usefulness of the ISV concept is also examined by comparing the result of the present research effort with available experimental and theoretical studies in the open literature. The generalization of the theoretical model is then described for cross-ply laminates together with further applicability of the ISV concept for analyzing angle-ply laminates containing arbitrarily shaped matrix cracks.

LITERATURE SURVEY

All existing theories can be categorized into five types according to their main assumptions and mathematical techniques:

1. Shear-Lag Model ... Highsmith and Reifsnider[1]

2. Self-Consistent Model ... Laws and other authors[4-5]

3. Complementary Strain Energy Method ... Hashin[6]

4. Strain Energy Method ... Aboudi[7]

5. Internal State Variable Method ... Talreja[8] and Allen et al.[9-10]

Each model has its own advantages as well as disadvantages for predicting the stiffness reduction in a fibrous laminated composite with matrix cracks. A brief review of the existing models and the necessity of a new model is discussed in this section.

The shear-lag model has been used by Highsmith and Reifsnider[1] for predicting the stiffness reduction of various types of laminates due to matrix cracks. In the shear-lag model, the far-field tensile stress was assumed to transfer to the cracked layer via shear deformation of a thin boundary layer in the vicinity of the layer interface. Also, the shear stress was assumed to be dominant within the boundary layer or so called shear transfer region. The procedure for shear lag analysis is relatively simple and results in a reasonably accurate prediction of stiffness reduction as a function of the crack density, even though it is not clear how to determine the boundary layer thickness in

a systematic way.

Laws and other authors[4-5] have utilized the self-consistent model together with classical laminated plate theory for estimating the stiffness reduction due to matrix cracking. The self-consistent method is a variation of the method for evaluating the overall stiffness of a composite material with various constituents including voids [11]. For an isotropic material with stacked cracks, the self-consistent method retrieves the average crack opening displacement which may be directly obtained from the fracture mechanics solution to a single crack imbedded in an infinite medium.

Hashin's model has utilized a relatively simple procedure based on the principle of minimum complementary strain energy to calculate out-of-plane stress components and the effective stiffness in a very explicit way[6]. For analyzing a $[0_q/90_r]_s$ type laminate, Hashin's model is obviously the most effective one. However, difficulties arise when Hashin's model is generalized for a multi-layered laminate of the types $[0_p/90_q/0_r/90_t]_s$, because of the cumbersome nature of the complementary strain energy method associated with assumed stress functions and traction boundary conditions.

Aboudi has expanded the displacement fields of a unit cell representing a body with aligned cracks in Legendre polynomials[7]. The effective elastic moduli of a cracked solid were calculated from the elastic energy stored in the cracked body. Aboudi's model gives approximately the same result as the shear-lag method, and requires higher

order expansions of the assumed displacement to increase the accuracy of the model prediction.

Talreja has utilized the damage vector concept for modelling a two-dimensional solid containing oriented crack arrays[8]. By assuming the energy density in a representing volume as a function of the strain tensor and the damage vector set, he reconstructed the constitutive equations with the observable strains and the effective stiffness tensor. This model may be considered as an alternative to the ISV method described below.

Allen et al. have developed a model for predicting stiffness loss as a function of damage state in composite materials[9-10]. Their model utilizes a set of second order tensorial quantities previously proposed by Kachanov[12] to describe each internal damage state. These tensorial quantities have been named as internal state variables, defined by

$$\alpha_{ij}^{\eta} = \frac{1}{V} \int_{S_2^{\eta}} u_i n_j \, dS \qquad (1)$$

where

$\eta = 1, 2, \ldots$ to the number of damage modes in the laminate.

$u_i =$ displacements on the crack faces

$n_j =$ unit normal to the crack surface

$V =$ local volume over which cracks are arranged

$S_2^{\eta} =$ surface area of cracks in V.

The stress-strain relations at the ply level are given by

$$\sigma_{ij} = C_{ijkl}\, \epsilon_{kl} + I^{\eta}_{ijkl}\, \alpha^{\eta}_{kl} \tag{2}$$

The ISV model described by eqs. (1) and (2) together with experimentally determined energy release rates for the $[0/90/0]_s$ laminate has been utilized to predict axial stiffness loss due to matrix damage in several graphite/epoxy cross-ply and quasi-isotropic laminates[13]. This last model has also been utilized to predict stiffness loss due to delamination[14].

Among these models, the ISV method can be considered as a general tool for predicting the overall effect of each damage mode on the global response of a fibrous composite laminate. In order to predict the upper bounds of effective Young's moduli for $[0_q/90_r]_{n,s}$ type laminates with matrix cracks, the authors present a relatively simple procedure based on the strain energy method to estimate the internal state variable representing the effect of the average matrix crack opening displacement on the effective Young's modulus.

MODEL FORMULATION

Consider a laminated composite material with infinite number of 0 and 90 degree layers as illustrated in Fig. 2-a. Since the crack patterns in 90 degree layers may be random, displacement fields in each crack element surrounded by two adjacent crack surfaces and two material interfaces are different. It is apparent from Fig. 2-a that a solution to the boundary value problem for all possible displacement boundary conditions is impractical, or at least very cumbersome to obtain. A relatively simple solution may be obtained by postulating a fictitious boundary value problem which represents a statistically arranged volume element shown in Fig. 2-b. The mutual influence between cracks in different 90 degree layers may be implicitly taken into account by assuming the y and z plane to remain plane throughout deformation under the axial tensile loading, P, at far-field. The displacement fields may then be assumed as

$$u = (u_o/a)x + \sum_m \sum_n a_{mn} \sin\alpha x \cos\beta y \qquad (3\text{-}a)$$

$$v = -(v_o/t)y \qquad (3\text{-}b)$$

$$w = -(w_o/b)z \qquad (3\text{-}c)$$

where   m, n = 1, 2, 3, ..., k

$$\alpha = (2m\text{-}1)\pi/2a$$

$$\beta = (2n\text{-}1)\pi/2t$$

Strain components are given by

$$\epsilon_{xx} = u_o/a + \sum_m \sum_n a_{mn} \, \alpha \, \cos\alpha x \, \cos\beta y \tag{4-a}$$

$$\epsilon_{yy} = -v_o/t \tag{4-b}$$

$$\epsilon_{zz} = -w_o/b \tag{4-c}$$

$$\gamma_{xy} = -\sum_m \sum_n a_{mn} \, \beta \, \sin\alpha x \, \sin\beta y \tag{4-d}$$

Otherwise, $\epsilon_{ij} = 0$.

The total potential energy in the volume($a \times 2t \times 2b$) is then described by

$$\Pi = U + V_E$$

$$= \frac{1}{2} \int_{-b}^{b} \int_{-t}^{t} \int_{0}^{a} C_{ijkl} \, \epsilon_{ij} \, \epsilon_{kl} \, dx \, dy \, dz - P \, u \Big|_{\substack{x=a \\ y=t}} \tag{5-a}$$

$$\frac{\Pi}{2b} = C_{xx} \left[(u_o/a)^2 at + 2(u_o/a)\sum_m \sum_n (-1)^{m+n} a_{mn}/\beta + \sum_m \sum_n (a_{mn}\alpha)^2 at/4 \right]$$

$$+ C_{yy} (v_o/t)^2 at + C_{zz} (w_o/b)^2 at + 2C_{yz} v_o w_o \, a/b$$

$$- 2C_{zx} \left[(u_o w_o(t/b) + (w_o/b)\sum_m \sum_n (-1)^{(m+n)} a_{mn}/\beta \right]$$

$$- 2C_{xy} \left[(u_o v_o + (v_o/t)\sum_m \sum_n (-1)^{(m+n)} a_{mn}/\beta \right]$$

$$+ G_{xy} \sum_m \sum_n (a_{mn}\beta)^2 at/4 - p u_o \tag{5-b}$$

where $p = P/2b$.

Differentiating the total potential energy with respect to unknown constants gives the following mxn+3 algebraic equations to solve.

$$p/2t = C_{xx}(u_o/a) - C_{xy}(v_o/t) - C_{zx}(w_o/b) \tag{6-a}$$

$$+ (C_{xx}/at) \sum_m \sum_n (-1)^{(m+n)} a_{mn}/\beta$$

$$0 = C_{yy}(v_o/t) - C_{xy}(u_o/a) + C_{yz}(w_o/b) \tag{6-b}$$

$$- (C_{xy}/at) \sum_m \sum_n (-1)^{(m+n)} a_{mn}/\beta$$

$$0 = C_{zz}(w_o/b) + C_{yz}(v_o/t) - C_{zx}(u_o/a) \tag{6-c}$$

$$- (C_{zx}/at) \sum_m \sum_n (-1)^{(m+n)} a_{mn}/\beta$$

$$0 = [C_{xx}(u_o/a) - C_{xy}(v_o/t) - C_{zx}(w_o/b)](-1)^{(m+n)}/\beta \tag{6-d}$$

$$+ a_{mn}(at/4)[C_{xx}\alpha^2 + G_{xy}\beta^2]$$

From eqs. (6-a), (6-b), and (6-c), v_o/t and w_o/b are determined.

$$v_o/t = (p/2t) \frac{C_{xy}C_{zz} - C_{yz}C_{zx}}{\det[C_{ij}]} \tag{7-a}$$

$$w_o/b = (p/2t) \frac{C_{yy}C_{zx} - C_{xy}C_{yz}}{\det[C_{ij}]} \tag{7-b}$$

From eqs. (6-d), a_{mn} are expressed in terms of other constants.

$$a_{mn} = \frac{4(-1)^{(m+n)} [-C_{xx}(u_o/a) + C_{xy}(v_o/t) + C_{zx}(w_o/b)]}{at\beta [C_{xx}\alpha^2 + G_{xy}\beta^2]} \quad (8\text{-}a)$$

$$\sum_m \sum_n (-1)^{(m+n)} a_{mn}/\beta = \frac{64at}{\pi^4}[-C_{xx}(u_o/a) + C_{xy}(v_o/t) + C_{zx}(w_o/b)]\xi \quad (8\text{-}b)$$

where

$$\xi = \sum_m \sum_n \frac{1}{C_{xx}(2m-1)^2(2n-1)^2 + G_{xy}(a/t)^2(2n-1)^4} \quad (8\text{-}c)$$

From eqs. (6-a) and (8-b), u_o/a is determined.

$$u_o/a = (p/2t)\left[\frac{C_{yy}C_{zz} - C_{yz}^2}{det[C_{ij}]} + \frac{1}{\dfrac{\pi^4}{64\xi} - C_{xx}}\right] \quad (8\text{-}d)$$

Utilizing eqs. (1), (7-a), (7-b), (8-a), and (8-d), α_{xx} is explicitly given by

$$\alpha_{xx} = \frac{(-1)p/2t}{\dfrac{\pi^4}{64\xi} - C_{xx}} \quad (8\text{-}e)$$

All other components of α_{ij} are assumed to be negligible.

The ISV, α_{xx}, given by eq. (8-e) represents the contribution of crack opening displacement to the observable axial strain which can be measured from a specimen with matrix cracks under uniaxial tensile loading. α_{xx} can be rewritten in terms of observable strain, u_o/a, using eqs. (8-d) and (8-e).

$$\alpha_{xx} = \frac{-(u_o/a)}{1 + \left[\dfrac{C_{yy}C_{zz} - C_{yz}^2}{\det[C_{ij}]} \right] \left[\dfrac{\pi^4}{64\xi} - C_{xx} \right]} \qquad (8\text{-}f)$$

The average value of the actual strain is then given by

$$\epsilon_{xx}^{act} = \epsilon_{xx}^{ind} [1 + \alpha_{xx}] \qquad (9\text{-}a)$$

$$\epsilon_{yy}^{act} = \epsilon_{yy}^{ind} \qquad (9\text{-}b)$$

$$\epsilon_{zz}^{act} = \epsilon_{zz}^{ind} \qquad (9\text{-}c)$$

where

$$\epsilon_{xx}^{ind} = u_o/a, \qquad \epsilon_{yy}^{ind} = -v_o/t, \qquad \epsilon_{zz}^{ind} = -w_o/b.$$

The stress-strain relations are given by

$$\begin{Bmatrix} \sigma_{xx} \\ \sigma_{yy} \\ \sigma_{zz} \end{Bmatrix} = \begin{bmatrix} C_{xx} & C_{xy} & C_{xz} \\ & C_{yy} & C_{yz} \\ \text{SYM.} & & C_{zz} \end{bmatrix} \begin{Bmatrix} \epsilon_{xx}^{act} \\ \epsilon_{yy}^{act} \\ \epsilon_{zz}^{act} \end{Bmatrix} \qquad (10\text{-}a)$$

Substituting eq. (9-a), (9-b), and (9-c) into eq. (10-a) gives the average values of stress components expressed in terms of observable strain components and effective stiffnesses.

$$
\begin{Bmatrix} p/2t \\ 0 \\ 0 \end{Bmatrix} = \begin{bmatrix} C_{xx}(1-\varsigma) & C_{xy} & C_{xz} \\ C_{xy}(1-\varsigma) & C_{yy} & C_{yz} \\ C_{xz}(1-\varsigma) & C_{yz} & C_{zz} \end{bmatrix} \begin{Bmatrix} \epsilon_{xx}^{ind} \\ \epsilon_{yy}^{ind} \\ \epsilon_{zz}^{ind} \end{Bmatrix}
\tag{10-b}
$$

where

$$
\varsigma = \cfrac{1}{1 + \left[\cfrac{C_{yy}C_{zz} - C_{yz}^2}{\det[C_{ij}]} \right]\left[\cfrac{\pi^4}{64\xi} - C_{xx} \right]}
\tag{10-c}
$$

Since the average value of the out-of-plane normal stress, σ_{yy}, is zero in eq. (10-b), classical laminated plate theory can be directly applied for expressing the effective Young's modulus of a damaged $[0_q/90_r]_s$ laminate as a function of the crack density, t/a, and the elastic properties of an undamaged material. For a $[0_q/90_r]_s$ laminate under uniaxial tensile loading, a compact analytical solution to the effective Young's modulus is obtained as follows.

By replacing subscripts x and z with L and T, respectively, and rearranging terms, plane stress constitutive relations are obtained.

$$
\begin{Bmatrix} \sigma_{LL} \\ \sigma_{TT} \end{Bmatrix} = \begin{bmatrix} C_{LL} & C_{LT}(1-\varsigma) \\ C_{LT} & C_{TT}(1-\varsigma) \end{bmatrix} \begin{Bmatrix} \epsilon_{LL} \\ \epsilon_{TT} \end{Bmatrix}
\tag{11-a}
$$

The effective stiffness matrix for a $[0_q/90_r]_s$ laminate under in-plane biaxial tensile loading becomes

$$
\left[\bar{C}_{ij}\right] = \begin{bmatrix} qC_{LL}+r(1-\varsigma_2)C_{TT} & [q(1-\varsigma_1)+r]C_{LT} \\ \\ [q+r(1-\varsigma_2)]C_{LT} & q(1-\varsigma_1)C_{TT}+rC_{LL} \end{bmatrix} \tag{11-b}
$$

where ς_1 and ς_2 represent the effects of matrix cracks in 0 and 90 degree layers given by eq. (10-c), respectively.

If 0 degree layers are assumed to remain undamaged during deformation, the inverse of eq. (11-b) can be written as

$$
\left[\bar{S}_{ij}\right] = \frac{q+r}{C_{TT}\det[\bar{C}_{ij}]} \begin{bmatrix} r(E_L/E_T)+q & -\nu_{LT}[q+r(1-\varsigma_2)] \\ \\ -\nu_{LT}r & q(E_L/E_T)+r(1-\varsigma_2) \end{bmatrix} \tag{11-c}
$$

The effective compliance matrix of an undamaged $[0_q/90_r]_s$ laminate, $[S_{ij}]$, is retrieved by setting $a/t = \infty$. The normalized axial stiffness, $S_{11}/\bar{S}_{11}$, then can be described by

$$
S_{11}/\bar{S}_{11} = 1 - \frac{\varsigma_2 r[\ r(E_L/E_T) + q - \nu_{LT}^2(q+r)\ ]}{(r+qE_L/E_T)(q+rE_L/E_T) - \nu_{LT}^2(q+r)^2} \tag{12-a}
$$

where

$$\zeta_2 = \cfrac{1}{1 + \rho \left[\dfrac{\pi^4}{64\lambda} - 1 \right]}$$ (12-b)

$$\lambda = \sum_m \sum_n \cfrac{1}{(2m-1)^2(2n-1)^2 + \dfrac{G_T(a/t)^2}{\rho E_T}(2n-1)^4}$$ (12-c)

$$\rho = \cfrac{1 - \nu_{LT}\nu_{TL}}{(1 - \nu_{TT} - 2\nu_{LT}\nu_{TL})(1 + \nu_{TT})}$$ (12-d)

The non-dimensionalized crack opening displacement, δ, is given by

$$\delta = (\ u|_{\substack{x=a \\ y=t}} - u|_{x=a}\ )/u|_{\substack{x=a \\ y=t}} = 1 - \frac{u|_{x=a}}{u_o}$$

$$= - \frac{\pi\zeta_2}{2\lambda} \sum_m \sum_n \cfrac{(-1)^{n-1}\cos\beta y}{(2m-1)^2(2n-1) + \dfrac{G_T(a/t)^2}{\rho E_T}(2n-1)^3}\ ,$$ (12-e)

and the variation of δ is illustrated in Figs. 3-a and 3-b for typical isotropic and orthotropic material systems, respectively. The crack parameter, ζ_2, computed from eq. (12-a) is listed in Table 1 for most commonly used fibrous composite materials given in Table 2. Also, it should be noticed that the ISV for matrix cracks described herein can be obtained by assuming fixed grip mode, in which u_o/a is treated as a known variable.

For an isotropic material, the normalized axial stiffness from the self consistent model[4] is given by

$$S_{11}/\bar{S}_{11} = \frac{1}{1 + (\pi/2)(1-\nu^2)(t/a)} = 1 - \varsigma_{2,s} \qquad (13\text{-}a)$$

Thus,

$$\varsigma_{2,s} = \frac{1}{1 + \dfrac{2\,(a/t)}{\pi(1-\nu^2)}} \qquad (13\text{-}b)$$

Please notice that eq. (13-a) can be directly obtained from the crack opening displacement calculated from fracture mechanics as described below.

The mode I crack opening displacement, u_x, is given by

$$u_x = \frac{2(1-\nu^2)\sigma}{E}\sqrt{(t^2-y^2)} \qquad (14\text{-}a)$$

The average value of u_x along the crack surface becomes

$$u_{x,ave} = \frac{2(1-\nu^2)\sigma}{E}\frac{\int_{-t}^{t}\sqrt{(t^2-y^2)}\,dy}{2t}$$

$$= \frac{\pi t(1-\nu^2)\sigma}{2E}$$

The contribution of $u_{x,ave}$ to the observable strain is then given by

$$u_{x,ave}/a = (\pi/2)(1-\nu^2)(t/a)(\sigma/E) \qquad (14\text{-}c)$$

when the representing volume is $4at$. The normalized axial stiffness
is expressed by

$$S_{11}/\bar{S}_{11} = \frac{1}{1 + (\pi/2)(1-\nu^2)(t/a)} \; ,$$

which is identical to eq. (13-a) obtained from the self consistent
model.

The matrix crack parameter, ζ_2, is plotted in Fig. 4-a for iso-
tropic materials with various Poisson's ratios. Fig. 4-b shows that ζ_2
is almost independent of the material systems which have been commonly
used for measuring the effect of matrix cracks on the axial stiffness.
In Fig. 5, the crack parameters for various isotropic materials are
compared with those calculated from the self-consistent model.

RESULTS AND DISCUSSION

The suitability of any theoretical model must be assessed by comparing the model with other models and/or experimentally measured data. This is accomplished herein by comparing the present model predictions with the non-dimensionalized effective Young's moduli (normalized stiffnesses) of glass/epoxy and graphite/epoxy specimens in the open literature[1, 10]. Among published experimental data, the stiffness reduction in $[0/90_3]_s$ glass/epoxy specimen reported by Highsmith and Reifsnider [1] has been frequently cited by other researchers[5, 6, 7]. For this specific experimental data, the authors compared the present model with other models [1, 5, 6, 7] in Fig. 6-a. Also, the experimental data from AS-4/3502 graphite/epoxy specimens with a number of cross-ply stacking sequences[3] are compared with the present model predictions in Figs. 7-a to 7-d.

The comparisons illustrated in Fig. 6 and Fig. 7 verify that the present model gives a fairly accurate prediction of the degraded axial stiffness as a function of the crack density for two commonly used material systems. Furthermore, it should be noticed that the crack density(number of cracks per unit length) is not appropriate for representing the matrix crack characteristics. As an example, consider $[0_n/90_n]_s$ specimens. If the crack density is utilized as an independent parameter, the normalized stiffnesses of $[0/90]_s$ and $[0_2/90_2]_s$ will be different at the same crack density as shown in Figs. 7-a and 7-b. This violates the most important assumption in the continuum mechanics, i. e., observable state variables are independent of the size of the

domain of interest. On the contrary, the ratio of the crack length to the distance between two adjacent cracks, t/a, eliminates this inconsistency as illustrated in the same figures. Also, the study of Talreja (Fig. 17 of ref.[8]) shows a similar result. Thus, the authors strongly recommend to use a non-dimensional parameter, t/a, as an independent parameter instead of the crack density for characterizing matrix cracks in fibrous composite materials. This type of non-dimensional parameter as an independent variable is an essential tool especially for describing history dependent phenomena such as plastic deformation of the constituents of metal matrix composites.

Since the Internal State Variable defined by eq. (1) is a general expression for an arbitrary damage mode, the entire mathematical formulation presented herein can be easily modified for $[0_q/90_r]_{n,s}$ type laminates or angle-ply laminates with arbitrarily shaped matrix cracks and interfacial delaminations. For a $[0_q/90_r]_{n,s}$ laminate, the present model can be directly applicable without any correction if our interest is restricted to the effective axial Young's modulus as a function of t/a. For off-axis or curved matrix cracks, the present model can be generalized by utilizing the conventional tensor transformation law for α_{ij}. However, another ISV is required for modelling the effect of interfacial delaminations on the observable stiffnesses. This will be accomplished by assuming relatively simple displacement fields similar to eq. (3-a) to eq. (3-c) for matrix cracks together with a series/parallel spring model for regions adjacent to interfacial delaminations.

The analytical solution to the crack parameter, ζ_2, includes the crack interaction in an explicit form. Furthermore, the internal state variable, α_{xx}, results directly from the strain energy loss due to matrix cracks[9]. By combining the present problem solving technique with the study of Allen et al.[9], strain energy release rate at a given matrix crack damage state can be predicted analytically. However, the internal state variable presented herein may not be exact under the following conditions.

(1) When the matrix crack size and spacing cannot be assumed to be homogeneous.

(2) When the matrix material should be assumed viscoelastic.

(3) When the matrix cracks are dominated by micro-cracks rather than by those that cross the entire specimen width.

Even though the actual shapes of matrix cracks are quite different from the idealized straight one illustrated in Fig. 2, the comparison between the present model prediction and experimental data from two different material systems shows very close agreement.

REFERENCES

[1] Highsmith, A. L., Reifsnider, K. L., "Stiffness-Reduction Mechanisms in Composite Laminates,"Damage in Composite Materials, ASTM STP 775, K. L. Reifsnider, Ed., American Society for Testing and Materials, 1982, pp. 103-117.

[2] Ogin, S. L., Smith, P. A., Beaumont, P. W. R., "Matrix Cracking and Stiffness Reduction during the Fatigue of a $[0/90]_s$ GFRF Laminate," Composite Science and Technology, Vol. 22, 1985, pp. 22-31.

[3] Groves, S. E., "A Study of Damage Mechanics in Continuous Fiber Composite Laminates with Matrix Cracking and Interply Delaminations," Dissertation, Texas A&M University, 1986.

[4] Laws, N., Dvorak, G. J., Hejazi, M., "Stiffness Changes in Unidirectional Composites Caused by Crack Systems," Mechanics of Materials 2, North Holland, pp. 123-137, 1983.

[5] Dvorak, G. J., "Analysis of Progressive Matrix Cracking in Composite Laminates," AFOSR-82-0308, Rensselaer Polytechnic Institute, March 1985.

[6] Hashin, Z., "Analysis of Cracked Laminates: A Variational Approach," Mechanics of Materials 4, North Holland, pp. 121-136, 1985.

[7] Aboudi, J., "Stiffness Reduction of Cracked Solids," Engineering Fracture Mechanics, Vol. 26, No. 5, pp. 637-650, 1987.

[8] Talreja, R., "Transverse Cracking and Stiffness Reduction in Composite Laminates," J. of Composite Materials, Vol. 19, pp. 355-375, 1985.

[9] Allen, D. H., Harris, C. E., Groves, S. E., " A Thermomechanical Constitutive Theory for Elastic Composites with Distributed Damage-Part I: Theoretical Development," Int. J. of Solids and Structures, 23(9), pp. 1301-1318, 1987.

[10] Allen, D. H., Harris, C. E., Groves, S. E., " A Thermomechanical Constitutive Theory for Elastic Composites with Distributed Damage-Part II: Application to Matrix Cracking in Laminated Composites ," Int. J. of Solids and Structures, 23(9), pp. 1319-1338, 1987.

[11] Mura T., "Micromechanics of Defects in Solids," Mechanics of Elastic and Inelastic Solids 3, Martinus Nijhoff Publishers, Printed in the Netherlands, 1982.

[12] Kachanov, M., " Continuum Theory of Media with Cracks," Izv. AN SSSR, Mekhanika Tverdogo Tela, ASCE, Vol. 7, pp. 54-59, 1972.

[13] Harris, C. E., Allen, D. H., Norttorf, E. W., Groves, S. E.,
      "Modelling Stiffness Loss in Quasi-Isotropic Laminates due to
      Microstructural Damage," to appear in J. of Engineering Materials
      and Technology, 1988.

[14] Allen, D. H., Groves, S. E., Harris, C. E., "A Cumulative Damage
      Model for Continuous Fiber Composite Laminates with Matrix Crack-
      ing and Interply Delaminations," to appear in ASTM STP for 8th
      Symposium on Composite Materials: Testing and Design, American
      Society for Testing and Materials, 1987.

Table 1. Crack Parameter

t/a	Crack Parameter (ζ_2)	
	Glass/Epoxy	Graphite/Epoxy
0.0	0.0000	0.0000
0.1	0.0812	0.0828
0.2	0.1673	0.1704
0.3	0.2559	0.2603
0.4	0.3415	0.3469
0.5	0.4189	0.4247
0.6	0.4857	0.4917
0.7	0.5421	0.5480
0.8	0.5891	0.5948
0.9	0.6284	0.6338
1.0	0.6613	0.6664

I

Table 2. Material Properties

Property	Material	
	Glass/Epoxy Ref. [1]	Graphite/Epoxy Ref. [10]
E_{LL}(Msi)	6.048	21.0
E_{TT}(Msi)	1.885	1.39
G_{LT}(Msi)	0.493	0.694
ν_{LT}	0.300	0.310
ν_{TT}	0.420*	0.461*
One Ply Thickness(in.)	0.008	0.005

* Assumed Values

II
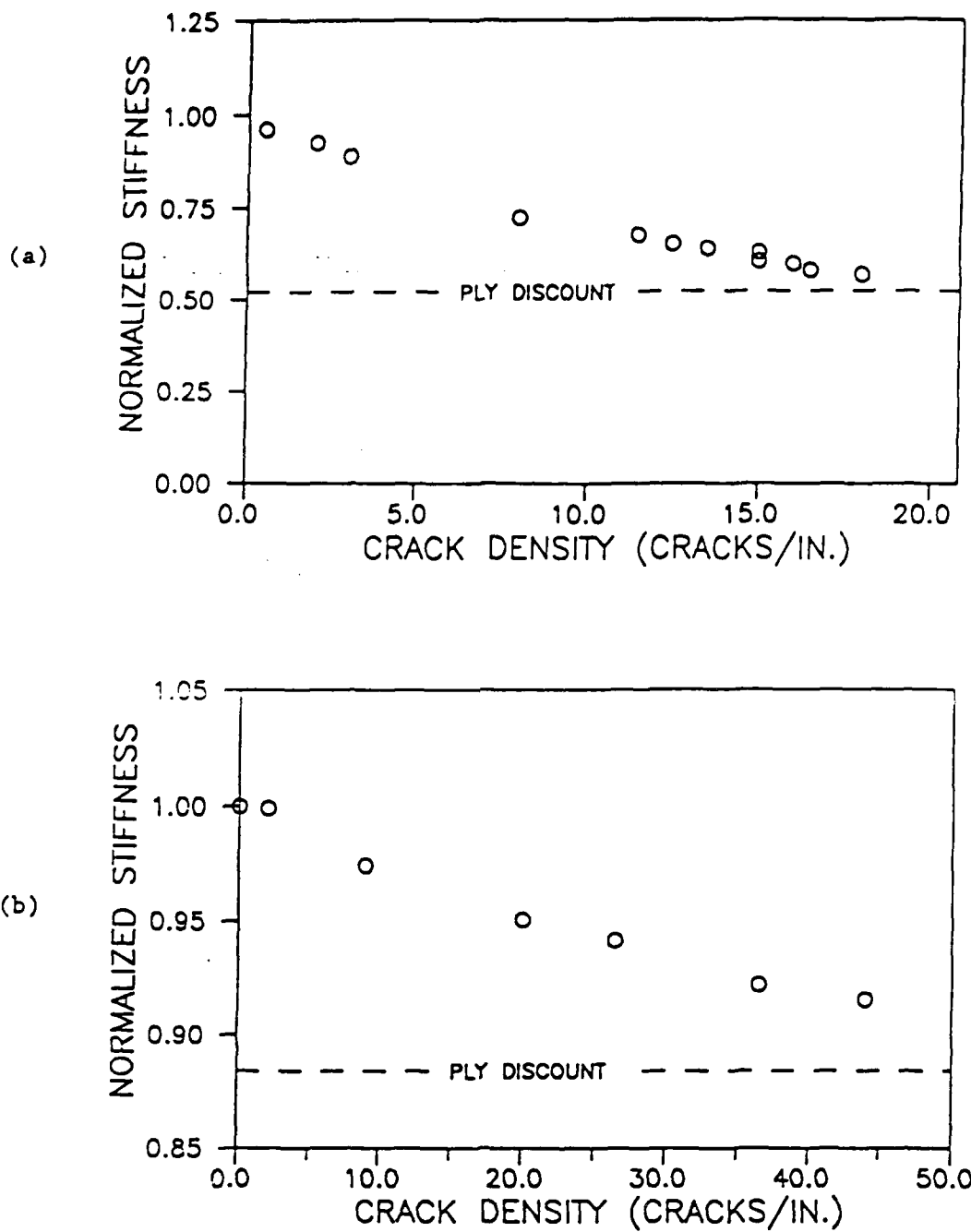
Fig. 1. Discrepancies between the Classical Ply Discount Method
and Experimental Observations

(a) $[0/90_3]_s$ Glass/Epoxy[1]

(b) $[0/90_2]_s$ Graphite/Epoxy[3]
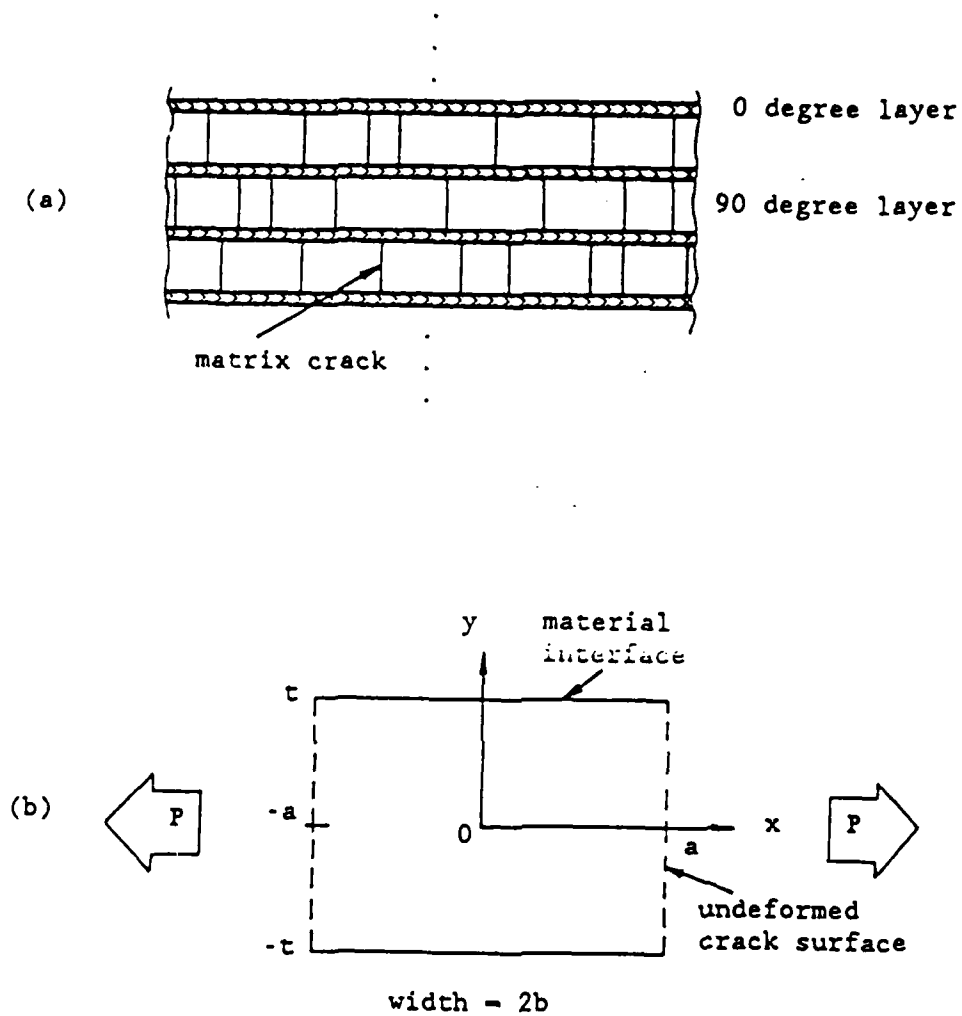
Fig. 2 $[0_q/90_r]_{n,s}$ Type Laminate with Matrix Cracks

(a) Overall Configuration

(b) One Representing 90 Degree Layer Element
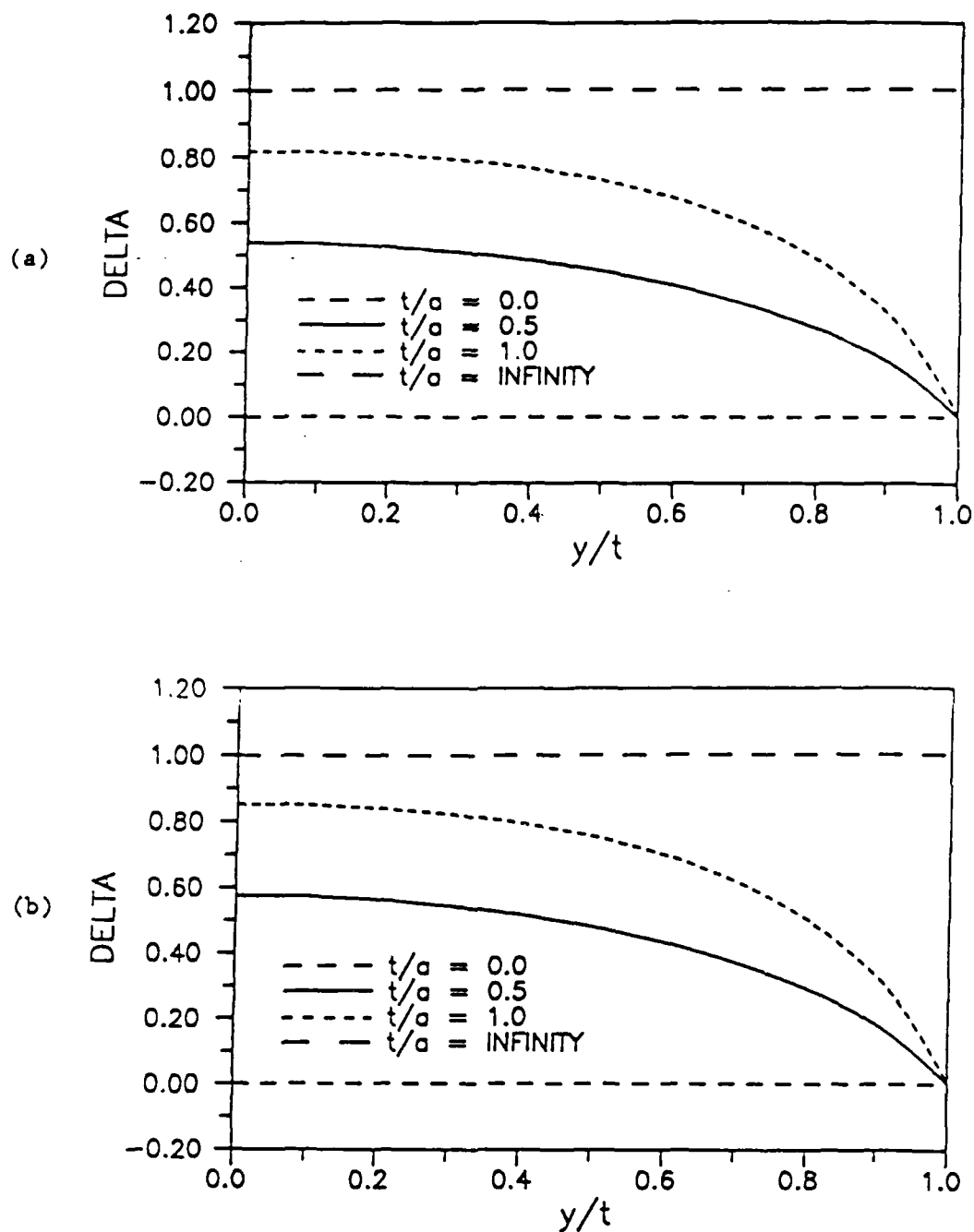
Fig. 3. Non-Dimensionalized Crack Opening Displacement

(a) Isotropic Material ($\nu = 0.333$)

(b) Graphite/Epoxy (Table 2)

(a)

(b)
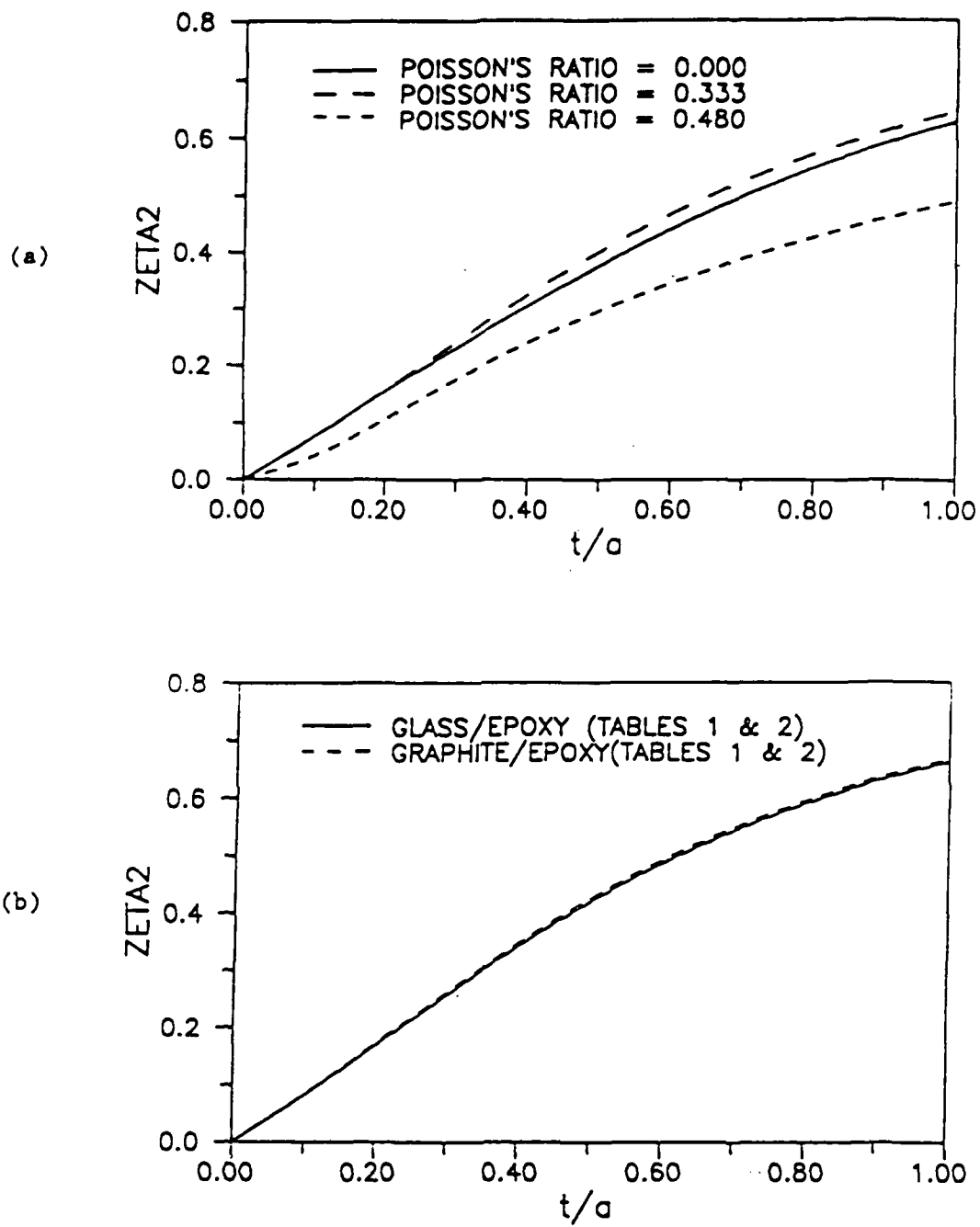
Fig. 4.   Crack Parameters

(a) Isotropic Materials

(b) Orthotropic Materials
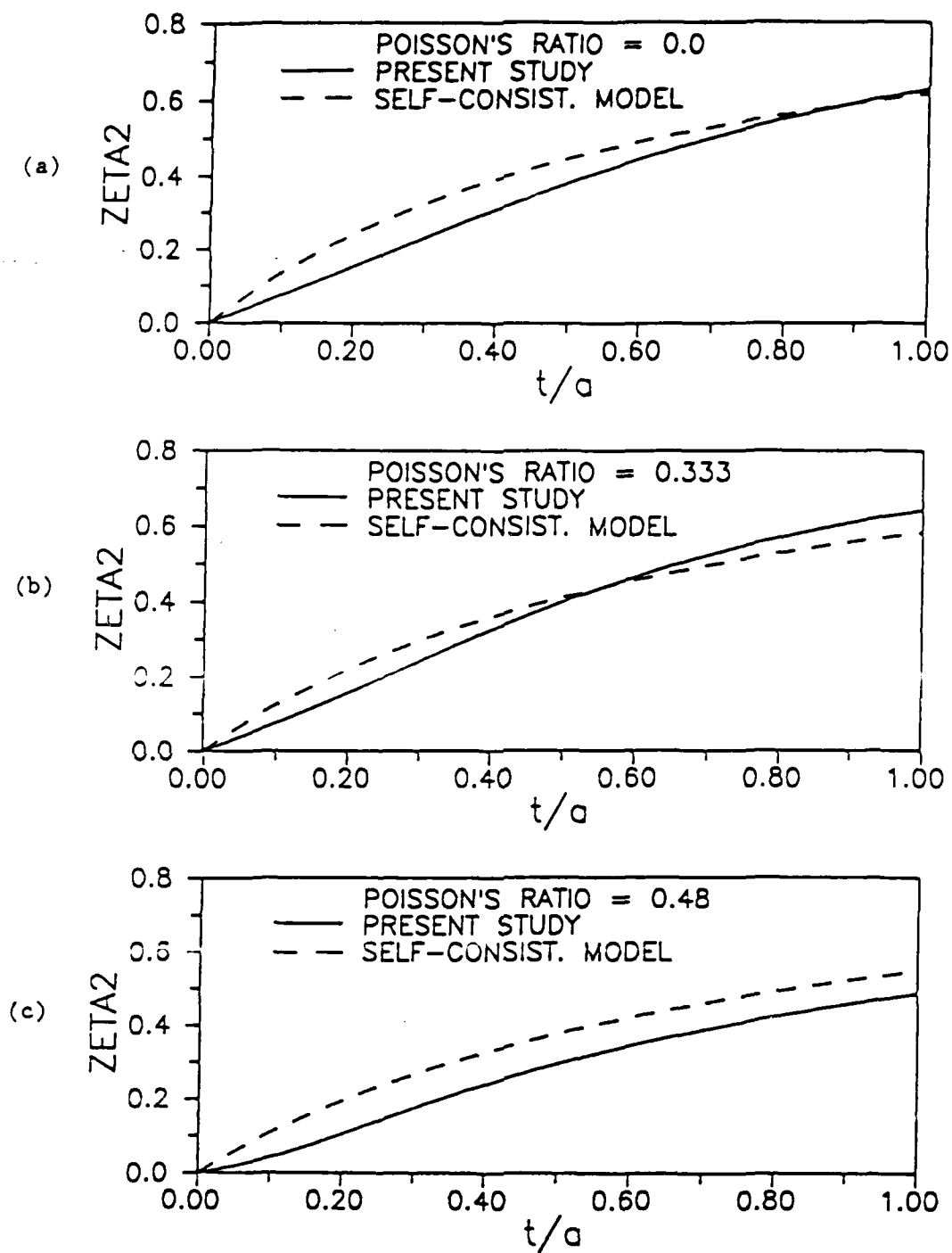
Fig. 5. Crack Parameters from the Present Study and Ref. [4]
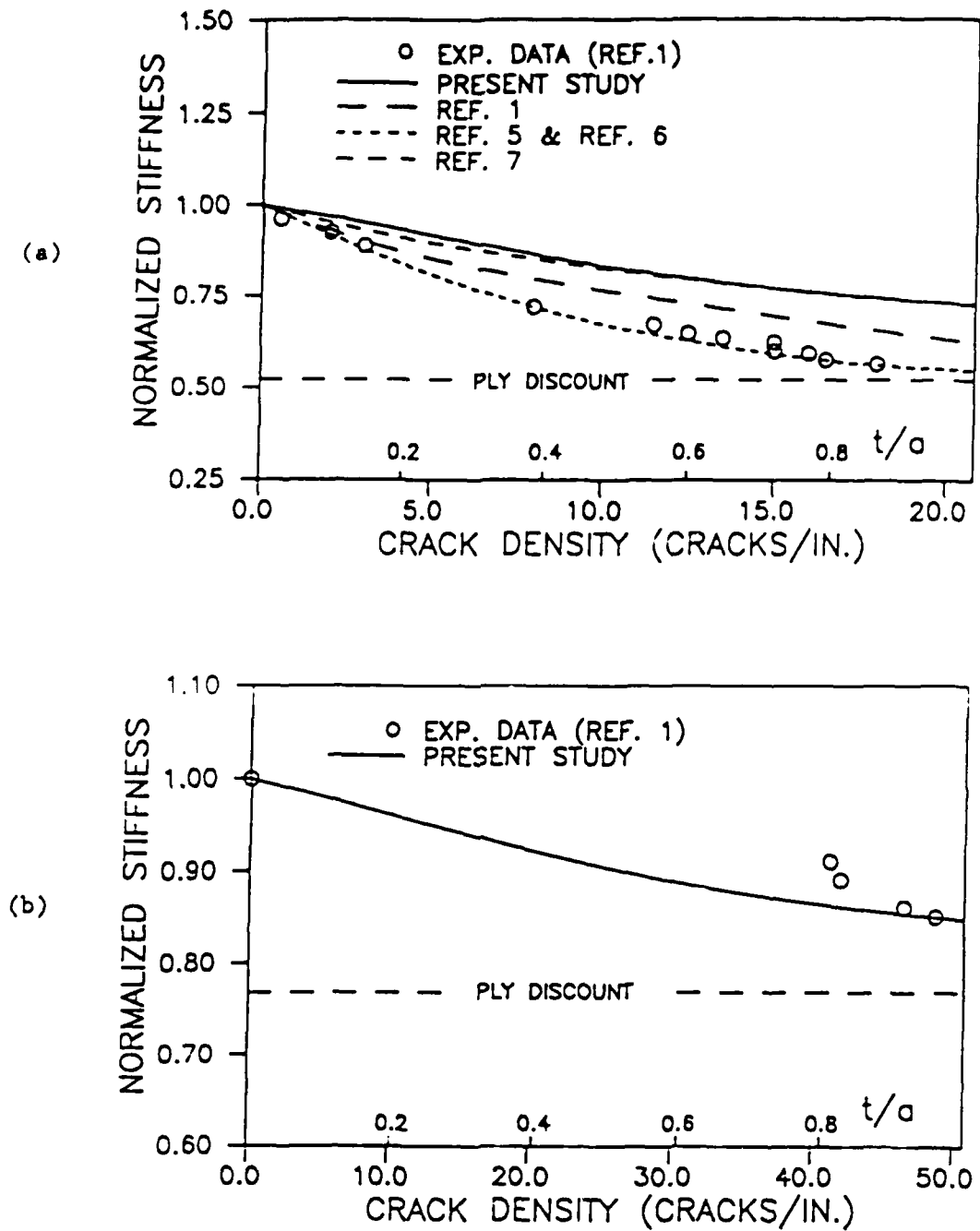
(a) $\nu = 0.0$

(b) $\nu = 0.333$

(c) $\nu = 0.48$

(a)

(b)

Fig. 6. Stiffness Reduction in Glass/Epoxy Specimens

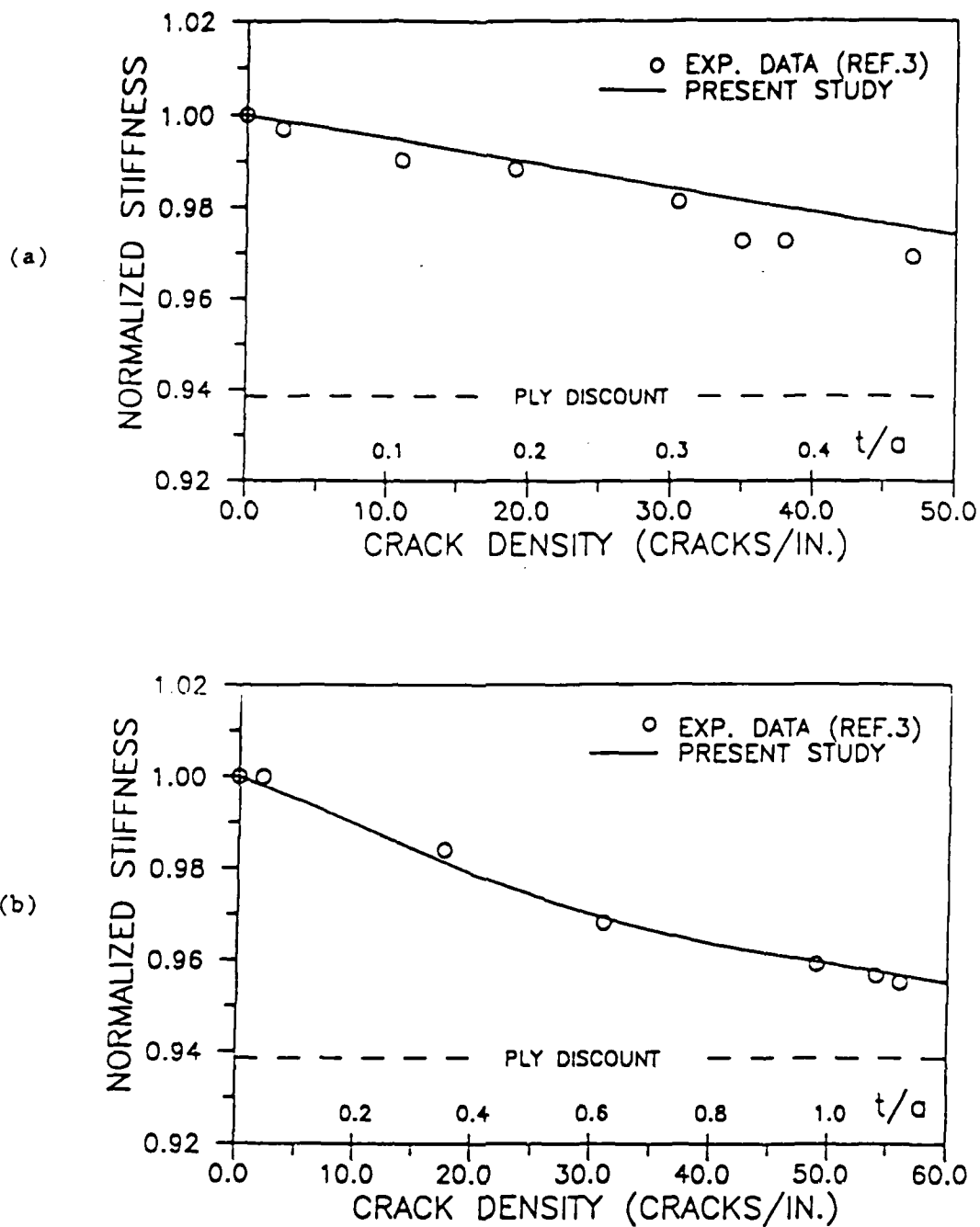(a) $[0/90_3]_s$ laminate

(b) $[0/90]_s$ laminate

Fig. 7. Stiffness Reduction in Graphite/Epoxy Specimens

       (a) $[0/90]_s$ laminate

       (b) $[0_2/90_2]_s$ laminate

       (c) $[0/90_2]_s$ laminate

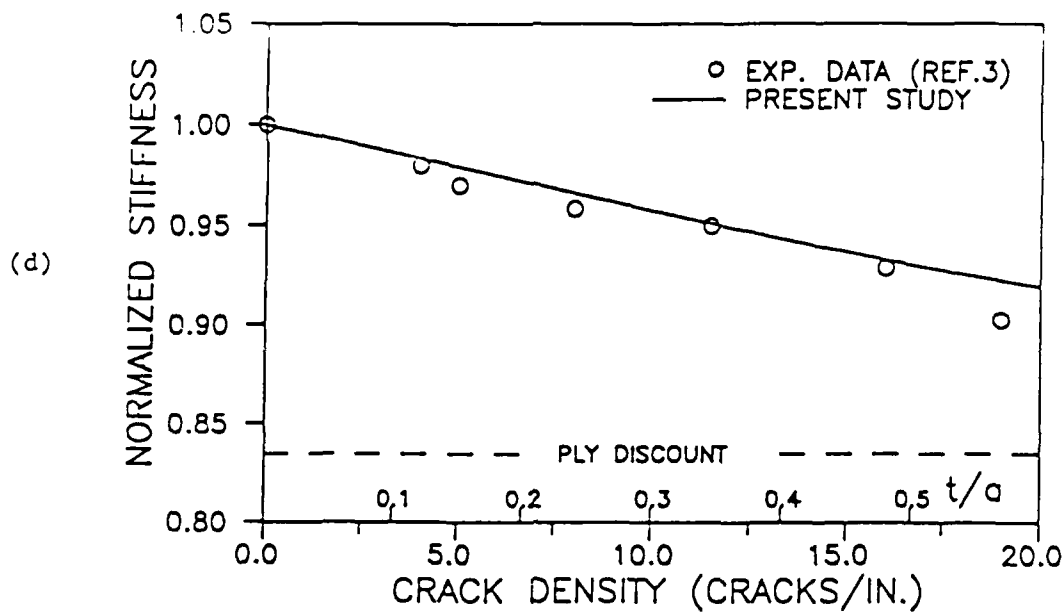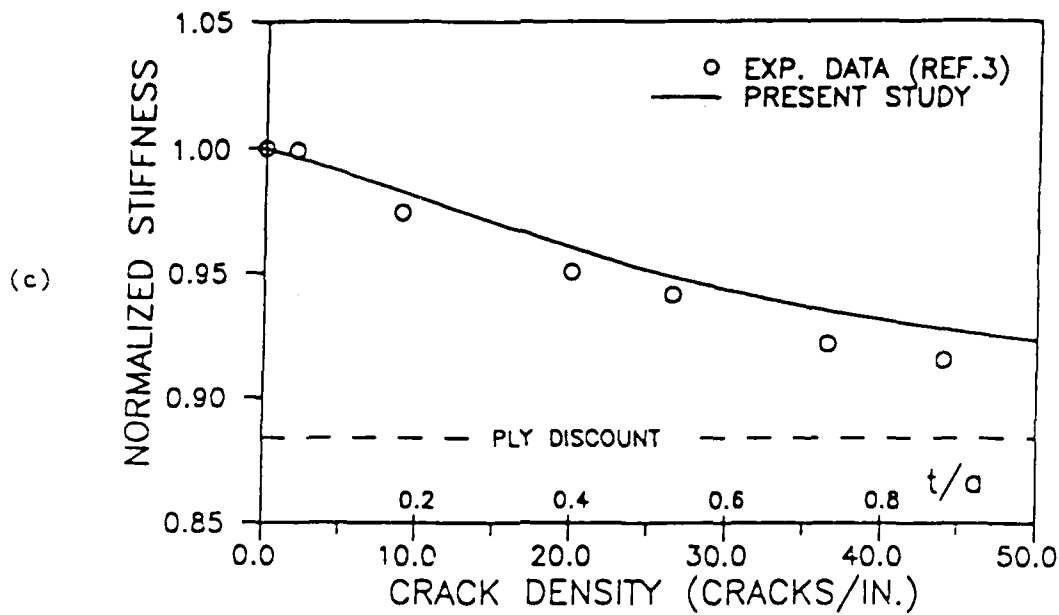   (d) $[0/90_3]_s$ laminate   (continued to next page)

Fig. 7. Stiffness Reduction in Graphite/Epoxy Specimens

(a) $[0/90]_s$ laminate

(b) $[0_2/90_2]_s$ laminate

(c) $[0/90_2]_s$ laminate

(d) $[0/90_3]_s$ laminate